CONTROL OF PHOSPHOLIPID METABOLISM IN MAMMALIAN TISSUES

By

Biao Lu

A thesis submitted to the Faculty of Graduate Studies

in partial fulfillment of the requirements for the degree

of Doctor of Philosophy

Department of Biochemistry and Medical Genetics

University of Manitoba

2003

THE UNIVERSITY OF MANITOBA

FACULTY OF GRADUATE STUDIES

*****

COPYRIGHT PERMISSION PAGE

Control of Phospholipid Metabolism in Mammalian Tissues

BY

Biao Lu

A Thesis/Practicum submitted to the Faculty of Graduate Studies of The University of Manitoba in partial fulfillment of the requirements of the degree of

DOCTOR OF PHILOSOPHY

To my family,

My wife Jenny, and my son Frank

ACKNOWLEDGEMENTS

I wish to express my gratitude to my supervisor Dr. Patrick C. Choy for his guidance, inspiration and above all his support of my endeavors. Pat, you have shown me multi-facets in science and in life. It is a privilege to be a student under your tutelage. I shall always be in your debt.

A big "Thank you" is also extended to members of my advisory committee, Dr. Edwin Kroeger, Dr. Grant Hatch, and Dr. Yuewen Gong. I am grateful for your help and support. I would like to thank Dr. Roy Baker for his critical assessment of this thesis.

I also extend my gratitude to members of the department who have enriched my scientific life during my graduate training.

I wish to thank my special friends and colleagues in the department: Monroe, Yaling, and Sun for all the fun and happy times we have shared.

Financial support was provided by the Manitoba Health Research Council and the Canadian Institutes of Health Research.

Life so short, the craft so long to learn…

-- Hippocrates

TABLE OF CONTENTS

LIST OF FIGURES x

LIST OF TABLES xv

LIST OF ABBREVIATIONS xvi

ABSTRACT xix

INTRODUCTION AND LITERATURE REVIEW

I. BIOLOGICAL MEMBRANE

1.1 Structure of Biological Membrane 1

1.2 Membrane Lipids 3

1.2.1 Phospholipids (phosphoglycerides) 3

1.2.2 Sphingolipids 6

1.2.3 Cholesterol 6

1.2.4 Asymmetry of Lipid Bilayers 8

1.3 Membrane Proteins 11

1.4 Membrane Sugars 11

II. CELL SIGNALING

2.1 Three Forms of Cell Signaling 13

2.2 Mitogen-activated Protein Kinases (MAPKs) Signaling 13

2.3 Protein Kinase C (PKC) Signaling 18

2.4 Inflammatory Signaling 20

2.5 Apoptotic Signaling 22

2.6 Nuclear Receptor Signaling 24

2.6.1 Classification of Nuclear Receptors 24

2.6.2 Estrogen Receptor Actions 26

2.6.3 RXR and RAR Actions 29

III. CONTROL OF PHOSPHOLIPID METABOLISM

3.1 Classification and Nomenclature 30

3.2 Function of Phospholipids 30

3.3 Phospholipid Biosynthesis in Mammalian Tissues 31

3.3.1 The *de novo* Biosynthesis Pathways 32

3.3.2 Glycerol Kinase (EC 2.7.1.30) and *sn*-glycerol-3-phosphate Dehydrogenase (EC 1.1.1.94) 34

3.3.3 Dihydroxyacetone-phosphate Acyltransferase (EC 2.3.1.42) 34

3.3.4 *sn*-glycerol-3-phosphate Acyltransferase (EC 2.3.1.15) 35

3.3.5 1-acyl-*sn*-glycerol-3-phosphate Acyltransferase (EC 2.3.1.51) 36

3.3.6 Phosphatidic Acid Phosphohydrolase (EC 3.1.27) 37

3.3.7 Monoacylglycerol Acyltransferase (EC 2.3.1.22) 39

3.3.8 Diacylglycerol Acyltransferase (EC 2.3.1.21) 41

3.3.9 Biosynthesis of Polyglycerophospholipids 41

3.3.10 Biosynthesis of Phosphatidylcholine 44

3.3.11 Biosynthesis of Phosphatidylethanolamine 44

3.4 Remodeling of Phospholipids 45

3.5 Phospholipid Catabolism in Mammalian Tissues 51

3.5.1 Phospholipases 51

3.5.2 Phospholipase A_2 52

3.5.3 Regulation of Cytosolic Phospholipase A_2 54

3.5.4 Arachidonate-eicosanoid Cascade 56

3.5.5 Prostanoid Biosynthesis 58

3.5.6 Function of Eicosanoids 59

3.5.7 Cyclooxygenases and Their Regulations 62

IV. BIOINFORMATICS

4.1 Bioinformatics 65

4.2 Biotechnology 65

4.3 Bioinformatic Databases and Information Retrieval 67

4.4 Software Tools and Data Analysis 69

4.5 Knowledge Discovery in Databases 69

4.6 Bioinformatic Resources 72

4.6.1 Expressed Sequence Tag (EST) 72

4.6.2 Conserved Domain Database (CDD) 72

4.6.3 Basic Local Alignment Search Tool (BLAST) 73

4.6.4 Multiple Sequence Alignments 74

4.7 Applications of Bioinformatics in Lipid Research 75

V. RESEARCH AIMS AND HYPOTHESES 77

MATERIALS AND METHODS

I. MATERIALS

1.1 Experimental Animals and Cell Lines 80

1.2 Radioisotopes 80

1.3 Antibodies 80

1.4 Biochemicals, Hormones, and Cytokines 81

1.5 Restriction Enzymes and Modifying Enzymes 81

1.6 Commercial Kits and Experiment Systems 81

1.7 Cell Culture Medium, Lipid Standards, and Other Materials 82

II. METHODS

2.1 Culture of Human Premonocytic U937 Cells 83

2.2 Cell Differentiation Method and Treatment 83

2.3 Culture of Rat Heart Myoblast H9c2 Cells 84

2.4 Culture of COS-1 and NIH3T3 Cells for Transfection Studies 84

2.5 Giemsa Staining and Morphological Observation 84

2.6 Immunocytochemical Staining of Human ER-α 85

2.7 Fluorescence-activated Cell Sorting (FACS) 85

2.8 Determination of Cell Viability 86

2.9 Whole Cell, Cytosolic, and Nuclear Extraction Preparation 86

2.10 Protein Determination 87

2.11 Immunoblotting Analysis of Enzyme Protein Levels 88

2.12 Measurement of AA Release 89

2.13 Measurement of PGE_2 Production 89

2.14 Isolation of Total RNA 90

2.15 RNA Denaturing Electrophoresis and Northern Blotting Analysis 90

2.16 PCR Primers and RT-PCR Conditions 91

2.17 Double-stranded DNA Sequence Analysis 94

2.18 Construction of Expression Vectors for Murine AGPATs 94

2.19 Plasmids and Transient Transfection 95

2.20 *In vitro* transcription and translation 96

2.21 1-acyl-*sn*-glycerol-3-phosphate Acyltransferase Enzyme Assay 96

2.22 Monolysocardiolipin Acyltransferase Enzyme Assay 97

2.23 Statistical Analysis 98

EXPERIMENTAL RESULTS

PART I. STUDIES ON THE BIOSYNTHESIS OF PHOSPHOLIPID

I. IDENTIFICATION AND MOLECULAR CLONING OF MAMMALIAN 1-ACYL-SN-GLYCEROL-3-PHOSPHATE ACYLTRANSFERASES

1.1.1 Identification of Murine AGPAT1/2/3/4/5 and Human N456 100

1.1.2 cDNA Cloning and Construction of Expression Vectors 103

1.1.3 Alignment Study and Identification of Conserved Motifs 104

1.1.4 Detection of Hypothetical AGPAT mRNA in Murine Tissues 108

1.1.5 Expression of AGPATs *in vitro* and *in vivo* 110

1.1.6 Determination of 1-acyl-*sn*-glycerol-3-phosphate Acyltransferase Activity 113

II. COMPLEX EXPRESSION PATTERN OF THE BARTH SYNDROM GENE TAZ IN HUMAN AND MURINE TISSUES

1.2.1 Expression of TAZ in Human and Murine Tissues 117

1.2.2 Identification of Evolutionarily Conserved and Potentially Functional Form of TAZ 122

1.2.3 Alternative Translation of Human and Murine TAZs 126

1.2.4 Determination of Potential Acyltransferase Activity of Human Full-length TAZ and Murine Exon 5-deleted TAZ 129

PART II. STUDIES ON PHOSPHOLIPID CATABOLISM

I. REGULATION OF CYTOSOLIC PSHOSPHOLIPASE A_2, COX-1 AND –2 EXPRESSIONS BY PMA, TNFα, LPS AND M-CSF IN HUMAN MONOCYTES AND MACROPHAGE

2.1.1 PMA, TNFα, LPS and M-CSF Enhance AA Release in U937 Premonocytes and Macrophages. 131

2.1.2 PMA, TNFα, LPS and M-CSF Differentially Affect PGE_2 Production in U937 Cells and Macrophages 134

2.1.3 Differential Expression of $cPLA_2$, COX-1 and COX-2 by PMA, TNFα, LPS and M-CSF in U937 Cells and Macrophages 136

II. REGULATION OF ARACHIDONIC ACID METABOLISM BY PHOBOL 12-MYRISTATE 13-ACETATE IN MONOCYTES AND MYOCYTES

2.2.1 PMA Induced Arachidonic Acid Release in U937 Cells 143

2.2.2 PMA Induced PGE_2 Release in U937 and H9c2 Cells 145

2.2.3 Effect of PMA on $cPLA_2$, COX-1, and COX-2 in U937 and H9c2 Cells 148

2.2.4 The Efficacy of PMA in the Modulation of COX-1 and COX-2 151

III. 17-β-ESTRADIOL ENHANCES PROSTAGLANDIN E2 PRODUCTION IN HUMAN U937 DERIVED MACROPHAGES

2.3.1 Assessment of PMA-induced U937 Cell Differentiation by Morphologic Observation and Cell Surface Antigen Expression 153

2.3.2 Increase in the Expression of ER-α in PMA-differentiated U937 Cells 155

2.3.3 17-β Estradiol Enhance PGE_2 Production in PMA-differentiated U937 Cells 157

2.3.4 17-β Estradiol Enhanced AA Release and Up-regulated COX-1 and COX-2 in PMA-differentiated U937 Cells 158

2.3.5 Attenuation of PGE_2 Production by Selective Estrogen Receptor Modulators (SERMs) 162

IV. CYTOOXYGENASE EXPRESSION IS ELEVATED IN RETINOIC ACID-DIFFERENTIATED U937 CELLS

2.4.1 Cell Differentiation by RA 164

2.4.2 The Effect of RA on PGE_2 Production 167

2.4.3 The Effect of RA on COX-1 or COX-2 Protein Expression 171

2.4.4 The Effect of RA on COX-1 mRNA Levels 175

DISCUSSIONS

I. STUDIES ON THE BIOSYNTHESIS OF PHOSPHOLIPID

1.1 Identification and Characterization of Acyltransferases in Phospholipid Biosynthesis 178

1.2 Complex Expression Pattern of in Barth Syndrome Gene Tafazzin in Human and Murine Tissues 179

II. STUDIES ON THE CATABOLISM OF PHOSPHOLIPID

2.1 Regulation of Cytosolic Phospholipase A2, Cyclooxygenase-1 and –2 Expression by PMA, TNFα, LPS and M-CSF in Human Monocytes and Macrophages 181

2.2 Modulation of Arachidonic Acid Metabolism by Phorbol 12-Myristate 13-Acetate in Monocytes and Myocytes 183

2.3 17-β Estradiol Enhances PGE_2 Production in U937-derived Macrophages 186

2.4 Cyclooxygenase Expression Is Elevated in Retinoic Acid-differentiated U937 Cells 188

SUMMARY 192

REFERENCES 194

LIST OF FIGURES

		Page
Figure 1.	The fluid mosaic model of eucaryotic plasma membrane	2
Figure 2.	General structure of a phospholipid molecule	4
Figure 3.	Five major types of phospholipids found in mammalian tissues	5
Figure 4.	Structures of sphigolipids found in mammalian tissues	7
Figure 5.	The structure of cholesterol and cholesterol in a lipid bilayer	8
Figure 6.	Phospholipid asymmetry in mammalian plasma membranes	10
Figure 7.	Six ways in which membrane proteins associate with the lipid bilayer	12
Figure 8.	Three parallel MAPK pathways in mammalian cells	15
Figure 9.	M-CSF action and signaling via the MAPK/ERK pathway	17
Figure 10.	Diacylglycerol action and PKC signaling pathway	19
Figure 11.	LPS and TNF-α action and signaling via the SAPK/JNK pathway	21
Figure 12.	TNF-α action and apoptotic signaling pathway	23
Figure 13.	Estrogen action and ER modular structure and function domains	28
Figure 14.	Phospholipid biosynthetic pathways in mammalian cells	33
Figure 15.	Biosynthesis of phosphatidylglycerol and cardiolipin	43
Figure 16.	Biosynthesis of phosphatidylcholine and phosphatidylethanolamine	46
Figure 17.	Sites of phospholipase action	48
Figure 18.	The deacylation-reacylation of phosphatidylcholine	49

Figure 19.	Gene structure, transcript, and protein functional domains of human cytosolic phospholipase A_2	55
Figure 20.	Pathways in arachidonate cascade	57
Figure 21.	Biosynthetic stages of prostanoids derived from AA	61
Figure 22.	Gene structure, promoter sequence, transcript, and protein functional domains of human COX-1	63
Figure 23.	Gene structure, promoter sequence, transcript, and protein functional domains of human COX-2	64
Figure 24.	Important advancements of Biotechnology	66
Figure 25.	Processes of knowledge discovery via data mining	71
Figure 26	Scheme of the research	79
Figure 27	Identification AGPATs via data mining	101
Figure 28	Candidate AGPATs and their domain structure	102
Figure 29	Dendrogram of the murine AGPAT gene family members and the subgrouping classification	106
Figure 30	Alignment of predicted protein sequences of the murine AGPAT gene family members	107
Figure 31	Differential expression AGPATs in various murine tissues	109
Figure 32	Transcription coupled *in vitro* translation of AGPATs	111
Figure 33	Expression of AGPATs in COS-1 cells	112
Figure 34	TLC analysis of AGPAT activity in lysate of *in vitro* generated AGPAT gene products	114

Figure 35	TLC analysis of AGPAT activity in cells transfected with AGPAT candidate expression plasmids	115
Figure 36	Expression of TAZ mRNA in various murine tissues	119
Figure 37	Exon/Intron structure and PCR primer design	120
Figure 38	Detection of full-length and various splicing forms of TAZ mRNA in mouse tissues and human cells	121
Figure 39	Exon 5-deleted TAZ is evolutionarily conserved among different species	124
Figure 40	Alignment of human full-length TAZ with CD sequences of acyltransferases in glycerolipid biosynthesis	125
Figure 41	*In vitro* translation of mouse exon 5-deleted TAZ and human full-length TAZ	127
Figure 42	Putative tafazzins encoded by human and mouse mRNAs	128
Figure 43	TLC analysis of MLCL acyltransferase activity of in vitro and in vivo generated TAZ proteins	130
Figure 44	The effect of stimuli on AA release in U937 cells and macrophages	133
Figure 45	The effect of stimuli on PGE_2 production in U937 cells and macrophages	135
Figure 46	The effect of stimuli on $cPLA_2$ protein expression in U937 cells	138
Figure 47	The effect of stimuli on $cPLA_2$ protein expression in macrophages	139
Figure 48	The effect of stimuli on COX-1 protein expression in U937 cells	140
Figure 49	The effect of stimuli on COX-1 protein expression in macrophages	141

Figure 50	The effect of stimuli on COX-2 protein expression in macrophages	142
Figure 51	PMA-induced arachidonic acid release in U937 cells	144
Figure 52	PMA-induced PGE_2 release in U937 and H9c2 cells	146
Figure 53	Effects of PMA on $cPLA_2$, COX-1, and COX-2 in U937 and H9c2	150
Figure 54	Does response for the effects of PMA on enzyme protein synthesis of COX-1, and COX-2 in U937 and H9c2 cells	152
Figure 55	Changes in morphology and cell surface markers of U937 cells upon PMA induction	154
Figure 56	ER-α expression in U937 and PMA-differentiated U937 cells	156
Figure 57	Effects on PGE_2 production by different ligands of estrogen receptors	158
Figure 58	Effects on AA release by 17-β estradiol	160
Figure 59	17-β estradiol enhances PGE_2 production through up-regulation Of COX-1 and COX-2 enzymes	161
Figure 60	Attenuation of PGE_2 production and the up-regulation of COX-1/-2 and by pure ER antagonist ICI 182 780 but not partial antagonist 4-OH-TAM	163
Figure 61	Time course of morphological changes to U937 cells during RA treatment	165
Figure 62	The effect of all-*trans*-RA on PGE_2 production in U937 cells	169
Figure 63	The effect of 9-*cis*-RA on PGE_2 production in U937 cells	170

Figure 64	The effect of RA on COX-2 protein expression in U937 cells	172
Figure 65	The effect of all-*trans*-RA on COX-1 protein expression in U937 cells	173
Figure 66	The effect of 9-*cis*-RA on COX-1 protein expression in U937 cells	174
Figure 67	The effect of all-*trans*-RA on COX-1 mRNA expression measured by Northern blot analysis	176
Figure 68	The effect of 9-*cis*-RA on COX-1 mRNA expression measured by Northern blot analysis	177

LIST OF TABLES

		Page
Table 1.	Characteristics of major classes of nuclear receptors	25
Table 2.	Cloning and characterization of PAP-1 and PAP-2	38
Table 3.	Cloning and characterization of MGAT1, MGAT2, and MGAT3	40
Table 4.	Characteristics of the major groups of phospholipase A_2	53
Table 5.	Functions of prostanoids	60
Table 6.	Databases in National Center for Biotechnology Information	68
Table 7.	Selected analysis software tools	70
Table 8.	Description of BLAST services in NCBI	74
Table 9.	Selected published reports involving applications of Bioinfromatics in lipid research	76
Table 10.	PCR primer design	92
Table 11.	PCR conditions	93
Table 12.	Feature of constructed expression vectors	103
Table 13.	Amino acid alignment scores of murine AGPATs	105
Table 14.	The effect of PMA on PGE_2 release in U937 cells	147
Table 15.	The effect of all-*trans*-RA on cell surface CD11b expression in U937 cells	166

LIST OF ABBREVIATIONS

aa	amino acid
AA	arachidonic acid
AGPAT	1-acyl-*sn*-glycerol-3-phosphate acyltransferase
AP1	activation protein-1
ATCC	American type culture collection
ATP	adenosine triphosphate
BLAST	basic local alignment search tool
BSA	bovine serum albumin
CaLB	calcium binding
CD	conserved domain
CDD	CD database
cDNA	complementary deoxyribonucleic acid
COX	cyclooxygenase
CL	cardiolipin
$cPLA_2$	cytosolic phospholipase A_2
DG	1,2-diacyl-*sn*-glycerol
DGAT	1,2-diacyl-*sn*-glycerol acyltransferase
DMSO	dimethylsulfoxide
DNTP	deoxynucleotides
dpm	disintegrations per minute
EDTA	ethylene glycol-bis(β-aminoethyl ether)-*N,N,N',N'*-tetraacetic acid
EGTA	ethylenediaminetetraacetic acid
ER	estrogen receptor
ER-α	ER-alpha
ER-β	ER-beta
ERK	extracellular signal-regulated protein kinase
EST	expressed sequence tag
FACS	fluorescence-activated cell sorting

FXR	farnesoid X receptor
GPAT	*sn*-glycerol-3-phosphate acyltransferase
GPCR	G protein-coupled receptor
h	hour
HEPES	*N*-2-hydroxyethylpiperazine-N'-2-ethanesulfonic acid
IAP	inhibitor of apoptotic protein
IL-1	interleukine-1
IP_3	inositol triphosphate
kDa	killodalton
LPA	lysophosphatidic acid
LPAAT	LPA acyltransferase
LPS	lipopolysaccharide
LXR	liver X receptors
JNK	c-Jun N-terminal kinase
Km	Michaelis-Menten coefficient
MAb	monoclonal antibody
MAPK	mitogen-activated protein kinase
MAPKK	MAPK kinase
MAPKKK	MAPKK kinase
M-CSF	macrophage-colony stimulating factor
MG	monoacylglycerol
MGAT	MG acyltransferase
M-MLV	Moloney murine leukemia virus
M-MLV RT	M-MLV reverse transcriptase
MEK	MAPK/ERK kinase
mRNA	messenger ribonucleic acid
NCBI	National Center for Biotechnology Information
ORF	open reading frame
PA	phosphatidic acid
PCR	polymerase chain reaction
PG	prostaglandin

PIP_2	phosphatidylinositol biphosphate
PKA	protein kinase A
PKC	protein kinase C
PLA_2	phospholipase A_2
PMA	phorbol 12-myristate 13-acetate
PPAR	peroxisome proliferator-activated receptors
PVDF	polyvinylidene difluoride
RA	retinoic acid
RAR	RA receptor
RXR	retinoid X-activated receptor
RNAsin	Ribonuclease inhibitor
SAPK	stress-activated protein kinase
S.D.	standard deviation
SDS	sodium dodecylsulfate
SDS-PAGE	SDS-polyacrylamide gel electrophoresis
SERM	selective estrogen receptor modulator
$sPLA_2$	secretory phospholipase A_2
SRE	serum response element
TG	1,2,3-triacyl-*sn*-glycerol
TNF-α	tumor necrosis factor alpha
Tris	tris (hydroxymethyl) aminomethane
Tx	thromboxane
UTR	untranslated region
WST-1	4-[3-(4-iodophenyl)-2-(4-nitrophenyl)-2H-5-tetrazolio]-1,3-benzene disulfonate

ABSTRACT

The biological membrane is essential to the life and function of the cell. Phospholipids form building blocks of the biological membrane and the hydrolysis of phospholipids provides a source of lipid signaling molecules that are involved in many biological processes and human diseases. In this study, the identification of novel acyltransferases in phospholipid biosynthesis and the control of arachidonate-eicosanoid cascade were investigated.

1-acyl-*sn*-glycerol-3-phosphate acyltransferase (AGPAT) catalyzes the acylation of 1-acyl-*sn*-glycerol-3-phosphate to yield phosphatidic acid in the major phospholipid biosynthesis pathway. Using conserved domain sequences and BLAST algorithms; several acyltransferases were identified from murine and human EST databases. Molecular cloning and sequence analysis revealed that these enzymes were convergence in sequence similarities and domain structures. The initial enzyme characterization demonstrated that proteins encoded by these genes had AGPAT activities.

Barth syndrome is an X-linked inherited disorder characterized by cardioskeletal myopathy with neutropenia and abnormal mitochondria abnormalities. The causative gene was mapped to Xq28.12 and was termed TAZ that was thought to belong to a family of acyltransferase in glycerolipid biosynthesis. In this study, a comparative genomic approach was employed to examine the complex express pattern of TAZ in both human and murine tissues. Multiple alternative splice variants were identified in both species. However, the full-length TAZ expressed in human tissues was not found in other species. Rather, exon 5-deleted TAZ was the most abundant expressed and evolutionarily

conserved form in all species analyzed. The present study indicates that exon 5-deleted TAZ is the evolutionarily conserved form and thus the potential functional form.

Arachidonaic acid is an essential fatty acid and an important precursor for the biosynthesis of bioactive lipid mediator eicosanoids. The control of arachidonate-eicosanoid cascade in monocytes and myocytes was assessed by activating differential signaling pathways. The data showed that PMA, M-CSF, TNF-α, LPS, estrogens, and retinoid acids exerted differential regulation effect on $cPLA_2$ and/or COX-1/-2 enzymes. Both transcriptional activation and posttranslational modulation/modification of these enzymes were contributed to the control of arachidonic acid release and subsequent prostaglandin production. These studies clearly demonstrated that arachidonate-eicosanoid cascade was controlled by multiple interconnected pathways at multiple stages via different mechanism.

INTRODUCTION AND LITERATURE REVIEW

I. BIOLOGICAL MEMBRANE

1.1 Structure of Biological Membrane

Cell membranes are essential to the function of the cell. Biological membrane provides a semi-permeable barrier and a matrix for membrane proteins. The plasma membrane encloses the cells and provides a selective barrier to regulate the transport of compounds such as salts, nutrients, and signaling molecules. Inside the cell the membrane delineates organelles in eucaryotic cells to maintain microenvironments for their proper function. There are six major types of organelles present in most eucaryotic cells: endoplasmic reticulum, Golgi apparatus, mitochondria, lysosomes, peroxisomes and the nucleus. Each organelle has specialized functions that are carried out by the unique enzymes within the organelle.

The membrane is composed predominantly of lipids and proteins but may contain carbohydrates. Figure 1 illustrates the topography of lipids, proteins, and carbohydrates in the "fluid mosaic model" of a typical eukaryotic plasma membrane (Singer and Nicolson 1972). The bilayer structure is attributed to the amphipathic property of lipid molecules, which causes them to assemble into a bilayer. Under physiological conditions, membrane lipid is in the liquid crystalline state. The fluidity of plasma membrane is dependent on the nature of the acyl-chain region comprising the hydrophobic domain of the membrane. In the plasma membrane, fluidity is also dependent on the cholesterol content of the membrane. The movement of lipid or membrane protein along the plane is generally unrestricted. Alternatively, the movement of lipid or membrane protein in the

transverse plane of the bilayer is thermodynamically unfavorable and thus would not occur spontaneously (Singer and Nicolson 1972; Cullis et al. 1996; Dowhan and Bogdanov 2002). Membrane carbohydrate is localized exclusively on the extracellular side of the plasma membrane either in the form of glycolipid or glycoprotein.

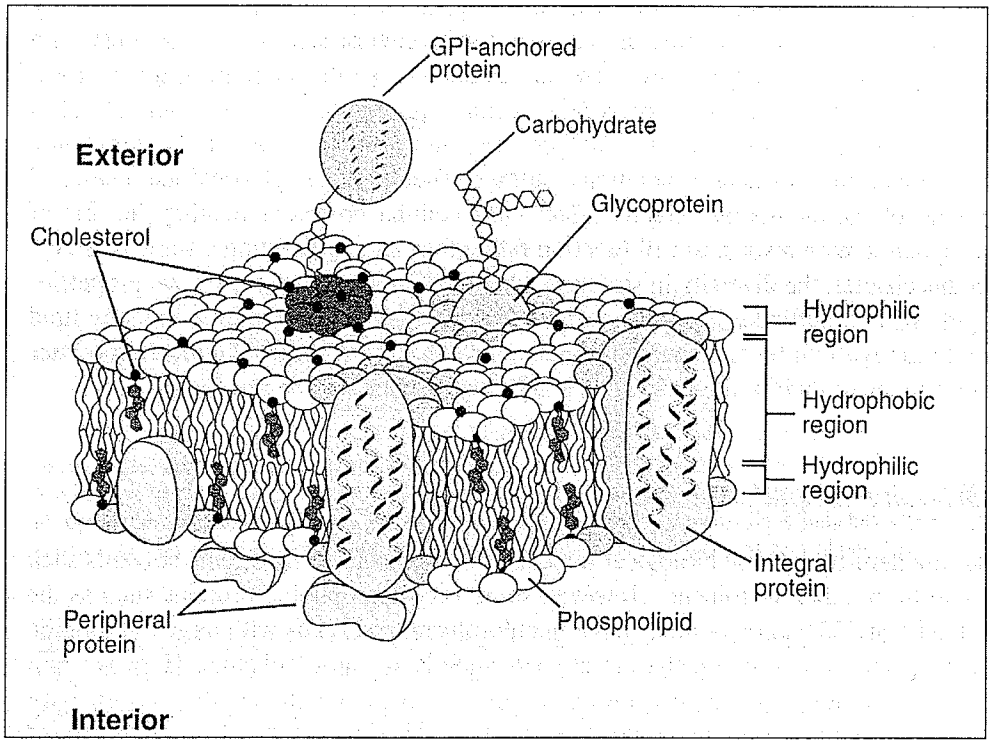

Figure 1. The fluid mosaic model of eukaryotic plasma membrane. (Adapted from Dowhan and Bogdonov, 2002)

Inner and outer leaflets of membrane phospholipid bilayers are depicted. Carbohydrate moieties on lipids and proteins face the extracellular space.

1.2 Membrane Lipids

Lipid molecules constitute about 50% of the mass of a typical mammalian cell membrane, nearly all of the remainder being protein. Major classes of lipids found in eukaryotic membranes include glycerol-based phospholipids (phosphoglycerides) and sphingosine-based lipids (sphingolipids). The most abundant lipids are the phospholipids. Sphingosine based lipids are important constituents, and cholesterol functions as a key modulator of membrane fluidity (Ansell and Spanner 1982; Bloch 1991; Dowhan and Bogdanov 2002).

1.2.1 Phospholipids (phosphoglycerides)

All phospholipid molecules in cell membranes are amphipathic. The general structure of a phospholipid is shown in Figure 2. The phospholipid molecule is composed of a polar head group and two long hydrophobic hydrocarbon tails. The head group is linked to the glycerol moiety at the *sn*-3 position via a phosphate moiety, which in turn is linked to the hydroxyl moiety of choline, ethanolamine, serine, inositol, glycerol or phosphatidylglycerol. Two hydrocarbon tails composed of acyl chains are varied in chain lengths (C14 to C24). The tail at the *sn*-1 position is usually saturated while the other at the *sn*-2 position has one or more *cis*-double bonds. These double bonds are rigid and create kinks in the chain (Figure 2). The rest of the chain is free to rotate about the other C-C bond. Phosphatidylcholine and phosphatidylethanolamine are the two most abundant phosphoglycerides in mammalian tissues (White 1973; Ansell and Spanner 1982). Structures of five major types of phospholipid in mammalian tissues are depicted in Figure 3.

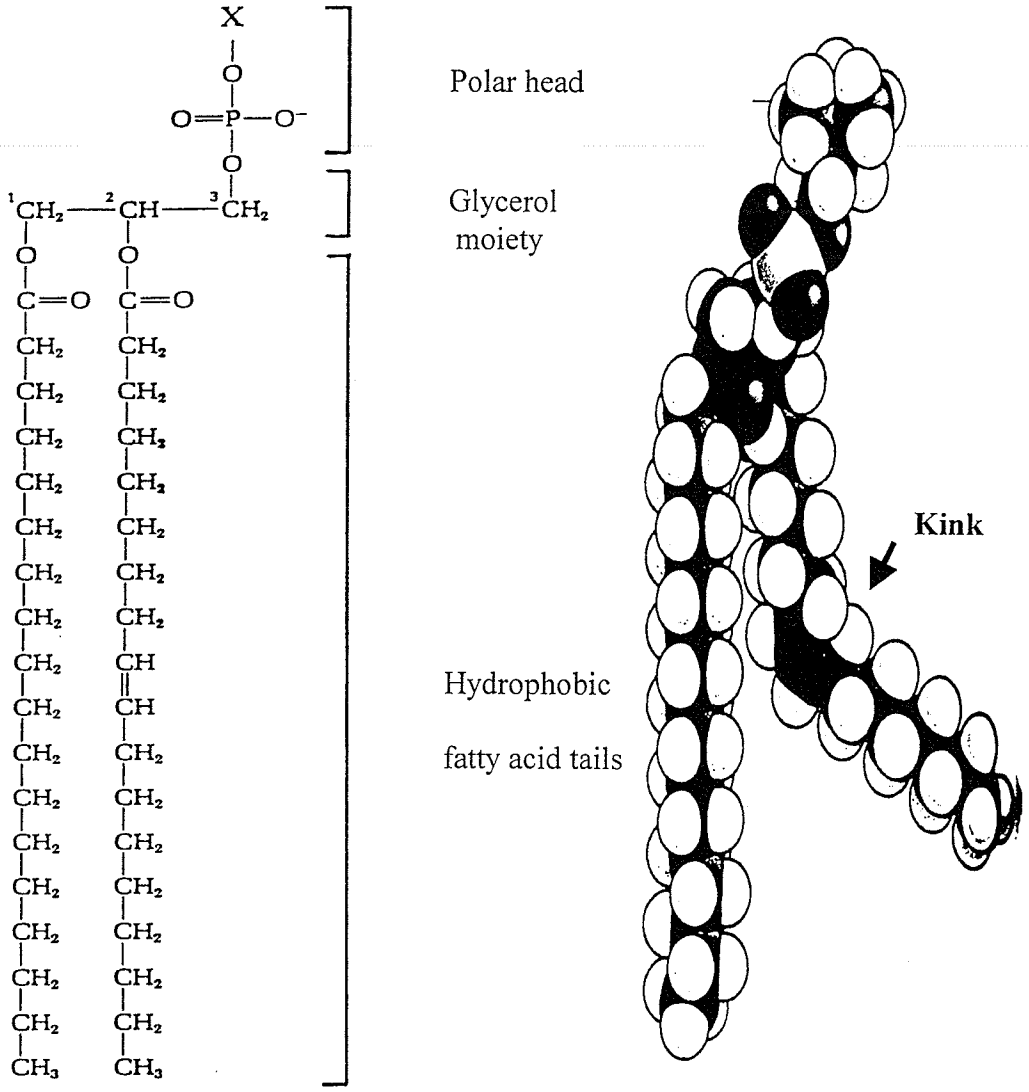

Figure 2. General structure of a phospholipid molecule.

X is the small head group alcohol moiety, usually choline, ethanolamine, serine or inositol. Arrow shows a kink that is created by a double bond in the fatty acid chain.

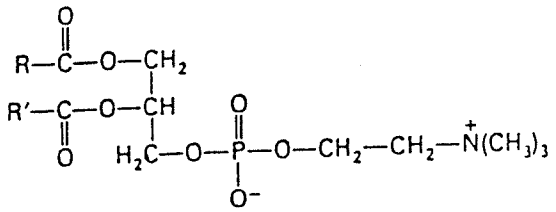

Phosphatidyl choline

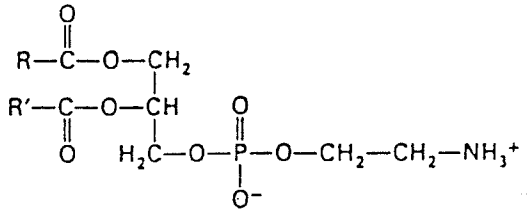

Phosphatidyl ethanolamine

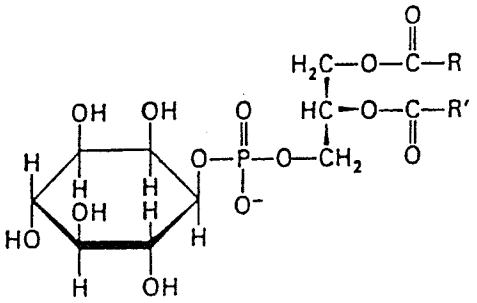

Phosphatidyl inositol

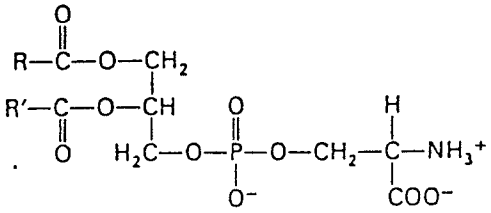

Phosphatidyl serine

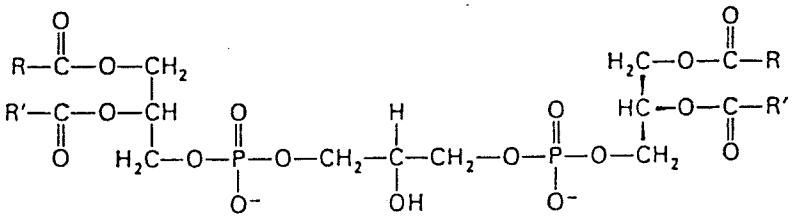

Diphosphatidyl glycerol
(Cardiolipin)

Figure 3. Five major types of phospholipids found in mammalian tissues.

R and R' are acyl groups.

1.2.2 Sphingolipids

Sphingosine-based lipids, including sphingomyelin and glycosphingolipids, also constitute a major fraction of biological membrane (Merrill and Sandhoff 2002). Sphingomyelin is predominantly found in the plasma membrane of mammalian cells. Phosphocholine is linked to the terminal hydroxyl group of ceramide to form sphingomyelin (Figure 4). Ceramide is a N-acylated derivative of sphingosine and structurally similar to the glycerol backbone of phospholipid molecule. A glycosphingolipid molecule consists of a carbohydrate moiety linked to the terminal hydroxyl group of the ceramide. In cerebroside, the terminal hydroxyl group of ceramide is linked to a single glucosyl or galactosyl residue (Figure 4). More complex glycolipid such as ganglioside contains oligosaccharide chains with one or more N-acetylneuraminic acid residues (Figure 4). It is worth noting that glycolipids including carbohydrate-containing glycerol-based lipids play major roles in cell-surface-associated antigens and recognition factors in eukaryotes (Merrill and Sandhoff 2002).

1.2.3 Cholesterol

The precise fluidity of plasma membrane is biologically important and the fluidity of a lipid bilayer is dependent on its composition. Bacterial plasma membranes are often composed of one main type of phospholipid and contain no cholesterol (Dowhan and Bogdanov 2002). In contrast, mammalian plasma membrane contains large amounts of cholesterol and sometimes up to one molecule for every phospholipid molecule. A small amount of cholesterol can be found in the mitochondria, endoplasmic reticulum, and Golgi

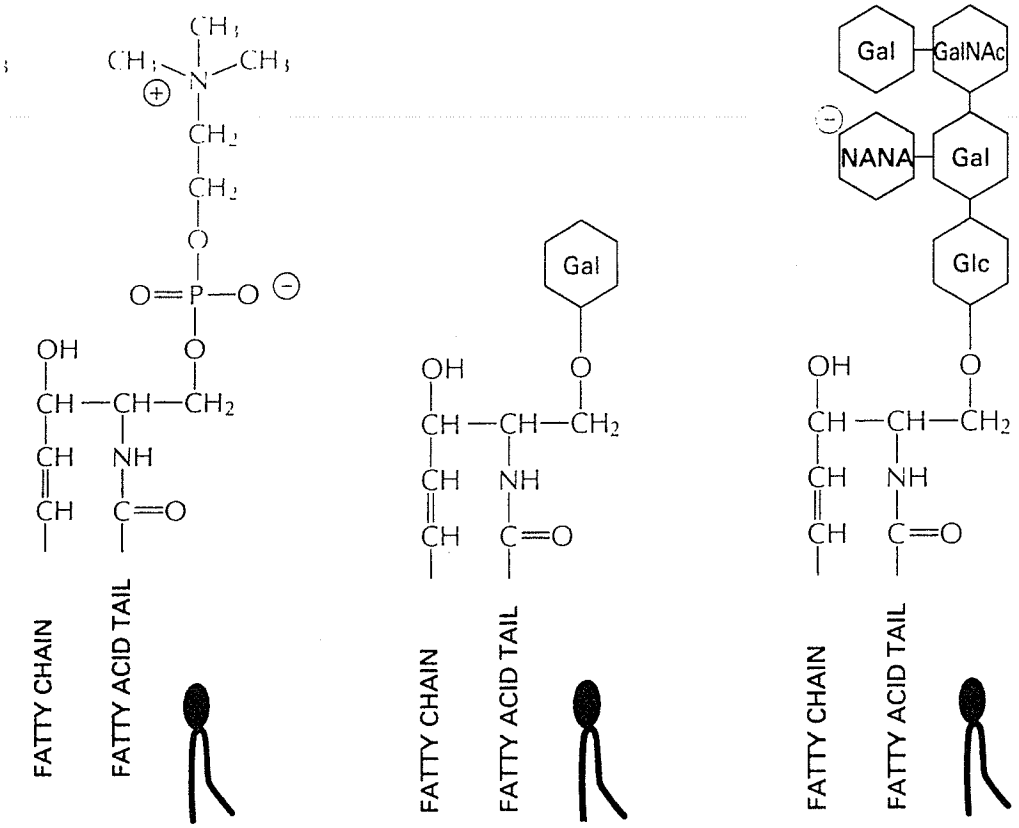

Sphingomyelin **Galactocerebroside** **G_{M1} ganglioside**

Figure 4. Structures of sphingolipids found in mammalian tissues.

Galactocerebroside is a neutral glycolipid and ganglioside contains one or more negatively charged sialic acid residues. Three uncharged sugars are Gal = galactose; Glc = glucose; GalNac = N-acetylgalactoseamine.

membranes. Cholesterol functions to modulate membrane fluidity (Bloch 1991; Dowhan and Bogdanov 2002). The cholesterol molecule orients itself in the bilayer with its hydroxyl group close to the polar head groups of phospholipid molecules, its rigid steroid rings interact with the first few CH_2 groups of the hydrocarbon chains of the phospholipid molecules, and thereby lowering membrane fluidity (Figure 5). Cholesterol is also biologically important as a metabolic precursor of bile acids and steroid hormones.

1.2.4 Asymmetry of Lipid Bilayers

Lipid compositions of two leaflets of the lipid bilayer are strikingly different (Cullis et al. 1996; Voelker 2002). Figure 6 summarizes the phospholipid asymmetry in various mammalian plasma membranes. A common feature is that amino-containing phospholipids are mainly limited to the cytosolic side of plasma membranes, whereas almost all the lipid molecules that have choline in their head groups are in the outer half leaflet. The lipid asymmetry can be biologically significant. For example, the phosphatidylserine is largely located on the cytoplasmic face. When extracellular signals activate protein kinase C (PKC), the kinase attaches to the cytoplasmic face of the plasma membrane, and the negatively charged phosphatidylserine provides a milieu for the kinase to act (McPhail 2002). Similarly, the phosphatidylinositol 4, 5-bisphosphate is also largely located on the cytoplasmic half of plasma membrane. Upon stimulation, this phospholipid molecule is cleaved into inositol trisphosphate and diacylglycerol, both molecules play crucial parts in intracellular signaling (Marks and Gschwendt 1996; McPhail 2002).

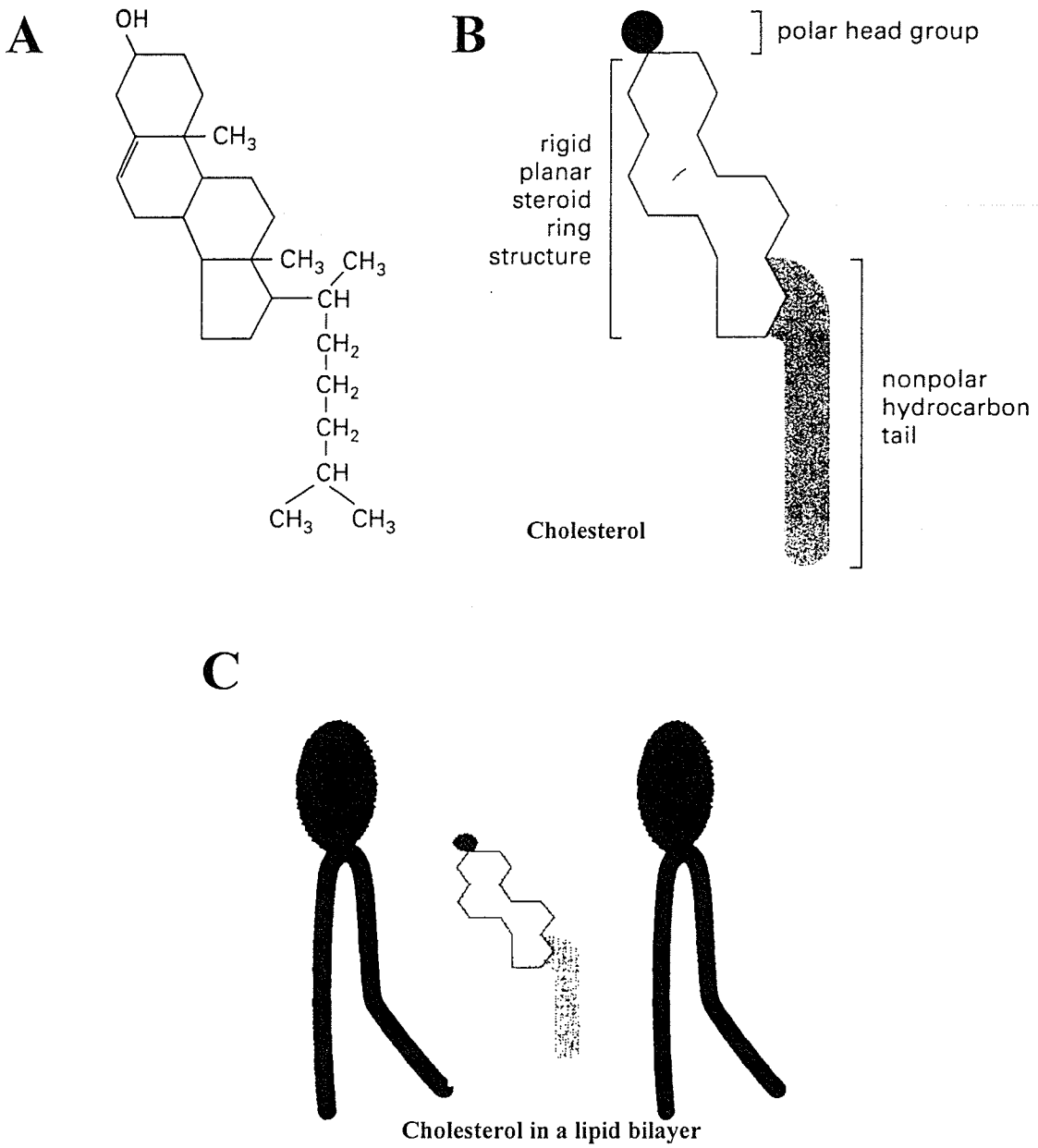

Figure 5. The structure of cholesterol and cholesterol in a lipid bilayer. (Modified from Alberts et al. 1994)

(A): cholesterol is represented by a formula; (B): a corresponding schematic drawing of a cholesterol molecule; (C) a cholesterol molecule interacting with two phospholipid molecules in one leaflet of a lipid bilayer.

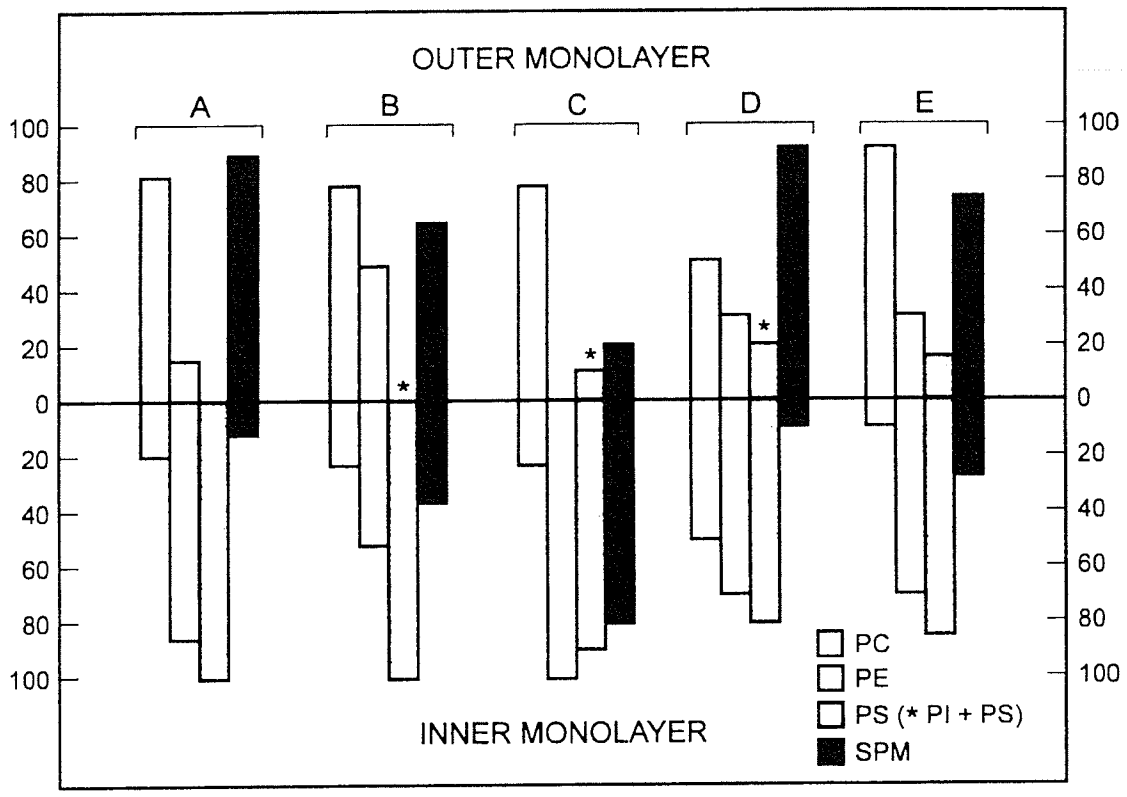

Figure 6. Phospholipid asymmetry in mammalian plasma membranes.
(Adapted from Cullis et al. 1996)

(A) human erythrocyte membrane; (B) rat liver blood sinusoidal plasma membrane; (C) rat liver splasma membrane; (D) pig platelet plasma membrane; (E) VSV envelope derived from hamster kidney BHK-21 cells.

1.3 Membrane Proteins

The basic structure of the biological membrane is provided by the lipid bilayer, most specific functions, however, are carried out by membrane proteins. According to their association with the lipid bilayer, membrane proteins are classified into two categories: extrinsic membrane proteins and integral membrane proteins. The peripheral or extrinsic membrane proteins that do not extend into the hydrophobic interior of the lipid bilayer bound to one or the other face of the membrane by non-covalent interactions with other membrane proteins or lipids. The integral membrane proteins are held by interaction with the hydrophobic core of the lipid bilayer. In most transmembrane proteins the polypeptide chain crossing the lipid bilayer is in an α-helical conformation. Six ways in which membrane proteins associate with the lipid bilayer have been identified and are depicted in Figure 7. The lipid microenvironment surrounding membrane proteins can influence protein function (Yeagle 1989). Most enzymes involved in phospholipid metabolism are either integral membrane proteins or peripheral/extrinsic membrane proteins (Vance 2002).

1.4 Membrane Sugars

The cell surface is coated with sugar residues. These carbohydrates exist as either oligosaccharide or polysaccharide chains covalently bound to membrane proteins and/or lipids. Carbohydrate moieties of glycolipids and glycoproteins are located exclusively on the extracellular side of plasma membranes (Paulson 1989; Paulson and Colley 1989; Rudd et al. 2001). Oligosaccharide side chains of glycoproteins and glycolipids usually contain fewer than 15 sugar residues. Some plasma membranes contain integral

proteoglycan molecules with surface-exposed polysaccharide chains. The role of this sugar coating is multifaceted: (1) to protect the cell from mechanical and chemical damage; (2) to mediate specific cell-cell adhesion events; and (3) to be involved in specific cell-recognition process (Paulson 1989; Paulson and Colley 1989; Nathan and Sporn 1991; Alberts et al. 1994; Lodish et al. 2000; Rudd et al. 2001).

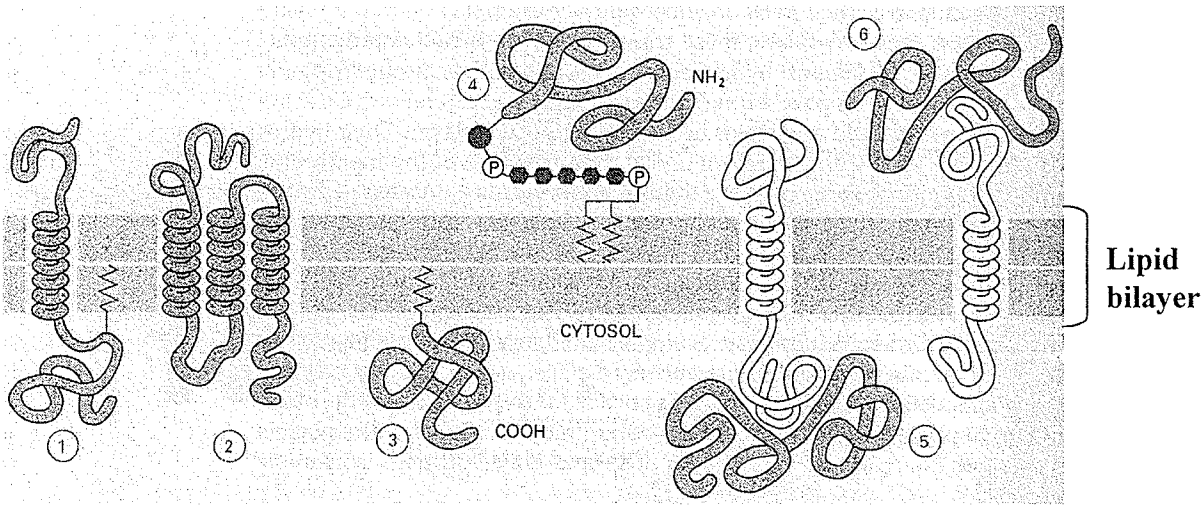

Figure 7. Six ways in which membrane proteins associate with the lipid bilayer. (Adapted from Alberts et al. 1994)

(1) single transmembrane α-helix; (2) multiple transmembrane α-helices; (3) covalently attached to a lipid molecule; (4) covalently attached to phospholipid via an oligosaccharide; (5) and (6) noncovalent interactions with other membrane proteins.

II. CELL SIGNALING

2.1 Three Forms of Cell Signaling

Cell signaling is the mechanism that enables one cell to influence the behavior of others in multicellular organisms. In the mammalian system, secreted molecules mediate three basic forms of signaling: (1) endocrine, (2) paracrine/autocrine, and (3) synaptic. Endocrine cells secrete their signaling molecules, called hormones, into the bloodstream, which signal to target cells distributed widely throughout the body. Local mediators, affecting cells in the immediate environment of signaling cells, transmit paracrine/autocrine signals. Other specialized signaling cells are neurons, which send signals among themselves or to their target cells by molecules termed as neurotransmitters.

Extracellular signaling molecules are recognized by specific receptors on or in target cells. Receptors specifically bind the signaling molecules and then initiate a response in the target cell. Many of the extracellular signaling molecules act through membrane receptors or they may diffuse into cells and bind to nuclear receptors. The following sections discuss the importance of signaling pathways that are relevant to this study.

2.2 Mitogen-activated Protein Kinases (MAPKs) Signaling

MAPKs are members from a widely conserved family of serine/threonine kinases that involve in many cellular processes such as cell proliferation, cell differentiation, inflammation, and cell death (Yeagle 1989; Lewis et al. 1998; Cobb 1999; Garrington

and Johnson 1999; Schaeffer and Weber 1999; Weston and Davis 2002; Weston et al. 2002). There exist at least three parallel MAPK pathways, and each can be considered as a three-tiered kinase (Cobb and Goldsmith 1995; Cobb 1999). MAPKs are phosphorylated and activated by MAPK-kinases (MAPKKs), which in turn are phosphorylated and activated by MAPKK-kinases (MAPKKKs) as illustrated in Figure 8. The MAPKKKs are activated by external stimuli that are mediated by cell surface receptors and other protein kinases and/or GTPases. Kinases in each pathway have been given specific names. The first two closely related MAPKs identified are termed as p44 and p42 MAPKs, or extracellular signal-regulated protein kinases 1 and 2 (ERK1 and ERK2), respectively (Cobb and Goldsmith 1995; Cobb 1999). The MAPKKs that phosphorylate and activate the ERKs are then termed as MAPK/ERK kinases 1 and 2 (MEK1 and MEK2), and the corresponding MAPKKK is termed as MEK kinase (MEKK). MEKKs include A-Raf, B-Raf, C-Raf, Mos, and Tpl2. Signaling through ERK pathway mediates cell growth or differentiation. The other two parallel MAPK pathways are referred to as the c-Jun N-terminal kinase/stress-activated protein kinase (JNK/SAPK) pathway and p38 MAPK pathway (Weston and Davis 2002). Signaling through p38 MAPK mediates inflammatory and stress responses to stimuli such as cytokines and TNF-α. The JNK/SAPK pathway transduces a variety of signals including growth, differentiation, death, inflammation, and stresses such as ultraviolet radiation, osmotic shock, oxidation, and DNA damage (Figure 8).

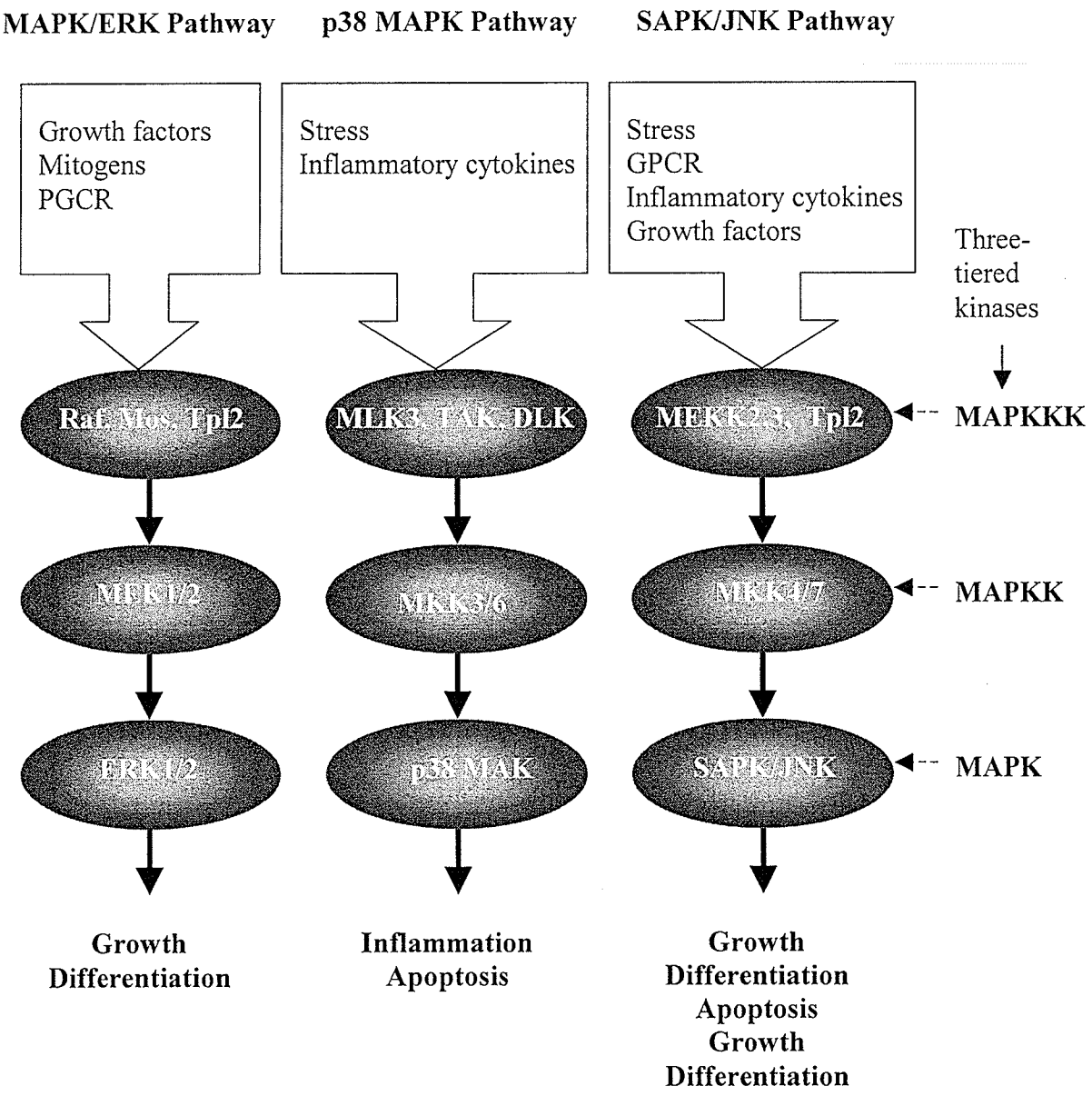

Figure 8. Three parallel MAPK pathways in mammalian cells.

Abbreviation: MLK, mixed lineage kinase

Many receptors of growth factors belong to the family of receptor tyrosine kinases. These include receptors for platelet-derived growth factor (PDGF), fibroblast growth factors (FGF), hepatocyte growth factor (HGF), insulin, insulin-like growth factor-1 (IGF-1), nerve growth factor (NGF), vascular endothelial growth factor (VEGF), and macrophage colony stimulating factor (M-CSF) (Menard et al. 2003; Ria et al. 2003; Yeung and Richard Stanley 2003). M-CSF activates mitogen-activated protein kinase pathways via specifically binding to its receptors (Figure 9). Once bound, the receptor becomes phosphorylated on tyrosines and is thereby activated. The autophosphorylation is thought to serve as a switch to trigger the transient assembly of an intracellular signaling complex to relay the signal into the nucleus. The p44/42 MAP kinase pathway that consists of a protein kinase cascade linking growth and differentiation signals with transcription in the nucleus has been analyzed in great detail (Figure 9).

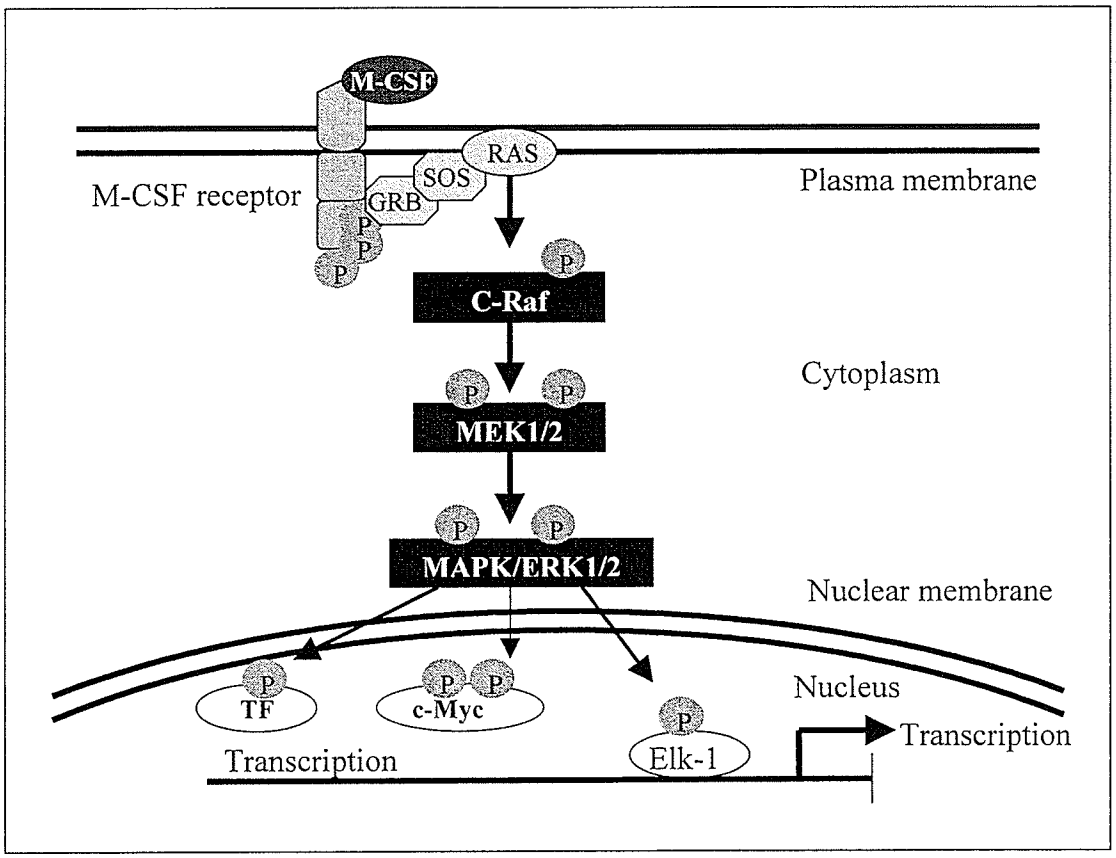

Figure 9. M-CSF action and signaling via the MAPK/ERK pathway.

2.3 Protein Kinase C (PKC) Signaling

Phosphatidylinositol bisphosphate (PIP_2) hydrolysis produces inositol trisphosphate (IP_3) and diacylglycerol. Diacylglycerol has two signaling roles (Marks and Gschwendt 1996; McPhail 2002). First, it can be further cleaved to release arachidonic acid, which may act as a messenger in its own right or be used to synthesize eicosanoids (see Section on Arachidonate-eicosanoid Cascade). Second, diacylglycerol can activate a crucial serine/threonine protein kinase called protein kinase C (PKC), which in turn phosphorylates selected proteins in the target cell.

There are two intracellular pathways by which PKC activates the transcription of specific genes in the target cell (Figure 10). In one case, PKC activates a phosphorylation cascade by cross-talking to MAP-kinase, which in turn activates the transcription factor Elk-1 (Marks and Gschwendt 1996; McPhail 2002). Elk-1 is bound to a serum response element (SRE) within the promoter region of targeted gene. In the other pathway, PKC phosphorylates Iκ-B, which causes the release of NF-κB so that NF-κB translocates into the nucleus and activates the transcription of targeted genes.

The effect of diacylglycerol can be mimicked by a phorbol ester, which binds to PKC and activates it directly. For example, a number of cell types can be stimulated to proliferate or differentiate in culture when treated with phorbol esters (Yang et al. 2002; Niles 2003; Paik et al. 2003; Paydas et al. 2003).

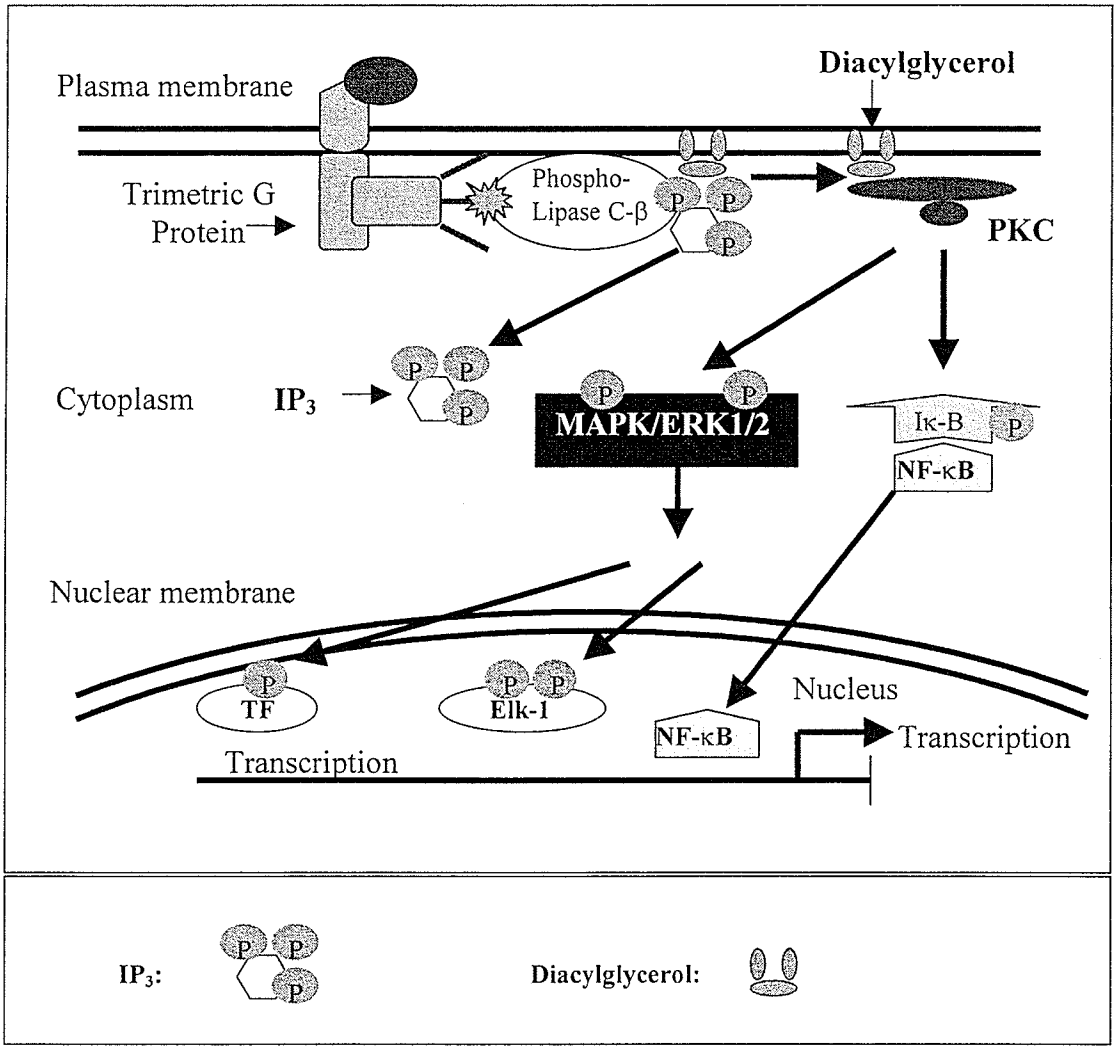

Figure 10. Diacylglycerol action and PKC signaling pathway.

2.4 Inflammatory Signaling

Inflammatory cytokines such as interleukin-1 (IL-1), tumor necrosis factor (TNF-α), and lipopolysaccharide (LPS) appear to activate SAPK/JNK pathway via the Rho family (Rac, Rho, cdc42) of small GTP binding proteins (Agrawal et al. 2003; Welch et al. 2003). LPS from Gram-negative bacteria can elicit the excessive release of proinflammatory cytokines from immune cells, which contribute to many of the pathological processes of bacterial infection (Raetz 1990; Gupta et al. 1995). Tool-like receptors (TLRs) function as pattern-recognition receptors for these bacterial ligands (Lien et al. 1999; Murakami et al. 2002). TLRs possess an intracellular domain homologous to that of interleukin-1 receptor and participate in NF-κB signaling cascades elicited by LPS (Figure 10 and Figure 11). Activated MEKK1/4 and a member of mixed lineage kinase (MLK) phosphorylate SEK1 or called MKK3/6, the p38 MAP kinase upstream kinase. Alternatively, MKK3/6 can also be directly phosphorylated by ASKs, which are regulated by apoptotic stimuli. MKKs in turn activate SAPK also known as JNK. After phosphorylation and activation, SAPK/JNK becomes dimerized and translocates to the nucleus where it regulates transcription through its effects on c-Jun, ATF-2 and other transcription factors (Figure 11).

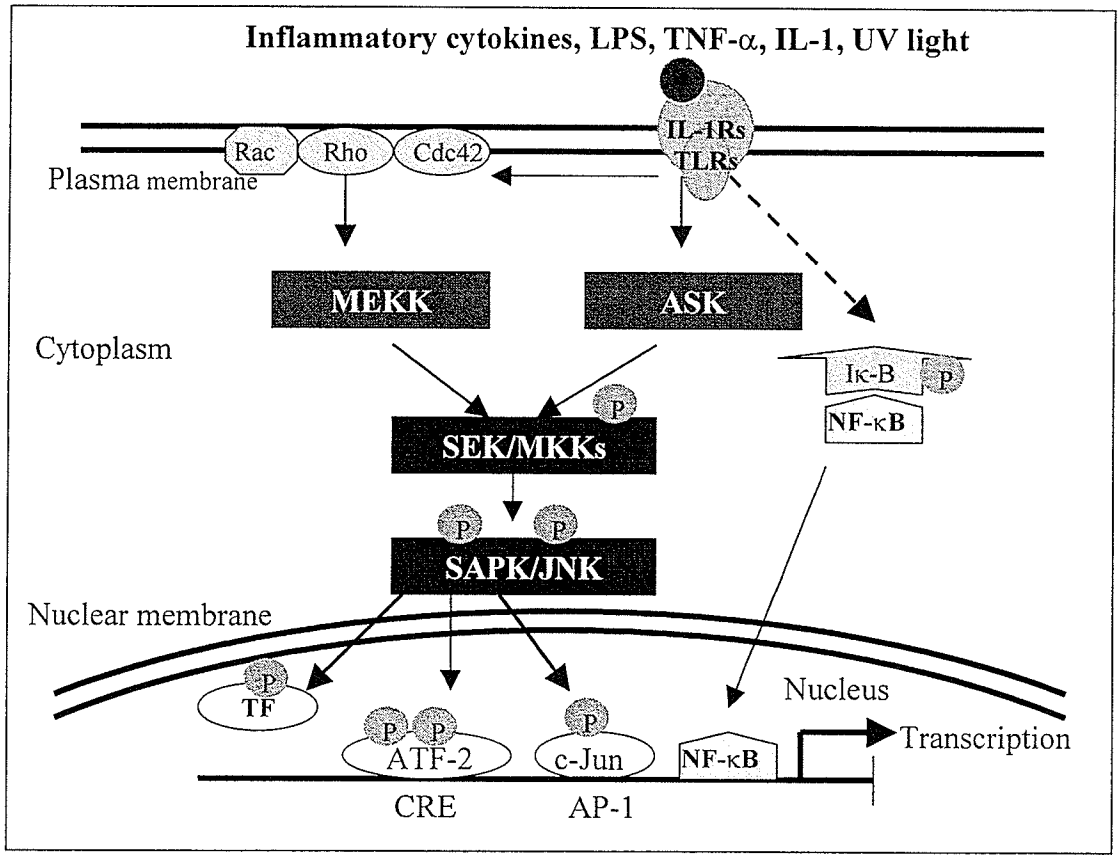

Figure 11. LPS and TNF-α action and signaling via the SAPK/JNK pathway.

2.5 Apoptotic Signaling

Apoptosis, or programmed cell death, is a regulated process leading to cell death. Active signaling from death receptors such as CD95/Fas, DNA damage, or mitochondrial malfunction induces cascades of cysteine aspartate-specific proteases (caspases). Initiator caspases, caspase-8, -9, and –12 are closely coupled to proapoptotic signals (Chen and Wang 2002). Once activated, these caspases cleave and activate downstream effector caspases, caspase-3, -6, and -12, which in turn cleave essential cellular components and degrade the genomic DNA (Figure 12). Cytochrome c release from mitochondria is also coupled to the activation of initiator caspase -9 (Baker and Reddy 1998). Death stimuli include the FasL, TNF-α, DNA damage, and ER stress. TNF-α, when bound to its receptor (TNFR-1) activates caspase -8 and -10 (Budihardjo et al. 1999). TNFR-2 may stimulate an anti-apoptotic pathway by inducing inhibitors of apoptosis protein (IAP), which directly inhibits caspases -3, -7, and- 9 (Deveraux et al. 1998; Li et al. 1998; Du et al. 2000).

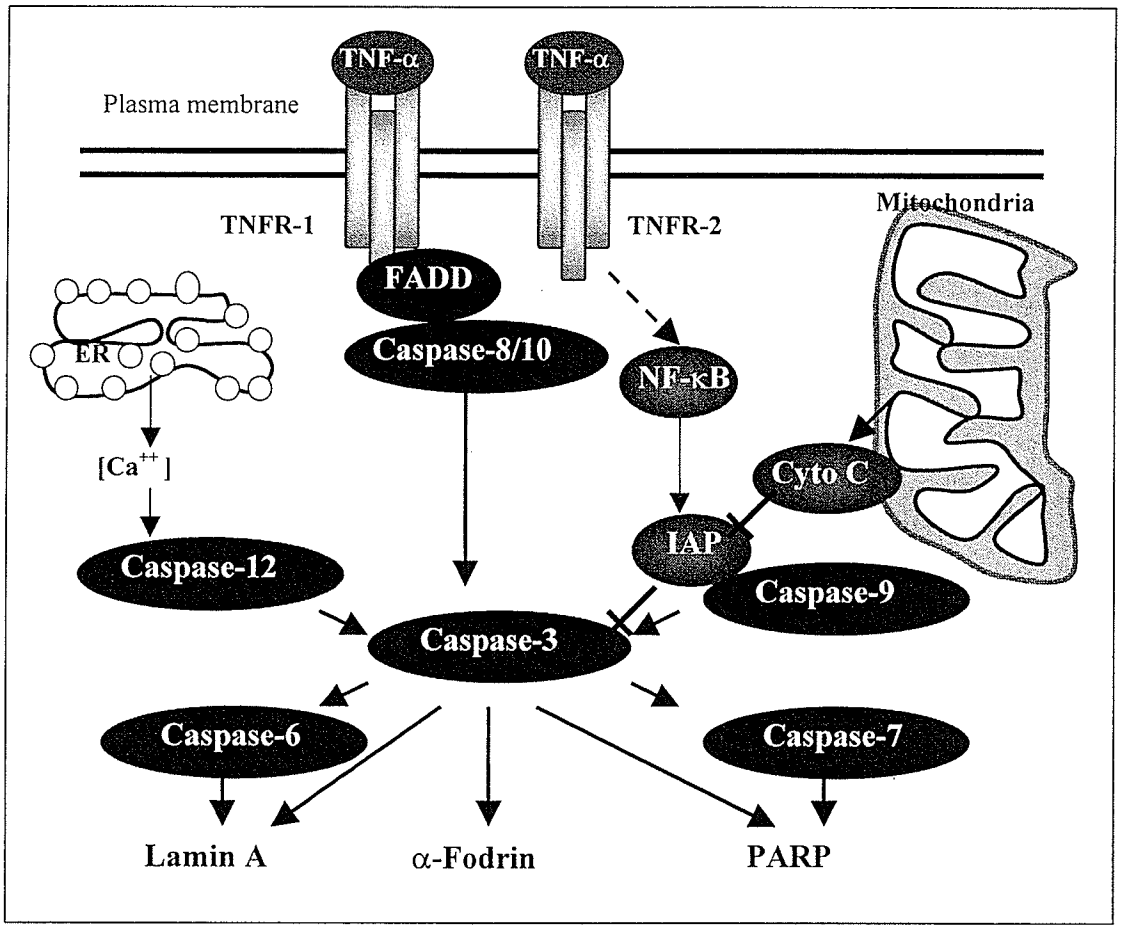

Figure 12. TNF-α action and apoptotic signaling pathway.

Cyto C: cytochrome C. Initiator caspases includes -8, -9, and -10 are closely coupled to proapototic signals. Once these caspases are activated, they in turn cleave and activate downstream effector caspases, which include caspases -3, -6, and -7.

2.6 Nuclear Receptor Signaling

2.6.1 Classification of Nuclear Receptors

Nuclear receptors function as ligand-activated transcription factors that regulate the expression of target genes to exert effects on a diversity of processes such as reproduction, development, and metabolism. More than 150 members have been identified and they can be divided into four subclasses according to their DNA binding mode and ligand binding affinity (Table 1) (Forman and Evans 1995; Mangelsdorf et al. 1995). Class I receptors include the steroid hormone receptors which function as ligand-induced homodimers and bind to their cognate DNA half-sites organized as inverted repeats or palindrome structure. Their ligands are usually hormonal lipids and have high-affinity to their receptors. Class I receptors include estrogen receptor alpha and beta (ER-α, ER-β), progesterone receptor (PR), androgen receptor (AR), glucocorticoid receptor (GR), and mineralcorticoid receptor (MR) (Evans 1988). Class II receptors function as heterodimers (usually dimerized with the retinoid X-activated receptor (RXR)) and bind to direct DNA repeats, hence RXRs typically do not function alone but rather serve as master regulators of several regulatory pathways (Forman et al. 1995a; Forman et al. 1995b; Mangelsdorf and Evans 1995). Class III receptors bind primarily to direct repeats as homodimers such as RAR and COUP (Kurokawa et al. 1994). Finally, Class IV receptors are orphan receptors that typically bind to their responsive elements as monomers.

Unlike water-soluble peptide hormones and growth factors, which bind to cell surface receptors and activate a cascade of second messengers, ligands of nuclear receptors can enter the cell by simple diffusion and relay their signals to the genome via

intracellular receptors (Forman et al. 1995c). After binding to its receptor, the ligand induces conformational change of the receptor so that it can dissociate from its associated heat shock protein and then bind directly to the high affinity DNA sequence in the promoter region of the regulated gene.

Table 1. Characteristics of major classes of nuclear receptors.

Class	Members	Ligands	DNA Binding Sequences & Binding Mode
Class I	Glucocorticoid receptor Mineralcorticoid receptor Progesterone receptor Estrogen receptor Androgen receptor	High-affinity, Hormonal lipids	Homodimers, Inverted repeats
Class II	Thyroid hormone receptor (TR) Retinoid X receptor (RXR) 1,25-$(OH)_2$-VD3 receptor (VDR) PPAR Liver X receptors (LXR) Farnesoid X receptor (FXR)	High affinity (TR, VDR) Low-affinity dietary lipids (PPAR, LXR, FXR)	Heterodimers, Direct repeats
Class III	Retinoid acid receptor (RAR)	Low-affinity dietary lipids	Homodimers Direct repeats
Class IV	Orphan receptors	Not known	Monomer

2.6.2 Estrogen Receptor Actions

Estrogen receptors are activated by estradiol, and phytoestrogens. Several synthetic substances, including 4-hydrotamoxifen (4-OH-TAM), ICI146 187, ICI182 780 and Reloxifens also bind to and either activate or inhibit ER with a high degree of specificity (Couse and Korach 1999a; Mcewen and Alves 1999). 4-OH-TAM is a partial agonist and antagonist of ER, whereas ICI 186164 is a full antagonist of ER. These synthetic agents are collectively termed as selected estrogen receptor modulators (SERMs)(Brazozowski et al. 1997).

The classical estrogen receptor, also called estrogen receptor alpha (ER-α), has been identified and studied for more than 30 years. The gene encoding human ER-α was cloned from a human breast cancer cell line MCF-7 (Walter et al. 1985; Green et al. 1986). At present, two types ERs (ER-α and ER-β) have been identified in vertebrates (Katzenellenbogen and Korach 1997; Giguere et al. 1998). They are encoded from separate genes, which have distinct tissue distribution and carry out different functions (Leygue et al. 1998; Lu et al. 1998; Lu et al. 1999; Lu et al. 2000; Peng et al. 2003). The mammalian ER-α is predominantly expressed in the female sex organs. This receptor is also present in endothelial and smooth muscle cells, heart, monocytes and monocyte-derived macrophages (Cutolo et al. 1993; Cutolo et al. 1996; Cutolo et al. 2001; Chambliss and Shaul 2002; Cid et al. 2002; Guo et al. 2002; Karas 2002; Rubanyi et al. 2002). The activation of ER-α produces pleiotropic effects such as the differentiation, proliferation, and maturation of female sex organs (Couse and Korach 1999a). The overexpression and altered activity of ER-α are involved in tumorigenesis and tumor progression of human breast cancers (Johnston et al. 1999).

The amino acid sequence inferred from the cDNA encodes a 67 kDa protein for ER-α, and 62 kDa protein for ER-β. Each receptor type has a wild type and various splice variants (Lu et al. 2000; Peng et al. 2003). The proposed 6 regions of the receptor consist of four functional domains (Figure 13). The conserved DNA binding domain is in the middle of the receptor and binds to a palindrome estrogen receptor response element (ERE) with zinc-figure motifs. The C-terminal is the ligand binding domain and a ligand-dependent transactivation function (AF-2) domain. The other transactivation domain (AF-1) has ligand-independent activity, which is within A/B regions (Figure 13).

Unlike the other nuclear receptors, ERs stay in the nucleus with/without ligand binding. After ligand binding, liganded ERs dissociate with inhibitory heat shock proteins and bind to EREs within the promoter region of the target gene (Shibata et al. 1997). The transcription of target genes by hormone-liganded receptors depends upon interactions between receptors and several members of co-regulators. Among co-regulators, co-activators are defined as proteins/RNAs that enhance transcription (Shibata et al. 1997; Lanz et al. 1999; McKenna et al. 1999a; McKenna et al. 1999b). It is believed that natural hormone 17-β estradiol functions as an agonist for ER to activate transcription since it favors the dimerized receptor to recruit co-activators. On the contrary, the antagonist ligand functions as an antagonist to abolish 17-β estradiol action by competitive receptor binding and the recruitment of co-repressors instead of co-activators (McKenna et al. 1999a).

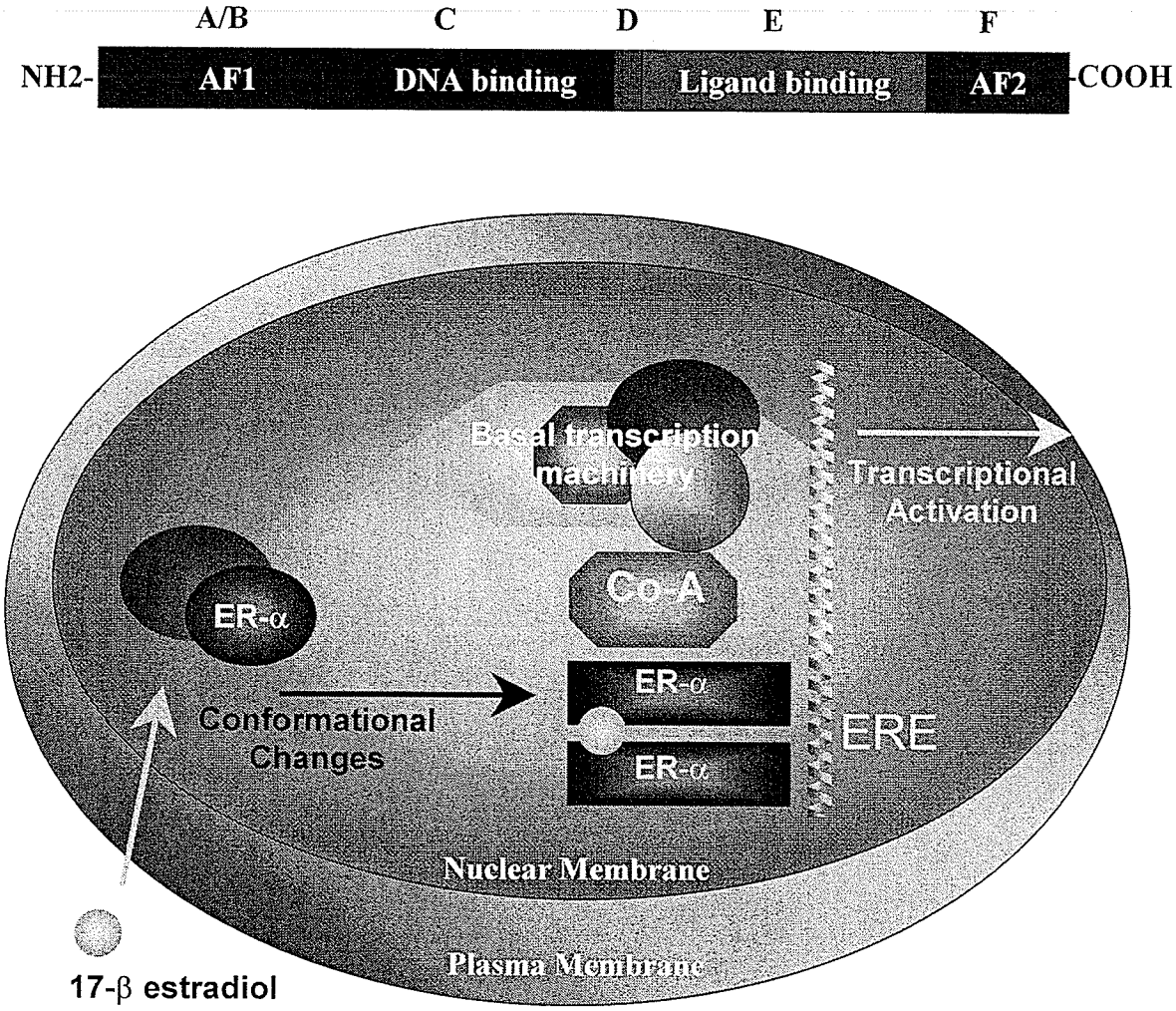

Figure 13. Estrogen action and ER modular structure and function domains. Top figure depicts the modular structure of the ER. Botton figure depicts estrogen signaling via ER-α. Abbreviations: ERE, estrogen response element; CoA, co-activators; AF: activating function

2.6.3 RAR and RXR Actions

The vitamin A derivative, 9-*cis* retinoid acid (RA), is the endogenous ligand for the RXRs, whereas *all-trans* RA binds to RARs with high specificity. Three subtypes of receptors exist for RAR and RXR (Chawla et al. 2001). RXRs function as obligate heterodimer partners for other nuclear receptors such as peroxisome proliferator-activated receptors (PPARs), liver X receptors (LXR), and farnesoid X receptor (FXR) (Willy et al. 1995; Willson et al. 2000; Chawla et al. 2001; Hwang et al. 2002; Urizar et al. 2002). RAR functions as homodimers or heterodimers and it may induce cell differentiation on varieties of tumor cell lines (Yang et al. 2002; Niles 2003; Paik et al. 2003; Paydas et al. 2003). Upon ligand binding, receptors undergo conformational changes by which the receptor coordinately dissociates the heat shock protein and translocates into the nucleus where it binds to the promoter region of the targeted gene to modulate gene transcription (Marill et al. 2003; Mehta 2003).

III. CONTROL OF PHOSPHOLIPID METABOLISM

3.1 Classification and Nomenclature

Phospholipids are the most abundant class of lipids in all mammalian membranes. Glycerol containing phospholipids, termed phosphoglycerides, may be divided into three distinct subclasses according to the type of bond at the *sn*-1 position: (1) 1, 2 diacyl-*sn*-phosphoglyceride (over 50%); (2) the most variablely tissue-distributed 1-alkenyl-2-acyl-*sn*-phosphoglyceride also known as plasmalogen (2-40%); (3) 1-alky-2-acyl-*sn*-phosphoglyceride (1-2%). Polyglycerophosphoglycerides are phospholipids that contain either 2 or 3 glycerol moieties. This class of phospholipid, which includes cardiolipin and bis-monoacylglycerophosphate, is a minor component in most cells but found in significant amounts in some tissues such as the lung and heart (Hatch 1998).

3.2 Function of Phospholipid

Phospholipids are building blocks of the biological membrane. The ability of phospholipids to assemble the basic lipid bilayer lies in their amphipathic character. As major components of the membrane, phospholipids provide the cell with a barrier where selective permeability protects cellular metabolism. Within the cell, these phospholipids participate in the membrane network that delineates individual organelles. In addition to their role in membrane formation, phospholipids are involved in the modulation of membrane bound enzymes or binding to membrane receptors (Coleman 1973; Hla et al. 2001). The developmentally critical protein Hedgehog is a prime example. Its lipid modification by cholesterol and palmitate and its action via a sterol-sensing domain have been recently demonstrated (Ingham 2001). Lipids may also help to direct proteins to

their proper locations in the cell. For example, many of these proteins that regulate vesicle trafficking bear a lipid-binding motif that targets them to distinct membrane localized phospholipids (Sato et al. 2001b). The direct involvement of phosphatidylcholine and phosphatidylethanolamine in the synthesis of lung surfactant, lipoprotein secretion and arachidonic acid release for the subsequent prostaglandin biosynthesis have been demonstrated (Cullis et al. 1996; Smith and Murphy 2002). Phosphatidylserine is required for surface recognition of apoptotic cells by phagocytes (Fadok et al. 1992). Cardiolipin plays a critical role in the apoptotic process in many cells (Newmeyer and Ferguson-Miller 2003). In addition, the role of phosphatidylinositol and its derivatives in signal transmission is well documented (Berridge and Irvine 1989; Exton 1990; Fukami and Takenawa 1992). It is clear from these studies that phospholipids also play an important role in the modulation of cellular activities, and their physiological involvement is well-beyond their primary function as building blocks of the biological membrane.

3.3 Phospholipid Biosynthesis in Mammalian Tissues

Studies on lipid biosynthesis have dated back to the 1950s and most of the biosynthetic pathways were elucidated largely through the work conducted in Eugene Kennedy's laboratory (Kennedy 1961; van den Bosch 1974; Kennedy 1992; Kent 1995). Since then a wealth of knowledge has been obtained on enzymes that catalyze lipid biosynthetic reactions.

3.3.1 The *de novo* Biosynthesis Pathways

In eukaryotes, enzymes catalyzing glycerolipid biosynthesis are present mainly in mitochondria and the endoplasmic reticulum (Paulauskis and Sul 1988; Haldar and Vancura 1992; Yet et al. 1993; Yet et al. 1995). The main site of cellular glycerolipid biosynthesis is believed to be at the endoplasmic reticulum, from which the lipids are transported to different subcellular compartments (Vance 2002). To date, two biosynthetic pathways have been established: (1) the *sn*-glycerol-3-phosphate pathway and (2) the monoacylglycerol pathway (Figure 14). In eukaryotes, both pathways may generate diacylglycerol that can be used as substrates for the synthesis of phospholipids and/or triacylglycerol. The *sn*-glycerol-3-phosphate pathway is present in most cell types. In this pathway, the 1-acyl-*sn*-glycerol-3-phosphate product formed from *sn*-glycerol-3-phosphate acyltransferase is esterified to yield 1, 2-diacyl-*sn*-glycerol-3-phosphate (phosphatidic acid, PA) by 1-acyl-*sn*-glycerol-3-phosphate acyltransferase, and diacylglycerols are derived from the hydrolysis of the phosphatidic acid. In contrast, the monacylglycerol pathway has been largely restricted to the enterocytes of the small intestine, in which diacylglycerol is formed directly from monoacylglycerol catalyzed by monoacylglycerol acyltransferase (Cases et al. 1998; Chen and Farese 2000; Cao et al. 2003a; Cao et al. 2003b). The monoacylglycerol pathway is believed to be critical for the packaging of dietary fat into chylomicron lipoprotein particles; however, its role in phospholipid biosynthesis remains to be unknown.

Phosphatidic acid is situated at the branch point in the common phospholipid biosynthesis pathway (Figure 14). Phosphatidic acid may be converted to 1,2-diacyl-*sn*-glycerol by phosphatidic acid phosphohydrolase (PAP), which can subsequently be used

for the biosynthesis of phosphatidylcholine, phosphatidylethanolamine, and 1,2,3-triacyl-*sn*-glycerol (TG) (Brindley and Waggoner 1998). Alternatively, phosphatidic acid may be converted to cytidine-5'-diphosphate-1,2-diacyl-*sn*-glycerol (CDP-DG) for the biosynthesis of phosphatidylinositol, phosphatidylglycerol and cardiolipin.

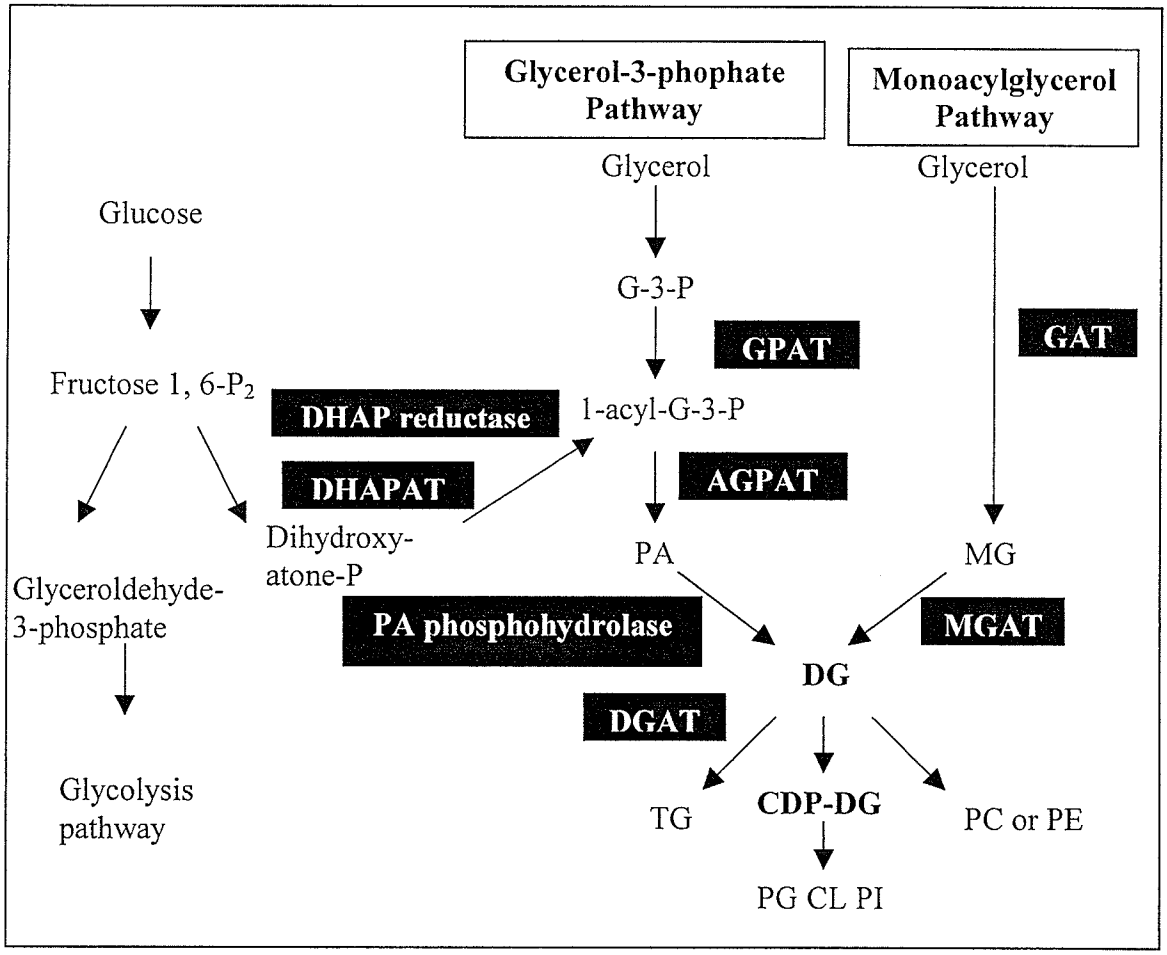

Figure 14. Phospholipid biosynthetic pathways in mammalian cells.

The abbreviation are: G-3-P, glycerol-3-phosphate; PA, phsphatidic acid; MG, monacylglycerol; DG, diacylglycerol; TG, triacylglycerol; PC, phosphatidycholine; PE, phosphatidylethanolamine; GPAT, glycerol-phosphate acyltransferase; AGPAT, 1-acyl-*sn*-glycerol-3-phosphate acyltransferase; MGAT, MG alcyltransferase; DGAT, DG acyltransferase; DHAP, dihydroxyacetone phosphate; DHAPAT, DHAP acyltransferase; PG, phosphatidylglycerol; CL, cardiolipin; PI, phosphatidylinositol.

3.3.2 Glycerol Kinase (EC 2.7.1.30) and *sn*-glycerol-3-phosphate Dehydrogenase (EC 1.1.1.94)

Glycerol kinase is the enzyme that transfers the phosphate group to glycerol molecule to form *sn*-glycerol-3-phosphate (ATP + glycerol = ADP + *sn*-glycerol-3-phosphate). *sn*-Glycerol-3-phosphate dehydrogenase can catalyze the *sn*-glycerol-3-phosphate to form dihydroxyacetone-3-phosphate (DHAP) (*sn*-glycerol-3-phosphate + $NAD(P)^+$ = dihydroxyacetone phosphate + NAD(P)H). Thus, 1-acyl-*sn*-glycerol-3-phosphate can be produced either through the direct acylation of *sn*-glycerol-3-phosphate or the reduction of the glycolytic intermediate dihydroxyacetone-3-phosphate in reactions catalyzed sequentially by dihydroxyacetone-phosphate acyltransferase and acyldihydroxyacetone-3-phosphate reductase (Figure 14) (Vance 1996; Vance 2002).

3.3.3 Dihydroxyacetone-phosphate Acyltransferase (EC 2.3.1.42)

Dihydroxyacetone phosphate acyltransferase (DHAPAT) is an integral membrane protein exclusively localized to the luminal side of peroxisomes of the liver (Singh et al. 1993). The enzyme uses DHAP as its substrate to produce acyldihydroxyacetone-phosphate, which also utilizes alkyldihydroxyacetone-phosphate as a substrate. Both 1-acyl-*sn*-glycerol-3-phosphate and alkyldihydroxyacetone-phosphate are reduced to 1-acyl-*sn*-glycerol-3-phosphate by a peroxisomal acyldihydroxyacetone-phosphate reductase. The route from DHAP to 1-acyl-*sn*-glycerol-3-phosphate serves as minor alternative circus for 1-acyl-*sn*-glycerol-3-phosphate synthesis (Singh et al. 1993; Vance 1996; Vance 2002).

3.3.4 *sn*-Glycerol-3-phosphate Acyltransferase (EC 2.3.1.15)

The acylation of *sn*-glycerol-3-phosphate represents the first committed step in glycerolipid biosynthesis. The *sn*-glycerol-3-phsphate acyltransferase (GPAT) is localized to both endoplasmic reticulum and mitochondrial membranes within mammalian cells (Dircks and Sul 1997). The two forms of GPAT can be distinguished by their sensitivity to sulfhydryl reagents such as N-ethylmaleimide for the microsomal form, whereas the mitochondrial form of enzyme is insensitive. Both microsomal and mitochondrial forms of the rat liver enzyme exhibit a broad pH optimum (between 6.6-9.0) and the Km for *sn*-glycerol-3-phosphate for the mitochondrial enzyme (1 mM) is much greater than the microsomal enzyme (0.1-0.2 mM). The mitochondrial GPAT prefers saturated fatty acyl CoA substrates and is extensively regulated under physiological and pathophysiological conditions and the nutritional status of the animal (Lewin et al. 2001; Hammond et al. 2002). A substantial amount of knowledge has accumulated on mitochondrial GPAT regarding its properties, purification, and cloning. Mitochondrial GPAT has been purified and its gene has been cloned from mouse and rat (Dircks and Sul 1997; Ganesh Bhat et al. 1999). The rat cDNA contains an open reading frame (ORF) of 828 amino acids that has 89% homology with the coding region of the mouse mitochondrial GPAT at DNA level and 96% identical at amino acid level. The topography of rat GPAT in the transverse plane of the mitochondrial outer membrane is dual spanning with the transmembrane protein adopts an inverted "U" conformation where the N and C termini are sequestered on the inner surface of the mitochondria, while the catalytic domain (aa 494-573) is exposed on the cytosolic surface of the mitochondria (Gonzalez-Baro et al. 2001). On the other hand, little is known about

microsomal form of GPAT. The microsomal GPAT has been purified to homogeneity; however, the gene coding for microsomal GPAT has not yet been cloned.

3.3.5 1-Acyl-*sn*-glycerol-3-phosphate Acyltransferase (EC 2.3.1.51)

The 1-acyl-*sn*-glycerol-3-phosphate product formed from *sn*-glycerol-3-phosphate acyltransferase is acylated to 1,2-diacyl-*sn*-glycerol-3-phosphate by 1-acyl-*sn*-glycerol-3-phosphate acyltransferase (AGPAT) also termed lysophosphatidic acid acyltransferase (LPAAT). Relatively less is known about the second step in the phosphatidic acid (PA) biosynthetic pathway. The activity of this acyltransferase is much lower in mitochondria than in endoplasmic reticulum (Vance 1996; Vance 2002). It is presumed that much of the AGPAT formed in mitochondria is transferred to endoplasmic reticulum for the second acylation. In endoplasmic reticulum membrane lyso-PA formed from *sn*-glycerol-3-phosphate in mitochondria is esterified to yield PA, the precursor of all glycerolipids. Multiple genes have been identified and postulated to encode ER transmembrane proteins that have AGPAT activities. The reason of existing multiple isoforms for this catalytic activity is not clear. In humans, two of these isozymes have been cloned and they locate at different chromosomes (Eberhardt et al. 1997; Stamps et al. 1997; West et al. 1997; Aguado and Campbell 1998). The cDNAs that encode proteins possessing AGPAT activities are termed AGPAT-α (283 aa) and AGPAT-β (278 aa) respectively. AGPAT-α (or AGPAT1) is expressed in all tissues with the highest expression being in skeletal muscle whereas AGPAT-β (or AGPAT2) is expressed predominantly in heart and liver tissues. By means of linkage studies, AGPAT-β has been found to be the causative gene for the human congenital generalized lipodystrophy (Agarwal et al. 2002).

3.3.6 Phosphatidic Acid Phosphohydrolase (EC 3.1.27)

Phosphatidic acid lies at a branch point in phospholipid biosynthesis. Phosphatidic acid may be converted to 1,2-diacyl-*sn*-glycerol by phosphatidic acid phosphohydrolase (PAP) (Jamal et al. 1991; Martin et al. 1991). Alternatively, phosphatidic acid may be converted to cytidine-5'-diphosphate-1,2-diacyl-sn-glycerol (CDP-DG) for biosynthesis of phosphatidylinositol (PI) and the polyglycerophospholipids, phosphatidylglycerol and cardiolipin (CL) in a reaction catalyzed by CTP: phosphatidic acid cytidylyltransferase. Two distinct PAPs have been found based on the differential inhibition by N-ethylmaleimide: N-ethylmaleimide-sensitive cytosolic and microsomal fractions (type I) and N-ethylmaleimide insensitive plasma membrane fraction (type II) (Jamal et al. 1991).

The type I PAP is Mg^{++}-independent and inactivated by N-ethylmaleimide. The enzyme translocates from the cytosol to the endoplasmic reticulum upon stimulation by fatty acids or acyl-CoAs. Hence the cytoplasmic form of PAP serves as a reservoir that moves onto the endoplasmic reticulum and becomes metabolically functional. The transition from a cytosolic inactive form to a membrane associated active form seems to be the main reason why this enzyme is so elusive and thus difficult to purify to homogeneity. It is believed that the cytoplasmic form is for TG and phospholipid biosynthesis. At present the type I (PAP-1) has not yet been cloned at the molecular level.

It has become clear that some members of PAPs play a role in signal transduction and these PAPs belong to the second type of PAP (PAP-2) (Waggoner et al. 1995;

Brindley and Waggoner 1998). Computer modeling predicts that the type II PAP is a channel-like integral membrane protein with six transmembrane domains. Several isoforms of mammalian PAP-2, PAP-2a, PAP-2b, and PAP-2c have been isolated and characterized (Kai et al. 1996; Hooks et al. 1998). Table 2 summarizes the cloning and characteristics of PAPs.

Table 2. Cloning and characterization of PAP-1 and PAP-2.

	PAP type I	**PAP type II**
N-ethylmaleimide	Sensitive	Insensitive
Localization	Cytosol or membrane association	Plasma membrane
Mg++	Dependent	Independent
Major function	Lipid biosynthesis	Signal transduction
cDNA	Not available	PAP-2a: 285 aa PAP-2b: 312 aa PAP-2c: 288 aa

3.3.7 Monoacylglycerol Acyltransferase (EC 2.3.1.22)

As discussed in previous sections, diacylglycerol (DG) is produced from phosphatidic acid in a reaction catalyzed by PAPs. Alternatively, DG is also synthesized from the direct acylation of monoacylglycerol (MG) that occurs readily in enterocytes of the small intestine and liver (Cao et al. 2003a). The reaction is catalyzed by acyl-CoA: monacylglycerol acyltransferase. The enzyme is also active in adipose tissue and cardiomyocytes. Recently, three isozymes have been cloned and characterized to have MGAT activity (Cases et al. 1998; Yen et al. 2002; Cao et al. 2003b; Yen and Farese 2003). MGAT1 belongs to a gene family that includes diacylglycerol acyltransferases (DGAT) and several other homologues that are uncharacterized. Murine MGAT1 is expressed in the stomach, kidney, adipose tissue, and liver but not in the intestine. The role of MGAT1 in tissues other than the intestine is unknown but may relate to the preservation of polyunsaturated fatty acids in tissues where cycles of TG degradation and resynthesis are prominent (Yen et al. 2002). MGAT2 is expressed in the small intestine in both mice and humans; whereas the RNA expression profile of human MGAT3 is highly restricted to gastrointestinal tract (Cheng et al. 2003; Yen and Farese 2003). Recombinant MGAT3 appears to possess superior substrate specificity for the acylation of 2-monoacylglycerol over other stereoisomers, thus the AGPAT3 gene product fulfills the essential criteria as the authentic intestinal MGAT. Characteristics of the three newly isolated mammalian MGATs are summarized in Table 3.

Table 3. Cloning and characterization of MGAT1, MGAT2, and MGAT3.

	MGAT1	MGAT2	MGAT3
Tissue expression	Stomach, kidney, adipose	Intestine, stomach, colon, kidney, adipose, liver	Intestine
Substrates	*sn*-2-MG, *sn*-1-MG	*sn*-2-MG > *sn*-1-MG	*sn*-2-MG
Human MGAT	334 aa	334 aa	341 aa
Localization	Membrane fraction	Membrane fraction	ER
Transmembrane domain	At least one	At least one	At least one
Chromosome Location	Murine Chromosome 1 Human Chromosome 2	Murine Chromosome 7 Human Chromosome 11q13.5	Not available

3.3.8 Diacylglycerol Acyltransferase (EC 2.3.1.21)

Triacylglycerols are the most important storage form of energy for eukaryotic cells. DGAT is the integral membrane protein that catalyzes the final and committed step in triacylglycerol synthesis. The enzyme is responsible for transferring an acyl group from acyl-Co-A to the *sn*-3 position of 1,2-diacylglycerol to yield TG. DGAT plays a key role in intestinal TG resynthesis, lipoprotein assembly, adipose tissue TG synthesis, and lactation (Lehner and Kuksis 1995; Chen and Farese 2000; Lockwood et al. 2003). To date, two DGATs, DGAT1 and DGAT2, have been cloned (Cases et al. 1998; Cases et al. 2001; Buhman et al. 2002). The full-length cDNA for DGAT1 predicts an ORF encoding a 498 aa protein with 6-12 possible transmembrane domains. Knockout of DGAT1 demonstrated that it is not essential for intestinal triacylglycerol absorption or chylomicron synthesis. The second mammalian DGAT, termed DGAT2, is expressed in many tissues with high expression levels in the liver and white adipose tissue, suggesting that it may play a significant role in mammalian TG metabolism. To date, the intestinal DGAT has not yet been cloned.

3.3.9 Biosynthesis of Polyglycerophospholipids

Cardiolipin, the first polyglycerophopholipid discovered is localized at both inner and outer mitochondrial membranes in eukaryotic cells (Hovius et al. 1990; Hovius et al. 1993). In the rat heart, cardiolipin is found exclusively in mitochondria and comprises approximately 12-15% of the total phospholipid mass (Hatch 1994). Phosphatidylglycerol is synthesized in mitochondria and microsomes and comprises 1-1.5% of the total phospholipid mass in mammalian tissues (Hostetler 1982). Cardiolipin

is required for the reconstituted activity of a number of key mitochondrial enzymes involved in cellular energy metabolism via holding the respiratory chain together (Zhang et al. 2002). In lower eukaryotes, phosphatidylglycerol and cardiolipin appear to be essential for growth and survival of yeast (Pluschke et al. 1978; Jiang et al. 1999). Phosphatidylglycerol is actively synthesized and secreted by alveolar type II cells and is a critical component of alveolar surfactant in the lung (Batenburg 1992).

The *de novo* biosynthesis of mammalian phosphatidylglycerol and cardiolipin via the CDP-diacylglycerol pathway was elucidated by Kennedy and co-workers (Kennedy 1961; Kennedy 1989; Kennedy 1992). In eukaryotic cells, phosphatidylglycerol and cardiolipin are actively synthesized from the newly formed phosphatidic acid. In the first step, phosphatidic acid is converted to CDP-diacylglycerol by CTP: phosphatidic acid cytidylytransferase. The CTP: phosphatidic acid cytidylyltransferase has been cloned from a human NT2 neuronal cell library (Heacock et al. 1996). The predicted reading frame encodes a protein of 444 amino acids with a molecular mass of 51.4 kDa. In the second and third steps of the CDP-diacylglycerol pathway CDP-diacylglycerol condenses with *sn*-glycerol-3-phosphate to form phosphatidylglycerol catalyzed by phosphatidylglycerolphosphate (PGP) synthase and phophatidylglycerolphosphate phosphatase (Cao and Hatch 1994). In the final step of the pathway, cardiolipin is formed from the condensation of phosphatidylglycerol and CDP-diacylglycerol catalyzed by cardiolipin synthase in eukaryotic cells (Figure 15) (Schlame et al. 1993). The cardiolipin synthase is localized exclusively on the inner side of the inner mitochondrial membrane. Pulse-chase heart perfusion studies have indicated that one of the rate-limiting steps of

phosphatidylglycerol and cardiolipin biosynthesis in the rat heart is the conversion of phosphatidic acid to CDP-diacylglycerol (Hatch 1994).

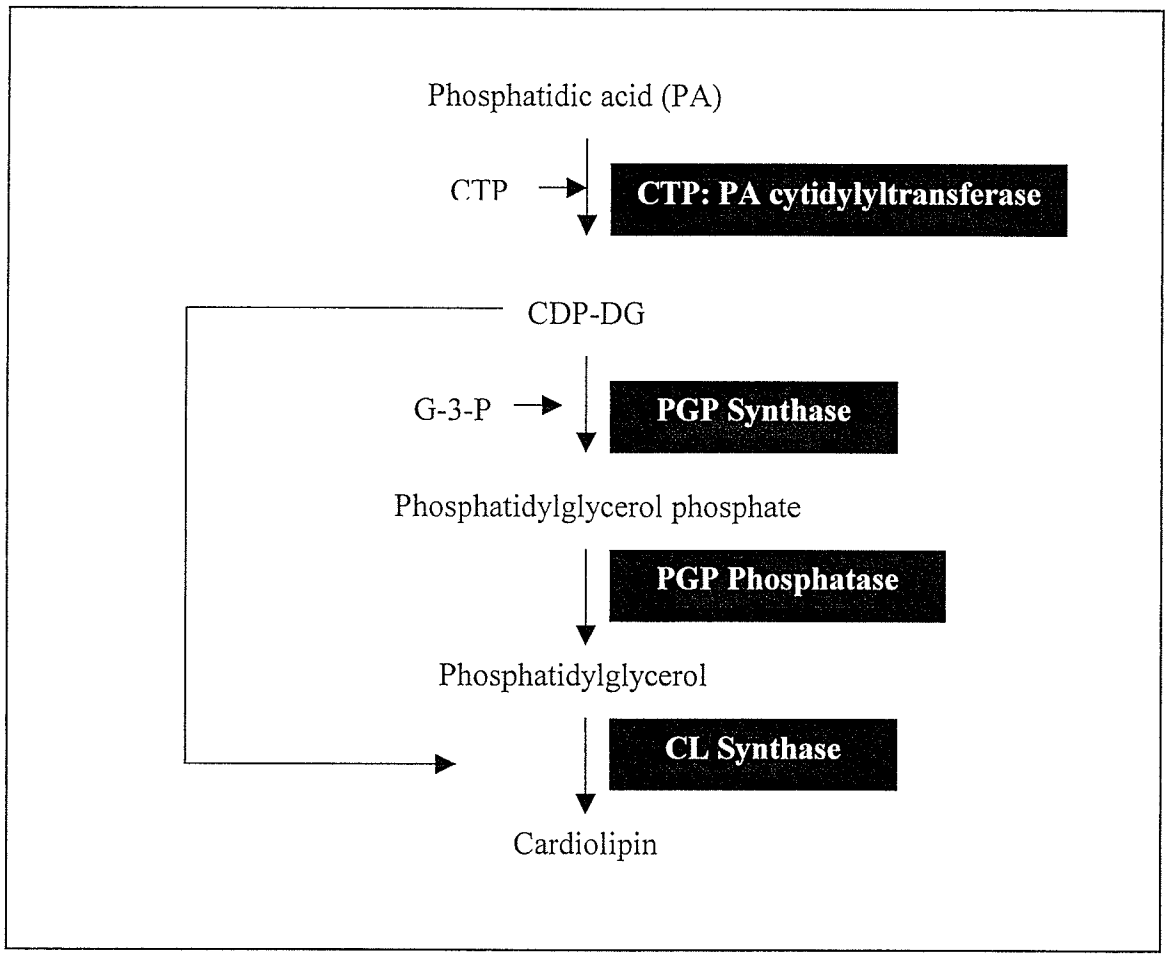

Figure 15. The biosynthesis of phosphatidylglycerol and cardiolipin.
Abbreviations: CDP-DG, CDP-diacylglycerol; PA, phosphatidic acid; PGP, phosphatidylglycerol phosphate; G-3-P, *sn*-glycerol-3-phosphate.

3.3.10 Biosynthesis of Phosphatidylcholine

Phosphatidylcholine is the major phospholipid in mammalian tissues. Three pathways are known for the formation of phosphatidylcholine: (1) CDP-choline pathway; (2) Methylation pathway; and (3) Base-exchange pathway (Figure 16). The majority of the phospholipid is formed from choline via the CDP-choline pathway (Kennedy 1989). In this pathway, choline is taken up by the cell and subsequently becomes phosphorylated by choline kinase (EC2.7.1.32). Phosphocholine is then converted to CDP-choline in a reaction catalyzed by CTP: phosphocholine cytidyltransferase (EC2.7.7.15). Phosphatidylcholine is formed by the condensation of CDP-choline and 1,2-diacylglycerol in a reaction catalyzed by CDP-choline: 1,2-diacylglycerol cholinephosphotransferase (EC 2.7.8.2).

Phosphatidylcholine can also be formed by the methylation pathway in which phosphatidylethanolamine is converted to phosphatidylcholine by the transfer of methyl groups from S-adenosylmethionine in a reaction catalyzed by phosphatidylethanolamine-N-methyltransferase (EC 2.1.1.17) (Ridgway and Vance 1992). This pathway contributes significantly to phosphatidylcholine formation in the liver but not in other organs (Vance 2002). Another pathway for phosphatidylcholine formation is the Ca^{2+}-mediated base exchange of choline for other phospholipid head groups(Dils and Hubscher 1961).

3.3.11 Biosynthesis of Phosphatidylethanolamine

The CDP-ethanolamine pathway is the major route for phosphatidylethanolamine biosynthesis in most mammalian tissues (Vance 2002). The decarboxylation of phosphatidylserine, however, has been recognized as an important pathway for

phosphatidylethanolamine biosynthesis in prokaryotes and some eukaryotic cells (Voelker 1984). The decarboxylation of phosphatidylserine is catalyzed by phosphatidylserine decarboxylase. The mammalian phosphatidylserine decarboxylase is localized to the inner mitochondrial membrane and contains mitochondrial membrane targeting and sorting sequences (Voelker 1997). A calcium mediated base-exchange pathway appears to be a minor route for the quantitative biosynthesis of phosphatidylethanolamine (Figure 16) (Vance 2002).

3.4 Remodeling of Phospholipids

In general, the content and composition of phospholipids in a membrane system are well defined. Structural studies of phospholipid molecules indicate that the acyl content is highly specific in terms of chain length, position and saturation (Arthur and Choy 1984). For example, the acyl moiety esterified to the glycerol backbone is usually saturated at the *sn*-1 position and unsaturated at the *sn*-2 position. The lipid moiety of phosphatidylcholine is synthesized via the *sn*-glycerol-3-phosphate pathway where phosphatidate is produced by the sequential action of *sn*-glycerol-3-phosphate and lysophosphatidate acyltransferases. It has been found that the newly formed phosphatidate contains predominately monoenoic and dienoic acyl species, which is different from the endogenous phospholipid pool. In the biosynthesis of phosphatidylcholine, the CDP-choline: 1,2-diacylglycerol choline phosphotransferase has only limited specificity for diacylglycerol species with specific acyl chain compositions.

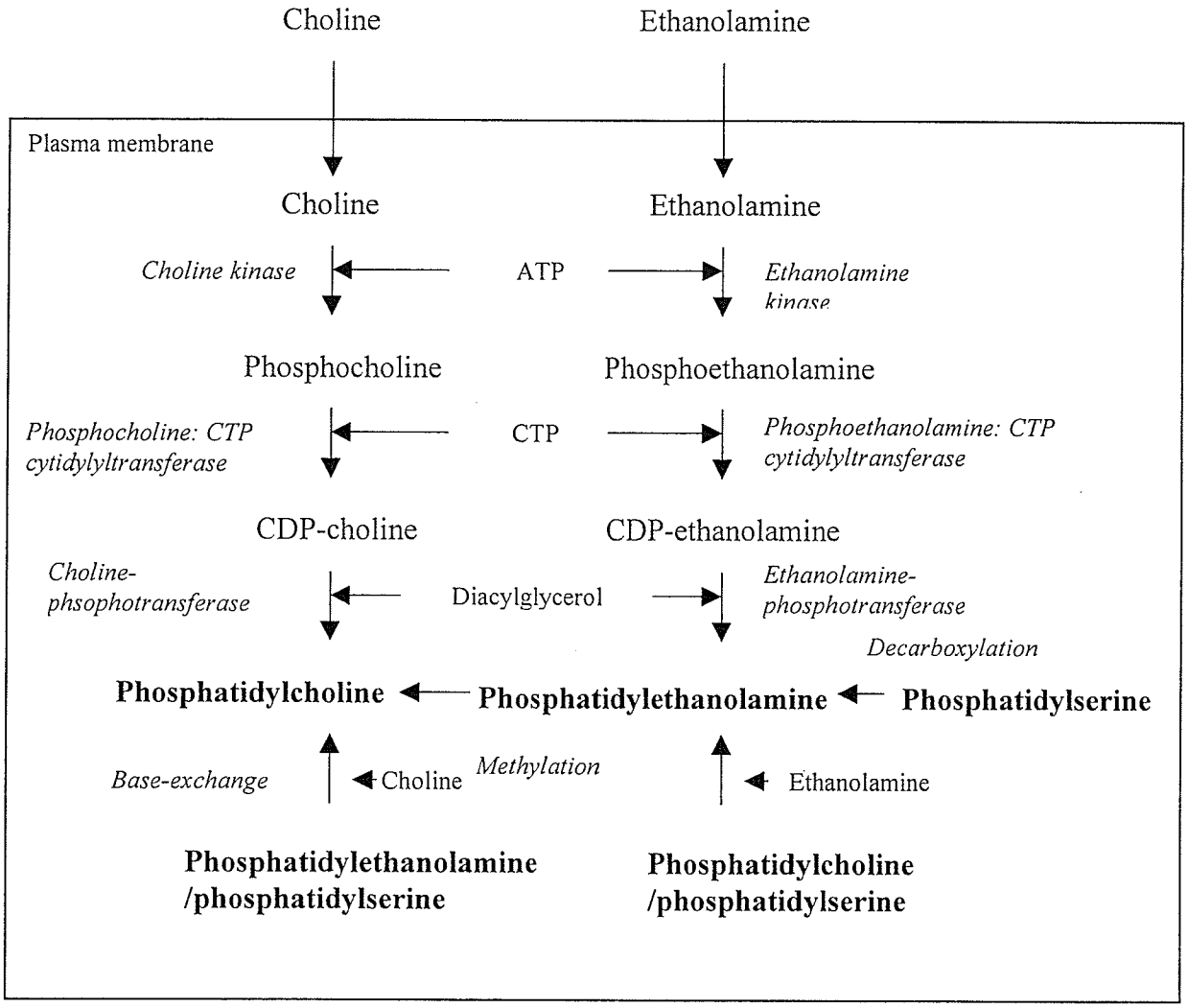

Figure 16. Biosynthesis of phosphatidylcholine and phosphatidylethanolamine.

In addition, the acyl composition of newly formed phosphatidylcholine is similar to the diacylglycerol produced from phosphatidate. Hence, the phospholipid acyl moieties are remodeled in a deacylation/reacylation process sometimes referred to as the Lands pathway (Lands and Hart 1965).

Phospholipases and acyltransferases are generally regarded as the principal enzymes involved in phospholipid remodeling in mammalian tissue. Phospholipids can be catabolized through the action of various phospholipases. The phospholipases can be categorized into four groups (A-D) according to the specific phospholipid bond they hydrolyze (Wilton and Waite 2002). Phospholipases A includes phospholipase A_1 (EC 3.1.1.32) and phospholipase A_2 (EC 3.1.1.4) that specifically cleave the ester bound at the *sn*-1 position or at the *sn*-2 position, while phospholipase B removes the acyl group at position 2 in addition to the acyl group at position 1. Phospholipase C (EC 3.1.4.3) cleaves the glycerophosphate bond, while phospholipase D (EC 3.1.4.4) removes the base group (Figure 17).

Since limited selectivity for the molecular species of diacylglycerol has been displayed by cholinephosphotransferase, the newly formed phospholipid must undergo extensive remodeling of the acyl group. Lands first introduced a scheme for the deacylation-reacylation of phospholipids, which was based on the presence of both phospholipase A_2 and acyltransferase activities in mammalian tissues (Lands and Hart 1965). The formation of phosphatidylcholine from lysophosphatidylcholine by an energy independent transfer of an acyl group was subsequently demonstrated (Figure 18). For example, phosphatidylcholine is converted to lysophosphatidylcholine by phospholipase A_2. Subsequently, lysophosphatidylcholine is reacylated back to phosphatidylcholine

with the proper acyl chain by acyl-CoA: 1-acyl-*sn*-glycerol-3-phosphocholine acyltransferase that highly prefers unsaturated acyl-CoA; while acyl-CoA: 2-acyl-*sn*-glycerol-3-phosphocholine acyltransferase highly prefers saturated acyl-CoA.

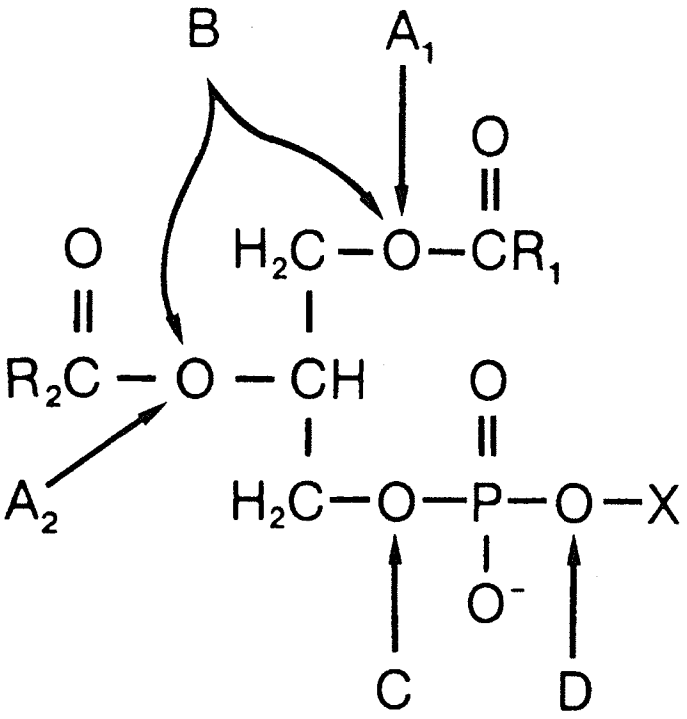

Figure 17. Sites of phospholipase action.
(Adapted from Wilton and Waite 2002)

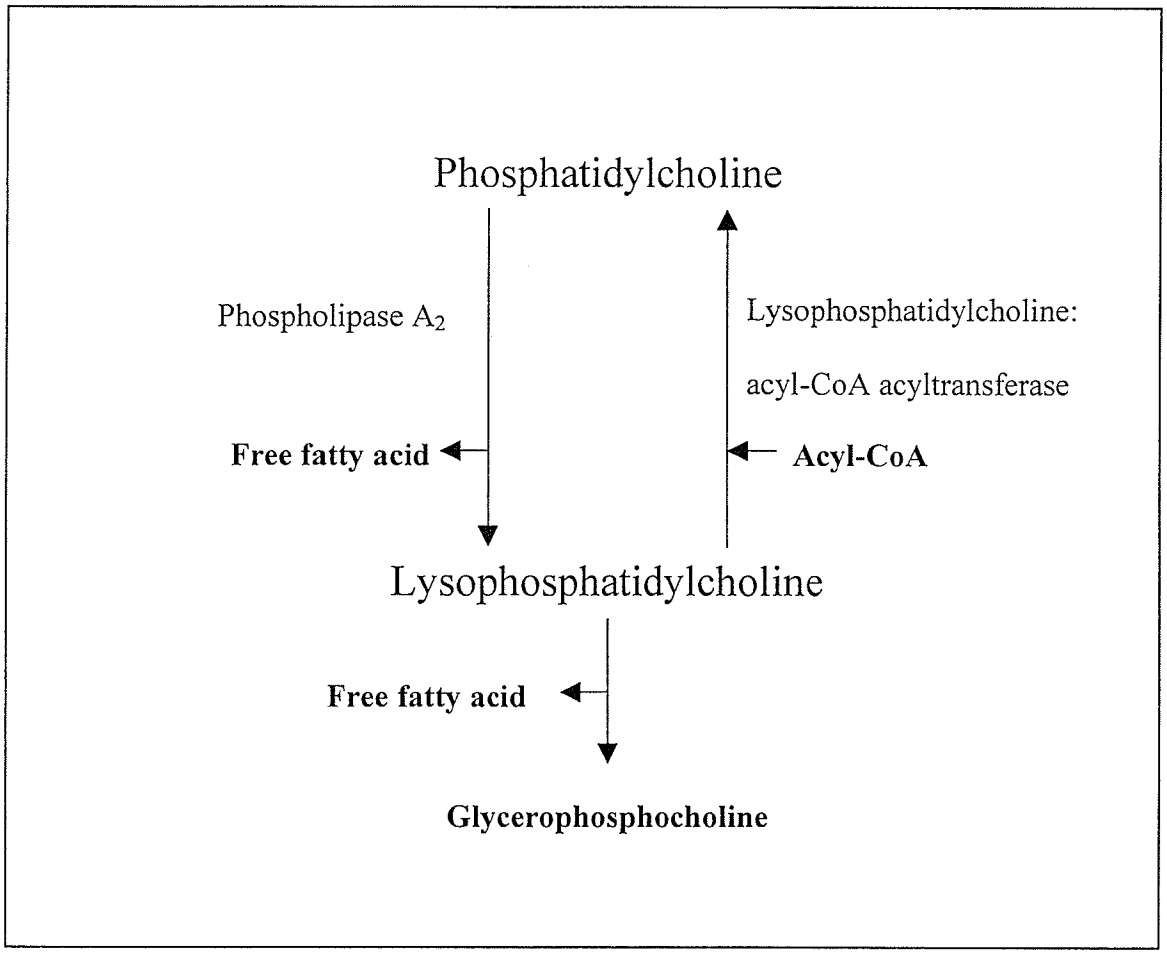

Figure 18. The deacylation-reacylation of phosphatidylcholine.

Lysophosphatidylcholine acyltransferase has been detected in all mammalian tissues studied. The enzyme activity was observed in both mitochondrial and microsomal fractions (Akesson et al. 1976; Cheng et al. 1996). In addition, lysophosphatidylcholine can be further catabolized to glycerophosphocholine.

The advances in delineating mechanisms that govern phospholipid remodeling of the acyl composition have been hampered by difficulties in purification and subsequently characterization of enzyme activities. The purification of lysophosphatidylcholine acyltransferase from the bovine brain and heart has been reported (Deka et al. 1986; Sanjanwala et al. 1988). The molecular weights of the proteins were 43 and 64 kDa respectively. In a separate study, lysophosphatidylcholine acyltransferase has also been identified as a 21 kDa protein band by solubilization with high concentrations of oleoyl-CoA and lysophosphatidylcholine into vesicular phosphatidylcholine (Fyrst et al. 1996). However, no further work has been reported on the purified enzymes. Hence information on the amino acid sequence of the enzyme is not available and attempts to obtain the cDNA have not been reported.

Mitochondrial cardiolipin is distinguished from other phospholipids by the great abundance of linoleoyl molecular species (Schlame et al. 1993). For example, the presence of an acylation-reacylation cycle by adding a labeled linoleoyl group to a mitochondrial preparation was observed in rat liver (Schlame and Rustow 1990). It was concluded that a cycle, comprising cardiolipin deacylation to monolysocardiolipin and its subsequent reacylation with linoleoyl-CoA, would previde a potential mechanism for the remodeling of molecular species of newly formed cardiolipin in the liver. To date,

information on the amino acid sequence and cDNA cloning of the enzyme is not available.

3.5 Phospholipid Catabolism in Mammalian Tissues

3.5.1 Phospholipases

Phospholipases are a group of enzymes that hydrolyze phospholipids. Phospholipases are critical to life since the continual remodeling of cellular membranes requires the action of one or more phospholipases (Wilton and Waite 2002). Under certain conditions, phospholipases go beyond their primary role in membrane homeostasis; they also function in such diverse roles from the digestion of nutrients to the formation of intracellular signaling molecules.

As discussed in the previous section, phospholipases can be categorized into four groups (A-D) according to the specific phospholipid bond it hydrolyzes as shown in Figure 17. In mammalian cells, phospholipase A_2 is important in the stimulus-coupled arachidonate metabolism (Smith 1989; Smith and Murphy 2002). Arachidonate is a precursor of a wide spectrum of lipid signaling molecules. Arachidonate and its metabolites possess diverse biological properties, many of which are related to vascular homeostasis (Moncada and Vane 1979; Funk 2001). In endothelial cells and cardiac myocytes, arachidonate is converted to prostacyclin, a potent vasodilator and platelet antiaggregator. Although different mechanisms have been proposed for the release of arachidonate in mammalian cells, the hydrolysis of the acyl chain at the *sn*-2 position of

glycerophospholipids by phospholipase A_2 is regarded as the primary pathway for this reaction. The following discussion is focused on phospholipase A_2.

3.5.2 Phospholipase A_2

Based on their structures, characteristics and amino acid sequences, phospholipases A_2 were classified into four groups in 1994, and more recently, into 11 distinct groups (Dennis 1997; Wilton and Waite 2002). A brief description of different classes of phospholipase A_2 is summarized in Table 4. In the last several years, major advances have been made towards the study of mammalian cytosolic phospholipase A_2 ($cPLA_2$) that is responsible for the release of arachidonic acid (Clark et al. 1991). The amino acid sequence from human cDNA encodes a 749-aa protein that migrates as a 110 kDa protein on sodium dodecylsulfate-polyacrylamide gel electrophoresis (SDS-PAGE). The human gene has been mapped to chromosome 1q25.3-q31.2 and contains no TATA box in its promoter region indicating a house-keeping-like gene. At the RNA level, it has three UAAAU unstable elements indicating potential regulation at transcriptional level. Functional domains of the cytosolic phospholipase A_2 include an N-terminal calcium-dependent regulatory domain and a C-terminal calcium-independent catalytic domain (Nalefski et al. 1994; Clark et al. 1995). The calcium-dependent lipid binding domain (CaLB) is similar to the C2 domain of protein kinase C. Distinct regions of the enzyme have been identified including the active-site serine 228 (Clark et al. 1995). Ser-505, which is phosphorylated by MAP-kinase, may play an important role in the regulation of enzyme activity (Lin et al. 1993).

Table 3. Characteristics of the major groups of phospholipase A_2. (Modified and condensed from Dennis 1997 & 2002)

Group	Source	Location	Size (kDa)	Ca-requmt	Characteristics
I-A	Cobras	Secreted	13-15	mM	7 disulfide bonds
I-B	Porcine/human Pancreas	Secreted	13-15	mM	7 disulfide bonds
II-A	Rattlesnake	Secreted	13-15	mM	7 disulfide bonds
III	Bees, Lizards	Secreted	16-18	mM	5 disulfide bonds
IV-A	Rat kidney, human platelet	Cytosolic	85	μM	Ser 505 phosphorylation Membrane translocation
IV-B	Human, liver, pancreas/brain	Cytosolic	114	μM	Membrane translocation
IV-C	Human heart, skeletal muscle	Cytosolic	64	None	Prenylated
V	Human/rat heart/lung	Secreted	14	mM	6 disulfide bonds
VI	Macrophages, hamster heart	Cytosolic	85-110	None	Phospholipase A_1 activity
VII	Human plasma	Secreted	45	None	
VIII	Bovine brain	Cytosolic	29	None	Ser 47 phosphorylation
IX	Marine snail	Secreted	14	μM	6 disulfide bonds
X	Human spleen/thymus	Secreted	14	Not available	8 disulfide bonds
XI	Green rice shoots	Secreted	12-13	Not available	6 disulfide bonds

3.5.3 Regulation of Cytosolic Phospholipase A_2

Type IV $cPLA_2$ is the key player for eicosanoid production since cells lacking $cPLA_2$ are generally devoid of eicosanoid synthesis (Dennis 1994; Leslie 1997; Fujishima et al. 1999). It is believed that cell-specific and agonist-dependent events coordinating translocation of $cPLA_2$ to the nuclear envelope, endoplasmic reticulum, and Golgi apparatus are essential for the enzyme activation (Evans et al. 2001; Funk 2001). Multiple mechanisms have been identified and are involved in the regulation of $cPLA_2$ (Figure 19). At the post-translational level, the enzyme is subjected to complex modulation including calcium-dependent translocation to the membrane and phosphorylation at serine 505 by MAP-kinase (Lin et al. 1993; Gijon et al. 1999; Xu et al. 2002; Pettus et al. 2003). At the transcriptional level, the $cPLA_2$ mRNA may be regulated in some cells by mediators such as IL-1, IFN-γ, macrophage colony stimulating factor, epidermal growth factor and glucocorticoid (Ozaki et al. 1994; Kramer and Sharp 1997; Hernandez et al. 1999; Yao et al. 1999; Sampey et al. 2001; Dieter et al. 2002). The existence of both GAS (interferon-gamma Activation Site) and γ-IRE (interferon-γ-Response Element) consensus elements in the 5'–flanking region of the $cPLA_2$ gene have been identified (Figure 19) (Morii et al. 1994; Wu et al. 1994). In addition, the promoter region of the $cPLA_2$ contains several inducible elements, including AP-1 binding sites and a potential NF-κB binding site, all of which may account for the transcriptional control of the enzyme. Recently, the regulation of $cPLA_2$ by peroxisome proliferator-activated receptor has been identified (Jiang et al. 2001).

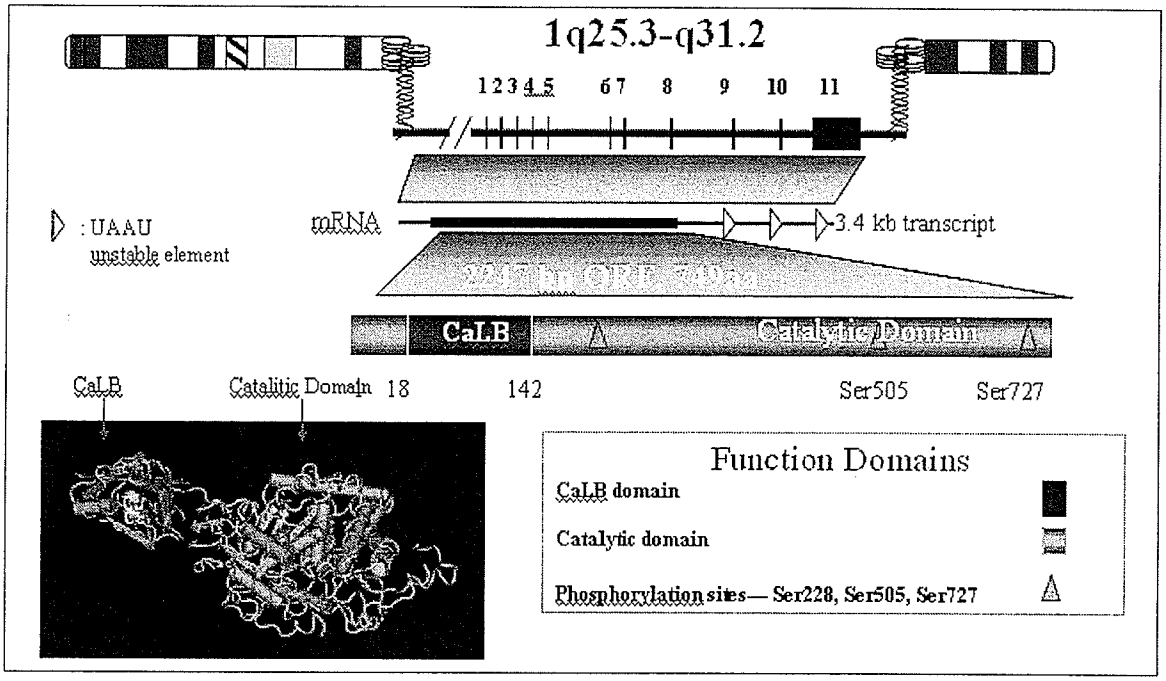

Figure 19. Gene Structure, promoter sequence, transcript, and functional domains of human cytosolic phospholipase A_2.

3.5.4 Arachidonate-eicosanoid Cascade

Eicosanoid comes from the Greek word *eicosa* (twenty), and is used to denote a group of 20 carbon fatty acids derived from phospholipase-released arachidonic acid. Eicosanoids are potent lipid mediators that are generated from cyclooxygenase, lipoxygenase, and epoxygenase pathways (Funk 2001; Smith and Murphy 2002). These three pathways are collectively termed as arachidonate-eicosanoid cascade (Figure 20). Among eicosanoids, prostaglandins and leukotrienes function as paracrine/autocrine signaling molecules and are involved in numerous homeostatic biological functions and inflammation. They are generated by cyclooxygenase isozymes and 5-lipoxygenase, respectively. The cytochrome P450 epoxygnase catalyzes the first step in the synthesis of the epoxyeicosatrienoic acid in epoxygenase pathway. The following discussion is focused on prostaglandins and leukotrienes (Funk 2001).

Prostaglandins are synthesized in most mammalian cells and act as autocrine and paracrine lipid mediators (Lambeth and Ryu 1996; Leslie 1997; Smith and Murphy 2002). They are not stored but rather synthesized *de novo* in response to extracellular stimuli. In contrast to prostaglandins, leukotrienes are made predominantly by inflammatory cells like polymorphonuclear leukocytes, macrophages, and mast cells. 5-lipoxygenase (5-LO) is the key enzyme in this cascade and is located in the nucleus in some cell types and in the cytosol of others. It transforms released free arachidonate to the epoxide LTA_4 with the help of 5-lipoxygenase-activating protein (FLAP) (Borgeat et al. 1985; Funk 2001).

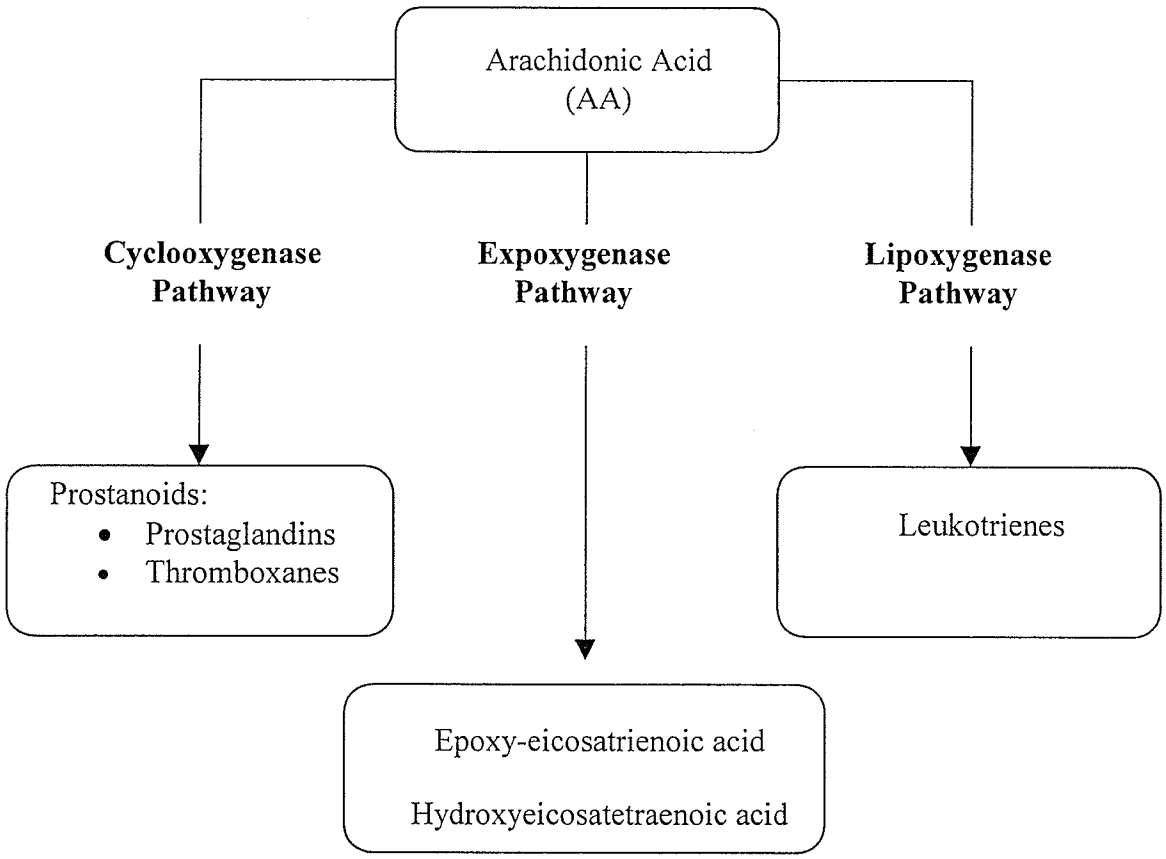

Figure 20. Pathways in arachidonate-eicosaniod cascade.

3.5.5 Prostanoid Biosynthesis

Prostanoid refers to a colletion of prostaglandin molecules synthesized through cyclooxygenase pathway. Prostanoid formation occurs in three stages: (1) the release of arachidonic acid from membrane phospholipids by $cPLA_2$; (2) the conversion of arachidonic acid to PGH_2 by COXs; and (3) conversion of PGH_2 to one of the prostanoids (Figure 21). It is believed that the last stage is cell-specific and is mediated by different synthases (Smith and Murphy 2002).

Arachidonic acid released by $cPLA_2$ is presented to either COX-1 or COX-2 at the endoplasmic reticulum and nuclear membrane (Yokoyama and Tanabe 1989; Hla and Neilson 1992; Funk 2001; Smith and Murphy 2002). Both COXs exhibit two different but complementary enzymatic activities: (1) a cyclooxygenase activity which converts arachidonic acid to PGG_2; and (2) a peroxidase activity which reduces PGG_2 to PGH_2 (Smith and Murphy 2002). The coupling of PGH_2 to effectors by downstream enzymes is intricately orchestrated in a tissue-specific fashion (Funk 2001). Thromboxane synthase is found in platelets and macrophages, prostacyclin synthase is found in endothelial cells and PGF synthase in uterus, and PGD synthases are found in brain and mast cells. Microsomal PGE synthase is responsible for PGE_2 synthesis and is particularly important in inflammatory settings.

3.5.6 Function of Eicosanoids

The role of eicosanoids in pain, fever, and inflammation has long been established. The renewed growth and rapid advances in the eicosanoid field over recent years is attributed to advances in several concerted approaches: (1) cloning of COX

isozymes and receptors of eicosanoids (Yokoyama and Tanabe 1989; Hla and Neilson 1992; Hirai et al. 2001; Monneret et al. 2001); (2) generation of crystal structures for the COX isozymes leading to discovery of isozyme specific inhibitors (FitzGerald et al. 2001; FitzGerald and Patrono 2001); (3) Gene –targeting technology and transgenic techniques to disrupt the genes encoding COXs and receptors in the prostaglandin and leukotriene pathways (Langenbach et al. 1999; Chulada et al. 2000; Morteau et al. 2000; Narumiya and FitzGerald 2001; Tilley et al. 2001). These studies are unraveling novel eicosanoid actions, and confirming long-held views.

The action of prostaglandins and leukotrienes are believed to be mediated through a distinct subfamily of the G protein-coupled receptor (GPCR) superfamily of seven-transmembrane spanning proteins. There are at least 9 known prostaglandin receptors in humans. Four of the receptors bind PGE_2 (EP_1-EP_4), two bind PGD_2 (DP1 and DP_2), each binds PGF_{2a}, PGI_2, and TxA_2 (FP, IP, and TP). In addition to action via plasma membrane receptors, some of eicosanoids are ligands for nuclear receptors. For example, LTB_4 and 8(S)-HETE bind to PPAR-α; 15-deoxy-delta 12,14-PGJ_2 binds to PPAR-γ; while prostacyclin analogs bind to PPAR-δ. Through both membrane and nuclear receptors, prostaglandins play a critical role in a variety of physiological and pathophysiological processes (Table 5).

Table 5. Functions of prostanoids.

Prostanoid	Source Cells	Receptor	Target Cells	Function
PGE_2	Most cells	EP1 EP2 EP3 EP4	Neurons Ovarian cumulus oophorus Neurons in preoptic area, Osteoblast	Pain response Maturation for ovulation and fertilization Fever generation Bone resorption
PGD_2	Mast Cells	DP1 DP2	Lung epithelial cells Th2 lymphocyte	Allergic asthma Chemotaxis
PGI_2	Endothelium	IP IP	Platelet Vascular smooth muscle cell	Platelet dechumping Vasodilation
TxA_2	Platelet	TPα TPβ	Platelet Vascular smooth muscle cell	Aggregation Vasoconstriction
$PGF_{2\alpha}$	Uterus	FP	Uterine smooth muscle	Constriction, parturition

Note: Prostaglandins could potentially enter cells, bind and activate nuclear hormone receptors such as PPARγ and PPARδ (PGJ_2 is a ligand for PPARγ and PGIs is a ligand for PPARδ).

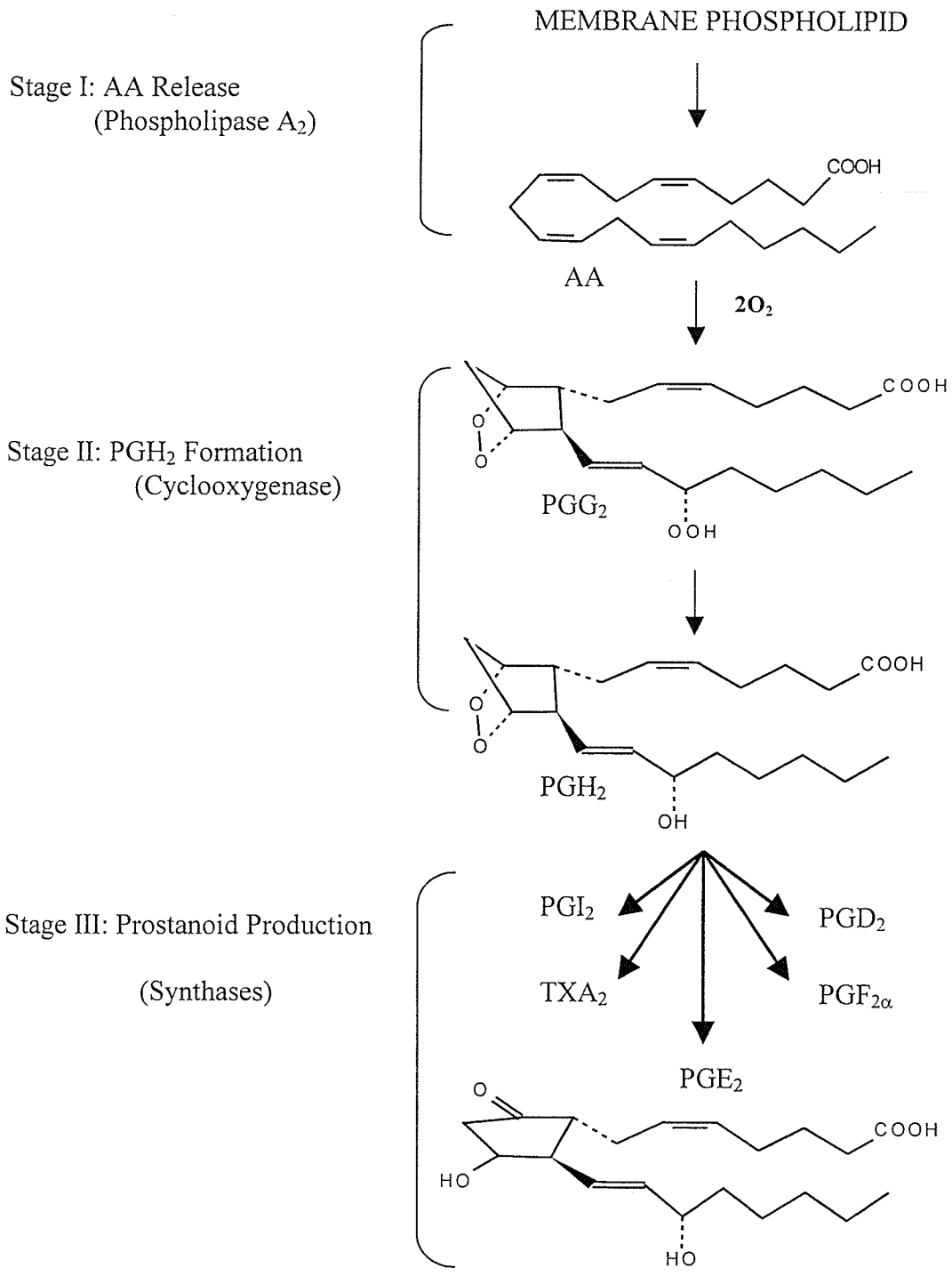

Figure 21. Biosynthetic stages of prostanoids derived from AA.

3.5.7 Cyclooxygenases and Their Regulation

COX-1 and COX-2 are encoded by separate genes and located at different chromosomes (Yokoyama and Tanabe 1989; Hla and Neilson 1992). Human COX-1 located at chromosome 9q32 is comprised of 11 exons which are spliced into 3.0 kb transcripts. The COX-1 mRNA contains a 1797 bp ORF that encodes a 70 kDa protein. From its N-terminal to C-terminal, human COX-1 enzyme consists of four functional domains: a signal peptide, an EGF domain, a membrane binding domain, and a catalytic domain. Human COX-2 gene is located at chromosome 1q25, the same chromosome region of human $cPLA_2$. Human COX-2 contains 10 exons and its 4.5 kb mRNA transcript has 9 AUUUA unstable elements in their 3' region. The domain architecture and crystal structure of COX-1 and COX-2 are remarkably similar, with one notable amino acid difference that leads to a larger binding pocket for substrate in COX-2.

The regulation of COX-1/COX-2 is distinctively different (Figure 22, 23). COX-1 is believed to be responsible for basal, constitutive prostaglandin synthesis, whereas COX-2 is induced under various conditions such as inflammation, oncogenesis, and stresses (Wu et al. 1994; Smith et al. 2000; Funk 2001). There are also exceptions in which COX-1 instead of COX-2 is transcriptionally regulated. Several inducible transcriptional protein binding elements exist in the promoter region of COX-1 such as AP2, NF-κb, and NF-IL6; For COX-2, there is a TATA box indicating a regulated gene and several regulatory elements are found in its promoter region such as CRE, NF-κB, and ERE. The regulation of both COX-1 and COX-2 may be tissue- or cell specific under some circumstances.

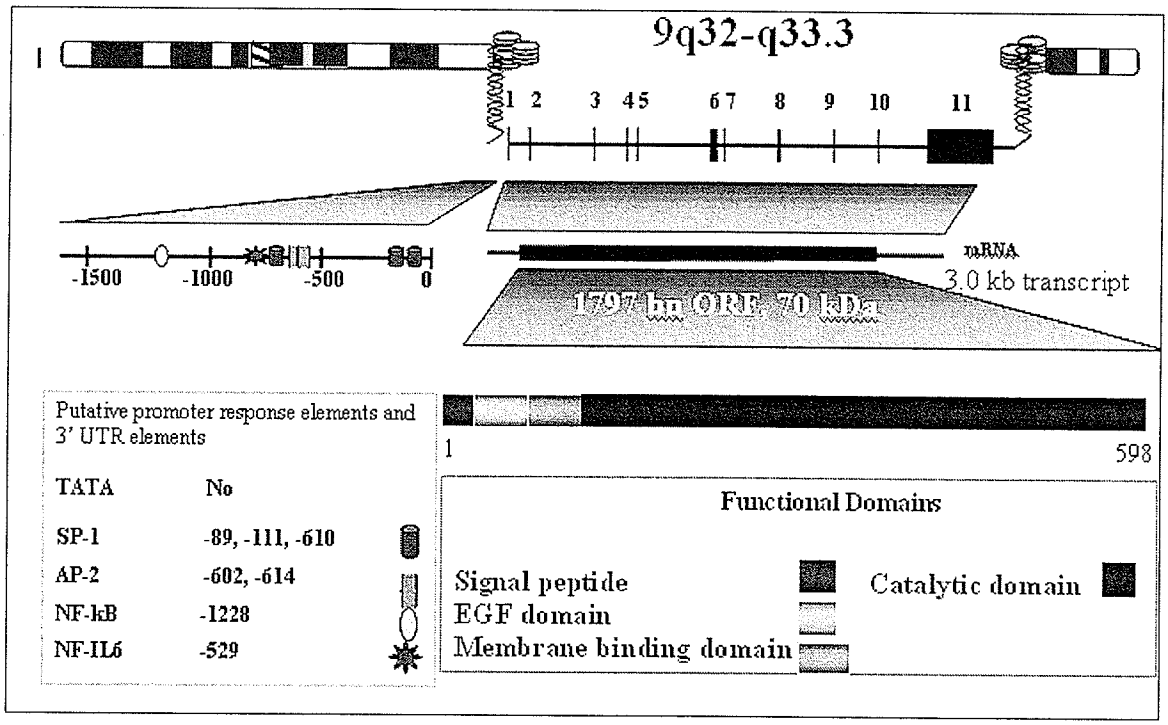

Figure 22. Gene Structure, promoter sequence, transcript, and functional domains of human COX-1. (Modified from CaymanChem.com)

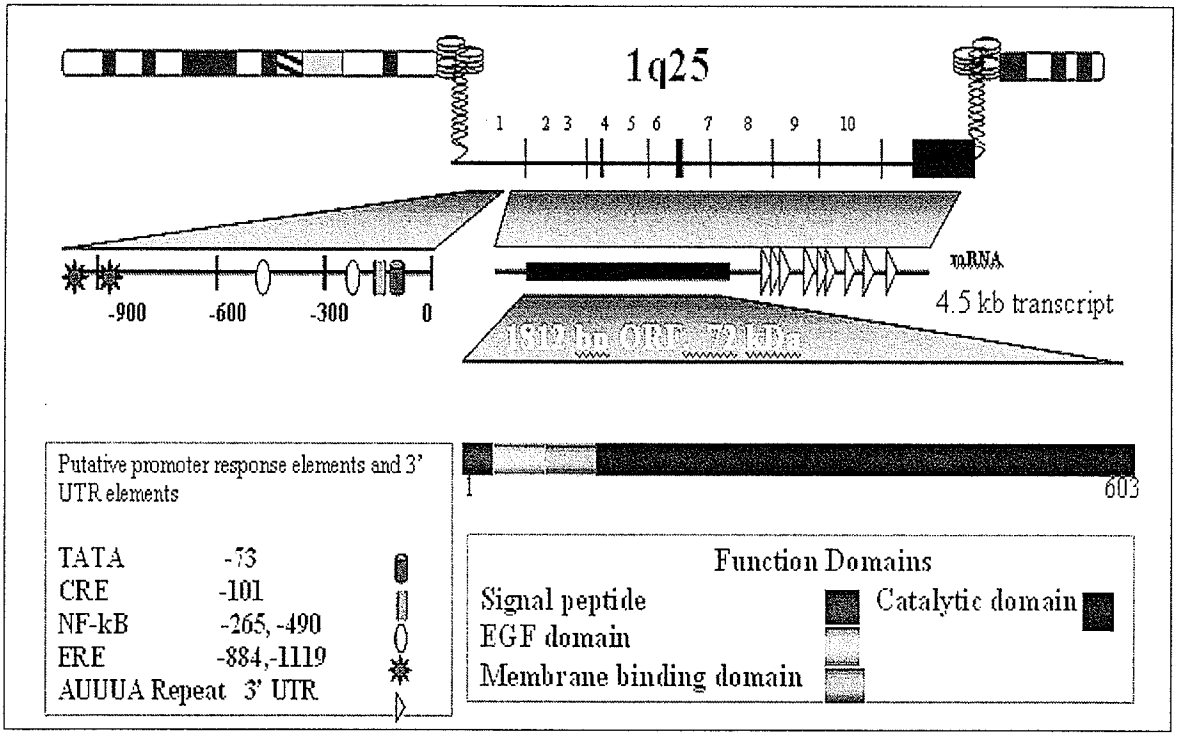

Figure 23. Gene Structure, promoter sequence, transcript, and functional domains of human COX-2. (Modified from CaymanChem.com)

IV APPLICATIONS OF BIOINFORMATICS IN LIPID RESEARCH

4.1 Bioinformatics

The definition of Bioinformatics has not been universally agreed upon. The NIH Bioinformatics Web Site defines Bioinformatics as "Research, development, or application of computational tools and approaches for use of biological, medical, behavioral or health data, including those to acquire, store, organize, archive, analyze, or visualize such data." Thus, Bioinformatics serves as an essential infrastructure underpinning biological research.

4.2 Biotechnology

Biotechnology has revolutionized the study of both cells and organisms. Mammalian cells can be engineered to express any desired proteins in a regulated manner, making it possible to analyze function of the protein and the effect on the cell or to use the gene product as a therapeutic drug or a vaccine for medical purposes (Alberts et al. 1994; Lodish et al. 2000). Driven by the discovery of DNA double helix and further decade-wise advancements of biotechnology, biomedical research is in an explosive phase (Figure 24). As information accumulates in ever more intimidating quantities, new techniques of data collection and analysis are in need to search for rational explanations to disconnected facts and mysteries (Alberts et al. 1994; Lodish et al. 2000). As a result, bioinformatics emerges as an elegant and dynamic multidisciplinary science that combines computer sciences, biosciences, and informatics.

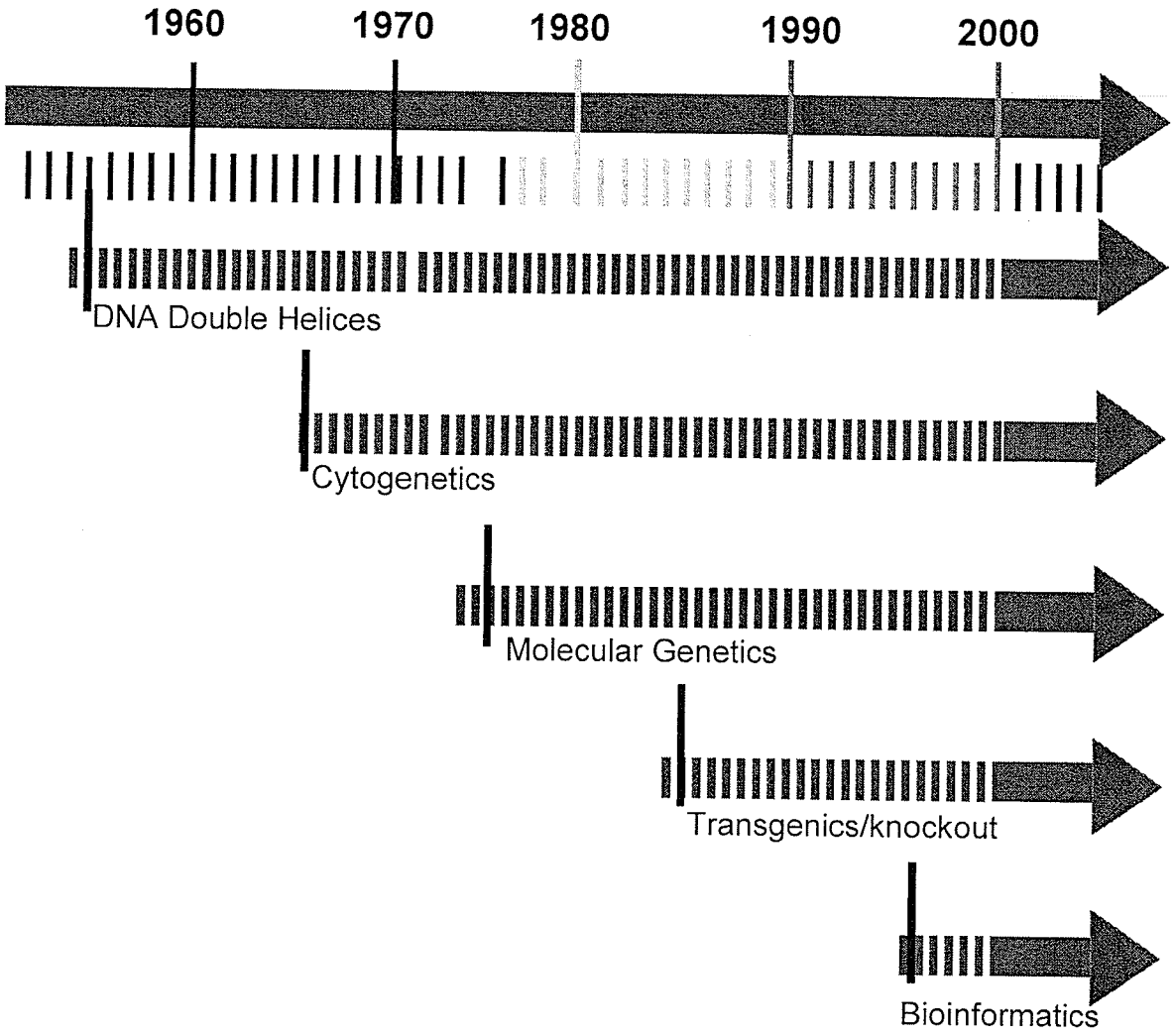

Figure 24. Important advancements of Biotechnology and the emergence of Bioinformatics.

4.3 Bioinformatic Databases and Information Retrieval

A database is a collection of data, typically describing activities of one or more related organizations. Bioinformatic databases refer to repositories for a collection of computerized biomedical data. Currently, several types of bioinformatic databases co-exist. These databases include: (1) general purpose database; (2) data type specific database; (3) organism specific database; (4) pathway information; and (5) National Center for Biotechnology Information (NCBI). NCBI is the largest repository of bioinformatic information and Entrez serves as a search and retrieval system for NCBI. Databases at NCBI provide access to various aspects of bioinformation including nucleotide sequences, protein sequences, macromolecular structures, whole genomes, and medical literatures via PubMed (Table 6).

Databases usually support operations including retrieval, insertion, updating, and deletion. Most databases offer the following features to allow easy searching: (1) restrict search to an organism; (2) restrict search to time frame; (3). Boolean searches by and/or/not Common identifiers for bioinformatic data provide another mechanism for fast retrieve of specific items. Commonly used identifiers include locus name, accession numbers, GenInfo (gi) ID, and Pubmed ID (PMID). Data are stored in servers and database models define data organization such as relational, object oriented/relational, hierachical/semistructured models. Upon retrieval, data can be presented in a variety of formats such as the FASTA, GenBank, SwissProt, XML, and internal standard format (ASN.1). For example, the most popular formats are FASTA and GenBank for nucleotide and protein sequences. FASTA tools use FASTA or Pearson format files and the files contain comment line followed by sequence data without annotation. GenBank is

a flat file format and contains detailed annotation (description of the sequences such as locus, organism, function domains, version, also authors, related information, and publications) of gene/protein sequences.

Table 6. Databases in National Center for Biotechnology Information. (up to August 25, 2003)

Database Name	Description
PubMed	Biomedical literature
Nucleotide	DbEST, dbGSS, dbSNP, dbSTS, Nucleotide, GenBank, HomoloGene, MGC, PopSet, RefSeq, TPA, TraceArchive, UniGene, UniSTS
Protein	Domains: Conserved Domains (CDD) Proteins: Sequence database PROW: Protein Review on the Web RefSeq: Nonredundent set of sequences
Structure	Domains: Conserved Domains (CDD) Structure (MMDB): 3-D macromolecular structure 3D Domains: domain from Structure
Genome	Genomes: over 800 organisms LocusLink: Curated sequence info bout gene loci COGs: Clusters of Orthologous Groups of Proteins
Expression	GEO: Gene Expression Omnibus SAGE: Serial Analysis of Gene Expression

4.4 Software Tools and Data Analysis

Software tools include management tools; retrieve tools; and analysis tools. Management tools are service tools that are not visible for end users. Tools for data collecting, storing, sorting, updating are in management category. Retrieve tools allow users to search and retrieve useful information. Analysis tools are particularly important for extracting, comparing and visualizing information retrieved. Table 7 summarizes commonly used analysis tools.

4.5 Knowledge Discovery in Databases

The knowledge discovery is a dynamic process involving data mining (Figure 25). Data mining is a complex process involving searching, filtering, extracting, comparing, evaluating and visualizing of data and information. In the process, various computational analysis tools are used. Figure 25 illustrates process of knowledge discovery in databases.

Table 7. Selected analysis software tools.

Genome Tools	RNA Tools	Protein Tools
Transcriptional factor binding sites	Expressed sequence tag (EST)	Basic local alignment search tool (BLAST)
Gene finder	Multiple sequence alignment (ClustalW)	Conserved domain database (CDD) and CD-search
Contig. construction	Translation	Multiple sequence alignment (ClustalW)
Basic local alignment search tool (BLAST)	RNA motif search program	Prediction of transmembrane regions
WWW submission tool for sequence submission	Serial Analysis of Gene Expression (SAGE)	Prediction of presence and location of signal peptide
LocusLink	Cancer Genome Anatomy Project (CGAP)	3-D structure and sequence alignment viewer

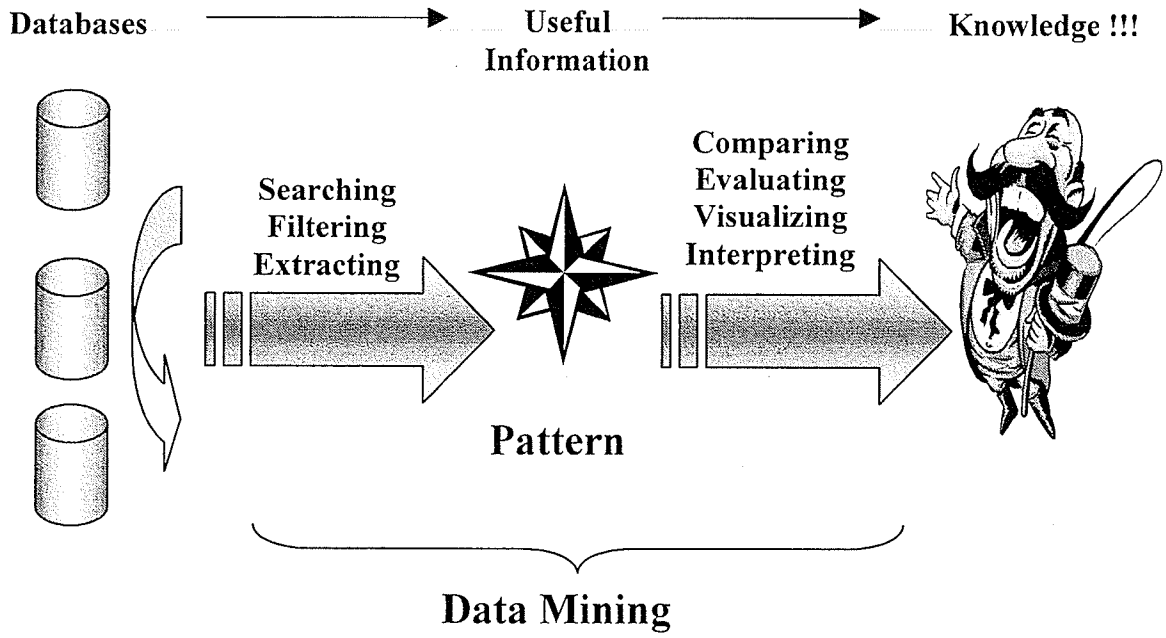

Figure 25. Process of knowledge discovery via data mining.

4.6 Bioinformatic Resources

4.6.1 Expressed Sequence Tag (EST)

EST is a collection of expressed sequence tags, or short, single-pass sequence reads from mRNA (cDNA) (Adams et al. 1991; Boguski et al. 1993). Most of the human cDNAs are derived from normalized libraries from several tissues, although tissue/cell line specific dbEST are also available. Read length are 300-500 bases, with a typical accuracy of 98%. dbEST also includes sequences that are longer than the traditional ESTs, or are produced as single sequences. Regardless of length, quality, or quantity, ESTs are scarcely annotated with respect to tissue and library source, 5' or 3' read, database similarities, and range of high quality data.

ESTs represent a snapshot of genes expressed in a given tissue and/or at a given developmental stages. They are tags of expression for a given cDNA library. ESTs have applications in the discovery of new human genes, mapping of the human genome, and identification of coding regions in genomic sequences. Four dbESTs are available for searching at NCBI: human dbEST, mouse dbEST, other dbEST, and the combined dbEST.

4.6.2 Conserved Domain Database (CDD)

In biological sciences, domain is defined as recurring functional and/or structural units of a protein. Proteins often contain several modules or domains, each with a distinct evolutionary origin. Molecular evolution might have utilized such domains as building blocks to modulate protein function. Conserved domains, in turn, contain conserved

sequence patterns or motifs, which allow for their detection. Computational biologists exploit conservation property of domains to identify domains in a protein sequence (CD-search). Conserved domain database (CDD) can be summarized with multiple local sequence alignments. CDD contains domains derived from three key collections, Smart, Pfam, and COG (Tatusov et al. 1997; Bateman et al. 2002; Letunic et al. 2002). Smart (Simple Modular Architecture Research Tool) and Pfam (Pfam-A seed alignments) are public domain databases, whereas COG (Clusters of Orthologous Groups) is an NCBI-curated protein classification resource. LOAD (Library Of Ancient Domains) constitutes a small set of CDD.

4.6.3 Basic Local Alignment Search Tool (BLAST)

BLAST is a set of similarity search programs designed to explore all of the available sequence databases including DNA or protein. BLAST uses a heuristic algorithm that seeks local as opposed to global alignments and is therefore able to detect relationships among sequences that share only isolated regions of similarity (Altschul et al. 1990; Gish and States 1993).

Many different types of BLAST are available for certain types of searches. The BLAST services in NCBI include four main categories: (1) nucleotide BLAST; (2) Protein BLAST; (3) Translating BLAST; (4) CD-search; and (5) Specialized BLAST. Table 8 is a brief description of BLAST services provided by NCBI (Table 8).

4.6.4 Multiple Sequence Alignments

Sequence alignment, based on an understanding of sequence variation, is one of the most fundamental principles explored by bioinformatic data mining (Altschul et al. 1990; Gish and States 1993). Alignment tools allow researchers to compare gene (DNA, RNA, protein) sequences in order to: (1) infer the structure of genes and gene products; 2) infer the function of genes; (3) infer the evolutionary history of genes/organisms; and (4) identify the variation responsible for disease and other complex phenotypes.

Table 8. Description of BLAST services in NCBI.

Type	Description
Nucleotide BLAST	Nucleotide sequences against other nucleotide sequences.
Protein BLAST	Protein sequences against other protein sequences.
Translating BLAST	Nucleotide/Protein sequences against other nucleotide/protein sequences
CD-Search	Protein sequence against the conserved domain database
Specialized BLAST	Sequences against Human Genome, Microbial Genome, Plasmodium falciparum, Vectors, Immunoglobulin sequences.

4.7 Applications of Bioinformatics in Lipid Research

The major task after the human genome has been fully sequenced is to understand the function and regulation of every encoded protein. However, mammalian genetic approaches to study gene function have been hampered by the lack of efficient tools to identify genes that are predicted to have membrane-spanning regions. As discussed in previous sections, most enzymes involved in lipid metabolism are either integral membrane proteins or peripheral membrane proteins. To overcome this limitation, two novel approaches have been under development. These approaches include global analysis of protein activities using proteome chips and data mining of biological databases using analytical software tools (Zhu et al. 2000; Yen et al. 2002; Yen and Farese 2003; Zhu and Snyder 2003).

Currently, significant advancements have been made and they come from mRNA expression patterns, gene disruption phenotypes, two-hybrid interactions, and protein subcellular localization (DeRisi et al. 1997; Lashkari et al. 1997; Ross-Macdonald et al. 1999; Uetz et al. 2000; Uetz and Hughes 2000). A novel protein chip technology that allows the high-throughput analysis of biochemical activities has been also developed and is proving to be extremely useful for lipid research (Zhu et al. 2001; Zhu and Snyder 2001; Phizicky et al. 2003). Conserved domain databases and the availability of 3-dimensional of certain enzymes would facilitate the identification and cloning of novel enzymes that have specific enzymatic activities in a very efficient and effective way (Yen et al. 2002; Yen and Farese 2003). Thus potential applications of Bioinformatics in lipid research could be enormous: to identify and clone novel enzymes; to define the identities, quantities, structures; to characterize the properties in different cellular contexts; and to

study the regulation of each enzyme. Several specific examples are listed in Table 7 to demonstrate potential usage of Bioinformatics in lipid research.

Table 7. Selected published reports involving applications of Bioinformatics in lipid research.

Author	Bioinformatic Approach Taken
Zhu et al. 2000	Analysis of yeast protein kinases using protein chips
Zhu et al. 2001	Phospholipid interacting proteins using protein chips
DeRisi et al. 1997	Gene expression and regulation using DNA arrays
Ross-Macdonald et al. 1999	Gene expression, localization, and function using gene disruption
Uetz et al. 2000	Protein interaction using yeast two-hybridization system
Aguado and Campbell 1998	Identification of a human LPAAT using gene finding and assembling tools
West et al. 1997	Identification of human LPAAT using homology searching tools.
Ganesh Bhat et al. 1999	Identification of rat AGPAT using homology searching tools
Cheng et al. 2003	Identification of MGAT-3 using homology searching tools and EST databases.
Vaz et al. 2003	Enzymatic activity using yeast and human genetics

V. RESEARCH AIMS AND HYPOTHESIS

Lipids are the building blocks of the biological membrane, and phospholipids are principal lipids in plasma membrane. In addition, the hydrolysis of phospholipids provides a source of lipid signaling molecules that are involved in many basic biological processes and human diseases. The general purpose of this research was to study the control of phospholipid metabolism in mammalian tissues. More specifically, the identification of novel acyltransferases in phospholipid biosynthesis and the control of arachidonate-eicosanoid cascade were investigated. The flowchart describing this study is depicted in Figure 26.

In the first part of the study, acyltransferases involved in phospholipid biosynthesis were identified via data mining. Since PA is the central phospholipid in metabolism, acyltransferases for PA biosynthesis was chosen for our study. We hypothesized that acyltransferase isoezymes for PA synthesis exist in multiple molecular forms, and acyltransferases exhibit convergence in sequence similarities and domain structures. In order to test this hypothesis, data mining of biological databases was conducted to identify novel enzymes (AGPAT) that catalyze the acylation of 1-acyl-*sn*-glycerol-3-phosphate to form 1,2-diacyl-*sn*-glycerol-3-phosphate. By using conserved sequences and BLAST algorithms, several acyltransferases were identified from murine and human EST databases and candidate gene expression profiles were studied at the mRNA level. Subsequently, these candidate genes were cloned and their encoded proteins were analyzed for acyltransferase activities. In addition the domain structure and catalytic motifs were also analyzed using computational analysis softwares. Data

obtained from this study supported our hypothesis that acyltransferase AGPATs are convergent in domain structures and sequence similarities.

Barth syndrome gene G4.5 or TAZ is one of 8 acyltransferases identified via data mining. Mutation of TAZ has been shown to cause a disease called Barth syndrome. G4.5 or TAZ may encode a group of proteins termed tafazzins due to alternative splicing. In the human, multiple splice variants have been identified with the two most abundant forms that differ in sequences due to alternative splicing of exon 5. We hypothesized that exon 5 deleted tafazzin is evolutionarily conserved form thus the potential functional form. The conservation of exon 5-deleted tafazzin was studied by comparative genomic approaches.

In the second part of the study, the arachidonate-eicosanoid cascade was studied. We hypothesize that the regulation of arachidonate-eicosanoid cascade is controlled by multiple signaling pathways, which are interconnected at multiple stages during the signal transduction processes. Our initial attempt was to identify and characterize signaling pathways that can regulate this catabolic pathway. Subsequently, detailed mechanisms of regulation were examined using two different cell models.

The knowledge gained from this study would contribute to our understanding of how phospholipid metabolism in mammalian tissues is maintained and regulated. Our findings may lead to the development of new strategies for the treatment and prevention of hereditary metabolic diseases as well as cardiovascular and inflammatory diseases.

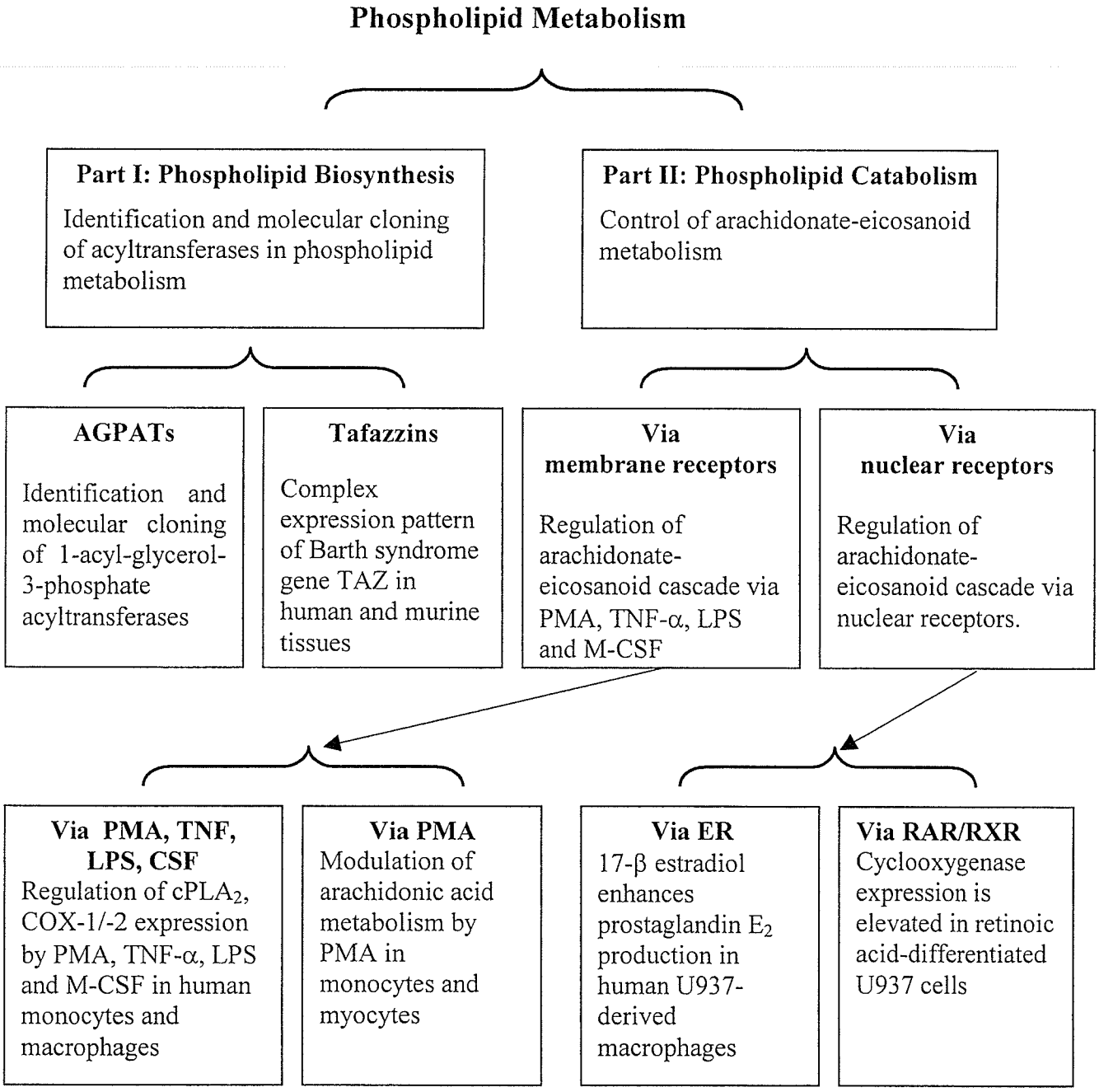

Figure 26. Scheme of the research.

MATERIALS AND METHODS

I. MATERIALS

1.1 Experimental Animals and Cell Lines

Male C57 mice (aged 8 – 9 weeks) were used for the isolation of total RNAs from various tissues. Total RNAs were used for the synthesis of cDNAs and Northern Blotting analysis. The human premonocytic cell line U-937, African green monkey SV40 transformed kidney cell line (COS-1), and mouse fibroblast cell line NIH3T3 were purchased from the American Type Culture Collection (ATCC). The human umbilical vein endothelial cells were purchased from Cascade Biologics, Inc. (Portland, Oregon).

1.2 Radioisotopes

α- [^{32}P] dCTP (800 Ci/mmol) at 10 mCi/ml, [^{35}S] methionine (>1,000 Ci/mmol) at 10 mCi/ml, and [5,6,8,9,11,12,14,15-^{3}H]-arachidonic acid (209 mCi/mmol) was purchased from Amersham Pharmacia Biotech (Buckinghamshire, England). γ- [^{32}P]ATP (6000 Ci/mmol at 10.0 mCi/ml) was purchased from Perkin Elmer Life Sciences, Inc. (Boston, MA). 1- [^{14}C] Oleoyl-coenzyme A (50 uCi/ml) in 0.01 M sodium acetate was purchased from Amersham Pharmacia Biotech (Buckinghamshire, England).

1.3 Antibodies

Polyclonal anti-COX-2 antibodies, monoclonal anti-cPLA$_2$ antibody, and polyclonal anti-Actin antibodies were purchased from Santa Cruz Biotechnology, Inc.

(Santa Cruz, CA). Monoclonal anti-COX-1 antibody was purchased form Cayman Chemical Co. (Ann Arbor, MI). Mouse monoclonal anti-ER-α antibody was from Novacastra Laboratories Ltd. (Newcastle upon Tyne, United Kingdom). Mouse monoclonal anti-V5 antibody was from Invitrogen Canada Inc. (Burlington, ON). Donkey anti-goat antibody was purchased from Santa Cruz Biotechnology, Inc. and sheep anti-rabbit antibody was purchased from Amersham Pharmacia Biotech (Buckinghamshire, England).

1.4 Biochemicals, Hormones, and Cytokines

17-β estradiol, 17-α estradiol, and 4-hydroxytamoxifen (4-OH-TAM) were purchased from Sigma Chemical Company. ICI 182,780 was purchased from TocrisCookson Inc. (Ellisville, USA). Phorbol 12-myristate 13-acetate (PMA), tumor necrosis factor-alpha (TNF-α), macrophage colony-stimulating factor (M-CSF), and lipopolysaccharide (LPS) were purchased form Sigma Chemical Company.

1.5 Restriction Enzymes and Modifying Enzymes

Restriction and modifying enzymes including BamHI, EcoRI, HindIII, KpnI, NcoI, NotI, PstI, Xho I, T4 DNA Ligase, T4 DNA Polynucleotide kinase, Taq DNA polymerase, Platinum Pfx DNA polymerase, and RNaseOUT Ribonuclease Inhibitor (Recombinant) were purchased form Invitrogen life technologies.

1.6 Commercial Kits and Experiment Systems

PGE_2 EIA assay kit was purchased form Cayman Chemical Co. (Ann Arbor, MI).

Cell Proliferation Reagent WST-1 was purchased from Boehringer Mannheim. Subcloning efficiency DH5α Chemically Competent E. Coli were purchased from Invitrogen life technologies. RNAzol Reagent of total RNA isolation was purchased from Invitrogen life technologies. Rapid-hyb buffer of Northern blotting hybridization was purchased from Amersham Pharmacia Biotech. (Little Chalfont Buckinghamshire, England). QIAprep Miniprep Kit and HiSpeed Plasmid Midi Kit for plasmid preparations were purchased from QIAGEN Inc. (Mississauga, ON). ECL Western Blotting Detection Reagents were purchased from Amersham Bioscience (Little Chalfont Buckinghamshire, England). TNT Coupled Reticulocyte Lysate Systems for *in vitro* protein synthesis were purchased from Promega Corporation (Madison, WI). pcDNA3.1/V5-His TOPO TA Expression kit was purchased from Invitrogen life technologies. BCA Protein Assay Reagent and BioRad Protein Assay Reagent for protein assay were purchased from PIERCE (Rockford, IL) and Bio-Rad Laboratories (Hercules, CA) respectively.

1.7 Cell Culture Medium, Lipid Standards, and Other Materials

Dulbecco's modified Eagle's medium, RPMI-1640 medium, phosphate-buffered saline, bovine serum albumin (BSA), and other chemicals were obtained from Sigma Chemical Company (St. Louis, MO). Ionomycin (a calcium ionophore) was obtained from Biomol Inc. (Plymouth Meeting, PA). All lipid standards were obtained from Doosan-Serdary (New Jersey, USA). Thin layer chromatography plates (SIL G-25) were the products of Mecherey-Nagel (Postfach, Germany).

II. METHODS

2.1 Culture of Human Premonocytic U937 Cells

The human premonocytic cell line U-937 (CRL-1593.2) was obtained from ATCC. These cells were grown in cell culture flasks with PRIM-1640 medium containing 10% fetal bovine serum, 100units/ml of penicillin G, 10μg/ml of streptomycin, and 0.25 μg/ml amphotericin B. For subculture, the cells were sedimented by centrifugation at 1000 rpm for 5 min. The cell pellet was resuspended in fresh medium and subcultured in a 1: 4 ratio. The cells used for experiments were seeded in culture dishes at a density of $3X10^5$/ml.

2.2 Cell Differentiation Method and Treatment

In macrophage cell model, the human premonocytic U-937 cells were differentiated into macrophages by incubation with PMA (cell density of $3X10^5$/ml in the presence of 162 nM PMA in the culture medium for 48 h). At the end of the induction, macrophages became firmly attached to the bottom of the cell culture dish. Undifferentiated floating cells and dead cells were washed away with three rinses of warmed serum-free RPMI-1640 medium containing 0.1% BSA. Subsequently, cells were incubated in the above serum-free medium with appropriate amount of reagents for the prescribed amount of time.

For estradiol treatment experiments, U-937 cells were switched to serum and phenol free medium containing 0.1% BSA and incubated for 12 hours before the appropriate amount of ER ligands in vehicle or vehicle alone (0.01% dimethylsulfoxide) were added for the prescribed period of time.

2.3 Culture of Rat Heart Myoblast H9c2 Cells

H9c2 cell, a rat heart myoblast cell line, was obtained from ATCC. These cells were grown in cell culture flasks with Dulbecco's modified Eagles medium containing 10% fetal bovine serum, 100 units/ml of penicillin G, 10μg/ml of streptomycin, and 0.25 μg/ml amphotericin B. The cells were incubated at 37 ^{0}C in an atmosphere of 95% humidified air and 5% carbon dioxide until 70% confluence was achieved. In some experiments, cells were switched to serum-free medium containing 0.1% BSA and incubated for 12 hours before the appropriate amount of PMA in vehicle or vehicle alone (0.01% dimethylsulfoxide) were added for the prescribed period of time.

2.4 Culture of COS-1 and NIH3T3 Cells for Transfection Studies

Two cell lines were used for transfection studies: COS-1 and NIH3T3. COS-1 line was a SV40 transformed African green monkey kidney cell line, and NIH3T3 was a mouse fibroblast cell line. Both cell lines were originally purchased from ATCC. Cells were maintained in culture flasks with Dulbecco's modified Eagles medium containing 10% fetal bovine serum, 100 units/ml of penicillin G, 10μg/ml of streptomycin, and 0.25 μg/ml amphotericin B. Upon experiments, cells were seeded in culture dishes at a density of 3-5 X10^{5} per 10-cm dish.

2.5 Giemsa Staining and Morphological Observation

U937 cells, PMA-treated U937 cells, and retinoid acid-treated U937 cells were collected and fixed in ice-cold methanol (100%) for 4 min. After fixation, cells were placed on slides and stained for 60 min at room temperature in freshly prepared Giemsa

solution (0.02% g/v Giemsa, 12% glycerin v/v, 12% methanol). Subsequently, the stained slides were mounted by Geltol Mounting Medium (*Immunon Thermo*, Shandon, Pittsburgh, PA) and images were taken and processed by Nikon ECLIPSE E1000 and Nikon ACT-1 Software (Version 2.00, Nikon).

2.6 Immunocytochemical Staining of Human ER-α

The expression of human ER-α in both undifferentiated and PMA-differentiated U937 cells were analyzed by immunocytochemical procedures. Briefly, cells were collected and fixed with 100% methanol for 5 min at room temperature. After washing with ice-cold PBS, the cells were exposed to a primary mouse anti-human ER-α monoclonal antibody (mAb) for 1 h at room temperature (Novocastra, Newcastle-upon-Tyne, UK). The specific binding of antibody and antigen was revealed through a secondary biotinylated anti-mouse-IgG, and the streptavidin-biotin-peroxidase amplification reagents according to the manufacturer's instruction (DAKO Corporation, Santa Barbara, CA).

2.7 Fluorescence-activated Cell Sorting (FACS)

Cell surface antigen CD11b was determined by fluorescence-activated cell sorting analysis (FACS). Untreated, PMA-differentiated U937 cells, or RA-treated U937 cells were harvested and washed once with PBS containing 0.2% BSA. Subsequently, aliquots of cell suspension (50 μl) were incubated with human monoclonal antibodies (Phycoerythrien (PE)-conjugated CD11b) for 30 min at 4 ^{0}C. Isotopic control antibody IgG1-PE was also included in the analysis. At the end of incubation, cells were washed

once with PBS/BSA buffer, fluorescence in the sample was determined by a Becton Dickinson FACS. Cursors were set to make sure that cells incubated with isotopic control antibody were less than 2% nonspecifically stained (This work was done by the help of Dr. Jie Yang in the Department of Microbiology, University of Manitoba).

2.8 Determination of Cell Viability

Cellular toxicity was determined by the WST-1 assay, which is based on the assessment of mitochondrial succinate dehydrogenase activity (Jiang et al. 2001). Subsequent to RA treatment, U937 cells were incubated at 37^0C for 3 h with the WST-1 reagent (0.2 mg/ml) dissolved in culture medium. The medium was collected and the extent of reduction of WST-1 to formazan within cells was quantitated by measuring the absorbance at $A_{440\ nm}$ with an ELISA reader.

2.9 Whole Cell, Cytosolic, and Nuclear Extracts Preparation

Cells were collected by centrifugation and washed once using ice-cold PBS. The cell pellets were then suspended in whole cell extraction buffer (WCEB: 20 mM Tris-HCl, pH 7.5; 0.4 M KCl; Glycerol 20% (v/v); 2 mM PMSF; 2 mM DTT; complete proteinase inhibitor tablet). Whole cell extracts were prepared by three rounds of freezing and thawing. Subsequently, cell debris were sedimented by centrifugation for 20 min at 12,000 x *g* and the cell extract in the supernatant was collected and stored in –70 ^{0}C. For the preparation of soluble and nuclear extracts, cells were first suspended in hypotonic buffer (HB: 15 mM Tris-HCl, pH 7.4; 15 mM NaCl; 60 mM KCl; 0.5 mM EDTA; 1 mM PMSF; 1 mM DTT and one unit of proteinase inhibitor /10 ml, 0.5% Triton X100). The

soluble extract was prepared by incubating cells in HB for 20 min on ice, and followed by centrifugation at 4,000 × g for 8 min. The sedimented nuclei fraction was then dissolved in nuclear extraction buffer (same as WCEB). Nuclear proteins were extracted by three rounds of freezing and thawing. Finally, the chromatin was sedimented by centrifugation for 20 min at 20,000 x *g* and nuclear extracts (supernatant) were and stored –70 ^{0}C.

2.10 Protein Determination

Bradford Assay and bicinchoninic acid assay (BCA Assay) were two methods used to determine protein content in solution. Bradford Assay is a rapid and reliable, whereas BCA Assay is a variation of the Lowry assay. The BCA Assay is a reliable method but the assay has slower reaction time compared to that of Bradford Assay.

For Bradford Assay, Bio-Rad kit with pre-mixed reagents was used. Briefly, protein solution was pipetted into microcentrifuge tube. Bio-Rad Bradford working solution (1 ml) was added and the absorption at $A_{595\ nm}$ was recorded. Sample protein concentration is calculated form a standard curve plotted by using BSA as protein standard.

For BCA Assay, Pierce kit with Reagent A and B was used. Briefly, 1 volume of sample was mixed with 20 volumes of standard working reagent (50 volumes of Reagent A and 1 volume of Reagent B). The mixture was incubated at 37^{0} C for 30 minutes and the absorption at $A_{562\ nm}$ was recorded. Sample protein concentration was calculated from a standard curve by using BSA as protein standard.

2.11 Immunoblotting Analysis of Enzyme Protein Levels

Cells were collected and washed in ice-cooled PBS buffer and the cell pellet was obtained by a centrifugation at 1000 × g for 10 min. at 4^0 C. The cell lysate was prepared by treating cells on ice for 20 min with the lysis buffer containing 15 mM Tris, pH 8.0, 0.5% Tween X-100, 1mM DTT, 0.5 mM EDTA, and 1 mM phenylmethysulfonyl fluoride (PMSF). Subsequently, the supernatant was obtained by centrifugation at 4,000 × g for 8 min. The protein concentration of the supernatant was determined by the Bio-Rad protein assay kit, using bovine serum albumin as standard.

Samples containing 30 to 50 μg of protein were subjected to sodium dodecylsulfate/8.0% polyacrylamide gel electrophoresis (SDS-PAGE) with pre-stained protein markers as references. Protein fractions in the gel were transferred to the Immobilon-P transfer membrane. The membrane was incubated with the monoclonal anti-cPLA$_2$ (1: 200 – 1:500), anti-COX-1 (1: 1000), polyclonal anti-COX-2 (1: 500), or polyclonal anti-Actin (1: 2000) antibodies. The membranes were then exposed to secondary antibodies that were coupled to horse-radish peroxidase. The protein bands were detected on film using a Western blotting detection reagent kit. The relative intensities of protein bands were acquired using Bio-Rad MultiImaging System (Bio-Rad Laboratories), and data were digitized and analyzed by the Quantity One software supplied by Bio-Rad Laboratories.

2.12 Measurement of AA-release

The AA released from the cells was determined as described previously (Tran et al. 1996; Wong et al. 1998). Briefly, cells treated with PMA or vehicle were stimulated

with 5 μM calcium ionophore for 15 min, and the labeled AA released into the medium was determined. The recovered medium was acidified with 50 μl of glacial acetic acid, an 0.8-ml aliquot was resolved by thin layer chromatography in a solvent system consisting of hexane/diethyl ether/acetic acid (70:30:1, v/v). The fatty acid fraction on the thin-layer chromatographic plate was visualized by iodine vapor, and its radioactivity was determined by liquid scintillation counting.

2.13 Measurement of PGE_2 Production

The production of PGE_2 in U937 and H9c2 cells were determined by enzyme immuno assay (EIA). After the treatment, the medium was collected to determine the endogenous production of PGE_2 by EIA using a commercial prostaglandin E_2 EIA Kit. Briefly, 50 μl of the standard PGE_2 or samples was added to the pre-coated mouse anti-rabbit IgG macrotitre plates. Subsequently, 50 μl PGE_2 tracer and 50 μl monoclonal antibody of PGE_2 were added into each well and the mixture was incubated for 18 h at 4^0 C. Following the incubation, the content in each well was removed and the wells were washed with PBS buffer containing 0.05% Tween-20 for 12 times. After the wash, wells were incubated with 200 μl Ellman's reagent for 90 min at room temperature on a shaker, or until a yellow color developed. The absorbance of solution was measured by a microplate reader at $A_{412\,nm}$. PGE_2 concentrations were calculated from a standard curve.

2.14 Isolation of Total RNA

Total RNA was extracted from cultured cells or murine organs (Lu et al. 1999). Briefly, cultured cell pellets or minced organs were homogenized with 1 ml TRIzol

reagent for one minute. The homogenates were poured into a microcentrifuge tube and 0.2 ml chloroform and shaken for 30 seconds. Samples were spun at 4 ^{0}C, 10,000×g for 15 min. After centrifugation, the upper aqueous phase was transferred to a sterile microcentrifuge tube followed by addition of an equal volume of ice-cold isopropanol. The solution was mixed well and stored at room temperature for 5 min. Samples were centrifuged again as same as the above condition to pellet the RNA. The pellet was washed with 1 ml of 75% ice-cold ethanol and RNA was finally collected by centrifugation. The total RNA was resuspended in double distilled water.

The purity and the yield of isolated RNA were determined by monitoring absorbance at $A_{260\ nm}$ and $A_{280\ nm}$. The integrity of the RNA was confirmed by performing denaturing agarose gel electrophoresis on the isolated RNA samples.

2.15 RNA Denaturing Electrophoresis and Northern Blot Analysis

Total cellular RNA was extracted from cells by the TRIZOL Reagent and 10-15 μg of total cellular RNA per lane were fractionated in formaldehyde-containing 1.0% agarose gels. Subsequently, the RNA was transferred to nylon-supported Hybond-N+ membrane. After UV-cross-linking, membranes were hybridized within Rapid-hyb buffer for 2 hours at 65 ^{0}C with a radiolabeled human Cox-1 or Cox-2 cDNA probe. After hybridization, membranes were washed for 20 min at room temperature in 2XSSC with 0.1% SDS, and twice for 20 min in 0.1XSSC with 0.1 SDS. Washed membranes were then subjected to autoradiograph. Cox-1 and Cox-2 cDNA probes (Cayman Chemical, MI) were labeled with $\alpha[^{32}P]$dCTP by Random Prime Labeling System following the

manufacturer's instruction. The density of the bands was scanned and quantified by Molecular Imager FX and QuantityOne software (BioRad, CA).

2.16 PCR Primers and RT-PCR Conditions

The cDNA of each of murine AGPAT1/2/3/4/5 was amplified with a pair of specific primers. Using the computationally constructed gene sequence as amplification template, the primers were designed using Vector NTI Suite software of InforMax (Vector NTI, Version 7, Oxford, United Kingdom). All primers were synthesized by Invitrogen Canada Inc. (Burlington, ON). Primers used to amplify human TAZ and murine TAZ were also similarly designed and synthesized. The sequence of primers and the length of predicted PCR products were listed in Table 9.

The first strand cDNA from 1 μg total RNA was synthesized as described previously (Lu et al. 1999). A typical reaction contained 150 U of Moloney murine leukemia virus (M-MLV) reverse transcriptase, 25 pmol of random hexamer primer, 20 U of ribonuclease inhibitor, 1 mM dithiothreitol (DTT), and 10 pmol each of the four deoxynucleotides (dNTPs), in a total volume of 15 μl. The reaction was incubated at 37 ^{0}C for 1 hour, and terminated by boiling at 95 ^{0}C for 5 min. An aliquot of 1.0 ~ 1.2 μl of the resultant cDNA preparation was used directly for each amplification reaction.

Polymerase chain reaction (PCR) was performed in 20 μl reaction mixtures containing 8 pmol of each primer, 8 pmol of each dNTP and 0.4 Taq DNA polymerase. The mixture was overlaid with 30 μl mineral oil to prevent evaporation. The reaction mixture was incubated in a Perkin-Elmer DNA Thermal Cycler under conditions listed in Table 8.

To clone cDNA, high fidelity Platinum pfx DNA polymerase was used to amplify cDNA (the extension temperature is 68 ^{0}C as opposed to 72 ^{0}C). At the end of PCR reaction, 10 U of Taq DNA polymerase were added into the reaction mixture and incubated for 60 more min at 72 ^{0}C to add an A nucleotide to 5' end of each strain to facilitate TA cloning.

Table 8. PCR primer design

Primer Name	Sequence	Product Length (Region)	GenBank Access No.
AGPAT1 (F)	5'-ACCAGAATGGAGCTGTGGCC-3'	846 bp (313-1158)	NM_018862
AGPAT1 (R)	5'-CGCTCCCCCAGGCTTCTTCA-3'		
AGPAT2 (F)	5'-CGCCGTCGGGGCTGGGGTGC-3'	861 bp (181-1041)	XM_130130
AGPAT2 (R)	5'-CTGGGCTGGCAAGACCCCAG-3'		
AGPAT3 (F)	5'-TGTTCTCAGTGAAGGACCGT-3'	1162 bp (70-1231)	NM_053014
AGPAT3 (R)	5'-CTTAAGCTCTTGGTTGCCAT-3'		
AGPAT4 (F)	5'-GATTTATCTCTTGAGAATCCCCACACC-3'	1161 bp (187-1347)	NM_026644
AGPAT4(R)	5'-GTCCGTTTGTTTCCGTTTGTTGTC-3'		
AGPAT5 (F)	5'-AGAGGATGCTGCTGTCCT-3'	1091 bp (721-1811)	XM_133988
AGPAT5 (R)	5'AACAAACCACAGGCAGCC-3'		
Beta-actin (F)	5'-GTGGGGCGCCCCAGGCACCA-3'	540 bp	
Beta-actin (R)	5'-CTCCTTAATGTCACGCACGATTTG-3'		

Table 10. PCR conditions

Primer Name	PCR Conditions	Cycles
AGPAT1(F)	Start: 94 ^{0}C 4 min. End: 72 ^{0}C 7 min.	25-32
AGPAT1 (R)	Cycle: 94 ^{0}C 1 min. 62^{0}C 30s. 72 ^{0}C 3 min.	
AGPAT2 (F)	Start: 94 ^{0}C 4 min. End: 72 ^{0}C 7 min.	25-32
AGPAT2 (R)	Cycle: 94 ^{0}C 1 min. 72 ^{0}C 3 min.	
AGPAT3 (F)	Start: 94 ^{0}C 4 min. End: 72 ^{0}C 7 min..	25-32
AGPAT3 (R)	Cycle: 94 ^{0}C 1 min. 55 ^{0}C 30s. 72 ^{0}C 2 min.	
AGPAT4 (F)	Start: 94 ^{0}C 4 min. End: 72 ^{0}C 7 min.	25-32
AGPAT4 (R)	Cycle: 94 ^{0}C 1 min. 55 ^{0}C 30s. 72 ^{0}C 2 min.	
AGPAT5 (F)	Start: 94 ^{0}C 4 min. End: 72 ^{0}C 7 min.	25-32
AGPAT5(R)	Cycle: 94 ^{0}C 1 min. 58 ^{0}C 30s. 72 ^{0}C 2 min.	
Beta-actin (F)	Start: 94 ^{0}C 4 min. End: 72 ^{0}C 7 min.	25
Beta-actin (R)	Cycle: 94 ^{0}C 1 min. 55 ^{0}C 30s. 72 ^{0}C 30s.	

2.17 Double-stranded DNA Sequence Analysis

The identity of each PCR product generated from RT-PCR using Taq or pfx DNA polymerase was verified by direct DNA sequencing. The gel fraction containing the target DNA, including AGPAT alpha, beta, gamma, delta, epsilon, and human and murine TAZ and their splicing forms, was excised and purified using standard methods. Briefly, the agarose band with DNA fractions were cut under UV light, each fraction was placed in a Spin-X centrifuge tube equipped with a filter and 100 μl H_2O was added. The solution containing the DNA fraction was obtained by centrifugation at 12,000 rpm for 5 min at 4 ^{0}C. The DNA in each fraction was extracted with phenol/chloroform, and the DNA in the aqueous fraction was allowed to precipitate in 1/10 volume of 3M sodium acetate (pH 5.5) mixed with 2.5 volume of 100% ethanol. The DNA was resuspended in H_2O, and an aliquot was submitted for double strained DNA sequencing analysis. The sequencing was performed using the Perkin-Elmer Applied Biosystems ABI310 Genetic Analyzer and the BigDye Terminator Cycle Sequencing Ready Reaction Kit at the Institute of Cell Biology, or Department of Microbiology, University of Manitoba, Winnipeg, Canada.

The nucleotide sequences obtained were used for homologous search by the Basic Local alignment Search Tool (BLAST) to confirm the identity of the sequences.

2.18 Construction of Expression Vectors for Murine AGPATs

The murine AGPAT2/3/4/5 expression plasmids were constructed using AT cloning strategy. Briefly, The RT-PCR fragments encompassing ORFs of the above genes were isolated and cloned into pcDNA3.1/V5-His-TOPO plasmid. Briefly, the RT-

PCR fragments were ligated into pcDNA3.1/V5-His-TOPO in a 6 μl reaction mixture (100 ng RT-PCR DNA fragment, 1 μl TOPO vector, 1 μl salt solution) for 5 min at room temperature. After ligation reaction, 2 μl of the ligation mixture was used to transform DH5α chemically competent E. coli. Positive colonies were picked up and cultured overnight in LB medium containing 50 μg/ml ampicillin. The plasmid DNA was isolated using Miniprep Kit. The identity and orientation of the inserted sequence was confirmed by both restriction enzyme digestion and double strained DNA sequencing.

2.19 Plasmids and Transient Transfection

For transient transfection analysis, either tagged or non-tagged enzyme expression vectors were generated. Murine AGPAT3, AGPAT4, AGPAT5 were tagged at their C-terminus with a polyhistidine and a V5 epitope tag using the pcDNA3.1/V5-His-TOPO plasmid. A murine exon-5 deleted TAZ was cloned into pcDNA3.1 was kindly provided by Dr. Grant Hatch. This murine exon-5 deleted TAZ has a C-terminus FlagTag sequence (DYKDDDDK). Full-length human TAZ in pCMV-SPORT6 (pCMV-SPORT6-hTAZ) was purchased from ResGen Invitrogen Corporation. The native cds was inserted in a direction controlled by both SP6 and CMV promoters. Murine AGPAT2 was cloned in pcDNA3.1 expression vector without an epitope tag.

For transient transfection experiments, Monkey kidney COS-1 cell line and murine fibroblast NIH3T3 cell line were used. The transfection was done using Effectene transfection reagent according to the manufacturer's instruction. Briefly, the day before transfection, the cells were seeded in 10-cm dishes at 3-5 X 10^5 cells per dish and left overnight. The dishes were 40% confluent on the day of transfection. The transfection

mixture was prepared according to the manufacturer's protocol, and then fresh medium was added to the transfection mixture. Finally, 3 ml per dish of the above mixture was added drop-wise into the medium and the dishes were gently swirled to ensure uniform distribution of the DNA-Effectene complexes. The cells were left for 48 h and then harvested. Cell extracts were prepared by sonification and were used to determine acyltransferase activity as described in enzyme assay section.

2.20 *In vitro* Transcription and Translation

In vitro transcription/translation reactions were performed using a coupled transcription/translation system (TnT coupled Reticulocyte Lysate System). Reactions were performed according to the manufacturer's instructions. TnT RNA polymerase SP6 or T7 was used to set up a translation reaction according to the promoter sequences available at the 5' of the inserted cds. Two setups for the transcription and translation preparations routinely used included radioactive reaction (using [^{35}S] methionine labeling) and non-radioactive reaction.

2.21 1-acyl-*sn*-glycerol-3-phosphate Acyltransferase Enzyme Assay

The activity of acyl-CoA: 1-acyl-*sn*-glycerol-3-phosphate acyltransferase was determined in reticulocyte lysates containing *in vitro* translated enzymes and cell extracts of transient transfected cells with corresponding plasmid DNA.

For *in vitro* translated enzymes, the assay mixture consisted of 100 mM Tris/HCl (pH7.4), 50 μM LPA (oleoyl-*sn*-glycerol –3-phosphate), 3 mM $MgCl_2$, 1 μl of 0.05 μCi [^{3}H]Oleoyl-CoA, and 10 μl reticulocyte lysate in a volume of 100 μl. The reaction was

incubated at 37 ^{0}C for 20 min, and terminated by addition of 0.62 ml methanol and 0.8 ml chloroform. A solution containing 3 μl saturated NaCl and 300 μl Tris/HCl (pH 7.4) was then added to the mixture to facilitate extraction and cause phase separation. The labeled phosphatidic acid in the lower phase was resolved by thin-layer chromatography (TLC) in a solvent system consisting of chloroform/ethanol/acetic acid/H_2O (50:20:6:2, by vol). The lipid standard on the thin-layer chromatographic plate was visualized by iodine vapor and the density of radioactive bands were scanned and quantified by a Molecular Imager FX equipped with QuantityOne software (Bio-Rad, CA) or visualized by exposure to Kodak X-OMAT X-ray film.

2.22 Monolysocardiolipin Acyltransferase Enzyme Assay

The activity of acyl-CoA: monolysocardiolipin acyltransferase was determined in cell extracts of transient transfected cells. For acylation of monolysocardiolipin (MLCL), the assay mixture consisted of 100 mM Tris/HCl (pH7.4), 1mM MLCL, 3 mM $MgCl_2$, 1 μl of 0.05 μCi [^{14}C]Oleoyl-CoA, and 20 μl cell extract containing 15 μg protein in a final volume of 100 μl. The reaction was incubated at 37 ^{0}C for 20 min, and terminated by addition of 0.62 ml methanol and 0.8 ml chloroform. A solution containing 3 μl saturated NaCl and 300 μl Tris/HCl (pH 7.4) was then added to the mixture to facilitate extraction and cause phase separation. The labeled cardiolipin in the lower phase was resolved by thin-layer chromatography (TLC) in a solvent system consisting of chloroform/hexane/methanol/acetic acid (50:30:15:5, by vol). The lipid standard on the thin-layer chromatographic plate was visualized by iodine vapor and the density of radioactive band was visualized by exposure to Kodak X-OMAT X-ray film.

2.24 Statistical Analysis

The data were analyzed by a two-tail independent Student's *t* test. In all cases, the level of significance was defined as two-tailed, $p < 0.05$. Results are presented as the mean ± standard deviation.

EXPERIMENTAL RESULTS

PART I. STUDIES ON PHOSPHOLIPID BIOSYNTHESIS

I. IDENTIFICATION AND MOLECULAR CLONING OF MAMMALIAN 1-ACYL-SN-GLYCEROL-3-PHOSPHATE ACYLTRANSFERASES

Acyltransferases in glycerol lipid biosynthesis are believed to be transmembrane enzymes. In this portion of study, the bioinformatic approach was used to identify and characterize acyltransferase enzymes in glycerol lipid biosynthesis. The acyltransferase and phospholipid acyltransferase domains are probably conserved across phyla and are present in several membrane proteins that have acyltransferase activities. Using the conserved domain database and BLAST algorithms, we conducted searches on the database of expressed sequenced tags (dbEST). Several transmembrane genes were identified that contain phospholipid acyltransferase domains in their translated peptides.

Sequence analysis of these cDNA sequences suggested the presence of several candidates for potential murine and human 1-acyl-*sn*-glycerol-3-phosphate acyltransferase (AGPAT), designated as murine AGPAT1/2/3/4/5, and human N456, respectively. The murine AGPAT1/2 correspond to the human AGPAT1/2 described in INTRODUCTION AND LITERATURE REVIEW Section 3.3.5. Through combined efforts of EST screening and RT-PCR amplification, cDNA clones containing the complete open reading frame of each candidate were cloned. Subsequently, enzyme activities and tissue expression profiles for each of gene product were examined.

1.1.1 Identification of Murine AGPAT1/2/3/4/5 and Human N456

A homology search of the GenBank™ EST database was performed using the conserved phosphate acyltransferase domain sequence (smart00563) as a query, which yielded several short stretches of cDNA sequences (Figure 27). Subsequently, complete open reading frames were discovered by incorporating more cDNAs (ESTs), through combined efforts of BLAST and assemblage. A comparison of the translated amino acid sequences of assembled cDNA clones revealed following features: (1) putative initiation sites for translation fulfilled the requirement of an adequate initiation site, which conforms Kozak sequences (Kozak 2002b; Kozak 2002a); (2) encoded polypeptides contained intact acyltransferase domain and several transmembrane domains (Figure 28); (3) a convergence in overall domain structures (Figure 28). It is interesting to note that these murine candidates (designated as murine AGPAT1/2/3/4/5) are similar in size and domain structure, whereas the human acyltransferase candidate (designated as human N456) is a longer enzyme (456 aa) with a shorter catalytic domain as compared to those of murine AGPATs (110 aa of N456 vs. 118 aa of AGPATs).

Most acyltransferases in lipid biosynthesis are transmembrane proteins. Domain analysis revealed that these candidate enzymes contained homologous sequences to conserved domains of phosphate acyltransferases (smart00563), acyltransferases (pfam01553), and 1-acyl-*sn*-glycerol-3-phosphate acyltransferase (COG0204). To identify potential transmembrane domains within enzyme, transmembrane stretches were predicted using transmembrane domain analysis program. Analysis results demonstrated that these enzymes have a similar hydrophobicity profile. The amino acid length and domain structure are summarized in Figure 28.

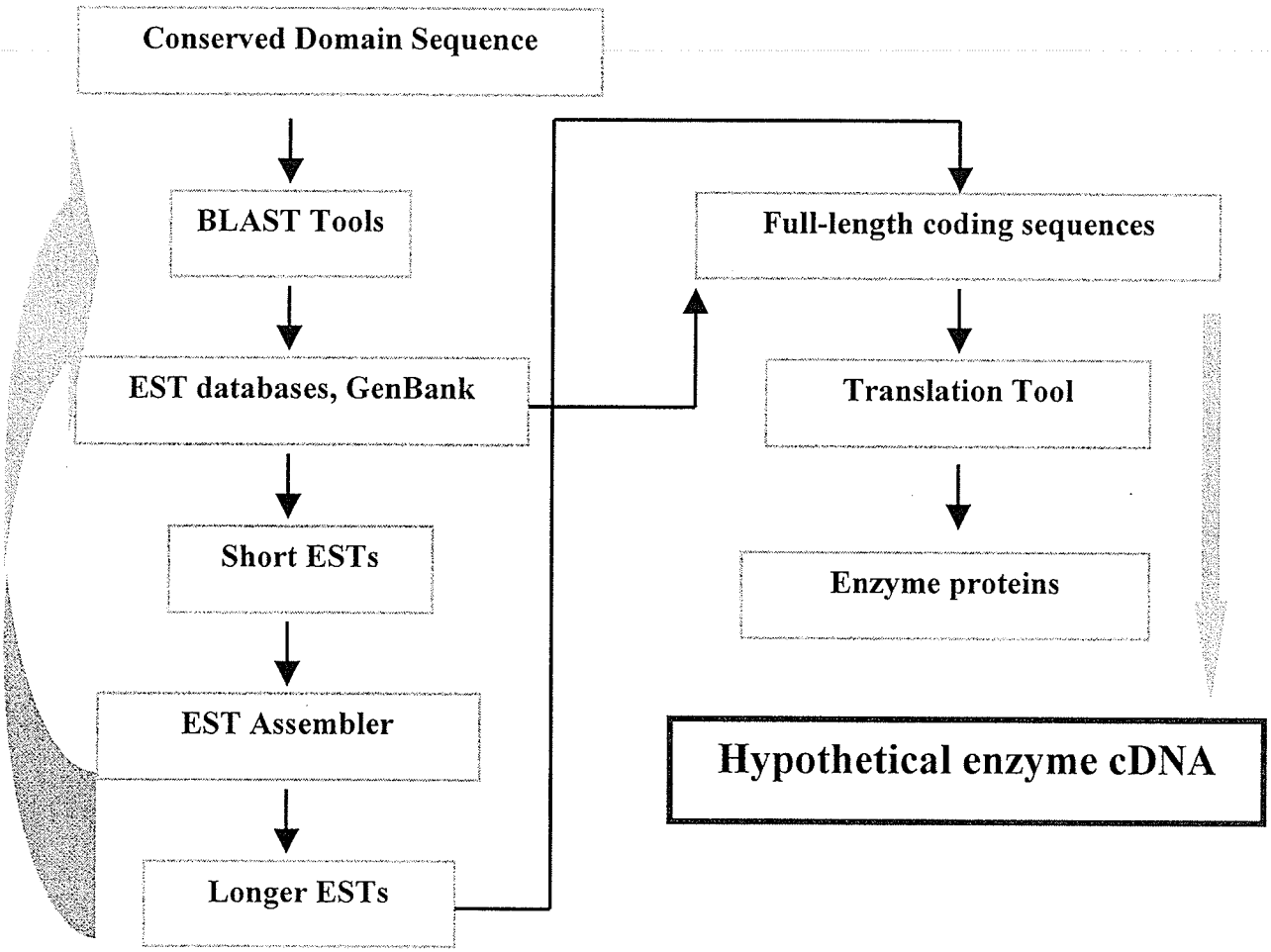

Figure 27. Identification of AGPATs via data mining

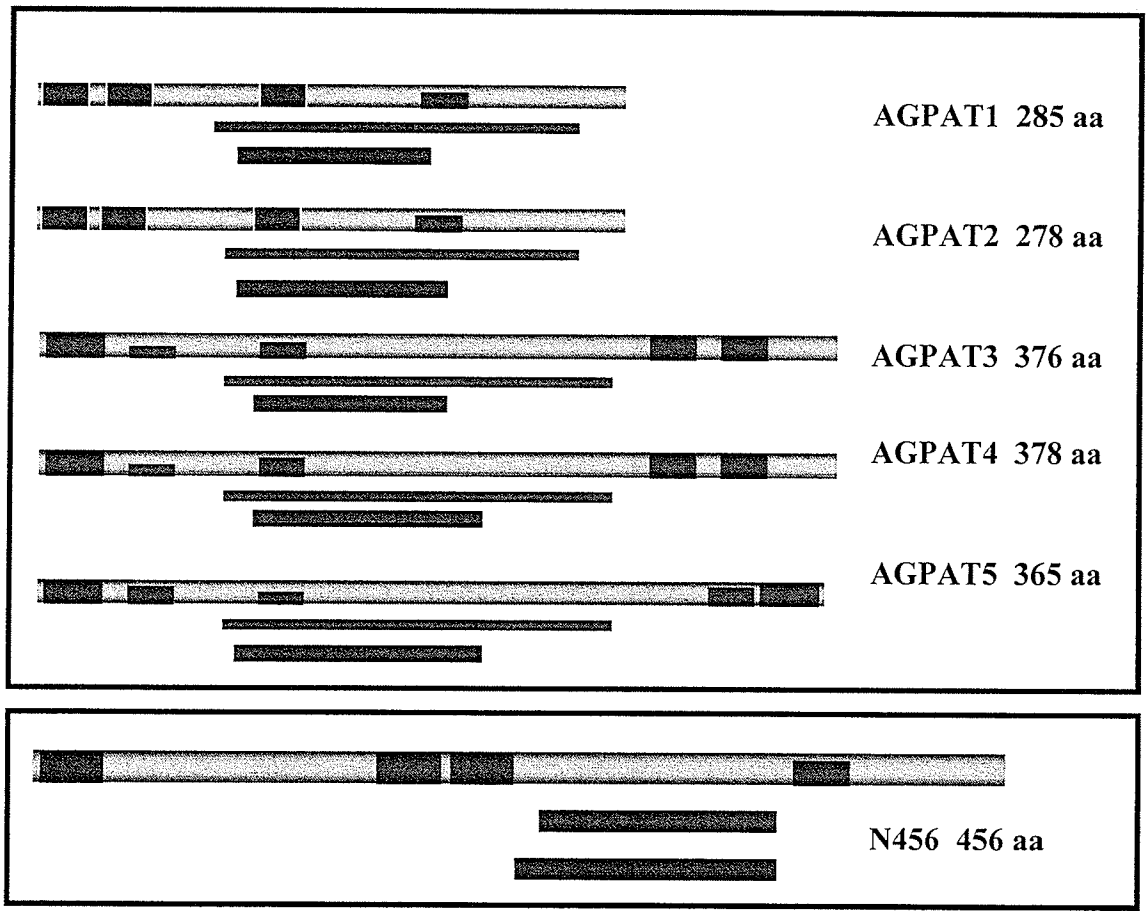

Figure 28. Candidate AGPATs and their domain structures

1.1.2 cDNA Cloning and Construction of Expression Vectors

Coding sequences of these enzymes were cloned into pcDNA3.1 or pcDNA3.1V5-His-TOPO expression vectors by a combination of RT-PCR and AT-cloning. Features of various expression vectors including expression vectors of commercial EST clones are summarized in Table 11. All constructs were verified by restriction enzyme digestion and DNA sequencing.

Table 11. Features of constructed expression vectors

Insert cDNA	Vectors	Promoters	Protein encoded
mAGPAT2	pBluescript SK-	T7, T3	Murine full-length
mAGPAT2	pcDNA3.1	T7, CMV	Murine full-length
mAGPAT3	pT7P3D-pac	T7, T3	Murine full-length
mAGPAT3	pcDNA3.1V5-his-TOPO	T7, CMV	C-terminal V5 and His fusion protein
mAGPAT4	PT7P3D-pac	T7, T3	Murine full-length
MAGPAT4	PcDNA3.1V5-his-TOPO	T7, CMV	C-terminal V5 and His fusion protein
mAGPAT5	pCMV-SPORT6	T7, SP6, CMV	Native full-length
mAGPAT5	pcDNA3.1V5-his-TOPO	T7, CMV	C-terminal V5 and His fusion protein
Murine TAZ	pCMV-SPORT6	T7, SP6, CMV	Murine exon 5 deleted TAZ
Murine TAZ	pcDNA3.1	T7, CMV	C-terminal flag-tagged murine exon 5 deleted
Human TAZ	pCMV-SPORT6	T7, SP6, CMV	Human full-length TAZ
Human N456	pCMV-SPORT6	T7, SP6, CMV	Human N456

1.1.3 Alignment Study and Identification of Conserved Motifs

Protein sequences of murine AGPATs were aligned with the ClustalW program. The amino acid alignment scores of five members are shown in Table 12. Overall matches among murine AGPATs range from 60% to 2%. According to their relative similarities, these candidate AGPATs can be subdivided into three subgroups: AGPAT1 and AGPAT2 in Group I; AGPAT3 and AGPAT4 in Group II; and AGPAT5 in Group III (Figure 29). Similar to human AGPATs, murine enzymes are predicted to have multiple hydrophobic regions that may serve as transmembrane domains (Figure 28). While the overall matches between members were highly varied, a core region containing highly conserved amino acid stretches was found within the catalytic domain. Two motifs that are critical for enzymatic activities appeared to be conserved (100%) among all five murine AGPATs. The catalytic motif NH(X4)D and the substrate binding motif EGTR were squared out (Figure 30). Interestingly, a conserved pattern K(X2)L(X6)G(X9)R that was underlined was also identified. This motif was found to lie between catalytic motif and substrate motif, which represents an unidentified novel motif for this gene family (Figure 30).

A similar search for conserved motif within human N456 gene was also conducted. The catalytic motif NH(X4)D was conserved. However, a change in the substrate-binding motif was identified (form conserved motif EGTR to a motif EGTC). These data indicated that the substrate of N456 might be distinct from other types of AGPATs in terms of its substrate binding specificity.

Table 12. Amino acid alignment scores of murine AGPATs

Identity	mAGPAT1	mAGPAT2	mAGPAT3	mAGPAT4	mAGPAT5
mAGPAT1	100%	44%	7%	11%	10%
mAGPAT2	44%	100%	9%	9%	2%
mAGPAT3	7%	9%	100%	60%	19%
mAGPAT4	11%	9%	60%	100%	17%
mAGPAT5	10%	2%	19%	17%	100%

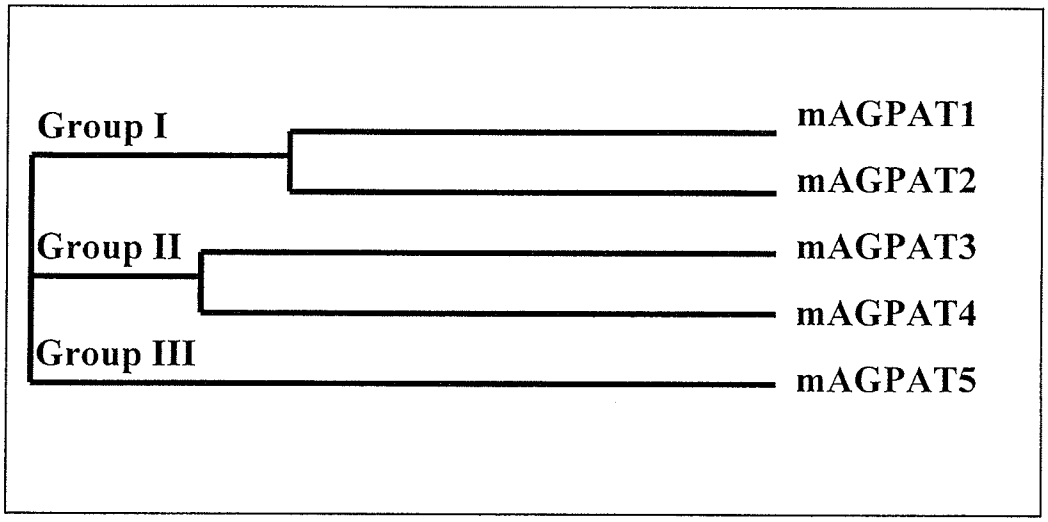

Figure 29. Dendrogram of the murine AGPAT gene family members and the subgrouping classification.

Predicted protein sequences were deduced from the sequences of complete coding sequences and aligned with the ClustalW Program (www.ebi.ac.uk)

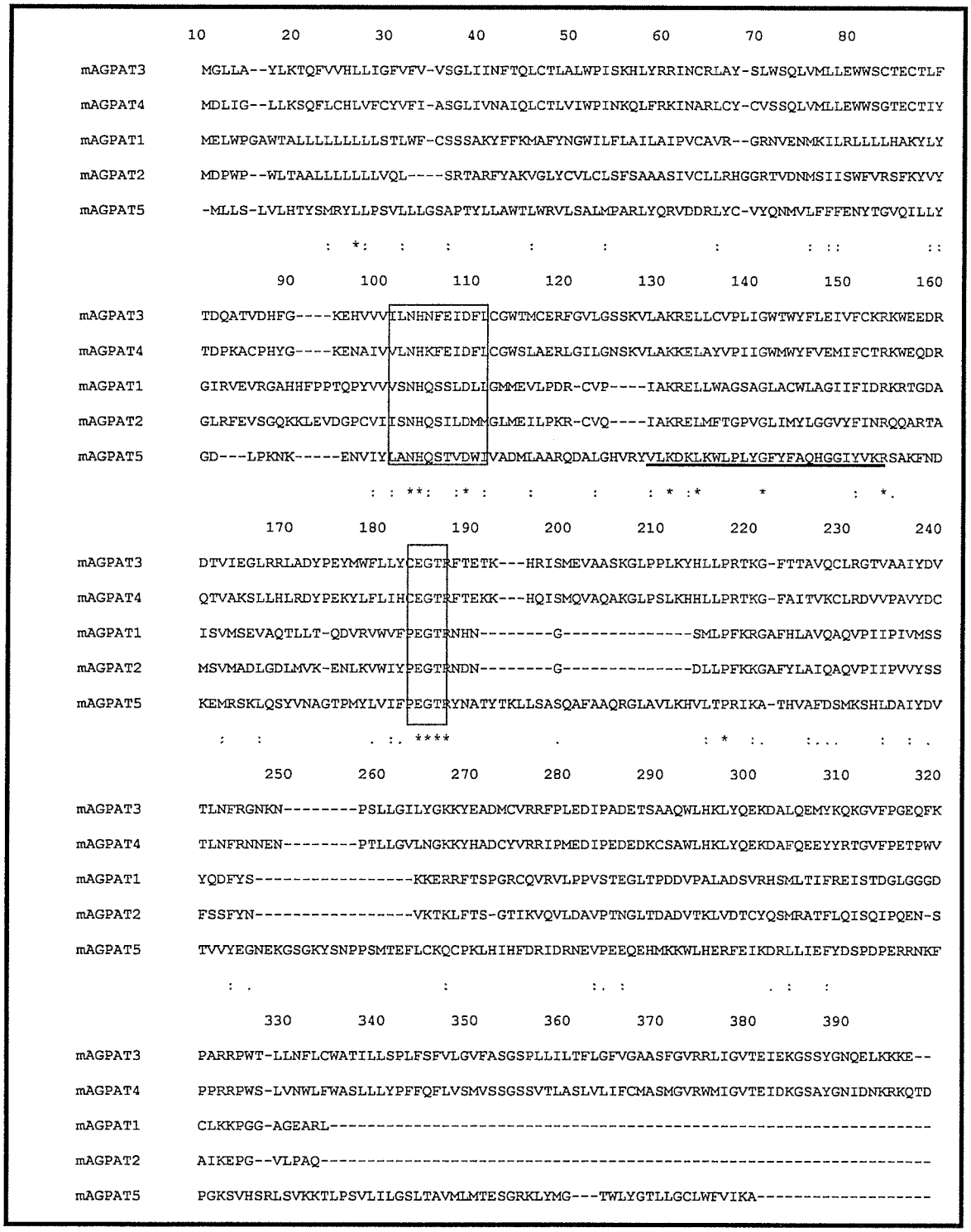

Figure 30. Alignment of predicted protein sequences of murine AGPAT gene family members.

Conserved motifs are boxed or underlined.

1.1.4 Detection of Hypothetical AGPAT mRNA in Murine Tissues

To check whether these AGPATs were expressed *de novo*, RT-PCR was used to detect transcripts of each candidate. In order to compare the relative abundance of each candidate, similar sets of primers (covering complete coding regions) and the same preparation of cDNAs were used in our experiments. RT-PCR results demonstrated that murine AGPAT1 was expressed ubiquitously at high levels (Figure 32). Similarly, AGPAT3 displayed a ubiquitous pattern with less abundance and some tissues variation. This pattern of expression is in marked contrast to patterns seen with AGPAT2/4/5. AGPAT2 was expressed at high levels in the liver and at intermediate levels in the kidney, the gut, and the skeletal muscle, but not seen in the brain and spleen. AGPAT4 is expressed at high levels in brain and at intermediate levels or low levels in skeletal muscles, the gut, the kidney, the spleen, and lung, but barely detectable in the heart and the liver. AGPAT5 was expressed in all tissues at different levels (at its highest in brain, then at decreasing levels in skeletal muscle, the heart, the kidney, the gut, the spleen, the lung, and the liver). The size of each PCR product was consistent with the predicted size, and the identity of the PCR product was also confirmed by direct DNA sequencing.

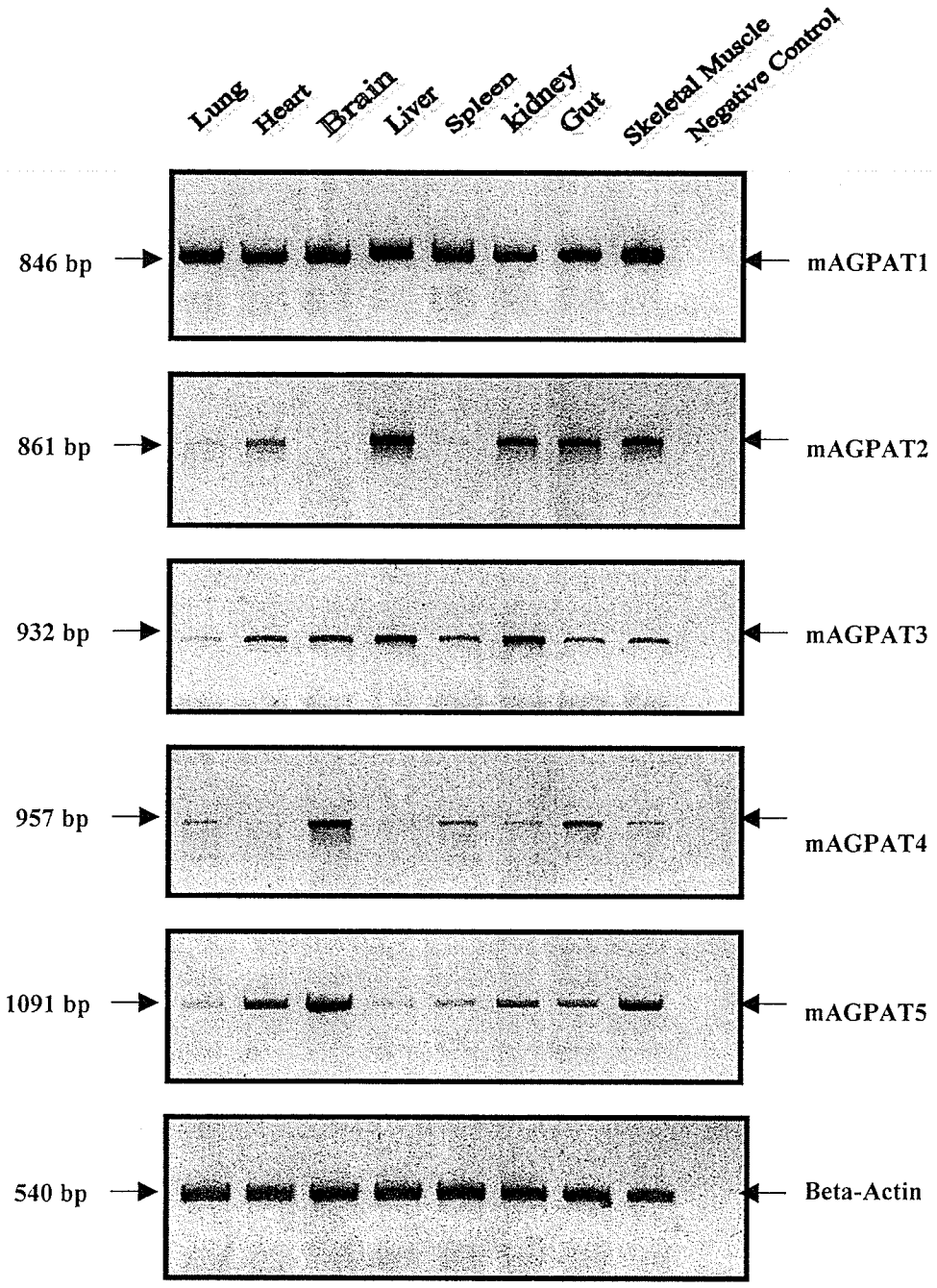

Figure 31. Expression profiles of AGPATs in various murine tissues

1.1.5 Expression of AGPATs *in vitro* and *in vivo*

To determine if the cDNAs isolated in our laboratory could be translated *in vitro*, expression vectors containing murine AGPATs, and human N456 downstream of a T7/SP6 polymerase promoter were used to generate enzyme proteins in a TnT coupled reticulocyte Lysate system as described in Materials and Methods. Stable enzyme proteins were produced under these conditions (Figure 32). The observed molecular masses were consistent with those predicted from their open reading frames (ORFs). Enzyme proteins were found to migrate at 30 kDa of native AGPAT2, at 46.3 kDa, 46.5 kDa, and 45.1 kDa for V5-His-tagged AGPAT3, AGPAT4, and AGPAT5 respectively.

To check whether the isolated cDNAs could be expressed and translated into enzyme *in vivo*, COS-1 cells were transiently transfected with expression vectors encoding murine AGPAT3/4/5 protein in frame with a C-terminal V5-His tag. The presence of AGPAT-tagged proteins in transfected cells was confirmed by determining fusion tag with Western blot. Lysates from transfected cells were prepared as described in Materials and Methods and the specific enzyme protein bands were detected using anti-V5 antibody. As shown Figure33, protein bands appeared in transfected cells vs. mock-transfected cells with empty vector plasmid DNAs. Multiple protein bands were seen for AGPAT3 indicating posttranslational processing and/or enzyme degradation.

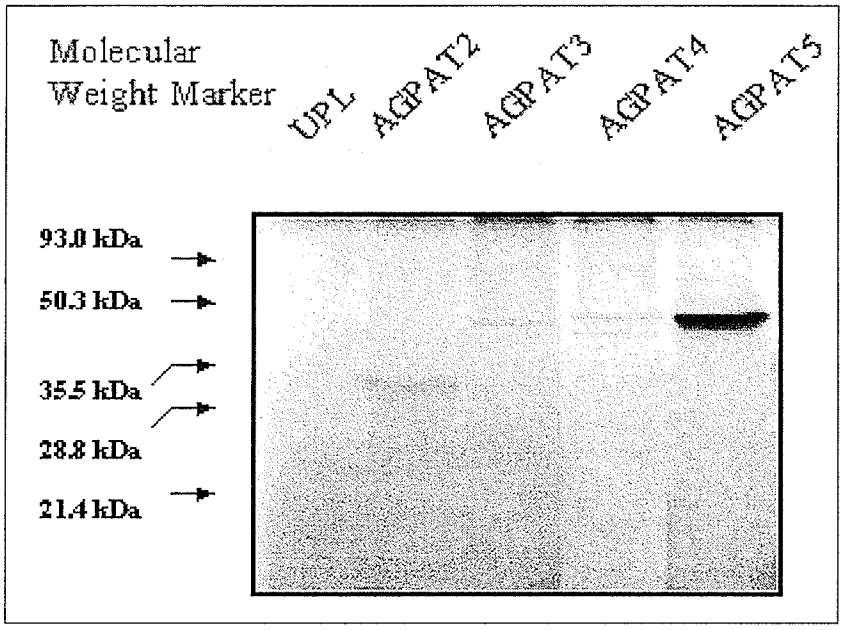

Figure 32. Transcription coupled in vitro translation of AGPATs. Abbreviation: UPL, unprogrammed cell lysate. Protein bands were [^{35}S] methionine radio-labeled and visualized by exposure to X-ray film as described in Materials and Methods section.

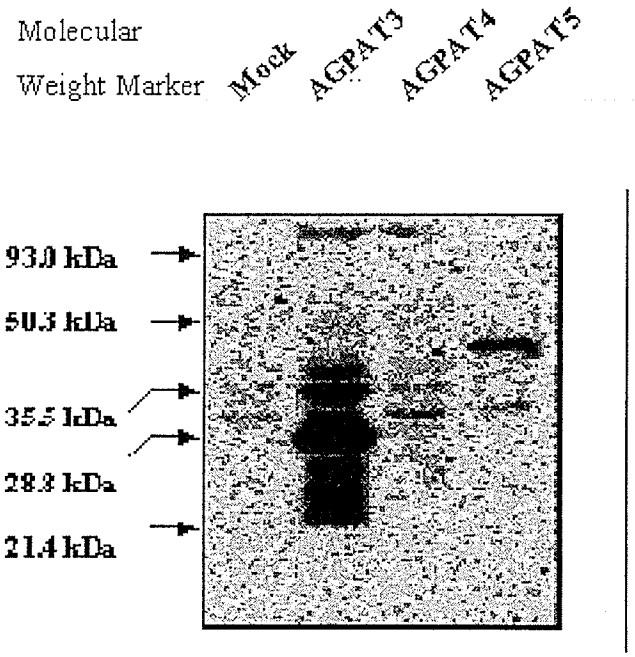

Figure 33. Expression of AGPATs in COS-1 cells.

COS-1 cells were transiently transfected with murine AGPAT C-terminal fusion proteins. 48 h later, cells were collected and whole cell extracts were prepared. Western blot analysis of cell extracts from transfected cells and mock control cells were done using anti-V5 antibody. The proteins and the molecular size markers are indicated in kDa.

1.1.6 Determination of 1-acyl-*sn*-glycerol-3-phosphate Acyltransferase Activity

To demonstrate that murine AGPAT gene products have 1-acyl-*sn*-glycerol-3-phosphate acyltransferase activity, activities of recombinant proteins expressed *in vitro* were examined. Similar amounts of each AGPAT proteins, determined as described in Materials and Methods, were used in the enzyme assays. As shown in Figure 34, murine AGPAT2/3/4/5 produced more radiolabeled PA as compared to that of unprogramed lysate. The efficiency of AGPAT3/4/5 was less than that of AGPAT2.

Under identical experimental conditions, human N456, human full-length TAZ, and murine exon 5-deleted TAZ were also examined for 1-acyl-*sn*-glycerol-3-phsophate acyltransferase activity. As shown in Figure 34, no radiolabeled PA was produced by human or murine TAZ, whereas both radiolabeled PA and LysoPA were produced by human N456.

To further demonstrate AGPAT activity of murine candidates, plasmid DNAs for AGPAT expression were transfected into a mammalian COS-1 cell line to determine if they would increase 1-acyl-*sn*-glycerol-3-phsophate acyltransferase activity. Whole cell extractions were made after COS-1 cells were transiently transfected with corresponding expression vectors. Equal amount of protein input was used to conduct the EA. Cells transfected with murine AGPAT2/3/5 produced more radiolabeled PA as compared to that of mock-transfected cells (Figure 35). Our result is consistent with the data obtained using *in vitro* translated enzyme proteins.

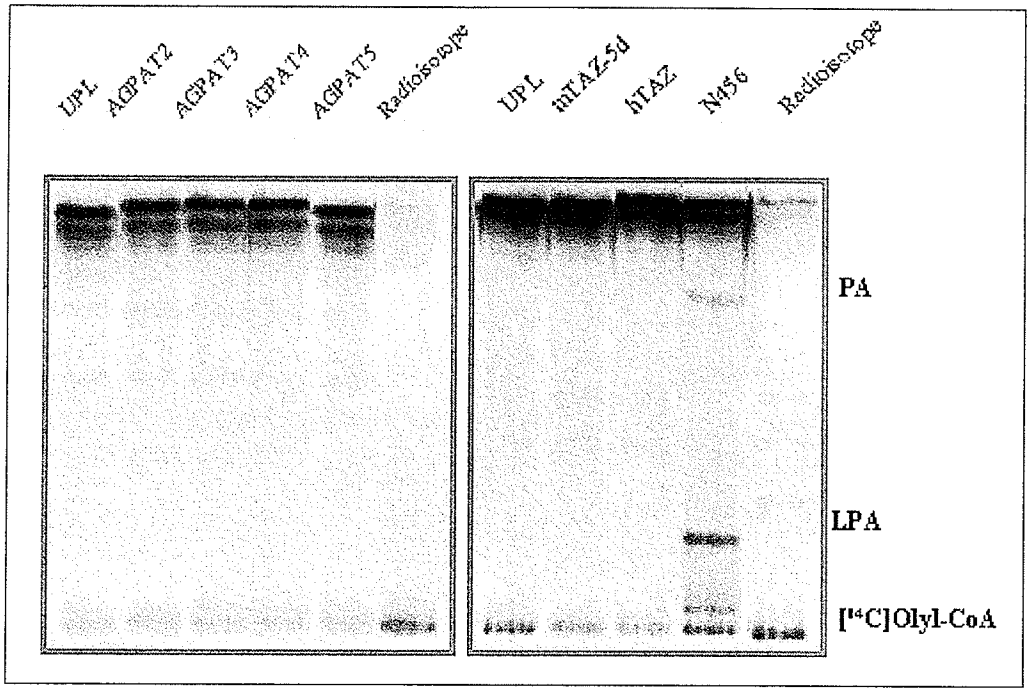

Figure 34. AGPAT activity in lysate of *in vitro* generated AGPAT proteins.

AGPAT assay with lysates of *in vitro* translated proteins or unprogrammed lysate. The positions of PA and LPA and acyl-CoA on the TLC plate are indicated.

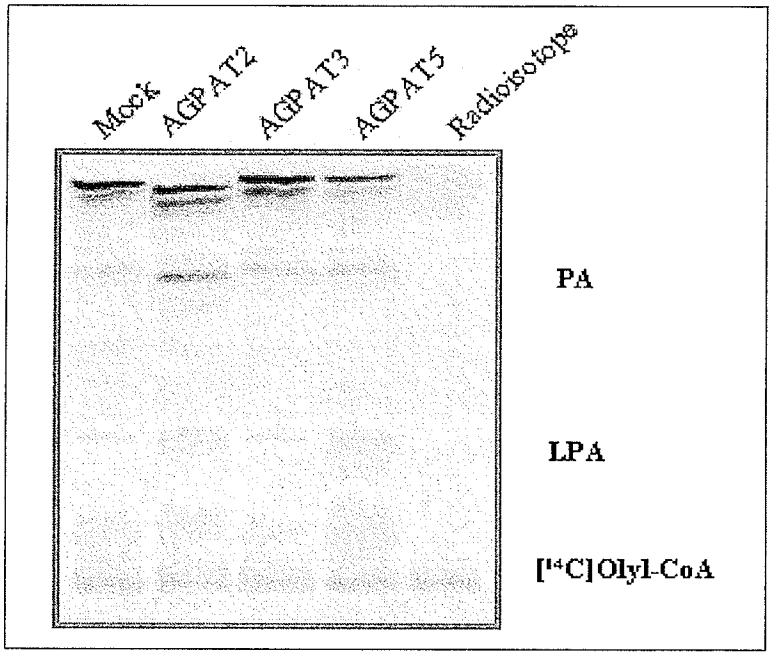

Figure 35. AGPAT activity in cells transfected with AGPAT candidate expression plasmids.

AGPAT assay with lysates of *in vivo* generated proteins from transient transfection of COS-1 cells. The positions of PA and LPA and acyl-CoA on the TLC plate are indicated.

II. COMPLEX EXPRESSION PATTERN OF THE BARTH SYNDROM GENE TAZ IN HUMAN AND MURINE TISSUES

One candidate for AGPAT we have identified through dataming is TAZ in which its mutation has been known to cause a human disease called Barth syndrome. Barth syndrome (MIM 302060) is an X-linked inherited disorder characterized by cardioskeletal myopathy with neutropenia and abnormal mitochondria abnormalities (Barth et al. 1981; Barth et al. 1983). Other characteristics include granulocytopenia, growth retardation and 3-methylglutaconicaciduria (Kelley et al. 1991; Chitayat et al. 1992). By means of linkage study, the causative gene has been mapped to Xq28.12 region and termed as G4.5 or TAZ (Barth et al. 1983; Bolhuis et al. 1991; Bione et al. 1996). The predicted proteins encoded by TAZ are thought to belong to a family of acyltransferase in glycerolipid biosynthesis (D'Adamo et al. 1997).

The G4.5 or TAZ is a small single-copy gene with a complex pattern of expression. As many as 10 mRNAs splice variants have been identified with the two most abundant and ubiquitously expressed forms differing in the sequence encoded in exon 5. However, there were no systematic studies addressing specifically the relative abundance of each form in human tissues, and the expression of tafazzins in rodent tissues was not investigated. In this portion of study, we undertook to examine the complex expression pattern of TAZ. In addition, we employed comparative genomics to identify the evolutionary conserved TAZ. We hypothesized that the most abundant expressed and evolutionarily conserved form is the potential function form of TAZ. Using comparative genomic approach, we were able to identify the most abundantly

expressed and evolutionarily conserved form of TAZ, and thus potential function form among various TAZ variants.

1.2.1 Expression of TAZ Gene in Human and Murine Tissues

The G4.5 or TAZ is a small single-copy gene with a complex pattern of expression. To determine the expression pattern of TAZ-mRNA in mouse tissues, total RNA was isolated from several tissue samples. The results shown in Figure 36 demonstrated that TAZ was expressed in all tissues analyzed and its highest expression was in skeletal muscle and kidney. The presence of a major ~2.1 kb band and a minor ~2.8 kb band indicate that more than one form of TAZ were expressed.

A large body of data supports the expression of multiple splice variants of TAZ, and the most prevalent pattern of variant TAZ transcript is the precise deletion of one or more exons. To examine the complex expression pattern and relatively abundant TAZ mRNA species, long range RT-PCR was carried out using mouse primer set exon 1-11 with murine RNA and human primer set exon 1-11 with human RNA. Although these primer sets are not exactly the same sequences between the two species they are similar in the sense that both primers are within the first and last protein coding exons of the appropriate species TAZ cDNA (Figure 37). Using the above primer we conducted RT-PCR on various murine samples. The results shown in Figure 38 A indicate that two RT-PCR products of 871 bp and 818 bp were detected in RNAs isolated from 8 murine tissues. No other RT-PCR products were detected in murine tissues, suggesting that little or no other TAZ mRNAs were expressed in murine tissues. Isolation and subsequent sequencing of each RT-PCR product revealed the identity of two bands that were precise deletions of exon 5 and exon 5 + 9, respectively.

This study is the first report on the detection of TAZ mRNA in various mouse tissues. We are the first to show that naturally expressed mouse TAZ mRNA species are exon 5-deleted and exon 5 + 9-deleted. It should also be emphasized that the so-called full-length TAZ mRNA was not detected under our experimental conditions suggesting no or very low expression level of full-length TAZ in mice.

In contrast to murine tissues, all three human cell lines in this study expressed TAZ mRNA with a similar but more complex and 4 distinct bands in RT-PCR (Figure 38). Isolation and sequencing of 879, 837, 789, and 747 bp fragments revealed four mRNA species: full-length TAZ, precise deletion of exon 7, deletion of exon 5, and deletion of exon 5 + 7, respectively. The 789 bp band was the most abundant TAZ transcript that corresponded to an exon 5-deleted TAZ.

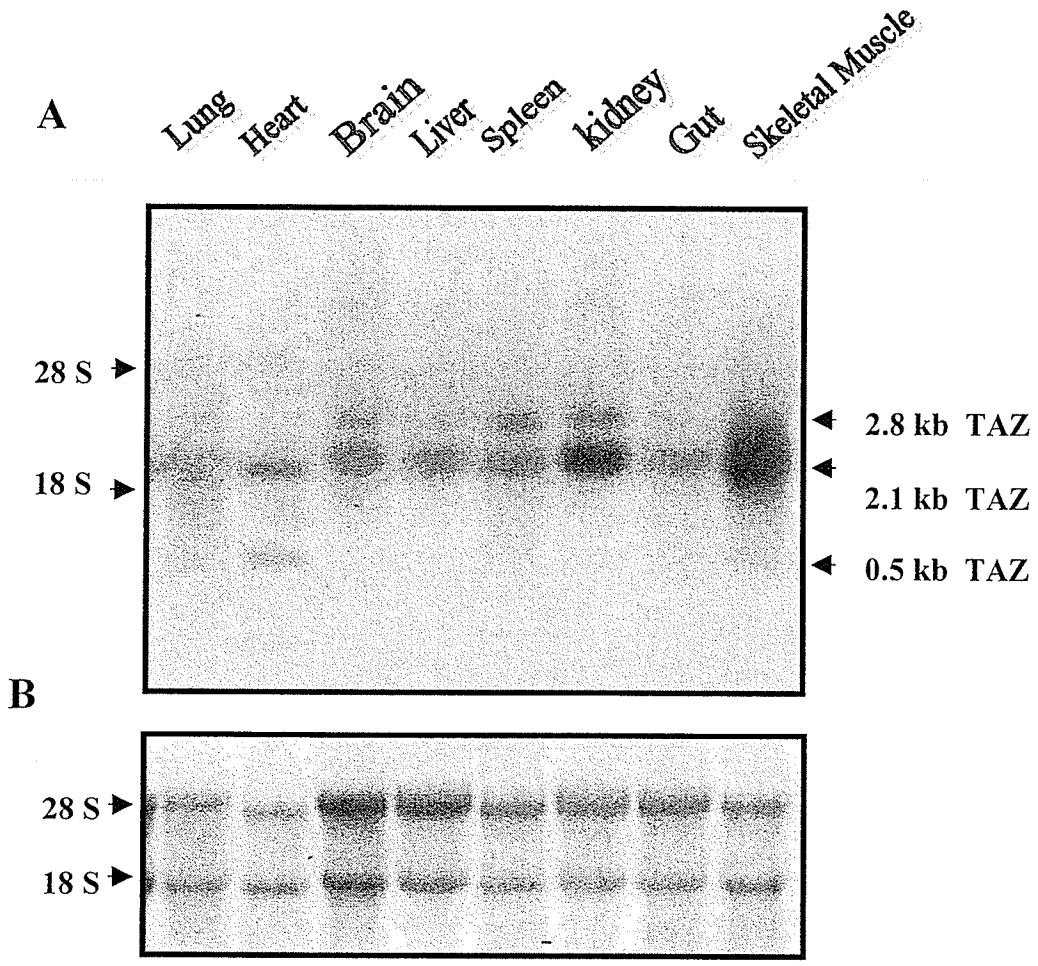

Figure 36. Expression of TAZ mRNA in various murine tissues.

(A) Nylon membrane containing 15 ug/lane total RNA from various murine tissues was hybridized with radiolabeled murine TAZ cDNA. The blot was exposed to PhosphoImage screen for 2 hours and image was scanned and analyzed by Molecular Imager FX equipped with QuantityOne software. (B) Ethidium bromide staining showed the equal loading of tissue RNAs for Northern hybridization.

A. Human TAZ

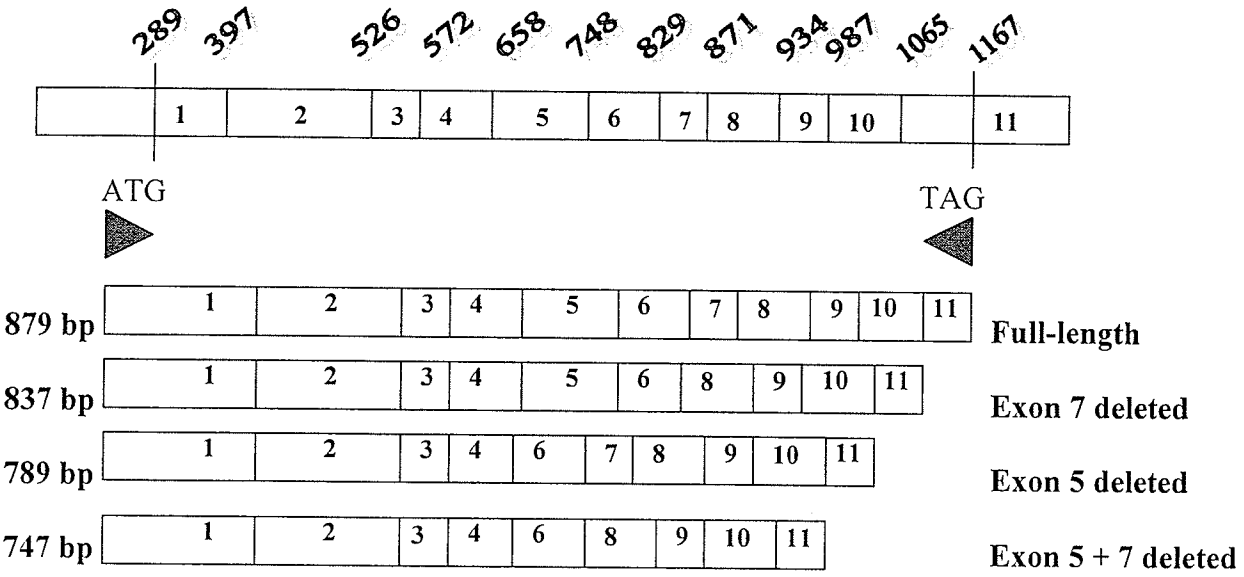

B. Mouse TAZ

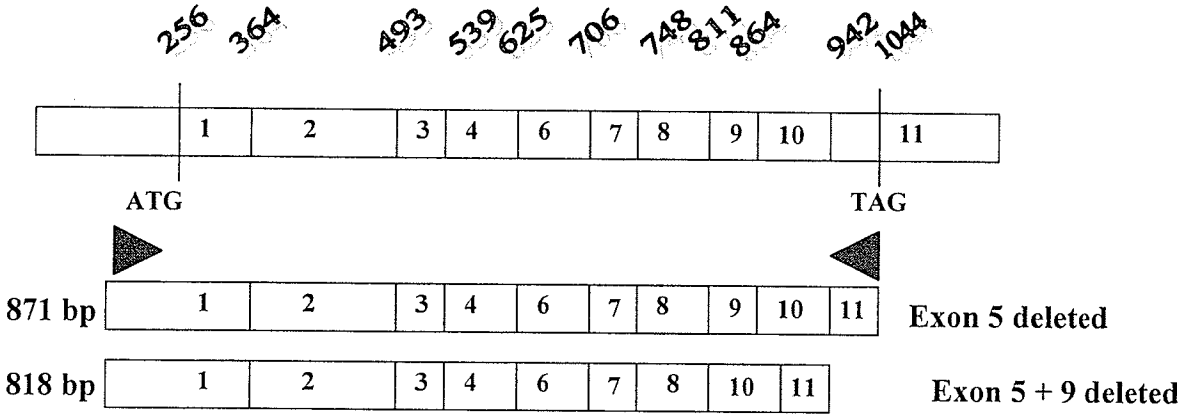

Figure 37. Exon/intron structure and PCR primer design. (A) Schematic diagram of human full-length TAZ cDNA showing positions of the primer sets used in PCR amplification are shown. (B) Schematic diagram of the exon 5-deleted mouse TAZ cDNA showing positions of the primer set used in PCR amplification (the numbering of exons of mouse TAZ is defined in this study by analogy to the human TAZ exon/intron structure to facilitate comparisons). Mouse TAZ primer set: mTAZ (sense) 5'-TCC TTC TCC TGA GTG GTA GAG-3', mTAZ (antisense) 5'-GTT CCT GTA CCA CCA CTT CC-3'. Human TAZ primer set: hTAZ (sense) 5'-GGG ATG CCT CTG CAC GTG AA-3' and hTAZ (antisense) TCT CCC AGG CTG GAG GTG GT-3'.

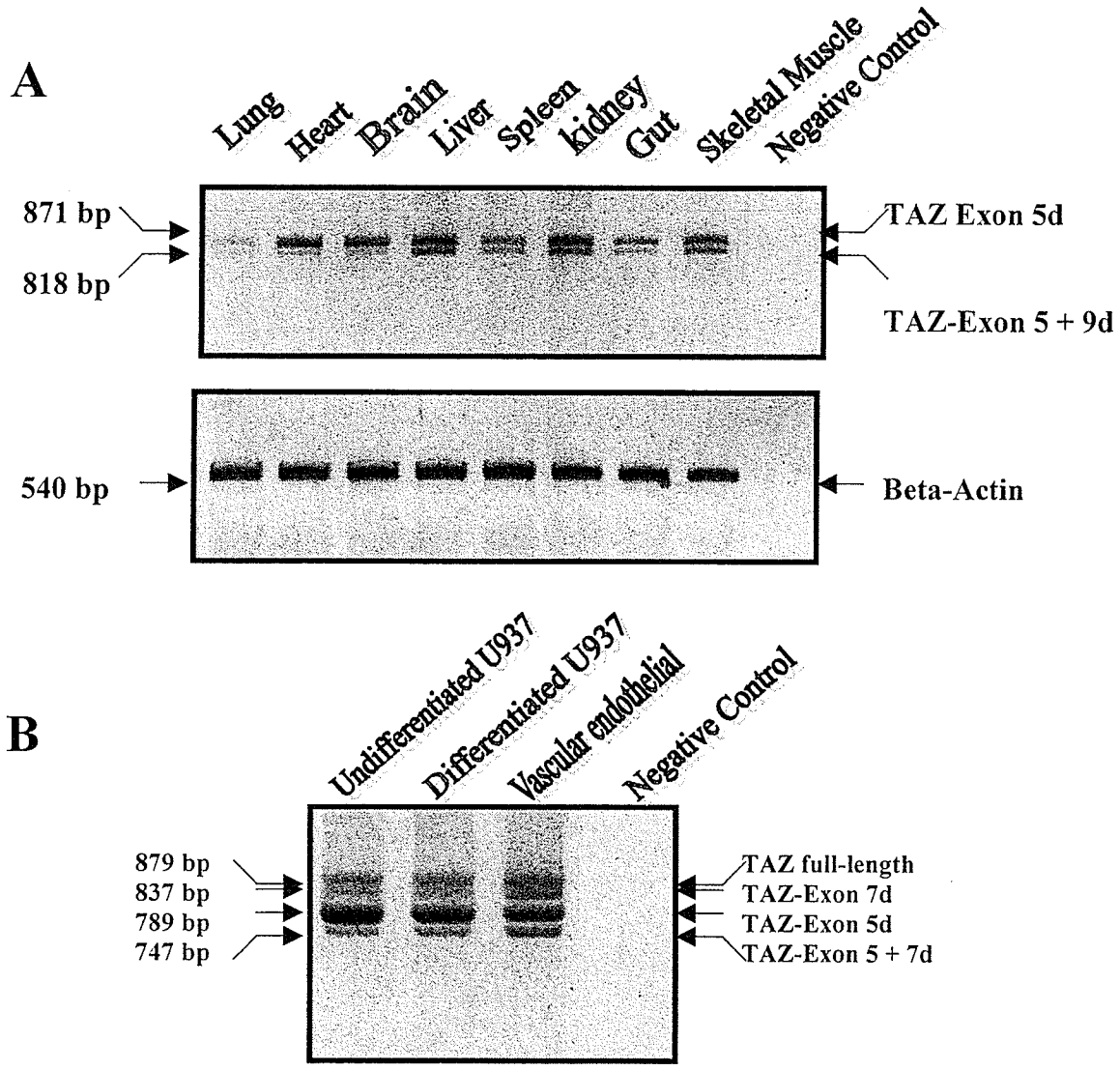

Figure 38. Detection of full-length and various splicing forms of TAZ mRNA in mouse tissues and human cells. (A) Total RNA extracted from various mouse tissues was reverse transcribed and amplified using primer set exon 1-11 PCR. PCR products were separated on a 1.5% agarose gel. PCR products migrating at 871 bp and 818 bp were isolated and sequenced and confirmed to be exon 5 and exon 5 +9 murine cDNAs, respectively. (B) Total RNA extracted from each of three human cell types was reversed transcribed and PCR amplified using exon 1-11 primer set. PCR products migrating at 879 bp, 837 bp, 789 bp, and 747 bp were isolated and sequenced and confirmed to be full-length, exon 7 deleted, exon 5 deleted, exon 5 + 7 deleted human TAZ cDNAs.

1.2.2 Identification of Evolutionarily Conserved and Potentially Functional Form of TAZ

The initial screening of mouse tissues using exon 1-11 primer set failed to reveal an analogous murine TAZ transcript containing exon 5. Since the exon 5 included transcripts were detected in all three human cells, a comparative genomics study was conducted to check the existence of exon 5 included transcripts in mouse by data mining approaches (Figure 39). In view of the fact that human and mouse TAZ shares 97% and 91% similarity in coding sequences and encoded amino acid sequences (ClastalW analysis), the coding cDNA sequences or encoded peptide sequences were employed to carry out similarity searches against different EST databases. First, we used human exon 5 cDNA sequence to conduct a similarity search against human EST database, mouse EST database, or non-human and non-mouse EST database. We found that only the expected human ESTs had sequences producing significant alignments, and no BLAST hits in mouse ESTs or non-human and non-mouse EST database had significant similarity suggesting non-existence of exon 5 included transcripts in other species. Secondly, we used 30 amino-acid long peptides encoded by human exon 5 to carry out a translated database search against the above databases to avoid biases produced by using human exon 5 cDNA sequence. Interestingly, the same result was obtained. Taken together, our results demonstrated that there was a species-specific difference in the expression of TAZ mRNAs. It is clear from our results that the exon 5-deleted TAZ was the most abundant form and might be the evolutionarily conserved one.

Since the screening of murine tissues using the exon 1-11 primer set failed to reveal an analogous human full-length TAZ, analysis of protein functional domains

encoded by exon 5-deleted transcript vs. full-length transcript was undertaken to confirm whether the exon-5 deletion would disrupt conserved domain(s) of potential TAZ enzyme. As shown in Figure 40, the human full-length TAZ demonstrated a high homology to each of three conserved domains of acyltransferases with scores of 100% aligned with phosphate acyltransferase, 100% aligned with acyltransferase, and 82.7% aligned with 1-acyl-glycerol-3-phosphate acyltransferase, respectively. The high similarity shared by TAZ and AGPAT indicated they might belong to one superfamily. However, a 30-amino acid insertion right within all conserved domains was created by exon-5 encoded sequences. Hence, the putative function of the full-length tafazzin remains unknown. Since the insertion was in the middle of the acyltransferase catalytic domain, it might either disrupt enzymatic activity or produce a different enzymatic activity and/or substrate specificity.

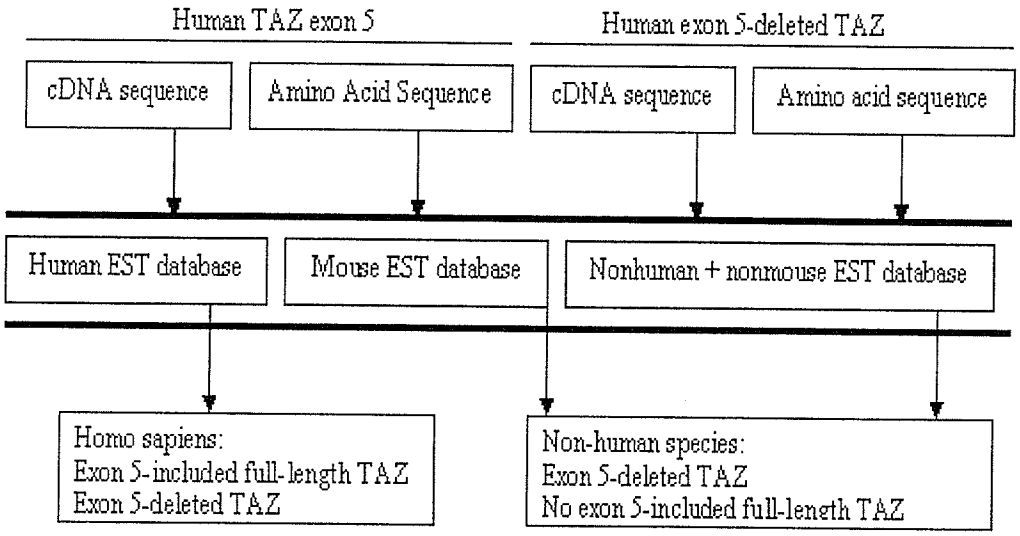

Figure 39. Exon 5-deleted TAZ is evolutionarily conserved among different species. Human TAZ exon 5 sequences or human exon 5-deleted TAZ sequences were used to BLAST human, mouse, and nonhuman and nonmouse EST databases. Exon 5-included TAZ was found only in humans and exon 5-deleted TAZ was retrieved from all three EST databases suggesting the exon 5-deleted TAZ is evolutionarily conserved among different species.

A.

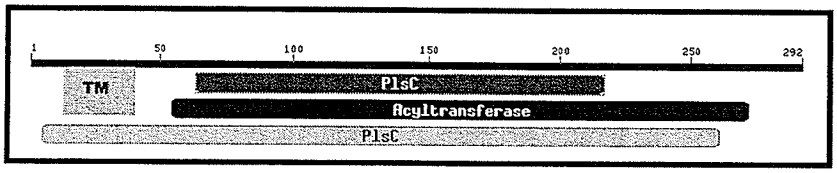

B.

```
            CD= Phosphate acyltransferases, 100.0% aligned
HumanTAZ:  63  LITVSNHQSCMDDPHLWGILKLRHIWNLKLMRWTPAAADICFTKELHSHFFSLGKCVPVC  122
PlsC:       1  ALVVANHQSFLDPLVLSALLPRKLR------RVRFVAKKELFYVPLLGWLLRLAGAIFID   54

           123 RGAEFFQAENEGKGVLDTGRHMPGAGKRREKGDGVYQKGMDFILEKLNHGDWVHIFPEGK  182
            55 RSR----------------------------GRKDRAALREAVRLLREGEWLLIFPEGT   85

           183 VNMSSEFLRFKWGIGRLIAECHLNPIILPLWHVGM  217
            86 RSRPGKLLPFKKGAARLALEAG--VPIVPVAIRGT  118

             CD = Acyltransferase, 99.5% aligned
HumanTAZ:  54  IEKRGPATPLITVSNHQSCMDDPHLWGILKLRHIWNLKLMRWTPAAADICFTKELHSHFF  113
Acylt:      1  LENLPKKGPAIVVANHRSYLDWLVLSAALPKRG-----RRLVFIAKKELLDIP-GFGWLM   54

           114 SLGKCVPVCRGAEFFQAENEGKGVLDTGRHMPGAGKRREKGDGV-YQKGMDFILEKLNH-GD 173
            55 RLAGAIFIDR----------------------------KNRADALAAADELVYVLERKGR  86

           174 WVHIFPEGKVNMSSEFLRFKWGIGRLIAECHLNPIILPLWHVGMNDV-LPNSPPYFPRFG  232
            87 SVLIFPEGTRSRGGELLPFKKGAFQLALKAGV--PIVPVVISGSELVEPKKEAKRLAPKL  144

           233 QKITVLIGKPFSALPVLERLRAENKSAVEMRKALTDFIQE  272
           145 GEVTVRVLPPIPLDDNSPEDIKEL--AERLRDIMVQALEE  182

              CD= AGPAT, 82.7% aligned
HumanTAZ:   5  VKWPFPAVPPLTWTLASSVVMGLVGTYSCFWTKYMNHLTVHNREVLYELIEKRGPATPLI  64
AGPAT:     10  VILFLLLPLPLALIALFRLRRPVLRRWLRFLVLLL--LLLFGLRVEVEGLENLPKGGPAL  67

           65  TVSNHQSCMDDPHLWGILKLRHIWNLKLMRWTPAAADICFTKELHSHFFSLGKCVPVCRG  124
           68  VVANHQSFLDPLLLSLALPRRG-------PVRFVAKKELFKVPLLGWLLRLLGAIPVDR-  117

          125  AEFFQAENEGKGVLDTGRHMPGAGKRREKGDGVYQKGMDFILEKLNHGDWVHIFPEGKVN  184
          118  -------------------------ENPDDETLRAAVARLKAG---GRSLVIFPEGTRS  150

          185  MS-SEFLRFKWGIGRLIAECHLNPIILPLWHVGMNDVLPNSPPYFPRFGQKITVLIGKPF  243
          151  RGGEELLPFKRGAARLALE--AGVPIVPVAIVGAEELFP------SLKKGKVKVRIGPPI  202

          244  SALPVLERLRAENKSAVE  261
          203  DISALPEPLLPELAEAVE  220
```

Figure 40. Alignment of human full-length TAZ with CD sequences of acyltransferases in glycerolipid biosynthesis. (A) Graphic representation of functional domain structure including putative transmembrane helices (15-35 aa), and acyltransferase catalytic domains. (B) Alignment of full-length TAZ with three CD sequences of acyltransferase in detail is shown and 30 aa encoded by exon 5 are underlined.

1.2.3 Alternative Translation of Human and Murine TAZs

As described in the previous section, our cloned TAZ-cDNAs showed three in-frame ATG codons in both human full-length form and murine exon 5-deleted form. To determine if the cDNAs isolated in our laboratory could be translated *in vitro*, expression vectors containing human full-length TAZ sequences (downstream of a SP6 polymerase promote) and murine exon-5 deleted TAZ sequences (downstream of a T7 polymerase promoter) were used in a TnT coupled Reticulocyte Lysate system as described in Materials and Methods. The two TAZ encodes stable TAZ proteins were produced under these conditions (Figure 41). It should be noted that two bands were detected for each construct, which is consistent with the possible use of the first two inframe initiating methionine codons. (Figure 42). The observed molecular masses for human full-length TAZ were ~35 kDa and ~32 kDa and for murine exon 5-deleted TAZ were ~32 kDa and 29 kDa. This alternative translation mechanism added another layer of complexity to the expression of TAZ in both human and mouse. Conceivably tafazzin proteins resulting from these two mechanisms could potentially generate various forms with a dominant exon 5-deleted form in both human and mouse (Figure 42). Translation starting at the second ATG produces N-terminal truncated tafazzin proteins (24 aa shorter than the longer one) without disruption of two acyltransferase conserved domains, but might affect AGPAT activity. Moreover, partial deletion of N-terminal putative transmembrane helices would be expected. This truncation of transmembrane helices might cause alteration of membrane anchoring in certain circumstances. Similar to exon 5-deleted tafazzin, exon 7-deleted tafazzin was also inframe but had significant deletion of the catalytic domain. The exon 9-deleted variant was not inframe and might produce

immature termination with a significant disruption of the putative catalytic domain of TAZ.

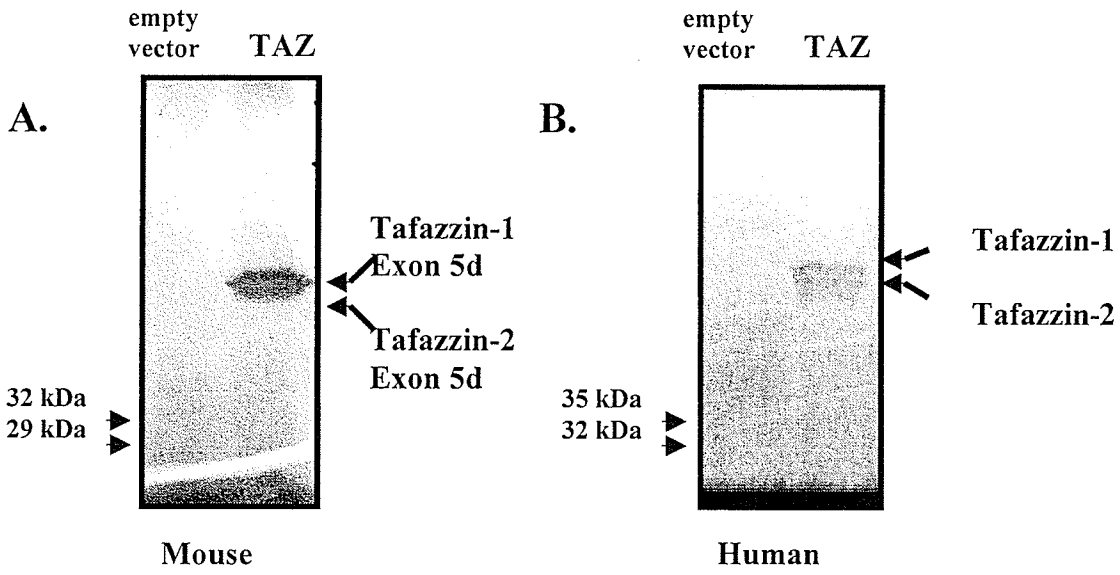

Figure 41. *In vitro* translation of mouse exon 5 deleted TAZ and human full-length TAZ.

In vitro transcription/translation reactions were performed using mouse exon 5 deleted and human full-length TAZ expression plasmids and labeled lysates analyzed as described in Materials and Methods. Sizes in kilodalton, corresponding to the stained marker are shown on the left.

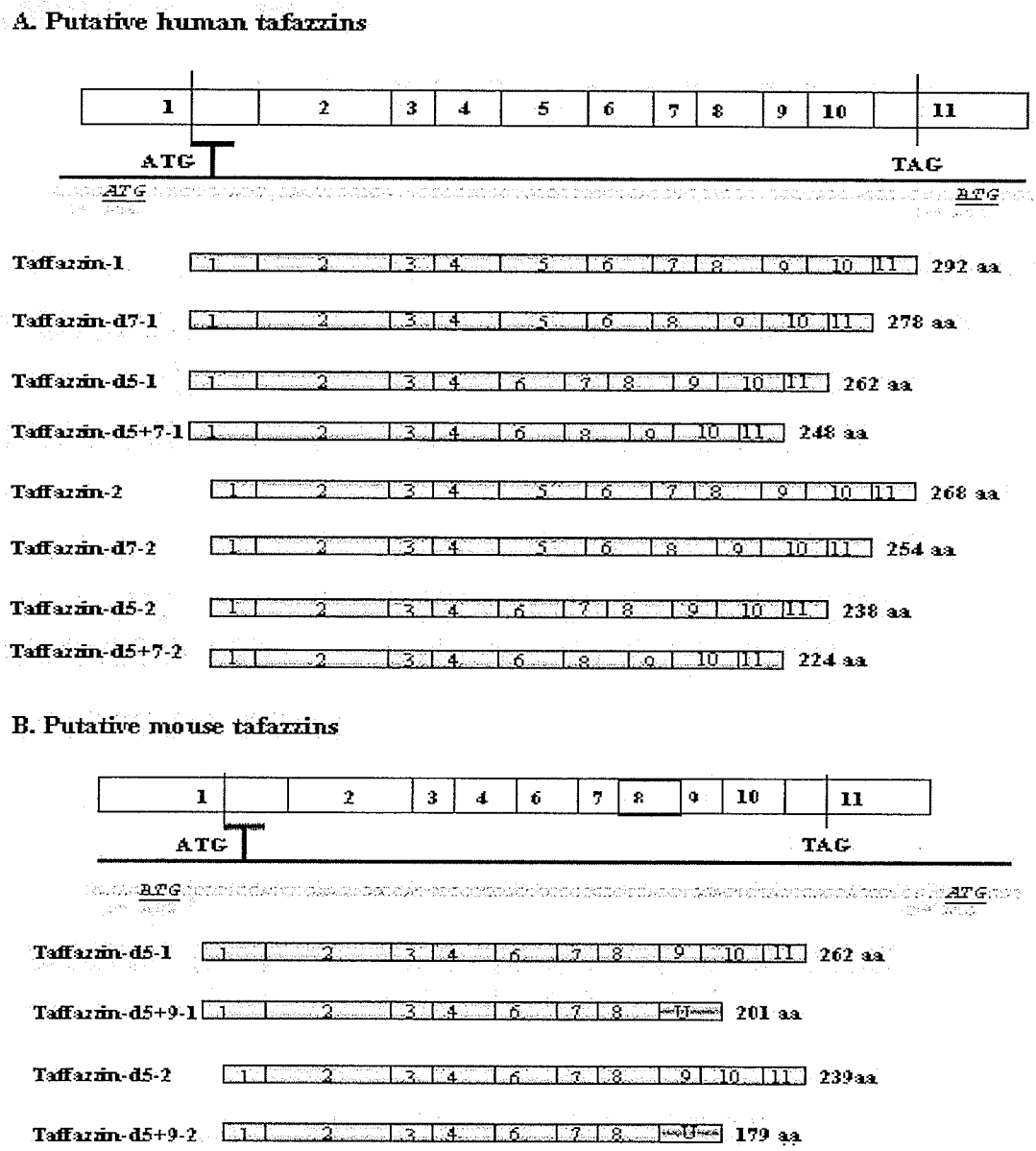

Figure 42. Putative tafazzins encoded by human and mouse mRNAs.

Putative tafazzins encoded by various human and mouse TAZ mRNAs coupled with alternative translations via the first and second in frame ATG codons. U: unique amino acid sequences created by out frame translation for exon 9 deleted mouse TAZ. The longest open reading frame is indicated by start and stop codons: ATG and TAG. The first two in frame start codons are underlined and labeled.

1.2.4 Determination of Potential Acyltransferase Activity of Human Full-length TAZ and Murine Exon 5-deleted TAZ

The alignment study indicated the presence of the phospholipid acyltransferase activity of TAZ proteins, lyso-PA activity was examined by using *in vitro* translated proteins. Similar amounts of each *in vitro* translated AGPAT proteins were used in the enzyme assays (Figure 35). Our assays demonstrated that all AGPATs including AGPAT2/3/4/5 produced radiolabeled PA. In contrast, human or murine TAZ failed to produce any radiolabeled PA. Further testing on monolyso-CL acyltransferase (MLCL) activity was also carried out by using *in vitro* and *in vivo* generated proteins. No MLCL acyltransferase activity was detected (Figure 43).

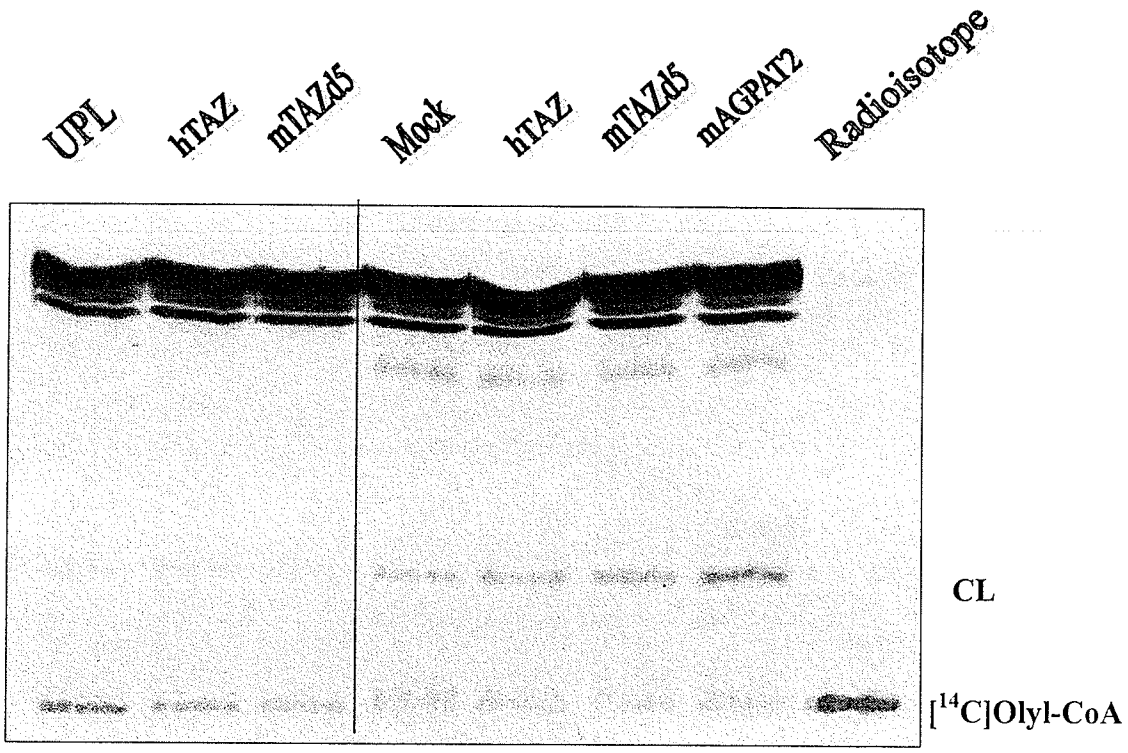

Figure 43. MLCL acyltransferase activity of in vitro and in vivo generated TAZ proteins.

MLCL acyltransferase assay with lysates of *in vitro* (first three lanes) and *in vivo* (last 5 lanes) generated proteins as described in Materials and Methods section. The positions of CL and acyl-CoA on the TLC plate are indicated.

PART II. STUDIES ON PHOSPHOLIPID CATABOLISM

I. REGULATION OF CYTOSLOLIC PHOSPHOLIPASE A_2, COX-1 AND –2 EXPRESSIONS BY PMA, TNFα, LPS AND M-CSF IN HUMAN MONOCYTES AND MACROPHAGE

Cytosolic phospholipase A_2 ($cPLA_2$) and cyclooxygenases-1 and -2 (COX-1 and -2) play a pivotal role in the metabolism of arachidonic acid (AA) and in eicosanoid production. The coordinate regulation and expression of these enzymes was not well defined. In this portion of study, the effect of phorbol 12-myristate 13-acetate (PMA), tumor necrosis factor α (TNFα), lipopolysaccharide (LPS) and macrophage-colony stimulating factor (M-CSF) on AA release and prostaglandin E_2 (PGE_2) production and the expression of $cPLA_2$ and COX-1 and -2 were investigated in U937 human pre-monocytic cells and fully differentiated macrophages.

2.1.1 PMA, TNF, LPS and M-CSF Enhance AA Release in U937 Pre-monocytes and Macrophages.

AA is released from cell membrane phospholipids via the action of a family of phospholipase A_2, mainly $cPLA_2$. The effect of stimuli on AA release was examined in undifferentiated U937 pre-monocytes and in differentiated macrophages. As shown in Figure 44A, treatment of U937 cells for 8 h with PMA, LPS and TNFα enhanced AA release. Prolonged incubation of cells for up to 24 h resulted in a higher amount of AA release (Figure 44 A). PMA (160 nM) had the maximal effect on AA release (40% increase at 8 h and 150% increase at 24 h compared to control). In macrophages,

treatment with TNFα and LPS resulted in an increase in AA release compared to controls (Figure 44 B). The amount of AA released from macrophages was greater than U937 cells after 8 h of treatment (Figure 44). Treatment of either U937 cells or macrophages for 8 h with M-CSF did not affect AA release. After prolonged (24 h) incubation, TNFα and LPS induced a further enhancement of AA release from macrophages (Figure 44 B). In both U937 cells and macrophages, M-CSF enhanced AA release after 24h treatment. These results demonstrated that PMA, TNFα, LPS and M-CSF were capable of inducing AA release in U937 cells and macrophages.

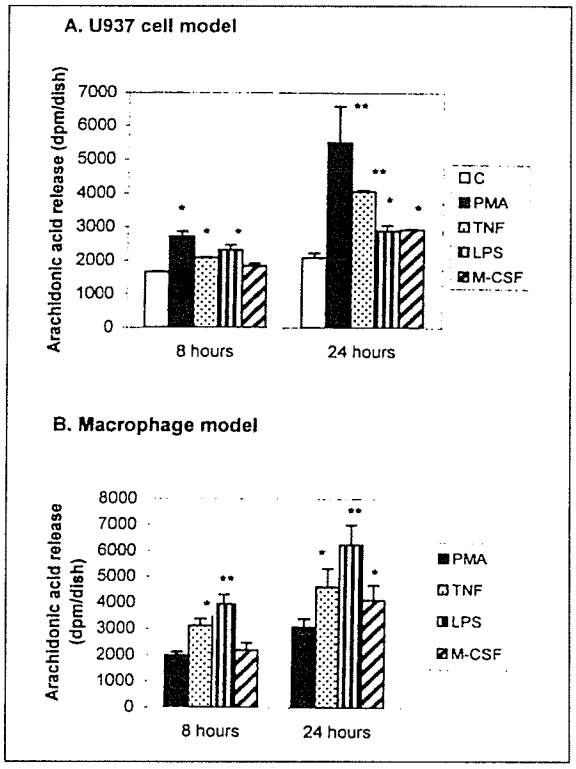

Figure 44. The effect of stimuli on arachidonic acid (AA) release in U937 cells and macrophages.

U937 cells or macrophages were incubated for 12 h with 1.0 μCi/ml [^{3}H] AA, washed and subsequently U937 cells were treated with PMA (160 nM), TNFα (10 ng/ml), LPS (100 ng/ml), or M-CSF (10 μg/ml) for 8 h or 24 h, respectively. Macrophages were treated with the same amount of TNFα, LPS, or M-CSF for same periods of time as in U937 cells. The AA released from cells was determined as described in *Methods*. **A.** U937 cells. **B**. Macrophages. Results presented are means ± SD of three independent experiments. * $p<0.05$. ** $p<0.01$.

2.1.2 PMA, TNFα, LPS and M-CSF Differentially Affect PGE_2 Production in U937 cells and Macrophages

PGE_2 is an important prostanoid produced via the cyclooxygenase pathway. The availability of AA and its subsequent metabolism by cyclooxygenases are responsible for PGE_2 biosynthesis. Hence, the effect of stimuli on PGE_2 production was examined in U937 cells and macrophages. As shown in Figure 45, the effects of stimuli on PGE_2 production were different from that of AA release. The basal level of PGE_2 production in U937 cells was low compared with macrophages (Figure 45). An 8 h challenge of U937 cells with stimuli had little effect on PGE_2 production. In contrast, PMA treatment of U937 cells for 24 h resulted in a 6.4-fold ($p<0.05$) stimulation of PGE_2 production (Figure 45 A). TNFα, LPS and M-CSF did not affect PGE_2 production in U937 cells. Treatment of macrophages with LPS stimulated PGE_2 production at 8 h and 24 h compared with the control (Figure 45 B). In contrast, TNFα and M-CSF did not affect PGE_2 production in macrophages.

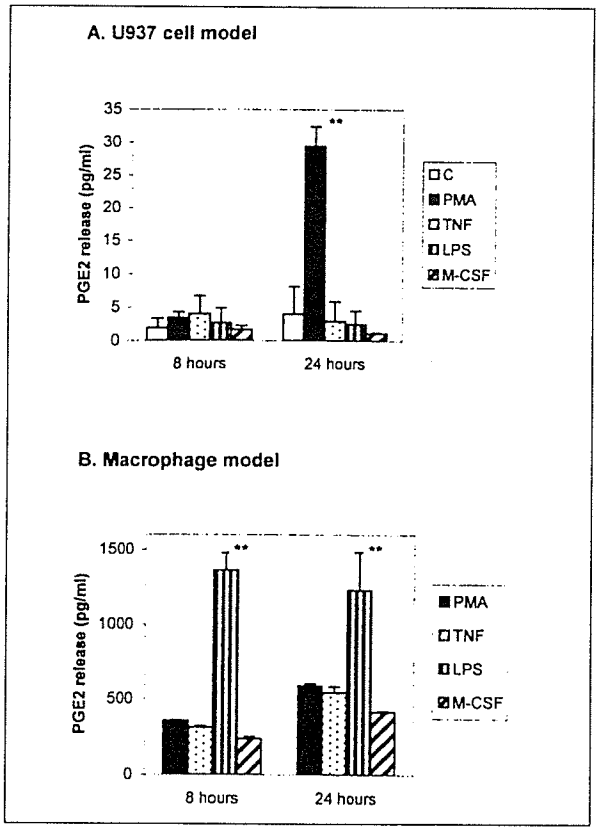

Figure 45. The effect of stimuli on PGE_2 production in U937 cells and macrophages. U937 cells were treated with PMA (160 nM), TNF (10 ng/ml), LPS (100 ng/ml), or M-CSF (10 μg/ml) for 8 h or 24 h, respectively. Macrophages were treated with the same amount of TNFα, LPS, or M-CSF for same periods of time as in U937 cells. PGE_2 released into the medium was measured by EIA, as described in *Methods*. ***A***. U937 cells. ***B***. Macrophages. Results presented are means ± SD of three independent experiments. ** $p < 0.01$.

2.1.3 Differential Expression of $cPLA_2$, COX-1 and COX-2 by PMA, TNFα, LPS and M-CSF in U937 Cells and Macrophages

The mechanism of the stimuli-mediated alterations in AA release and PGE_2 production was examined. The effects of PMA, TNFα, LPS and M-CSF on AA release and PGE_2 production in U937 cells and macrophages could result from altered enzyme activities and/or protein mass. Hence, the expressions of $cPLA_2$, COX-2 and COX-1 enzyme proteins were determined. PMA, TNFα, LPS and M-CSF treatment of U937 cells resulted in a bi-phasic alteration in $cPLA_2$ protein expression. During the early course (8 h) of treatment, $cPLA_2$ protein was up-regulated 1.8-3.4 fold ($p<0.05$) by all stimuli (Figure 46). Prolonged treatment (24 h) with the same stimuli attenuated $cPLA_2$ expression. The attenuation of $cPLA_2$ expression by TNFα was the greatest and presumably due to the pro-apoptotic action of this compound (Figure 46). Early (8 h) and prolonged (24 h) treatment of macrophages with TNFα and M-CSF did not affect $cPLA_2$ expression (Figure 47). In contrast, LPS increased $cPLA_2$ expression during the early course (8 h) but not during prolonged (24 h) incubation compared with control (Figure 47). These data were consistent with the LPS-mediated AA release and PGE_2 production in macrophages (Figure 44 and 45).

U937 cells expressed COX-1 protein and treatment with TNFα, LPS or M-CSF for 8 h or 24 h did not affect COX-1 expression compared with control (Figure 48). In contrast, PMA treatment for 8 h or 24 h enhanced expression of COX-1 protein (Figure 48). Macrophages expressed COX-1 protein at a level 2.5-3.5 fold ($p<0.05$) higher than in U937 cells (Figure 49). Treatment of macrophages with TNFα, LPS or M-CSF did not enhance expression of COX-1 protein (Figure 49). COX-2 was not expressed in U937

cells in the absence of PMA (Figure 50). COX-2 was expressed in macrophages and treatment of macrophages for 8 h or 24 h with LPS up-regulated COX-2 expression 3.3-4 fold ($p<0.05$) (Figure 50). TNFα and M-CSF did not affect COX-2 expression. These data were consistent with an LPS-mediated elevation in PGE_2 production in macrophages.

In summary, the data indicate that PMA induces AA release and PGE_2 production via up-regulation of $cPLA_2$ and COX1 protein expression in U937 pre-monocytes. In contrast, macrophages respond to LPS challenge by producing large quantities of AA and PGE_2 via up-regulation of $cPLA_2$ and induction of COX-2 enzyme protein. Thus, short term LPS-treatment of macrophages preferentially enhances AA release and PGE_2 production via up-regulation of $cPLA_2$ and COX-2 protein expression.

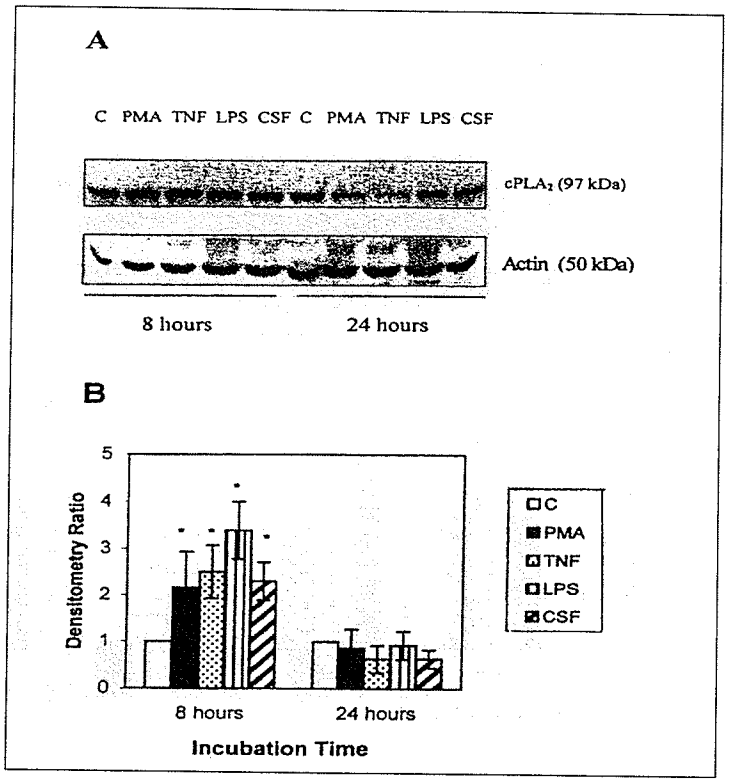

Figure 46. The effect of stimuli on $cPLA_2$ protein expression in U937 cells.

Cells were treated with stimuli as described in Figure 45. Following treatment, the cell lysate was subjected to western blot analysis, using specific antibodies for $cPLA_2$ and β-actin, as described in *Methods*. **A.** A representative blot is depicted. **B.** Densitometry ratio (target protein $cPLA_2$ over β-actin) plot of **A**. Results presented are means ± SD of three independent experiments. * $p<0.05$.

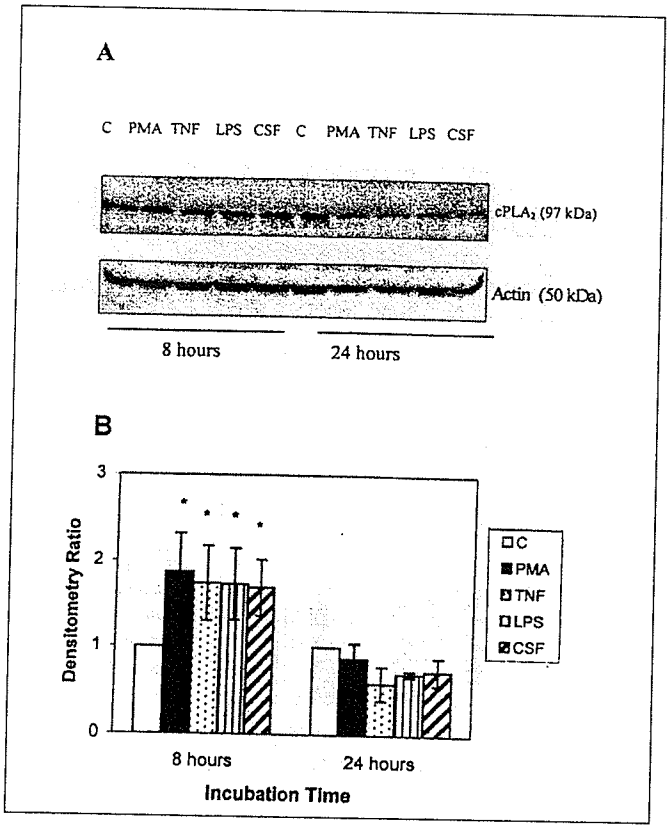

Figure 47. The effect of stimuli on $cPLA_2$ protein expression in macrophages.

Cells were treated with stimuli as described in Figure 45. Following treatment, the cell lysate was subjected to western blot analysis, using specific antibodies for $cPLA_2$ and β-actin. **A.** A representative blot is depicted. **B.** Densitometry ratio (target protein $cPLA_2$ over β-actin) plot of **A**. Results presented are means ± SD of three independent experiments. * $p<0.05$.

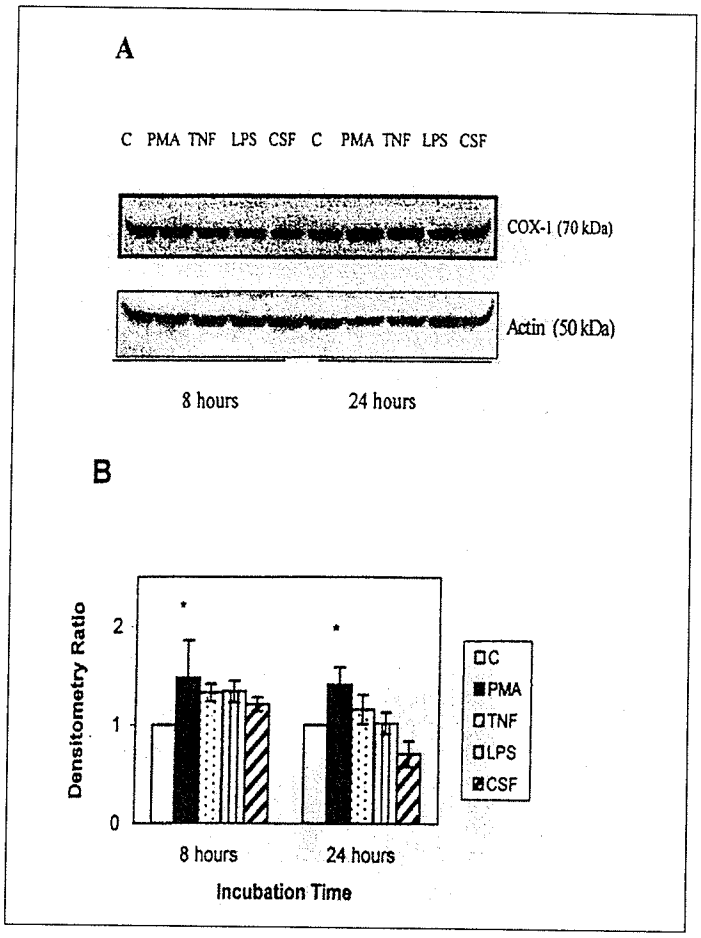

Figure 48. The effect of stimuli on COX-1 protein expression in U937 cells.

Cells were treated with stimuli as described in Figure 45. Following treatment, the cell lysate was subjected to western blot analysis, using specific antibodies for COX-1 and β-actin. **A.** A representative blot is depicted. **B.** Densitometry ratio (target protein COX-1 over β-actin) plot of **A**. Results presented are means ± SD of three independent experiments. * $p<0.05$.

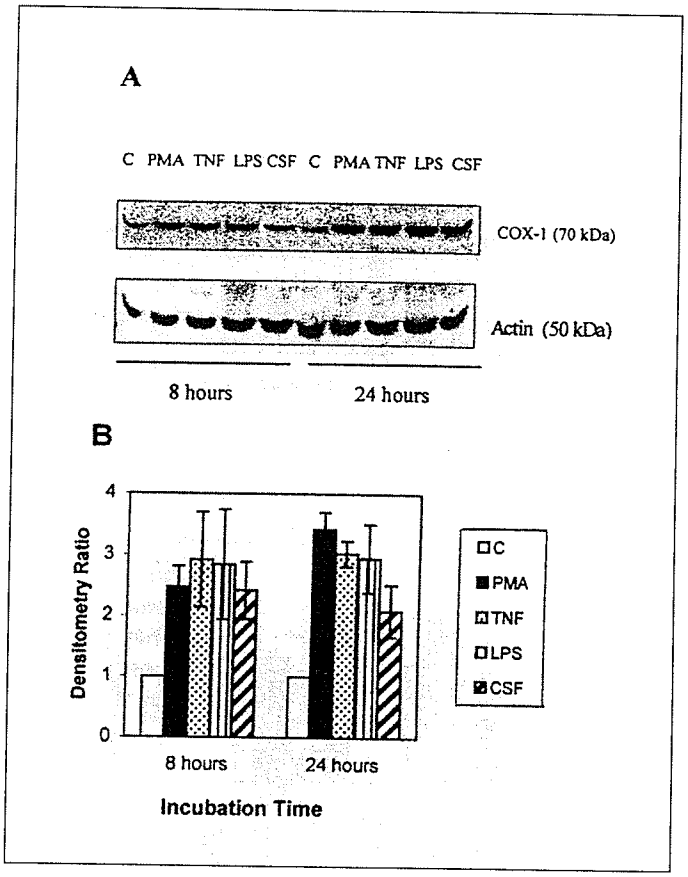

Figuer 49. The effect of stimuli on COX-1 protein expression in macrophages. Cells were treated with stimuli and the expression levels of COX-1 and β-actin were determined by western blot analysis, as described in Fiure 45. **A.** A representative blot is depicted. **B.** Densitometry ratio (target protein COX-1 over β-actin) plot of **A**. Results presented are means ± SD of three independent experiments.

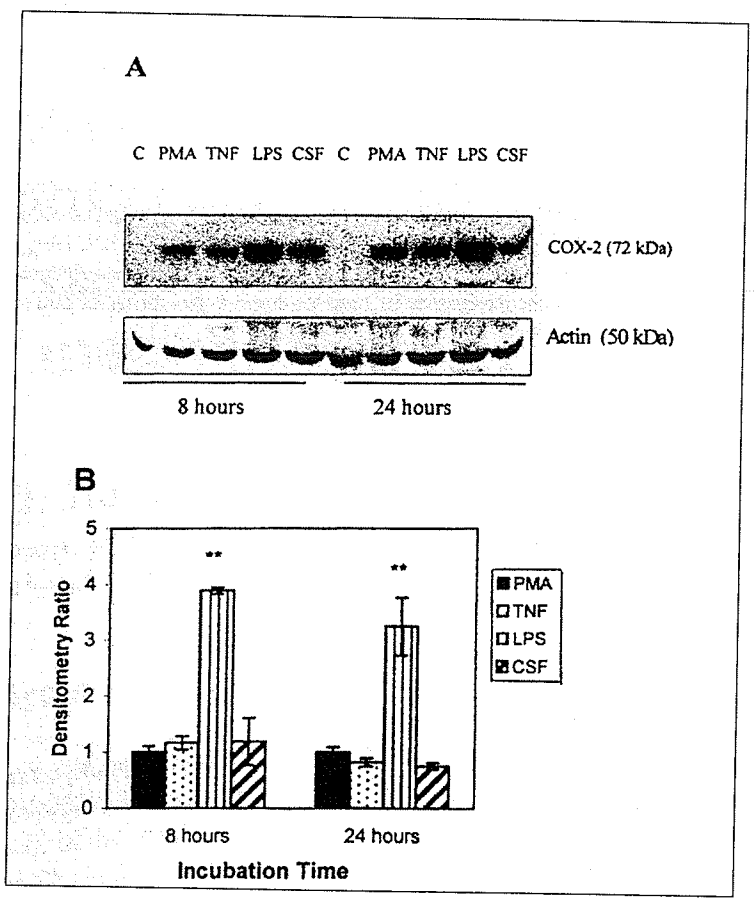

Figure 50. The effect of stimuli on COX-2 protein expression in macrophages. Cells were treated with stimuli and the expression levels of COX-2 and β-actin were determined. **A.** A representative blot is depicted. **B.** Densitometry ratio (target protein $cPLA_2$ over β-actin) plot of **A**. Results presented are means ± SD of three independent experiments. ** $p < 0.01$.

II. REGULATION OF ARACHIDONIC ACID METABOLISM BY PMA IN MONOCYTES AND MYOCYTES

The purpose of this section is to study coordinated regulation of the arachidonate-prostanoid cascade. The effect of phorbol 12-myristate 13-acetate (PMA) on AA release and PGE2 production was monitored in two different model cells: human monocytes and rat cardiac myocytes. The important roles of both $cPLA_2$ and COX-1/-2 in the regulation of the arachidonate-eicosanoid cascade were confirmed in both monocytes and cardiac myocytes.

2.2.1 PMA Induced Arachidonic Acid Release in U937 Cells

We reported earlier that PMA caused an enhancement of AA release in H9c2 cells (Tran et al. 1996). In this study, the effect of PMA on AA release in human premonocytic U937 cells was investigated. Labeled arachidonic acid was incorporated into U937 cells by incubating the cells in a serum-free RPMI-1640 medium containing 0.1% BSA, and [^{3}H] arachidonic acid (1.0 uCi/ml) was added into the incubating mixture. The cells were incubated for 12 h at 37^0 C, and then washed with the unlabeled medium. For each study, the labeled cells were incubated with the serum-free medium (with 1% BSA) and 160 nM PMA for various time periods. Subsequent to the prescribed period of incubation, the cells were stimulated with calcium ionophore (Ionomycin, 5 μM) for 15 min, and the amount of labeled AA released to the medium was determined. As shown in Figure 51, an increase in AA release was sustained at all time points (up to 72 h) of PMA treatment, but the maximum increase in AA release was obtained at 0.5 h of incubation. Our results indicate that the enhancement of AA release by PMA treatment in U937 cells was similar to that obtained in H9c2 cells (Tran et al. 1996).

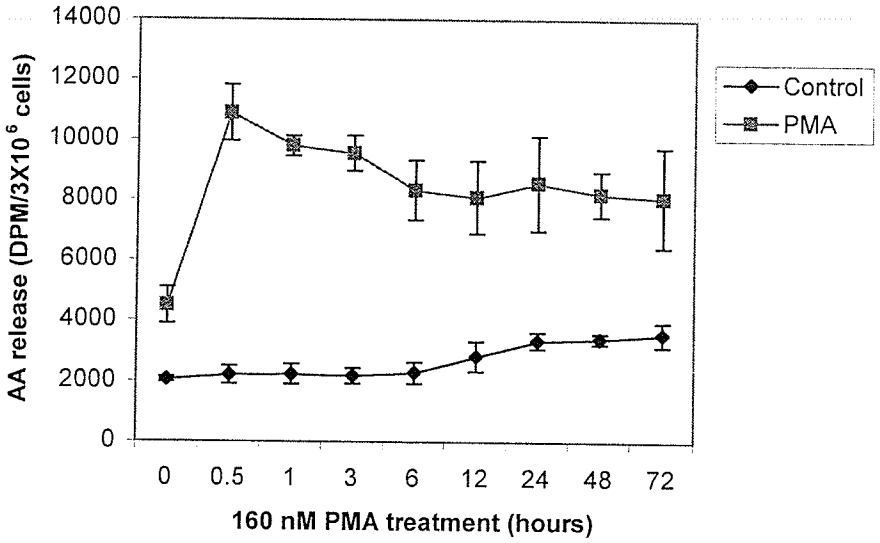

Figure 51. PMA-induced arachidonic acid release in U937 cells.

U937 cells were metabolically labeled with [^{3}H] arachidonic acid, washed, and then incubated in the absence or presence of 160 nM PMA for 0-72 h. After PMA treatment, the cells were stimulated with 5 μM Ionomycin for 15 min. An aliquot of the medium was recovered and labeled arachidonic acid was isolated by thin-layer chromatography (TLC) and quantified by scintillation counting. Data are expressed as means ± S.D. of three separate sets of experiments.

2.2.2 PMA Induced PGE_2 Release in U937 and H9c2 Cells

AA is the precursor for eicosanoid biosynthesis. In this study, the release of PGE_2 into the medium following PMA stimulation in U937 and H9c2 cells were determined. Cells were stimulated by PMA as described in the previous section, and the amount of PGE_2 released into the medium was determined by enzyme immunoassay (EIA). As shown in Figure 52a, the PMA treatment did not cause a detectable increase in PGE_2 production during the first 12-h treatment. Interestingly, the amount of PGE_2 in the medium was marginally elevated at 24 h of treatment, and a substantial increase was observed at 48 and 72 h of incubation. In a dose-response study, a 19-fold increase in PGE_2 production was observed when cells were treated with 1 nM PMA (Table 13.). Maximum increase in PGE_2 release (26-fold increase) was observed by the treatment with 100 nM PMA under identical experimental conditions.

PMA treatment also caused a moderate increase of PGE_2 release in H9c2 cells. In a time course study, an increase in PGE_2 release was observed at 3 h of incubation. A higher degree of increase in PGE_2 release was observed during 24 and 48 h of incubation. Further increase in the incubation time did not cause a high degree of increase in PGE_2 release in the H9c2 cells (Figure 52b). Our results indicated that PMA treatment caused a time dependent enhancement of PGE_2 release in both U937 and H9c2 cells. A more rapid response to PMA treatment was observed in H9c2 cells than U937 cells. In both cases, the enhancement of AA release by PMA precedes the increase in PGE_2 release in both cell types.

(a)

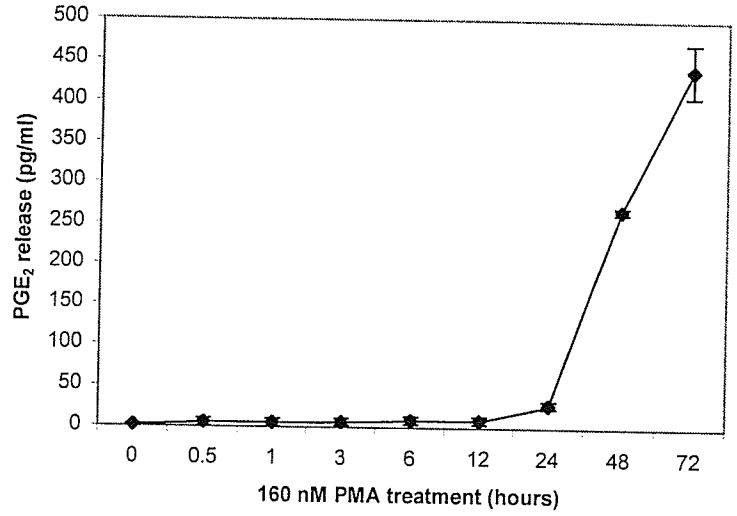

(b)

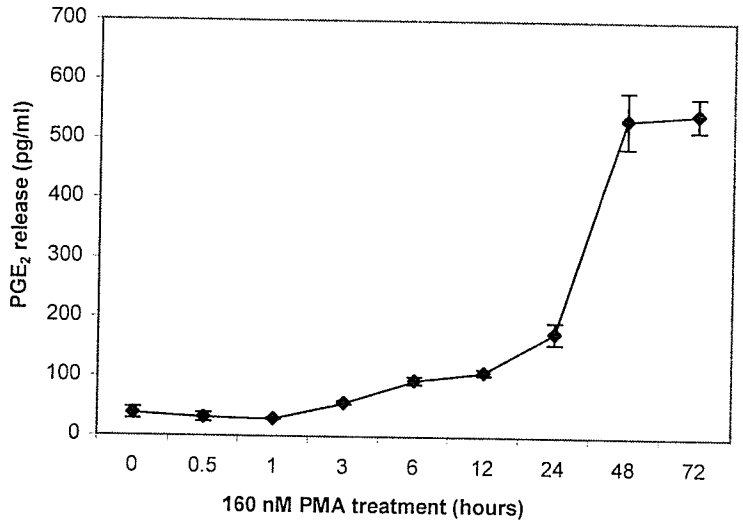

Figure 52. PMA-induced PGE_2 release in U937 and H9c2 cells.

U937 (Figure a) and H9c2 (Figure b) cells were incubated in serum-free PMRI or DMEM-medium containing 0.1% BSA in the presence of 160 nM PMA for 0-72 h. After PMA treatment, an aliquot of the medium was taken for the determination of PGE_2 production by EIA. Data are expressed as means ± S.D. of four separate sets of experiments.

Table 13. The effect of PMA on PGE_2 release in U937 cells

PMA treatment (nM)	PGE_2 release (pg/ml)
0	9.54 ± 2.08
1	193.56 ± 28.14 [a]
10	249.90 ± 27.12 [a]
100	256.37 ± 28.60 [a]
200	238.00 ± 4.51 [a]
400	217.68 ± 75.31 [a]

U937 cells were incubated in serum-free PMRI-1640 medium containing 0.1% BSA with increasing concentration of PMA for 48 h. The cell-free medium was recovered and PGE_2 concentration was determined by EIA. Results are means ± standard deviation of two separate sets of experiments. [a] $P < 0.05$ when compared with the control (untreated).

2.2.3 Effect of PMA on $cPLA_2$, COX-1, and COX-2 in U937 and H9c2 Cells

The PMA-induced enhancement of AA release and PGE_2 production could be caused by the increase in the respective enzymes. Hence, quantitative determination of enzymes obtained from the control and PMA treated cells were analyzed by SDS-PAGE. As shown in Figure 53a. $cPLA_2$ level was marginally higher in cells treated with 160 nM PMA during the first 0.5 h (116% ± 9%) and reached a maximum at 24 h (153% ± 12%). After 24 h of incubation, the level of $cPLA_2$ was drastically reduced (62% ± 10% at 48 h, 38% ± 1% at 72 h). It appears that PMA caused a biphasic response in the modulation of $cPLA_2$ enzyme levels, with an early up-regulation followed by a down-regulation. The biphasic change of $cPLA_2$ levels may in part contribute to the observed increase in AA release in the early phase of PMA stimulation, followed by a moderate reduction after prolonged treatment.

A similar pattern of response on the level of $cPLA_2$ by PMA treatment was also obtained in H9c2 cells. Treatment with PMA caused an immediate increase of the $cPLA_2$ level, and the stimulation was maintained at the first 6 h of incubation. The effect was diminishing at 12 h, and totally eliminated at 24 h of incubation. This observation is consistent with the observed biphasic response of PGE_2 release by PMA stimulation in H9c2 cells (Figure 52b).

The effect of PMA on the levels of COX-1 and COX-2 enzyme proteins was also studied under the same experimental conditions. In U937 cells, PMA treatment caused a slight decrease in COX-1 protein level during the first 6 h of incubation, and returned to the control level after 12 h of incubation (Figure 53a). The COX-1 level was subsequently up-regulated between 24-72 h, with a 6-fold increase in enzyme level at the

72 h time point. In contrast, COX-2 protein was not detected in untreated U937 cells. Upon PMA treatment, COX-2 protein was induced and became detectable 3 hours after PMA-treatment. The enzyme level was found to increase linearly between 3-24 h, and exponentially between 24-72 h of incubation. The change in COX-2 enzyme levels is consistent with the observed increase in PGE_2 release in U937 cells (Figure 52a), suggesting that it may play a significant role in PGE_2 production.

Treatment of H9c2 cells with PMA also caused a biphasic response in COX-1 level during a time course study (Figure 53b). The enzyme level was reduced during the first 6 hours of treatment, and subsequently returned to normal level after 24 hours of treatment. The level of COX-2 was slightly elevated between 3-24 h of incubation, and greatly stimulated at 48 h and 72 h of incubation (Figure 53b). The immunostaining of actin in the same blot was employed as a control to exclude the possibility of unequal loading of the protein sample into the gel. The change in COX-2 enzyme level is consistent with the observed increase in PGE_2 release in H9c2 cells (Figure 52b).

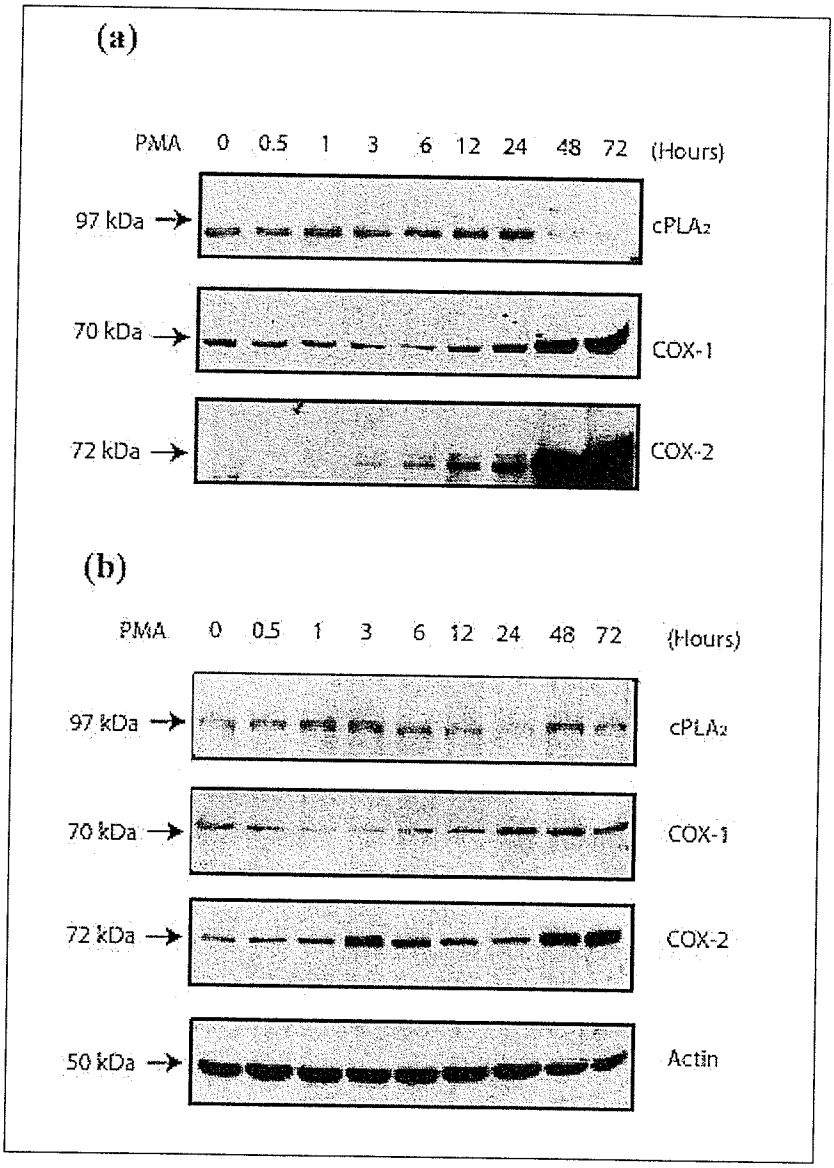

Figure 53. Effects of PMA on $cPLA_2$, COX-1, and COX-2 in U937 and H9c2 cells. U937 (Figure a) and H9c2 (Figure b) cells were incubated with 160 mM PMA for 0-72 h. The cell lysates containing 50 mg of protein were subjected to SDS-PAGE (8.0%). The protein bands in the gel were transferred to PVDF sheet and treated with respective primary antibodies. Protein bands corresponding to $cPLA_2$, COX-1, and COX-2 were detected by a coupled peroxidase color development system.

2.2.4 The Efficacy of PMA in the Modulation of COX-1 and COX-2

The efficacy of PMA in the modulation of COX-1 and COX-2 proteins in U937 and H9c2 cells was tested in a dose-response study. U937 cells were incubated with various concentrations of PMA (1-400 nM) in serum-free RPMI-1640 medium containing 0.1% BSA for 48 h. An aliquot of the cell lysate containing 50 μg of protein was subjected to SDS-PAGE (8.0%). As shown in Fig. 54a, COX-1 levels were effectively up-regulated at low PMA levels (1 nm PMA with 5-fold increase) and were not significantly affected by increasing PMA concentrations between 10-400 nM. In contrast, COX-2 was not detectable in U937 cells in the absence of PMA (Figure 54a). However, COX-2 was induced upon PMA treatment, and the levels increased in a dose-dependent manner with an optimal concentration of PMA between 50-200 nM. A similar set of experiments was conducted with H9c2 cells (Figure 54b). The COX-1 levels in these cells were not significantly affected by increasing PMA concentrations between 1-100 nM. A marginal increase was noticed with high dose of PMA treatment (>100 nM). However, COX-2 was significantly up-regulated by increasing PMA concentrations between 1-200 nM. The results obtained from this study indicate that an optimal concentration of PMA (160 nM) was used in our study. It also illustrates the diversity of response by different cell types to low concentrations of PMA in the modulation of enzyme levels.

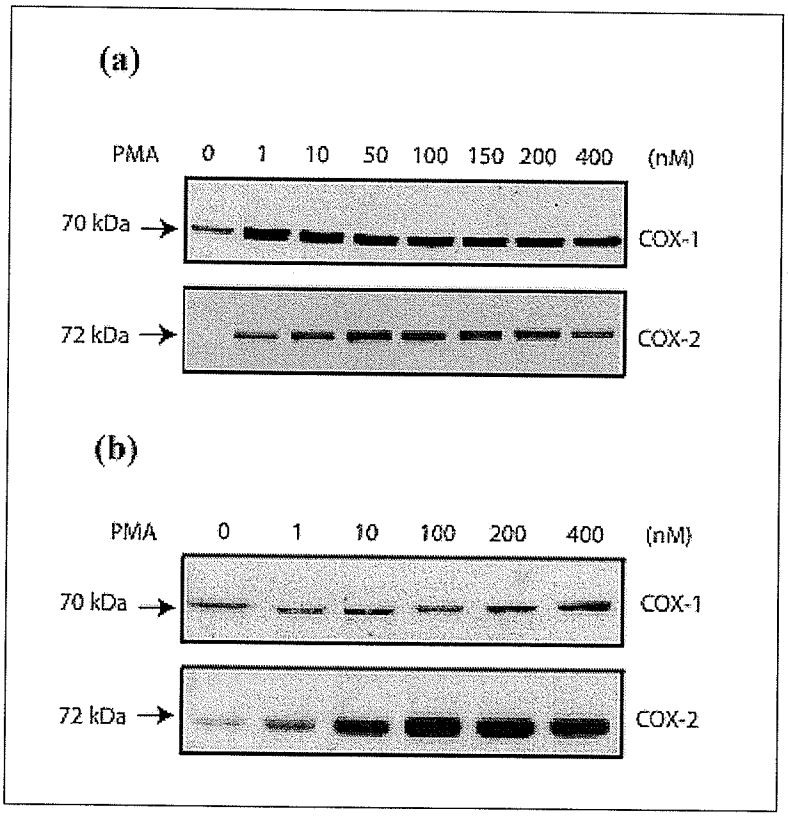

Figure 54. Dose response relationship for the effects of PMA on enzyme protein synthesis of COX-1, and COX-2 in U937 and H9c2 cells.

U937 (Figure a) AND H9c2 (Figure b) cells were incubated in serum-free medium containing 0.1% BSA with increasing concentration of PMA for 48 h. The cell lysates containing 50 μg of protein were subjected to SDS-PAGE (8.0%). The protein bands in the gel were transferred to PVDF sheet and treated with respective primary antibodies. Protein bands corresponding to COX-1, and COX-2 were detected by a coupled peroxidase color development system.

III. 17-β ESTRADIOL ENHANCES PROSTAGLANDIN E_2 PRODUCTION IN HUMAN U937-DERIVED MACROPHAGES

The regulation of the arachidonate-eicosanoid cascade in macrophages appears to be controlled by multiple interconnected pathways. Estrogens have been shown to regulate the expression of genes in lipid metabolism and macrophage activation. The purpose of this section is to study the modulatory effects of various estrogen receptor ligands on the production of PGE_2 using human U937-derived macrophages in culture.

2.3.1 Assessment of PMA-induced U937 Cell Differentiation by Morphologic Observation and Cell Surface Antigen Expression

Exposure of U937 cells to 162 nM PMA for 48 h resulted in a dramatic change in cell morphology from premonocyte (Figure 55A) to macrophage (Figure 55B). The differentiated cells were flat, and showed a decrease of nuclear/cytoplasmic ratio. In addition, the differentiated cells became firmly adhered to the bottom of the culture dishes, whereas the untreated control cells remained in suspension. Our results suggest that U937 cells underwent differentiation into macrophages upon PMA induction under our experimental condition.

CD11b, a surface marker of monocyte-macrophage lineage, is a 165-kDa adhesion glycoprotein that associates with integrin β2 to form CD11b/CD18 complex. PMA treatment of monocytes caused a two-fold increase in the number of cells expressing CD11b from premonocyte (Figure 55C) to macrophage (Figure 55D). The change in CD11b provided added evidence that cells were differentiated towards the mature macrophage phenotype under our experimental conditions (Hass et al. 1989).

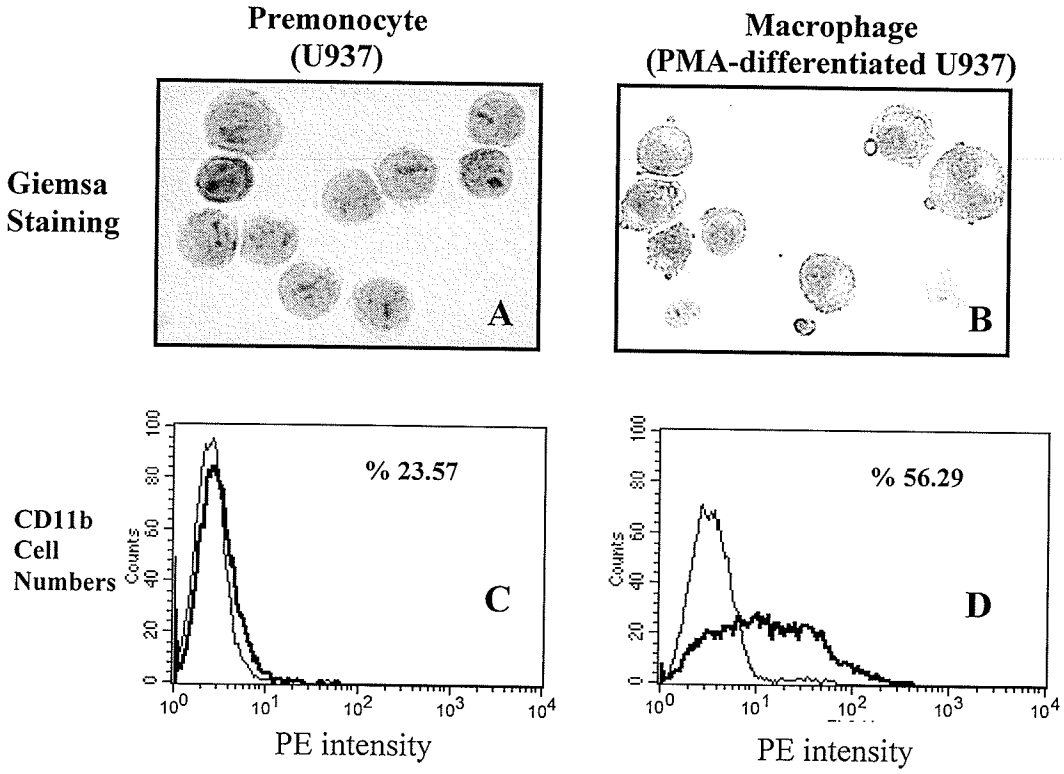

Figure 55. Changes in morphology and cell surface markers of U937 cells upon PMA induction.

U937 cells were incubated in the presence or absence of 162 nM PMA for 48 h. After PMA treatment, cells were collected, fixed, and stained with Giemsa (Figure A + B). Stained cells were photographed at high magnification (×600). For cell surface antigens, PMA-differentiated U937 cells as well as undifferentiated control U937 cells were exposed to primary anti-CD11b. The specific binding and positive cells of CD11b surface marker were measured by flow cytometric analysis as described under Materials and Methods (Figure C + D).

2.3.2 Increase in the Expression of ER-α in PMA Differentiated U937 Cells.

To address the expression of classical estrogen receptor alpha (ER-α) in U937 cells, two different approaches were employed. In the immunocytohistochemical study, a specific human ER-α staining was observed in only a small fraction of the cell population, and the immunostaining was confined to the nucleus of undifferentiated U937 cells (Figure 56A-a). Upon PMA treatment, cell numbers for positive staining increased from 37% to 56%, and there was a definite increase in the staining intensity (Figure 56A-b). The staining was not entirely confined to the nucleus, and some peri-nuclear staining was detected. To confirm the specificity of the immunostaining, the untreated U937 cells were incubated with biotinylated anti-mouse IgG only, and no immunostaining was observed (Figure 56A-c). In a separate set of experiments, the immuno-cytohistochemical finding was confirmed by determining the ER-α protein levels with Western blotting. Lysates from each subcelluar fraction were prepared as described in the previous section, and the specific ER-α bands were detected using anti-human ER-α mAb (Figure 56B). Treatment of U937 cells with 162 nM PMA for 48 h caused a two-fold increase in ER-α levels as compared to that of untreated controls, where the ER-α protein was confined to the nuclear fraction. Taken together, our results indicate that ER-α was expressed predominantly in the nuclei of U937 cells, and the expression level was increased in U937-derived macrophages.

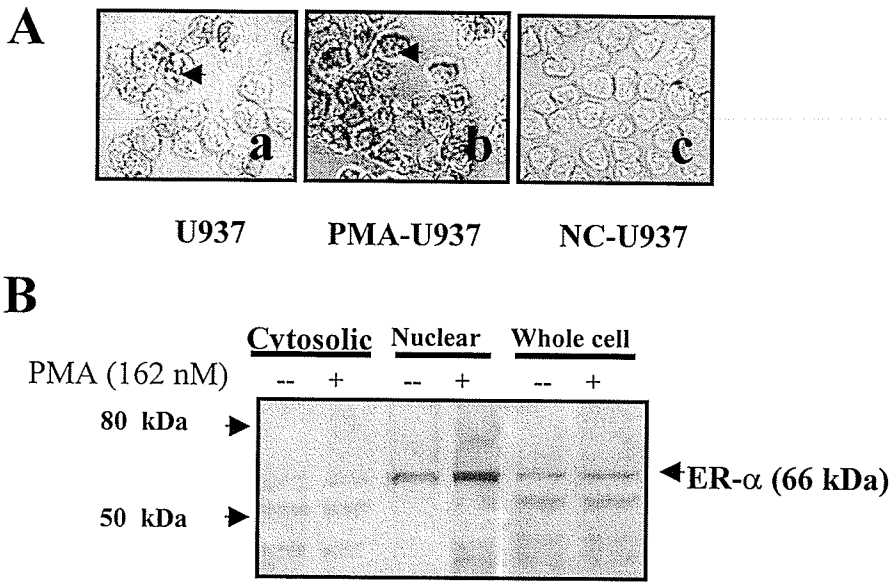

Figure 56. ER-α expression in U937 and PMA-differentiated U937 cells.

U937 cells were incubated in the presence or absence of 162 nM PMA for 48 h. The cells or cell lysates were subject to both immunocytochemical staining (Figure A) and Western blot analysis (Figure B) for human ER-α. Figure A: (a) immunocytochemical staining of human ER-α in unstimulated control U937cells, (b) PMA-differentiated U937 cells, and (c) primary antibody omitted negative control U937 cells. Staining was mostly located within the nucleus, with some peri-nuclear and plasma membrane straining (arrows). Figure B: Western blot analysis of human ER-α in subcellular fractions. Cytosolic lysate, nuclear lysate, and whole cell lysate containing 50 μg of protein were subjected SDS-PAGE (8%). The protein bands in the gel were transferred to a PVDF sheet and treated with mouse anti-ER monoclonal antibody (mAb). Protein bands corresponding to human ER-α (66 kDa) were detected by a coupled peroxidase color development system.

2.3.3 17-β Estradiol Enhanced PGE_2 Production in PMA-differentiated U937 Cells

PMA caused an induction of cell differentiation and an up-regulation of ER-α expression of U937 cells under our experimental condition. We reported earlier that U937 cells produced little PGE_2 (< 10 pg/ml) under normal culture conditions, and the release of PGE_2 into the medium following PMA stimulation increased significantly (Jiang et al. 2003). In this study, the effect of various ER ligands on PGE_2 production was tested on the U937-derived macrophages. After the induction of differentiation, the incubation medium was changed to a serum- and phenol- free medium in the presence or absence of an ER ligand for 48h. The amount of PGE_2 released into the medium was then determined by enzyme immunoassay (EIA). As shown in Figure 57A, 17-β estradiol caused a significant enhancement in PGE_2 production (2575 pg/ml vs. 381.3 pg/ml in the control). Alternatively, no effect on the PGE_2 production was observed when cells were incubated with the antiestrogens 4-OH-TAM and ICI182 780, the plant-derived nonsteroidal phytoestrogen Genestein, and the non-binding control reagent 17-α estradiol. In a dose-response study, a 1.9 fold increase in PGE_2 release was observed when macrophages were treated with 1 nM 17-β estradiol (Figure 57B). Maximum increase in PGE_2 release (6-8 fold increase) was achieved by 10 to 100 nM 17-β estradiol. A time-course study was also conducted to examine PGE_2 release by 17-β estradiol treatment. As shown in Figure 57C, significant increase was not observed until 48 h after 17-β estradiol treatment. The increase in PGE_2 production was sustained from 48-72 h.

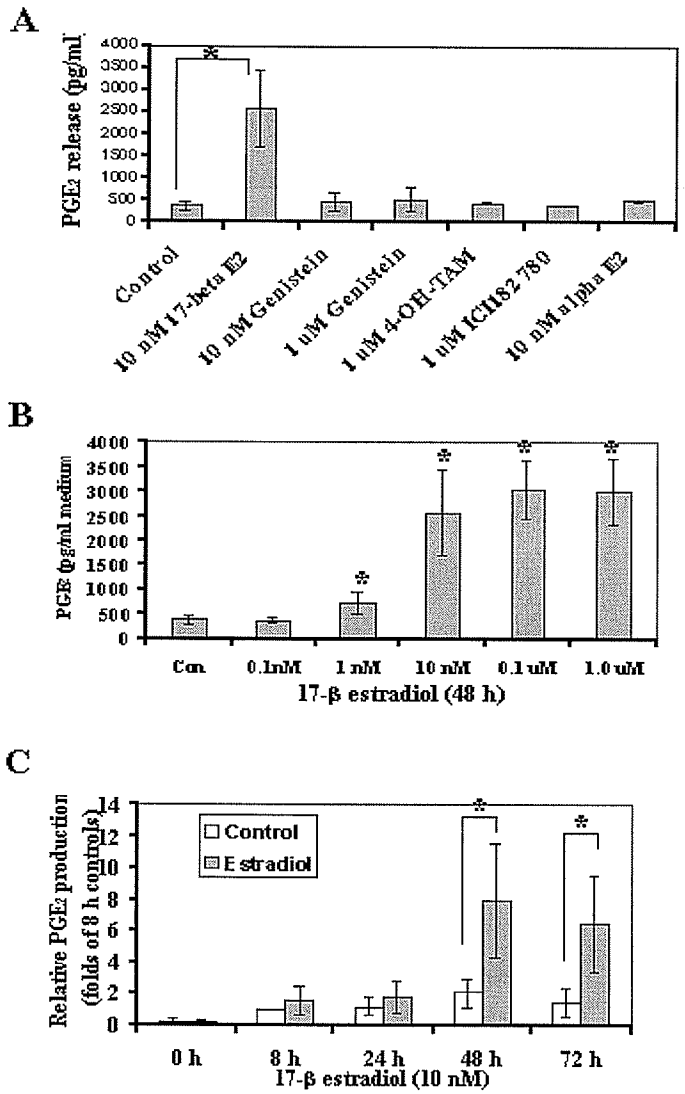

Figure 57. Effects on PGE_2 production by different ligands of estrogen receptors

PMA differentiated U937 cells were incubated in phenol-free and serum-free RPMI-1640 medium containing 0.1% BSA in the presence of indicated ER ligands. After ligand treatment, an aliquot of the medium was taken for the determination of PGE_2 production by EIA. Figure A: Cells were incubated with various ER ligands at the indicated concentration for 48 h. Figure B: cells were treated with various concentrations of 17-β estradiol for 48 h. Figure C: Cells were treated with 10 nM 17-β estradiol for 1-72 h. Results presented are mean ± S.D. of at least three independent experiments, each carried out in duplicate. * $P < 0.05$

2.3.4 17-β Estradiol Enhanced AA Release and Up-regulated COX-1 and COX-2 in PMA-differentiated U937 Cells

Arachidonic acid (AA) is released from membrane phospholipids via the action of $cPLA_2$. The effect of 17-β estradiol treatment on AA release was examined in PMA differentiated U937 cells. As shown in Figure 58, the addition of 10 nM 17-β estradiol caused an increase in AA release 24 h after stimulation, and the increase was sustained up to 72 hours. Our results indicate that the enhancement of AA release by 17-β estradiol treatment is a reflection of the enhancement of $cPLA_2$ activity and contributes to the increased production of PGE_2.

As the increase in PGE_2 production could also have resulted from an increase in COX-1 or COX-2, the quantitative determination of these enzymes in the control and 17-β estradiol treated cells were conducted. As shown in Figure 59A, both COX-1 and COX-2 enzyme protein levels were increased in a dose-dependent manner. The increase was 26% and 56% at 0.1 and 1 nM 17-β estradiol, respectively for COX-1, and greater than 180% increases was achieved at higher 17-β estradiol concentrations. Similar results were obtained for COX-2. The changes in COX-1/-2 enzyme levels were consistent with the observed enhancement of PGE_2 production in PMA-differentiated U937 cells. As a control, the house-keeping gene actin was also stained in the same blot to exclude unequal loading of the protein sample into the gel. Northern blotting analysis, using the same sample as the western blotting, indicated that the increase in enzyme protein was caused by a corresponding increase in the mRNA levels of both COX-1 and COX-2 (Figure 59B). Equal loading of the gel for the Northern blotting experiment was demonstrated by employing 28S/18S total RNAs as internal controls.

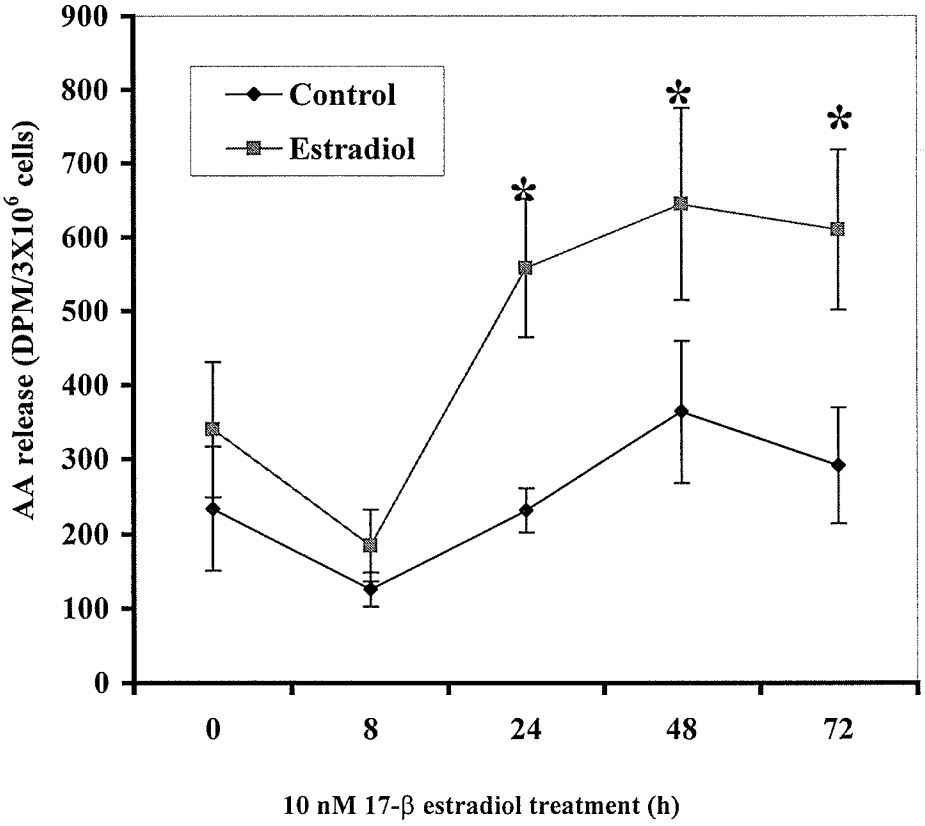

Figure 58. Effects on AA release by 17-β estradiol

PMA differentiated U937 cells were metabolically labeled with [^{3}H]arachidonic acid, and incubated in the absence or presence of 10 nM 17-β estradiol for 0-72 h. After 17-β estradiol treatment, the cells were stimulated at the lebelled time points with 5 μM Ionomycin for 15 min. An aliquot of the medium was taken and the labeled arachidonic acid was isolated by thin-layer chromatography (TLC) and quantified by scintillation counting. Data are expressed as mean ± S.D. of three separate sets of experiments. * $P < 0.05$.

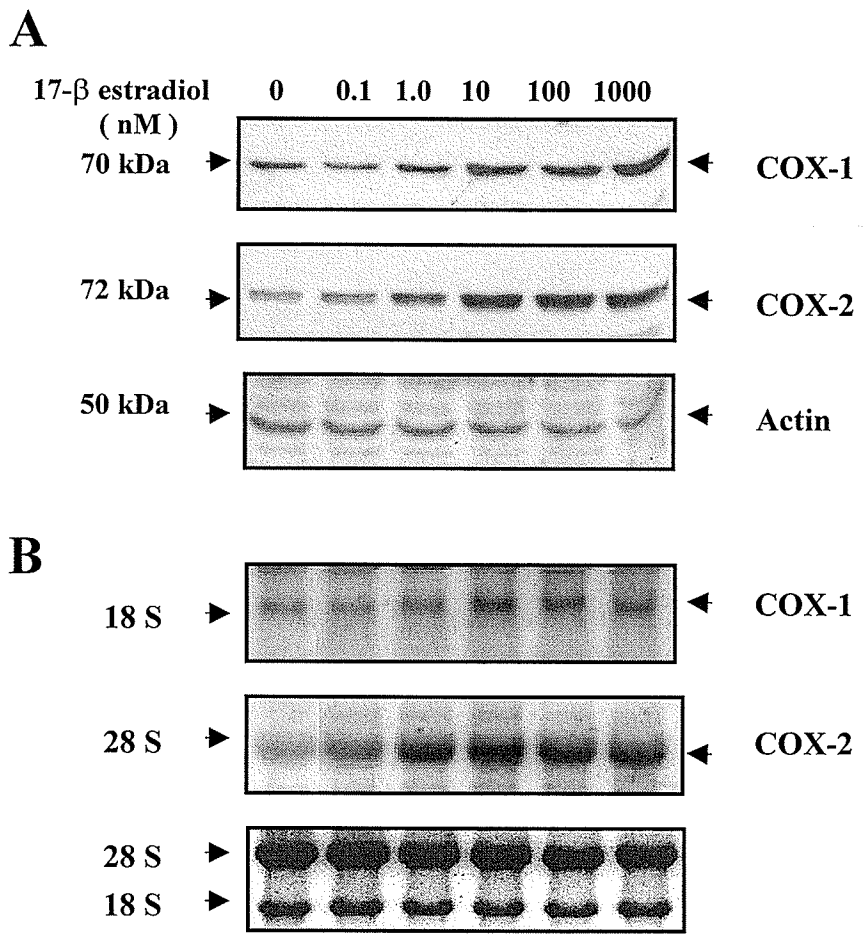

Fiure 59. 17-β estradiol enhances PGE_2 production through up-regulation of COX-1 and COX-2 enzymes

PMA differentiated U937 cells were incubated in phenol-free and serum-free PMRI-1640 medium containing 0.1% BSA in the presence of indicated amount of 17-β estradiol. Cell lysate and total RNAs were extracted and subject to Western blot analysis (Figure A) and Northern blot analysis (Figure B) as described under Material and Methods. For Western blot analysis, the cells were collected and cell lysates were made. Typically, lysates containing 50 μg of protein were subjected to SDS-PAGE (8.0%). The protein bands in the gel were transferred to PVDF sheet and treated with respective primary antibodies. Protein bands corresponding to COX-1 and COX-2 were detected by a coupled peroxidase color development system. Equal protein loading was checked by immunostaining of actin (Figure A). For Northern blot analysis, 10-20 μg of RNAs were loaded and separated by a denaturing gel. After Northern blotting and UV cross-linking, the membrane was hybridized with α-[^{32}P] labeled human COX-1/COX-2 probes respectively. Equal RNA loading was checked by ethidium bromide staining of 28S/18S RNAs in the gel (Figure B).

2.3.5 Attenuation of PGE_2 Production by Selective Estrogen Receptor Modulators (SERMs).

Co-treatment of macrophages with 17-β estradiol and SERMs was designed to further investigate the mechanism by which 17-β estradiol exerted its effect on PGE_2 production. As depicted in Figure 60A, 1 μM of 4-OH-TAM or ICI182 780 had no effects on the PGE_2 production. Treatment of the cells with 10 nM 17-β estradiol caused a 6.8-fold increase of PGE_2 production, and the enhanced PGE_2 release was not attenuated by co-treatment the cells with 1μM 4-OH-TAM. In contrast, the level of PGE_2 production was significantly reduced (38% reduction of 10 nM 17-β estradiol) by co-treatment with 1μM ICI182 780.

The modulatory effect of 4-OH-TAM and ICI182 780 on the expression of COX-1 and COX-2 proteins was studied. Using the Western blotting analysis, these two compounds had no effect on the expression of the enzyme proteins (lane 5 and 6 of Figure 60B). However, a partial reduction in both COX-1 and COX-2 levels was elicited by ICI in the 17-β estradiol treated cells (Figure 60B. lane 4 vs. 2). These results indicated that some selective estrogen receptor modulator, such as ICI182 780 inhibited the enhancement of PGE_2 production via blocking the up-regulation of COX-1 and COX-2.

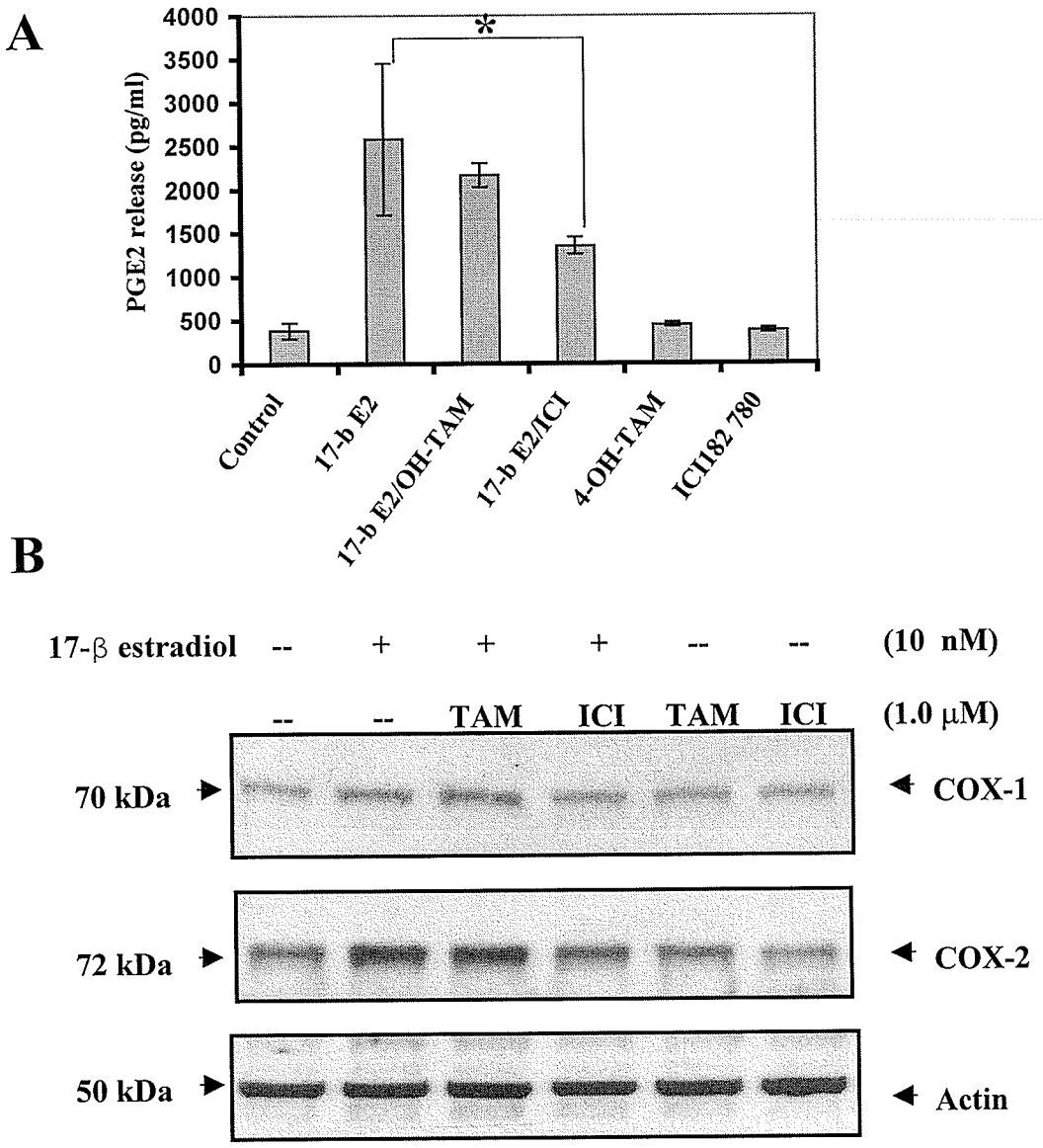

Figure 60. Attenuation of PGE_2 production and the up-regulation of COX-1/-2 by pure ER antagonist ICI 182 780 but not partial antagonist 4-OH-TAM. PMA differentiated U937 cells were incubated in the presence of a specific ligand or the combination of ligands as indicated. After ligand treatment, an aliquot of the medium was taken for the determination of PGE_2 production by EIA (Figure A). Data are expressed as means ± S.D. of at least three experiments for PGE_2 production. Cell lysates were subjected Western blot analysis of COX-1/-2 proteins (Figure B). Protein bands corresponding to COX-1, COX-2, and actin were detected by a coupled peroxidase color development system. A representative Western blot analysis was shown in Figure B.

IV. CYCLOOXYGENASE EPRESSION IS ELEVATED IN RETINOIC ACID DIFFERENTIATED U937 CELLS

3.3.9 Cell Differentiation by RA

The morphological changes induced by RA in U937 cells were examined. In the absence of RA, U937 cells in suspension reached the log phase of growth within 24 h of incubation. These cells contained large, round nuclei that are typical in premonocytes. In addition, the cytoplasm was basophilic and the nuclear/cytoplasmic ratio was relatively high (Figure 61a). In cultures treated with 500 nM of all-*trans*-RA, no clear morphologic change was detected within the first 24 h of incubation (Figure 61b-d). At 48 h of incubation, there was an increase in the number of differentiating cells (Figure 61e). These cells exhibited the following changes: smaller size, decreased nuclear/cytoplasmic ratio, matured nuclei and localization, which are consistent with cell differentiation described in a previous report (Hass et al. 1989).

The effect of all-*trans*-RA on cell surface antigen CD11b was examined by flow cytometric analysis. Cells were treated with 500 nM all-*trans*-RA for defined periods of time, and then incubated with CD11b fluorescent antibodies and subjected to FACS analysis. Similar to earlier findings, the CD11b was present in untreated U937 cells and its expression was elevated when cells were treated with all-*trans*-RA for 48 h (Table 15.). Similar results were obtained with 9-*cis*-RA. Thus, cell differentiation began to occur at 48 h of RA treatment.

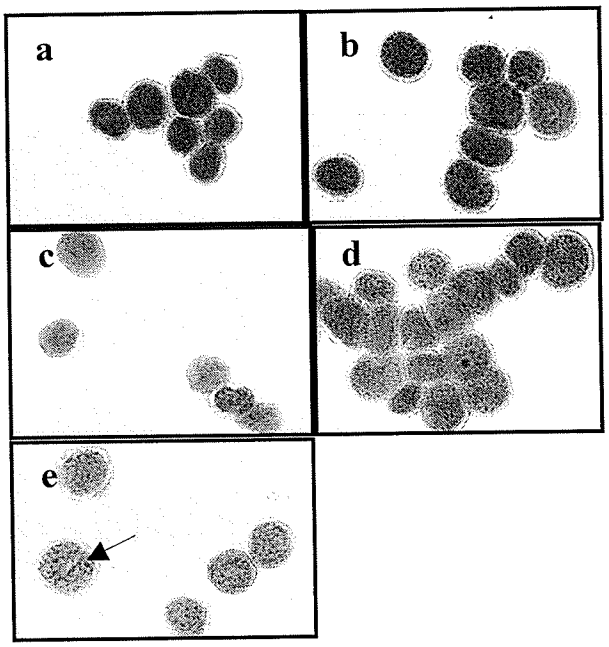

Figure 61. Time course of morphological changes to U937 cells during RA treatment. Cells were incubated in the absence or presence 500 nM all-*trans*-RA for 0–48 h. Cytospin slide preparations of suspension cell cultures stained with Wright–Giemsa were examined by light microscopy (magnification ×600). Cells cultured without RA (a). Cells cultured with RA for 6 (b), 12 (c), 24 (d) and 48 h (e). Arrowhead shows nuclear localization.

Table 15. The effect of all-*trans*-RA on cell surface CD11b expression in U937 cells

CD11b expression (h)	MFI ± S.D.
0	32.06 ± 3.15
6	34.94 ± 6.86
12	32.13 ± 4.10
24	28.07 ± 5.01
48	51.98 ± 5.18

U937 cells were treated with 500 nM all-*trans*-RA for indicated time periods or with 0.1% DMSO vehicle control (0 h). Cells were then incubated with CD11b fluorescent antibody and subjected to FACS analysis as described in Materials and Methods. Results are recorded as mean fluorescence index (MFI)±S.D., which is the product of the percentage of fluorescence and the mean fluorescence intensity. Values are representative of three independent experiments. *$P<0.05$.

2.4.2 The Effect of RA on PGE_2 Production

In a preliminary study, the amount of PGE_2 released into the culture medium by U937 cells was not detectable in either control or RA-treated cells. The addition of sodium arachidonate into the medium, however, caused an enhancement of PGE_2 production and release into the medium. Hence, exogenous sodium arachidonate (10 μM) was routinely added into the medium in all subsequent studies. The production of PGE_2 in the presence of all-*trans*-RA in U937 cells was investigated. When cells were incubated with all-*trans*-RA, the level of PGE_2 in the culture medium was increased in a time- and concentration-dependent manner (Figure 62). An increase in PGE_2 level was detected after 12 h of incubation with 500 nM all-*trans*-RA, and the increase reached a maximum at 48 h (Figure 62A). A 5–12-fold increase in PGE_2 level was observed when cells were incubated with 1–500 nM all-*trans*-RA for 48 h (Figure 62B). The effect of 9-*cis*-RA on PGE_2 released into culture medium was also examined. When cells were incubated with 9-*cis*-RA, an increase in PGE_2 level was detected in the medium in a time- and dose-dependent manner (Figure 63). The PGE_2 level was significantly increased after 12 h of incubation, and reached a maximum at 48 h (Figure 63A). A 3–8-fold increase in PGE_2 level was observed when cells were incubated with 1–500 nM 9-*cis*-RA for 48 h (Figure 63B). The results obtained from this study clearly indicate that both isomers of RA have the ability to enhance the amount of PGE_2 produced in U937 cells. The relative contribution of each isoform of COX for the enhancement of PGE_2 production in U937 cells was examined. Subsequent to stimulation by 500 nM of all-*trans*- or 9-*cis*-RA for 48 h, cells were incubated with 20 μM of SC-560 or Dup-697 for

10 min prior to the addition of sodium arachidonate. SC-560 is a specific inhibitor for COX-1, whereas Dup-697 is a highly selective inhibitor for COX-2. As depicted in Figure 62 and Figure 63, the RA-induced PGE_2 release was inhibited by SC-560 but not by Dup-697, indicating that the action of RA was mediated via COX-1. The small but not significant reduction of PGE_2 release produced by Dup-697 might result from its weak inhibition of COX-1. Thus, the increased PGE_2 production induced by both isomers of RA was likely to be mediated by COX-1 and not COX-2.

Since the synthesis of prostanoids is dependent on the availability of AA, RA treatment might cause an increase in the uptake of exogenous AA by U937 cells, resulting in a higher production of PGE_2. Hence, the rate of AA uptake by U937 cells in the presence of RA was examined. Cells were cultured in 24-well plates (10^5 cells/ml), and made quiescent by incubation in a basal medium for 12 h. Subsequently, cells were incubated with 0.1 μCi/ml [^{3}H]-AA in the presence or absence of 500 nM all-*trans*-RA for up to 48 h and the incorporation of [^{3}H]-AA into the U937 cells was determined. No difference in AA uptake was detected between the control and RA-treated cells, indicating that the increase in PGE_2 production mediated by RA was not caused by an increase in AA uptake (data not shown).

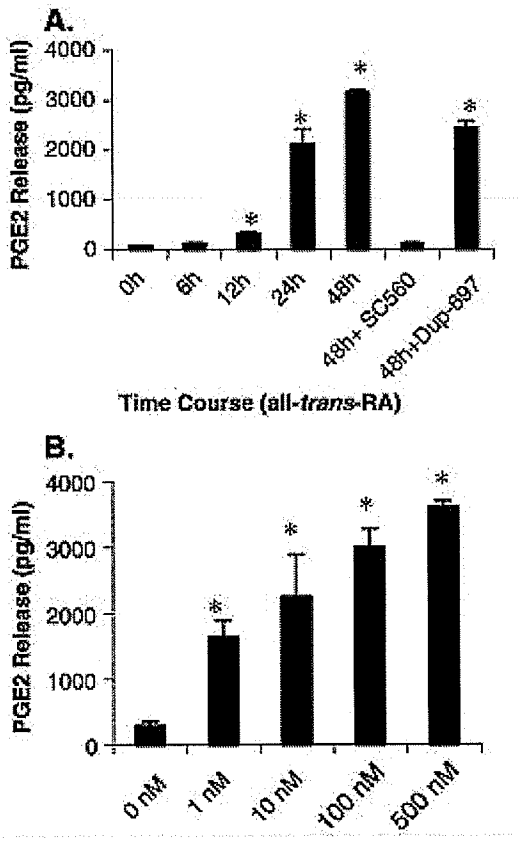

Figure 62. The effect of all-*trans*-RA on PGE_2 production in U937 cells.

Cells were treated with all-*trans*-RA for the indicated period of time. PGE_2 released into the medium was measured by EIA. (A) Cells were incubated with 500 nM all-*trans*-RA for 0–48 h. In separate experiments, cells were treated with all-*trans*-RA for 48 h in the presence of 20 μM SC-560 or 20 μM Dup-697. (B) Cells were treated with all-*trans*-RA (0–500 nM) for 48 h. Results presented are means±S.D. of three independent experiments, each carried out in duplicate. *P<0.05.

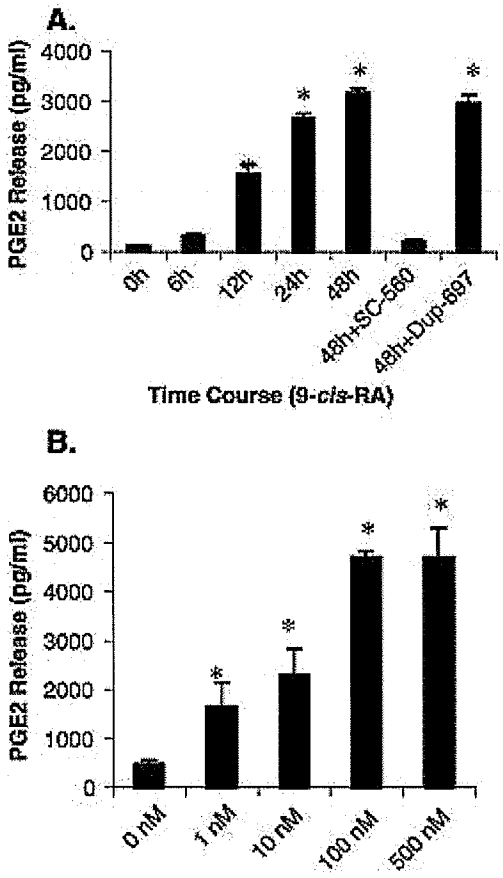

Figure. 63. The effect of 9-*cis*-RA on PGE_2 production in U937 cells.

Cells were treated with various concentrations of 9-*cis*-RA for the indicated period of time. PGE_2 released into the medium was measured by EIA. (A) Cells were incubated with 500 nM 9-*cis*-RA for 0–48 h. In separate experiments, cells were treated with 9-*cis*-RA for 48 h in the presence of 20 μM SC-560 or 20 μM Dup-697. (B) Cells were treated with 9-*cis*-RA (1–500 nM) for 48 h. Results presented are means±S.D. of three independent experiments, each carried out in duplicate.

2.4.3 The Effect of RA on COX-1 or COX-2 Protein Expression

The elevated PGE_2 level induced by RA in U937 cells might be caused by an increase in the production of COX-1 and/or COX-2. Hence, levels of these two enzymes before and after RA stimulation were quantitated by Western blot analysis. The conditions for the stimulation of U937 cells by RA were identical to that described in Figure 62 and Figure 63. The COX-2 protein level was too low to be detected in untreated or RA-treated U937 cells. As a positive control, the COX-2 protein level was also determined in U937 cells after PMA treatment. Our results show that PMA caused a significant increase in COX-2 production (Figure 64), which has been well-documented. In contrast, the level of COX-1 was readily detectable in untreated U937 cells (Figure 65 and Figure 66). Treatment of cells with 500 nM of all-*trans*-RA caused a 26% increase in COX-1 protein at 24 h of incubation, and an 86% increase at 48 h of incubation. (Figure 65). Treatment of cells with 1–500 nM of all-*trans*-RA stimulated COX-1 protein expression (Figure 65A).

The induction of COX-1 protein level by 9-*cis*-RA produced a pattern similar to that obtained by all-*trans*-RA. In a time course study, the level of COX-1 protein was elevated 41% at 24 h, and 3-fold at 48 h of incubation (Figure 66A). 9-*cis*-RA (1–100 nM) also stimulated the COX-1 protein expression (Figure 66B). Taken together, these data indicate that the enhancement of PGE_2 biosynthesis by RA in U937 cells was mediated by the enhancement of the level of COX-1 but not COX-2.

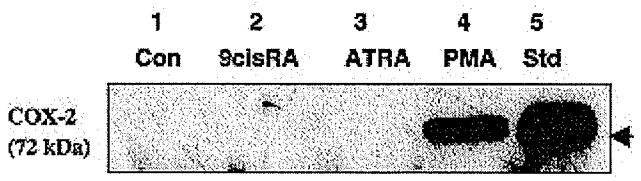

Figure 64. The effect of RA on COX-2 protein expression in U937 cells. Cells were treated with vehicle control (0.1% DMSO) (1), 500 nM 9-*cis*-RA (2), 500 nM all-*trans*-RA (3) or 162 nM PMA (4) for 48 h. Cell lysates and COX-2 standard protein (10 ng, lane 5) were subjected to Western blot analysis. A typical blot is depicted. Con: control. Std: COX-2 protein standard. ATRA: all-*trans*-RA

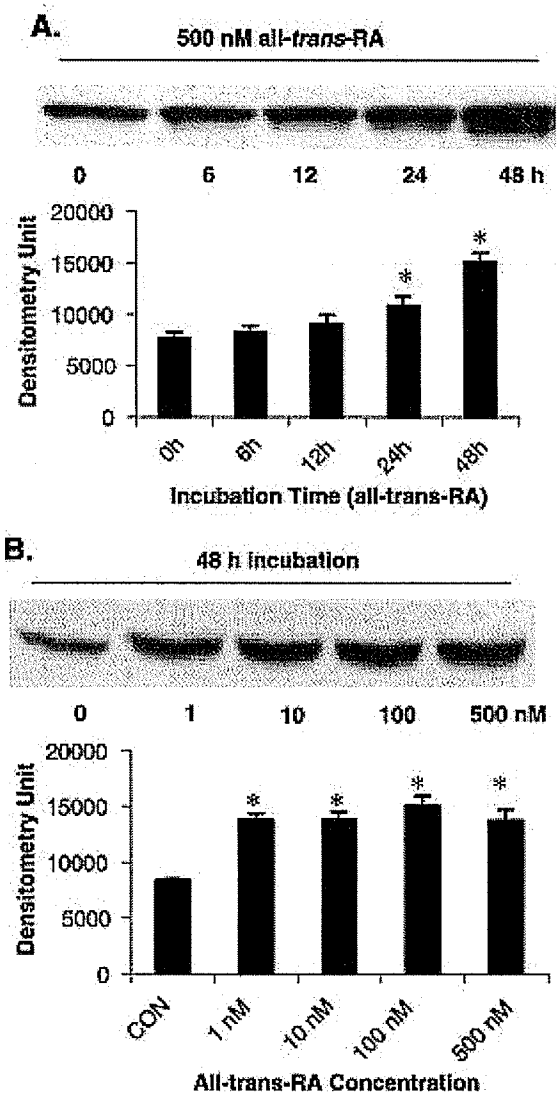

Figure 65. The effect of all-*trans*-RA on COX-1 protein expression in U937 cells. Cells were treated with all-*trans*-RA for the indicated period of time. The cell lysate was subjected to Western blot analysis. Each blot was scanned with a densitometer to determine relative protein levels. (A) Cells were treated with 500 nM all-*trans*-RA for 0–48 h. (B) Cells were treated with 0–500 nM RA for 48 h. Data represent the mean±S.D. of each protein from three independent experiments. A typical blot is depicted on the top of each plot. *P<0.05.

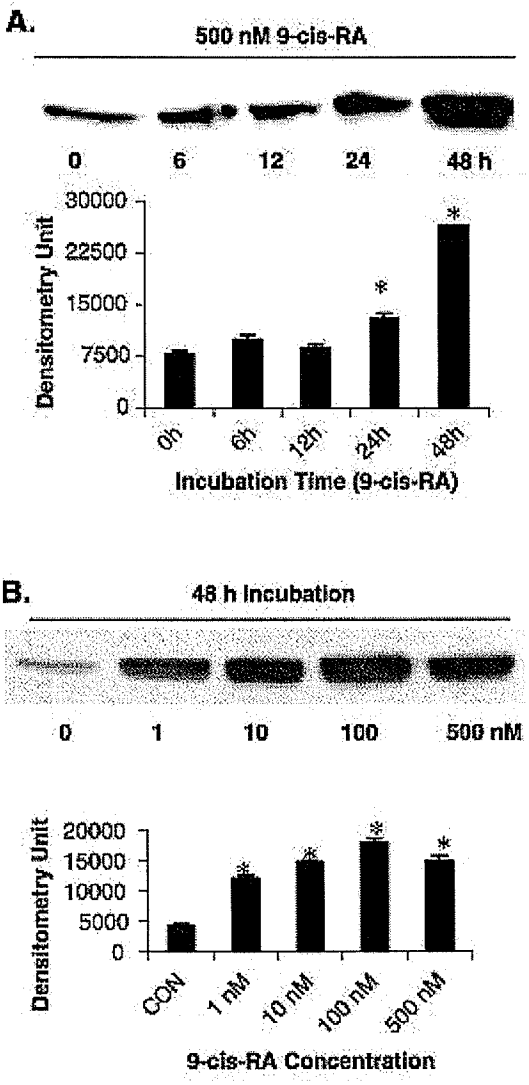

Figue 66. The effect of 9-*cis*-RA on COX-1 protein expression in U937 cells.

Cells were treated with 9-*cis*-RA for the indicated period of time. The cell lysate was subjected to Western blot analysis. Each blot was scanned with a densitometer to determine relative protein levels. (A) Cells were treated with 500 nM 9-*cis*-RA for 0–48 h. (B) Cells were treated with 0–500 nM RA for 48 h. Data represent the mean±S.D. of each protein from three independent experiments. A typical blot is depicted on the top of each plot. *$P<0.05$.

2.4.4 The Effect of RA on COX-1 mRNA Levels

Northern blot analysis was conducted to quantitate the changes in mRNA expression. The expression of COX-1 mRNA was stimulated by both isomers of RA within 6 h and reached the maximum value at 24 h of incubation (Figure 67 and Figure 68). In addition, an increase (1.7–6.6-fold) in COX-1 mRNA expression was observed in cells incubated with 1–500 nM of RA (Figure 67 and Figure 68). The results from the Northern blot analysis indicate that up-regulation of COX-1 protein expression by RA was due to an increase in COX-1 mRNA levels in U937 cells. The increase in COX-1 mRNA expression appears to precede the increase in COX-1 protein expression.

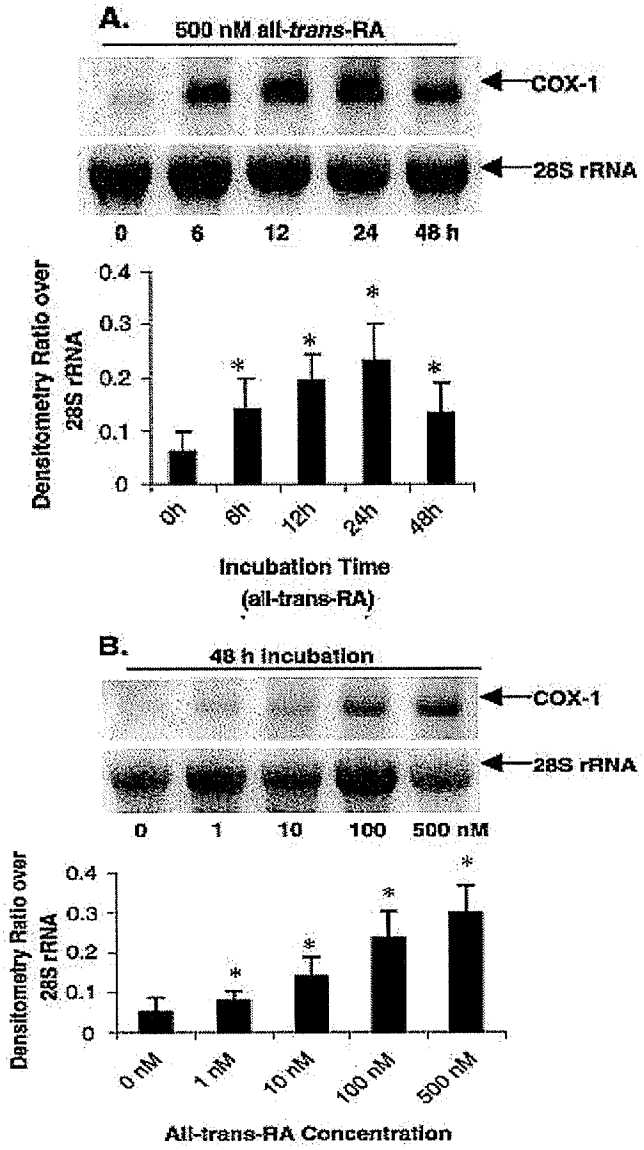

Figure 67. The effect of all-*trans*-RA on COX-1 or COX-2 mRNA expression—measured by Northern blot analysis.

Cells were treated with all-*trans*-RA and Northern blot analysis of COX-1 mRNA was performed as described under Materials and methods. The total RNA loading was checked by ethidium bromide staining of the gel, and ribosomal 28S was reported. Data represent three independent experiments and a typical blot is depicted. (A) Cells were treated with 500 nM all-*trans*-RA for 0–48 h. (B) Cells were treated with 0–500 nM all-*trans*-RA for 48 h. *$P<0.05$.

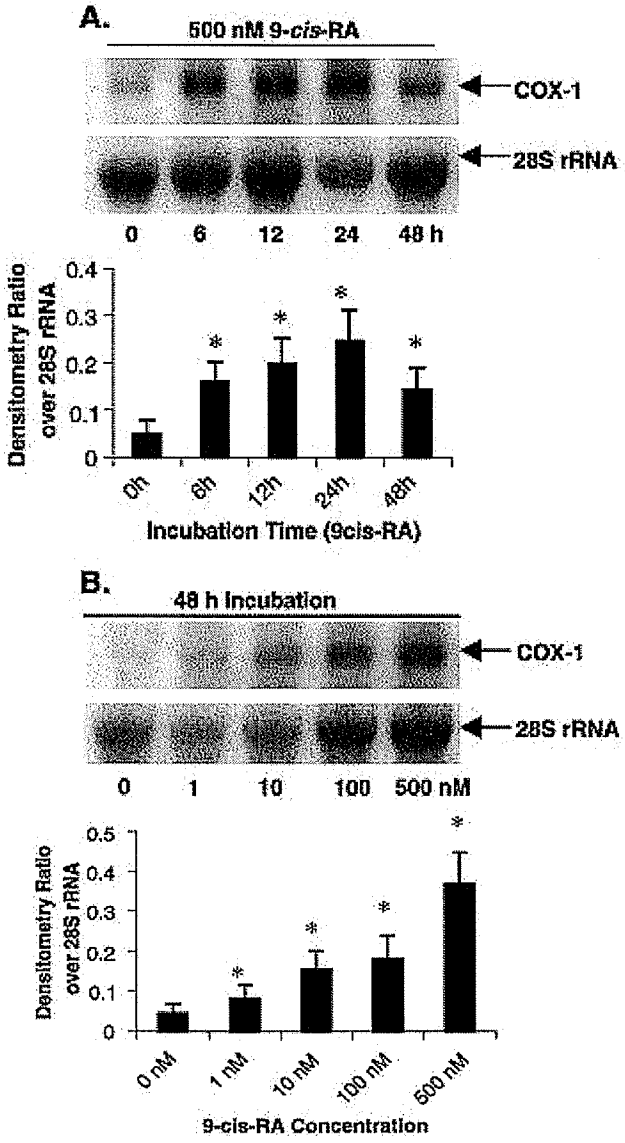

Figure 68. The effect of 9-*cis*-RA on COX-1 mRNA expression—measured by Northern blot analysis.

Cells were treated with 9-*cis*-RA and Northern blot analysis of COX-1 mRNA was performed as described under Materials and methods. The total RNA loading was checked by ethidium bromide staining of the gel, and ribosomal 28S was reported. Data represent three independent experiments and a typical blot is depicted. (A) Cells were treated with 500 nM all-*trans*-RA for 0–48 h. (B) Cells were treated with 0–500 nM all-*trans*-RA for 48 h. *$P<0.05$.

DISCUSSION

I. STUDIES ON THE BIOSYNTHESIS OF PHOSPHOLIPID

1.1 Identification and Characterization of Acyltransferases in Phospholipid Biosynthesis

The present study was conducted to identify and clone acyltransferases in lipid biosynthesis. Using the conserved domain database and BLAST algorithms, we identified several transmembrane genes that contain acyltransferase and phospholipid acyltransferase domains in their translated peptides. These candidate genes encoded several uncharacterized acyltransferases, which had 1-acyl-*sn*-glycerol-3-phosphate acyltransferase activities. Our findings support a model in which multiple AGPATs co-exist and they are differentially expressed in various tissues.

A variety of phospholipids are present in cells and tissues, considering difference in types, abundance, and turnover. It is unlikely a single enzyme will accomplish so much and this is especially true for 1-acyl-*sn*-glycerol-3-phosphate acyltransferase (as discussed in Introduction and Literature Review). Previous work suggested that multi-isozymes for 1-acyl-*sn*-glycerol-3-phosphate acyltransferase activities might exist in humans (Eberhardt et al. 1997; Stamps et al. 1997; West et al. 1997; Aguado and Campbell 1998). Several murine AGPAT isoezymes identified have been found to be differentially expressed in various tissues. However, little is known about the functional significance of tissue-specific expression.

The catalytic domain of each candidate contains two critical motifs for its functionality. The catalytic motif (NH(X4)D) and the substrate-binding motif (EGTR) are 100% conserved among five members. The conservation of two critical motif along with a novel motif (K(X2)L(X6)G(X9)R) signify that these enzymes belong to one gene family and they might have similar enzymatic activity.

It remains a mystery that these AGPATs have differential AGPAT activities when 1-oleoyl-*sn*-glycerol-3-phosphate was used as an acceptor and oleoyl—CoA as a donor. One should be cautious in the interpretation of these data. Nevertheless, other enzyme proteins such as human full length TAZ and murine exon 5-deleted TAZ showed no such activities at all under identical experimental conditions while human N456 displayed a differential profile.

In conclusion, we have identified and cloned several AGPATs in human and murine tissues. Our data suggest that multiple isozymes coexist and they have differential tissue distributions.

1.2 Complex Expression Pattern of in Barth Syndrome Gene Tafazzin in Humans and Murine Tissues

Tafazzins are a group of proteins that are produced by alternative splicing of the primary Barth syndrome gene G4.5 or TAZ. In humams, multiple splice variants have been identified with the two most abundant forms differing in their sequence due to alternative splicing of exon 5. However, the tissue expression pattern of tafazzins has not been investigated. To address this, RT-PCR and transcription-coupled *in vitro* translation analysis were undertaken in murine tisuues and human cell lines in order to determine the

transcriptional and translational regulation mechanisms. The data indicated that the complex pattern of tafazzin alternative splicing expressed in human tisuues was not apparent in murine tissues. Only two exon 5-deleted tafazzin transcripts, but not the full-length tafazzin, were expressed in murine tissues. Analysis of the open reading frames (ORFs) of both murine and human TAZ showed non consensues Kozak context for the first ATG initiation site and an in-frame down stream ATG that could serve as an alternative initiation site. Cloning and *in vitro* expression of both murine and human tafazzin cDNA revealed two prominent protein bands that corresponded to the expected sizes of alternative translation. The data support a species-specific difference in the expression of TAZ mRNAs between mouse and human and lend support to the recent hypothesis (Vaz et al. J. Bio. Chem. 2003 Aug 20 ahead of print) that the exon 5-deleted form of TAZ is the evolutionally conserved and functional form in mammalian cells.

Recently, a defect in cardiolipin and phosphatidylglycerol remodeling and a reduction in cardiolipin pool size were detected in cultured skin fibroblasts from Barth syndrome patients (Vreken et al. 2000). However, the mechanism responsible for the defect remains undefined. Since TAZ aligned to several consensus sequences of phospholipid acyltransferase enzymes, acyltransferases activities involved in cardiolipin biosynthesis and remodeling were examined using our *in vitro* and *in vivo* generated proteins. Neither AGPAT nor monolysocadiolipin acyltransferase activity was detected. Hence, the enzyme identity remains unknown.

II. STUDIES ON THE CATABOLISM OF PHOSPHOLIPID

2.1 Regulation of Cytosolic Phospholipase A_2, Cyclooxygenase-1 and Expression by PMA, TNFα, LPS and M-CSF in Human Monocytes and Macrophages

The phorbol ester PMA is a tumor-promoting factor commonly used as an inducer for U937 pre-monocyte differentiation into macrophages. PMA is a potent protein kinase C activator and regulates COX-2 expression via the mitogen-activated protein kinase (MAPK) signaling pathway. In this study, PMA induced a significant increase in AA release and PGE_2 production in U937 cells. The peak of AA release and PGE_2 production occurred 24h post-PMA addition. This dramatic increase in AA release at the late stage of treatment could not be explained solely by changes in $cPLA_2$ protein mass since 24 h post-incubation, $cPLA_2$ protein levels in PMA-treated cells were decreased. Previously, Rehfeldt *et al.* (1991) reported that PMA activated $cPLA_2$ by inducing enzyme translocation to the membrane fraction in U937 cells. Hence, the increase in AA release seen at 24 h post-PMA treatment could be caused by an increase in enzyme activation. Alternatively, the induction of $cPLA_2$ protein in the early stage (8 h) may trigger signaling that led to the expression of secretary PLA_2 and COX-2, which might be responsible for the late-phase PGE_2 synthesis (Fujishima et al. 1999). Our results also demonstrated that PMA not only induced COX-2 expression but also up-regulated COX-1 protein in U937 cells. Therefore, the elevated PGE_2 production in U937 cells induced by PMA was likely caused by a combined action of both COX-1 and COX-2 enzymes.

LPS is a bacteria-derived endotoxin and macrophages expressed COX-2 upon LPS stimulation, indicating a pro-inflammatory role of this enzyme. In addition to the

MAPK-mediated signaling pathway, LPS might mediate COX-2 transcription via NFκB or p38/RK/Mpk2 pathways (Dean et al. 1999; Zhang et al. 1999). In U937 cells, a significant AA release but not PGE_2 production was observed after LPS treatment. U937 cells were found to express COX-1 but not COX-2. The lack of PGE_2 production in LPS-treated U937 cells might result from the inability of this compound to induce COX-1 protein expression. In contrast, treatment of macrophages with LPS caused an enhancement of PGE_2 production (4-fold over control). Macrophages readily express CD14, a distinct cell surface marker, which is absent in monocyte and may function as the receptor for the complex of LPS with LPS-binding protein (Wright et al. 1990). The data from the present study revealed that the LPS-mediated enhancement of PGE_2 production was contributed by elevated COX-2 protein expression. Similar to the action of PMA, LPS might enhance the AA release in macrophages via directly increasing the enzyme activity of $cPLA_2$ or secretary PLA_2. Prolonged treatment (24 h) of macrophages with LPS attenuated $cPLA_2$ protein, indicating that both the bioavailability of AA as well as COX-1 and/or COX-2 expression were equally important in regulating PGE_2 biosynthesis in these cells.

TNF failed to induce PGE_2 production in macrophages or U937 cells, in spite of enhancing $cPLA_2$ protein expression and subsequently stimulating AA release. TNF has been found to induce COX-2 mRNA expression in mouse osteoblasts (Wright et al. 1990) but not in human monocytes (Glaser and Lock 1995). Our results were consistent with the published report on human monocytes (Glaser and Lock 1995) and suggested that TNF has limited influence in PGE_2 production. Hence, PGE_2 production likely requires the coordinated induction and functional coupling of $cPLA_2$, COX-1 and/or COX-2.

M-CSF has little capacity to release PGE_2 in U937 cells or macrophages, similar to the results obtained in bone marrow macrophages (Shibata et al. 1994). The cellular response to growth factor is generally regarded to be mediated by sequential activation of receptor tyrosine kinase, Src, Ras, and one or more of MAPK pathways (Smith et al. 2000). However, the activation of the COX-2 promoter by serum and platelet-derived growth factor has been shown to be inhibited by dominant negative Ras, MEKK-1 and Raf1 (Xie and Herschman 1996). The lack of COX-2 induction by M-CSF, therefore, may due to the inability of this compound to activate any of the Ras, MEKK-1 or Raf-1 pathways.

In summary, the enhancement of AA release in both U937 cells and macrophages may result from a combination of increased $cPLA_2$ activity and its $cPLA_2$ protein expression. PMA has been found to stimulate AA release and subsequent PGE_2 production via up-regulation of COX-1 and induction of COX-2 expression in U937 cells, whereas LPS elicits a similar effect via induction of COX-2 expression in macrophages. The complex regulation of AA release and PGE_2 production in U937 cells and in macrophages clearly depends upon the coordinated work of key enzymes in the cyclooxygenase pathway, $cPLA_2$, COX-2, COX-1, and probably other enzymes, such as secretary PLA_2 and PGE_2 synthase.

2.2 Modulation of Arachidonic Acid Metabolism by Phorbol 12-Myristate 13-Acetate in Monocytes and Myocytes

The central role of arachidonic acid metabolism in the production of eicosanoids in mammalian cells is well documented (Hla and Neilson 1992; Wu et al. 1994). The

production of prostanoids is regulated by the arachidonate-eicosanoid cascade. In this cascade, the $cPLA_2$ is responsible for the release of the free AA from the membrane phospholipids, whereas COX is responsible for the eicosanoid formation (Needleman et al. 1986; Herschman 1996; Leslie 1997; Funk 2001). Our results demonstrated that PMA caused an immediate increase of AA release followed by a subsequent enhancement of PGE_2 production in monocytes and myocytes.

The effect of PMA on the activation of $cPLA_2$ has been well-documented. PMA mediates its effect at both the transcriptional and post-translational levels (Nakamura et al. 1992; Lin et al. 1993; Kuroda et al. 1997; Funk 2001). It is clear that the increase in $cPLA_2$ level observed in this study was stimulated at the protein level. The increase in enzyme level does not seem to account for the increase in AA release after PMA treatment. Hence, PMA might modulate $cPLA_2$ at the post-translational level. We have shown in an earlier study that PMA causes the activation of $cPLA_2$, possibly via the indirect action of protein kinase C (Wong et al. 1998). Although protein kinase C has the ability to phosphorylate $cPLA_2$ *in vitro,* $cPLA_2$ is not activated by the phosphorylation process. In addition, protein kinase C does not have the ability to directly phosphorylate $cPLA_2$ under *in vivo* conditions (Lin et al. 1993; Seger and Krebs 1995). An alternate mechanism is that protein kinase C causes the activation of the p42/p44 MAPK cascade, which may result in the phosphorylation of $cPLA_2$.

In this study, the relationship between the up-regulation of COX and production of eicosanoids has been amply demonstrated. PMA elicited an immediate increase in AA release in both U937 and H9c2 cells, but the increase did not result in a comparable PGE_2 production in the first 24 h. The enhancement of PGE_2 production appears to result from

the elevated levels of COX-1 and COX-2 in both cell types under sustained stimulation of PMA.

There are two isoforms of cyclooxygenase, COX-1 and COX-2, which are coded by separate and distinct genes (Yokoyama and Tanabe 1989; Hla and Neilson 1992). COX-1 has been shown to be constitutively expressed in most tissues (Xu et al. 1997). COX-2 is an inducible enzyme, which is subjected to transcriptional regulation (Habib et al. 1993). It is clear from this study that the effect of PMA was more pronounced with COX-2 than COX-1. The fact that the temporal change in COX-2 level corresponded closely with the change in PGE_2 release in both cell types is indicative of the importance of COX-2 in the production of prostanoids under external stimuli.

The increase in COX-2 expression by PMA treatment was caused by an enhancement at the transcriptional level. Since PMA has been shown to cause the transformation of the premonocytic cells into monocytic cells, the increase in COX-2 expression in the U937 cells might be a consequence of cellular transformation. Alternatively, an increase in COX-2 expression was also observed in H9c2 cells, indicating that the enhancement of transcription might be independent of the transformation process.

In summary, our study clearly shows that PMA caused an increase in arachidonate release and the subsequent production of PGE_2 in both U937 and H9c2 cells. The action of PMA is mediated via the modulation of $cPLA_2$ and COX-2 expression in both cell types. Our results confirm the important roles of these two enzymes in the regulation of the arachidonate-eicosanoid cascade in both monocytes and cardiac myocytes.

2.3 17-β Estradiol Enhances PGE_2 Production in U937-derived Macrophages

The present study was conducted to examine the effect of female sex hormone on the production of PGE_2 in macrophages. Exposure of the cells to 17-β estradiol induced a dose-dependent increase in the production of PGE_2. Our findings support a model in which the enhancement of PGE_2 production is mediated by both an increase of AA release and an ER-mediated up-regulation of COX-1 and COX-2.

The effect of estrogen on the production of prostaglandins is well-documented. The modulation of cyclooxygenases by estrogen or selective estrogen receptor modulators such as tamoxifen, ICI182 780, and reloxifen has also been reported in several cellular systems. In vascular system, estrogen activates PGI_2 synthesis in endothelial cells and cerebrovessels by up-regulating the activity of COX-2 or COX-1, respectively (Akarasereenont et al. 2000; Ospina et al. 2002). In other cellular systems, however, estrogen exhibits a differential modulation effect on prostaglandin productions. For example, estrogen induces prostaglandin synthesis and COX-2 mRNA levels in the non-pregnant rat myometrium (Engstrom 2001), while estrogen prevents the lipopolysaccharide-induced PGE_2 release in microglia and inhibits PGE_2 and COX-2 production in rabbit uterine cervical fibroblasts (Sato et al. 2001a; Vegeto et al. 2001). The apparent discrepancy in the action of estrogen between cells types epitomizes the limitation of each study and illustrates the fragmented nature of our understanding on the role of estrogen in the regulation of prostaglandin production. Such differences illustrate the fact that estradiol modulation of cyclooxygenase expression and thus prostaglandin production are tissue-specific and cell-context dependent. Using human U937-derived macrophage cells as a model, we showed up-regulation of both COX-1 and COX-2 and

the enhancement of PGE_2 production upon treatment with 17-β estradiol. Neither tamoxifen and ICI182 780 nor plant-derived nonsteroidal phytoestrogen Genistein have any effect on PGE_2 production. In view that 17-α estradiol has a diphenolic ring structure, its inability to affect PGE_2 production under the same conditions eliminates the possibility that the observed estradiol effect was mediated via its antioxidant property.

Estrogen exerts its effect not only on female reproductive organs, but on other tissues including central nervous system, the vascular system, and the immune system (Couse and Korach 1999b; Hodis et al. 2002a; Hodis et al. 2002b; Rossouw 2002a; Rossouw 2002b). Genomic signaling via nuclear receptors is the dominant pathway that exists in reproductive organs, whereas both genomic and non-genomic signaling regulates cellular and molecular events in non-reproductive organs (Guo et al. 2002; Mendelsohn 2002; Rossouw 2002a; Rossouw 2002b). Our data suggest that 17-β estradiol acts at the cellular level via genomic signaling (possibly via the classical ER-α), which specifically modulates COX-1 and COX-2 expression in human PMA-differentiated macrophages. This view is supported by the fact that: (1) only 17-β estradiol but not the selective estrogen receptor modulators and 17-α estradiol is effective on PGE_2 release, (2) The enhanced presence of ER-α in the stained macrophages, (3) the up-regulation of both COX-1 and COX-2 are correlated with the increase of the corresponding mRNA levels. It should be noted that other possibilities, such as the estradiol-induced nongenomic signaling via membrane receptors or the cross-talk between the genomic and non-genomic signaling cannot be entirely excluded.

2.4 Cyclooxygenase Expression Is Elevated in Retinoic Acid-differentiated U937 Cells

The differentiation of monocytic cells is accompanied by changes in cellular morphology, enzymatic activity, the appearance of cell surface antigens and various biological responses (Hinds et al. 1997) These events are paralleled by complex alterations in gene regulation and expression (Spittler et al. 1997). RA has been widely used in differentiation studies in many cellular systems, including epithelial cells (Hill et al. 1996; Mestre et al. 1997), vascular smooth muscle cells (Neuville et al. 2000) (Miano and Berk 2001) and U937 cells (Hinds et al. 1997; Gonchar et al. 1998). In this study, the differentiation of premonocytic U937 cells by RA was monitored by light microscopy and by increased expression of monocytic surface antigen CD11b. Specifically, differentiation of U937 cells started to occur within 48 h of incubation with all-*trans*- or 9-*cis*-RA. It was shown previously that the incubation of U937 cells with a higher concentration of RA (all-*trans*- or 9-*cis*, 1000 nM) for a longer period (72–96 h) would induce several other markers for the mature monocyte such as CD18, but the treatment still failed to elicit the production of the macrophage marker CD14 (Nakajima et al. 1996; Hinds et al. 1997). CD14 is a glycosyl-phosphatidylinositol membrane protein that is strongly expressed by mature monocytes and macrophages (Hass et al. 1989). A similar observation on HL-60 cells incubated with RA (all-*trans*- or 9-*cis*, 100 nM) for 96 h has been reported (James et al. 1997). It is clear that the U937 cells used in this study had not been fully differentiated, which would allow us to study the early stage of differentiation. This notion is supported by the observation that: (1) none of the cells was found to attach to the culture dish, an indicator for full differentiation; (2) no induction of CD14 was

observed in RA-treated U937 cells. As a positive control, cells were also incubated with PMA, which is a known promoter of differentiation (Hass et al. 1989). Incubation with PMA for 24 h caused the complete cell differentiation, which was characterized by cell adhesion to each other and to the plate, the expression of monocyte/macrophage-specific CD14 antigen and the enhanced expression of COX-2 (Hass et al. 1989; Hoff et al. 1993). Hence, the stimulation of COX-1 by RA observed in this study may be regarded as a pre-differentiation process. The difference in cellular response between RA and phorbol ester for the induction of cellular differentiation and COX isoforms expression has not been defined.

In this study, both isomers of RA were shown to be effective in enhancing the production of PGE_2. RA caused the up-regulation of COX-1 expression, at both physiological (5–10 nM) and higher concentrations. The effect of RA on inducible PGE_2 synthase, however, has not been determined. The time course for the enhanced PGE_2 production did not directly correlate with morphologic changes, and hence, it is not possible to determine whether the occurrence of these events were parallel or sequential. Although PGE_2 alone can induce differentiation of HL-60 cells in a dose-dependent manner, the concentrations of PGE_2 required are much higher than the concentration induced by RA in this study (Olsson and Breitman 1982; Sellmayer et al. 1997). It is not clear if the enhanced release of PGE_2 by RA might potentiate the differentiation of the U937 cells. When HL-60 cells were incubated with PGE_2 and RA, PGE_2 would act effectively in a synergistic manner with RA to cause cellular differentiation. Both RA isomers caused the enhanced production of PGE_2, some subtle differences between these isomers were detected. U937 cells appeared to respond more readily to 9-*cis*-RA for the

release of PGE_2. Our result is consistent with an earlier study that 9-*cis*-RA was more effective than all-*trans*-RA for the induction of differentiation in HL-60 cells (Nagy et al. 1995).

Using specific inhibitors, our study indicated that the enhancement of PGE_2 production was mediated via COX-1 but not COX-2. This notion was further supported by the up-regulation of COX-1 protein expression in RA-treated cells. The up-regulation of COX-1 mRNA and protein was observed in murine neuroblastoma cells treated with all-*trans*-RA (Schneider et al. 2001) and in J774.1 macrophages treated with RA and activin A (Nusing et al. 1995). In addition, the induction of differentiation and COX-1 expression by phorbol ester in THP-1 cells has been documented (Smith et al. 1993). Thus, the induction of COX-1 expression appears to be a common theme in the early stage of cellular differentiation. Since the intrinsic COX activity was not an absolute requirement for U937 cell differentiation (Sellmayer et al. 1997), the augmentation of PGE_2 production via up-regulation of COX-1 might demonstrate a priming effect of RA on these cells.

An increase in COX-1 mRNA by RA was observed after 6 h of incubation, whereas the increase in COX-1 protein was detected at 24 h of incubation. Thus, it appears that the RA-induced COX-1 expression occurred first at the transcriptional level, and subsequently at the translational level. Based on the coexistence of RARs and RXRs in most cells (Zhuang et al. 1995), the COX-1 promoter may contain specific *cis*-elements that may respond to all-*trans*- or 9-*cis*-RA. Hence, the available nucleotide sequence of the *cox-1* promoter was examined. Unfortunately, we have not been able to

identify the sequences of the RARE. Thus, the molecular mechanism of COX-1 up-regulation by RA remains undefined.

SUMMARY

The research described in this thesis was designed to investigate the control of phospholipid metabolism in mammalian tissues. In the first part of the study, several acyltransferases involved in the biosynthesis of glycerolipids were identified and subsequently cloned and characterized. In the second part, the regulation of arachidonate-eicosanoid cascade was examined.

In the first part of the study, using conserved domain database and BLAST algorithm, several AGPATs were identified and subsequently cloned. Domain analysis demonstrated that proteins encoded by these genes contained the intact acyltransferase domain and several transmembrane domains and thus had a convergence in overall domain structures. *In vitro* and *in vivo* recombinant proteins were found to have 1-acyl-*sn*-glycerol-3-phosphate acyltransferase activities. In the study of human Barth syndrome gene TAZ, a comparative genomic approach was employed to examine the complex expression pattern of TAZ in human and murine tissues. Multiple alternative splice variants were identified in both species. However, the full-length TAZ expressed in human tissues was not found in other species. Rather, exon 5-deleted TAZ was found to be the most abundant expressed and evolutionarily conserved form in all species analyzed. The present study indicates that exon 5-deleted TAZ is the evolutionarily conserved form and thus the potential functional form.

In the second part of the study, the control of arachidonate-eicosanoid cascade was investigated. PMA, M-CSF, TNF-α, LPS, estrogens, and RAs were used to activate different signaling pathways via membrane receptors or nuclear receptors. The control of arachidonate-eicosanoid cascade was assessed in monocyte/macrophage and myocyte cell

models. The data showed that PMA, M-CSF, TNF-α, LPS, estrogens, and retinoic acids exerted a differential regulatory of $cPLA_2$ and/or COX-1/-2 enzymes. Both transcriptional activation and posttranslational modulation/modification of these enzymes contribute to the control of arachidonic acid release and subsequent production of prostaglandins. Our findings support a model in which the arachidonate-eicosanoid cascade is controlled by multiple signal transduction pathways, which are interconnected at multiple stages during the signal transduction processes.

REFERENCES

Adams MD, Kelley JM, Gocayne JD, Dubnick M, Polymeropoulos MH, Xiao H, Merril CR, Wu A, Olde B, Moreno RF, et al. (1991) Complementary DNA sequencing: expressed sequence tags and human genome project. Science 252:1651-1656

Agarwal AK, Arioglu E, De Almeida S, Akkoc N, Taylor SI, Bowcock AM, Barnes RI, Garg A (2002) AGPAT2 is mutated in congenital generalized lipodystrophy linked to chromosome 9q34. Nat Genet 31:21-23

Agrawal GK, Iwahashi H, Rakwal R (2003) Small GTPase 'Rop': molecular switch for plant defense responses. FEBS Lett 546:173-180

Aguado B, Campbell RD (1998) Characterization of a human lysophosphatidic acid acyltransferase that is encoded by a gene located in the class III region of the human major histocompatibility complex. J Biol Chem 273:4096-4105

Akarasereenont P, Techatraisak K, Thaworn A, Chotewuttakorn S (2000) The induction of cyclooxygenase-2 by 17beta-estradiol in endothelial cells is mediated through protein kinase C. Inflamm Res 49:460-465

Akesson B, Arner A, Sundler R (1976) Metabolism of different monoacylphospholipids in isolated hepatocytes and the intact rat. Biochim Biophys Acta 441:453-464

Alberts B, Bray D, Lewis J, Raff M, Roverts K, Watson JD (1994) Molecular biology of the cell. Garland Publishing, Inc., New York

Altschul SF, Gish W, Miller W, Myers EW, Lipman DJ (1990) Basic local alignment search tool. J Mol Biol 215:403-410

Ansell GB, Spanner S (1982) Phosphatidylserine, phosphatidylethanolamine and phosphatidylcholine. In: Hawthorne JN, Ansell GB (eds) Phospholipids. Elsevier Biomedical Press, Amsterdam, pp 1-49

Arthur G, Choy PC (1984) Acyl specificity of hamster heart CDP-choline 1,2-diacylglycerol phosphocholine transferase in phosphatidylcholine biosynthesis. Biochim Biophys Acta 795:221-229

Baker SJ, Reddy EP (1998) Modulation of life and death by the TNF receptor superfamily. Oncogene 17:3261-3270

Barth PG, Scholte HR, Berden JA, Van der Klei-Van Moorsel JM, Luyt-Houwen IE, Van 't Veer-Korthof ET, Van der Harten JJ, Sobotka-Plojhar MA (1983) An X-linked mitochondrial disease affecting cardiac muscle, skeletal muscle and neutrophil leucocytes. J Neurol Sci 62:327-355

Barth PG, Van't Veer-Korthof ET, Van Delden L, Van Dam K, Van der Harten JJ, Kuipers JR (1981) An X-linked mitochondrial disease affecting cardiac muscle, skeletal muscle and neutrophil leukocytes. In: Bush HF, Jennekens FG, Shotte HR (eds) Mitochondria and Muscular Diseases. Mefar, Beetsterzwaag, The Netherlands, pp 161-164

Bateman A, Birney E, Cerruti L, Durbin R, Etwiller L, Eddy SR, Griffiths-Jones S, Howe KL, Marshall M, Sonnhammer EL (2002) The Pfam protein families database. Nucleic Acids Res 30:276-280

Batenburg JJ (1992) Surfactant phospholipids: synthesis and storage. Am J Physiol 262:L367-385

Berridge MJ, Irvine RF (1989) Inositol phosphates and cell signalling. Nature 341:197-205

Bione S, D'Adamo P, Maestrini E, Gedeon AK, Bolhuis PA, Toniolo D (1996) A novel X-linked gene, G4.5. is responsible for Barth syndrome. Nat Genet 12:385-389

Bloch K (1991) Cholesterol:evolution of structure and function. In: Vance DE, Vance J (eds) Biochemistry of Lipids, Lipoproteins and Membranes. Elsevier Science Publishers, Amsterdam, pp 363-401

Boguski MS, Lowe TM, Tolstoshev CM (1993) dbEST--database for "expressed sequence tags". Nat Genet 4:332-333

Bolhuis PA, Hensels GW, Hulsebos TJ, Baas F, Barth PG (1991) Mapping of the locus for X-linked cardioskeletal myopathy with neutropenia and abnormal mitochondria (Barth syndrome) to Xq28. Am J Hum Genet 48:481-485

Borgeat P, Nadeau M, Salari H, Poubelle P, Fruteau de Laclos B (1985) Leukotrienes: biosynthesis, metabolism, and analysis. Adv Lipid Res 21:47-77

Brazozowski A, Pike A, Dauter Z, Hubbard R, Bonn T, Engstrom O, Ohman L, Green G, Gustafsson JA, Carlquist M (1997) Molecular basis of anogism and antagonism in the oestrogen receptor. Nature 389:753-758

Brindley DN, Waggoner DW (1998) Mammalian lipid phosphate phosphohydrolases. J Biol Chem 273:24281-24284

Budihardjo I, Oliver H, Lutter M, Luo X, Wang X (1999) Biochemical pathways of caspase activation during apoptosis. Annu Rev Cell Dev Biol 15:269-290

Buhman KK, Smith SJ, Stone SJ, Repa JJ, Wong JS, Knapp FF, Jr., Burri BJ, Hamilton RL, Abumrad NA, Farese RV, Jr. (2002) DGAT1 is not essential for intestinal triacylglycerol absorption or chylomicron synthesis. J Biol Chem 277:25474-25479

Cao J, Burn P, Shi Y (2003a) Properties of the mouse intestinal acyl-CoA:monoacylglycerol acyltransferase, MGAT2. J Biol Chem 278:25657-25663

Cao J, Lockwood J, Burn P, Shi Y (2003b) Cloning and functional characterization of a mouse intestinal acyl-CoA:monoacylglycerol acyltransferase, MGAT2. J Biol Chem 278:13860-13866

Cao SG, Hatch GM (1994) Stimulation of phosphatidylglycerolphosphate phosphatase activity by unsaturated fatty acids in rat heart. Lipids 29:475-480

Cases S, Smith SJ, Zheng YW, Myers HM, Lear SR, Sande E, Novak S, Collins C, Welch CB, Lusis AJ, Erickson SK, Farese RV, Jr. (1998) Identification of a gene encoding an acyl CoA:diacylglycerol acyltransferase, a key enzyme in triacylglycerol synthesis. Proc Natl Acad Sci U S A 95:13018-13023

Cases S, Stone SJ, Zhou P, Yen E, Tow B, Lardizabal KD, Voelker T, Farese RV, Jr. (2001) Cloning of DGAT2, a second mammalian diaylglycerol acyltransferase, and related family members. J Biol Chem 276:38870-38876

Chambliss KL, Shaul PW (2002) Estrogen modulation of endothelial nitric oxide synthase. Endocr Rev 23:665-686

Chawla A, Repa JJ, Evans RM, Mangelsdorf DJ (2001) Nuclear receptors and lipid physiology: opening the X-files. Science 294:1866-1870

Chen HC, Farese RV, Jr. (2000) DGAT and triglyceride synthesis: a new target for obesity treatment? Trends Cardiovasc Med 10:188-192

Chen M, Wang J (2002) Initiator caspases in apoptosis signaling pathways. Apoptosis 7:313-319

Cheng D, Nelson TC, Chen J, Walker SG, Wardwell-Swanson J, Meegalla R, Taub R, Billheimer JT, Ramaker M, Feder JN (2003) Identification of acyl coenzyme A:monoacylglycerol acyltransferase 3, an intestinal specific enzyme implicated in dietary fat absorption. J Biol Chem 278:13611-13614

Cheng P, Dolinsky V, Hatch GM (1996) The acylation of lysophosphatidylglycerol in rat heart: evidence for both in vitro and in vivo activities. Biochim Biophys Acta 1302:61-68

Chitayat D, Chemke J, Gibson KM, Mamer OA, Kronick JB, McGill JJ, Rosenblatt B, Sweetman L, Scriver CR (1992) 3-Methylglutaconic aciduria: a marker for as yet unspecified disorders and the relevance of prenatal diagnosis in a 'new' type ('type 4'). J Inherit Metab Dis 15:204-212

Chulada PC, Thompson MB, Mahler JF, Doyle CM, Gaul BW, Lee C, Tiano HF, Morham SG, Smithies O, Langenbach R (2000) Genetic disruption of Ptgs-1, as well as Ptgs-2, reduces intestinal tumorigenesis in Min mice. Cancer Res 60:4705-4708

Cid MC, Schnaper HW, Kleinman HK (2002) Estrogens and the vascular endothelium. Ann N Y Acad Sci 966:143-157

Clark JD, Lin LL, Kriz RW, Ramesha CS, Sultzman LA, Lin AY, Milona N, Knopf JL (1991) A novel arachidonic acid-selective cytosolic PLA2 contains a Ca(2+)-dependent translocation domain with homology to PKC and GAP. Cell 65:1043-1051

Clark JD, Schievella AR, Nalefski EA, Lin LL (1995) Cytosolic phospholipase A2. J Lipid Mediat Cell Signal 12:83-117

Cobb MH (1999) MAP kinase pathways. Prog Biophys Mol Biol 71:479-500
Cobb MH, Goldsmith EJ (1995) How MAP kinases are regulated. J Biol Chem 270:14843-14846

Coleman R (1973) Membrane-bound enzymes and membrane ultrastructure. Biochim Biophys Acta 300:1-30

Couse JF, Korach KS (1999a) Estrgoen receptor null mice: what have we learned and where will they lead us? Endocr Rev 20:358-417

Couse JF, Korach KS (1999b) Estrogen receptor null mice: what have we learned and where will they lead us? Endocr Rev 20:358-417

Cullis PR, Fenske DB, Hope MJ (1996) Physical properties and functional roles of lipids in membranes. In: Vance DE, Vance J (eds) Biochemistry of lipids, lipoproteins and membranes. Elsevier Science B.V., Amsterdam, pp 1-32

Cutolo M, Accardo S, Villaggio B, Barone A, Sulli A, Coviello DA, Carabbio C, Felli L, Miceli D, Farruggio R, Carruba G, Castagnetta L (1996) Androgen and estrogen receptors are present in primary cultures of human synovial macrophages. J Clin Endocrinol Metab 81:820-827

Cutolo M, Accardo S, Villaggio B, Clerico P, Bagnasco M, Coviello DA, Carruba G, lo Casto M, Castagnetta L (1993) Presence of estrogen-binding sites on macrophage-like synoviocytes and CD8+, CD29+, CD45RO+ T lymphocytes in normal and rheumatoid synovium. Arthritis Rheum 36:1087-1097

Cutolo M, Carruba G, Villaggio B, Coviello DA, Dayer JM, Campisi I, Miele M, Stefano R, Castagnetta LA (2001) Phorbol diester 12-O-tetradecanoylphorbol 13-acetate (TPA) up-regulates the expression of estrogen receptors in human THP-1 leukemia cells. J Cell Biochem 83:390-400

D'Adamo P, Fassone L, Gedeon A, Janssen EA, Bione S, Bolhuis PA, Barth PG, Wilson M, Haan E, Orstavik KH, Patton MA, Green AJ, Zammarchi E, Donati MA,

Toniolo D (1997) The X-linked gene G4.5 is responsible for different infantile dilated cardiomyopathies. Am J Hum Genet 61:862-867

Dean JL, Brook M, Clark AR, Saklatvala J (1999) p38 mitogen-activated protein kinase regulates cyclooxygenase-2 mRNA stability and transcription in lipopolysaccharide-treated human monocytes. J Biol Chem 274:264-269

Deka N, Sun GY, MacQuarrie R (1986) Purification and properties of acyl-CoA:1-acyl-sn-glycero-3-phosphocholine-O-acyltransferase from bovine brain microsomes. Arch Biochem Biophys 246:554-563

Dennis EA (1994) Diversity of group types, regulation, and function of phospholipase A2. J Biol Chem 269:13057-13060

Dennis EA (1997) The growing phospholipase A2 superfamily of signal transduction enzymes. Trends Biochem Sci 22:1-2

DeRisi JL, Iyer VR, Brown PO (1997) Exploring the metabolic and genetic control of gene expression on a genomic scale. Science 278:680-686

Deveraux QL, Roy N, Stennicke HR, Van Arsdale T, Zhou Q, Srinivasula SM, Alnemri ES, Salvesen GS, Reed JC (1998) IAPs block apoptotic events induced by caspase-8 and cytochrome c by direct inhibition of distinct caspases. Embo J 17:2215-2223

Dieter P, Kolada A, Kamionka S, Schadow A, Kaszkin M (2002) Lipopolysaccharide-induced release of arachidonic acid and prostaglandins in liver macrophages: regulation by Group IV cytosolic phospholipase A2, but not by Group V and Group IIA secretory phospholipase A2. Cell Signal 14:199-204

Dils RR, Hubscher G (1961) Metabolism of phospholipids. III. The effect of calcium ions on the incorporation of labelled choline into rat-liver microsomes. Biochim Biophys Acta 46:505-513

Dircks LK, Sul HS (1997) Mammalian mitochondrial glycerol-3-phosphate acyltransferase. Biochim Biophys Acta 1348:17-26

Dowhan W, Bogdanov M (2002) Functional roles of lipids in membrane. In: Vance DE, Vance J (eds) Biochemistry of Lipids, Lipoproteins and Membranes. Vol 36. Elsevier Science B.V., Amsterdam, pp 1-33

Du C, Fang M, Li Y, Li L, Wang X (2000) Smac, a mitochondrial protein that promotes cytochrome c-dependent caspase activation by eliminating IAP inhibition. Cell 102:33-42

Eberhardt C, Gray PW, Tjoelker LW (1997) Human lysophosphatidic acid acyltransferase. cDNA cloning, expression, and localization to chromosome 9q34.3. J Biol Chem 272:20299-20305

Engstrom T (2001) The regulation by ovarian steroids of prostaglandin synthesis and prostaglandin-induced contractility in non-pregnant rat myometrium. Modulating effects of isoproterenol. J Endocrinol 169:33-41

Evans JH, Spencer DM, Zweifach A, Leslie CC (2001) Intracellular calcium signals regulating cytosolic phospholipase A2 translocation to internal membranes. J Biol Chem 276:30150-30160

Evans RM (1988) The steroid and thyroid hormone receptor superfamily. Science 240:889-895

Exton JH (1990) Signaling through phosphatidylcholine breakdown. J Biol Chem 265:1-4

Fadok VA, Voelker DR, Campbell PA, Cohen JJ, Bratton DL, Henson PM (1992) Exposure of phosphatidylserine on the surface of apoptotic lymphocytes triggers specific recognition and removal by macrophages. J Immunol 148:2207-2216

FitzGerald GA, Cheng Y, Austin S (2001) COX-2 inhibitors and the cardiovascular system. Clin Exp Rheumatol 19:S31-36

FitzGerald GA, Patrono C (2001) The coxibs, selective inhibitors of cyclooxygenase-2. N Engl J Med 345:433-442

Forman BM, Evans RM (1995) Nuclear hormone receptors activate direct, inverted, and everted repeats. Ann N Y Acad Sci 761:29-37

Forman BM, Goode E, Chen J, Oro AE, Bradley DJ, Perlmann T, Noonan DJ, Burka LT, McMorris T, Lamph WW, et al. (1995a) Identification of a nuclear receptor that is activated by farnesol metabolites. Cell 81:687-693

Forman BM, Tontonoz P, Chen J, Brun RP, Spiegelman BM, Evans RM (1995b) 15-Deoxy-delta 12, 14-prostaglandin J2 is a ligand for the adipocyte determination factor PPAR gamma. Cell 83:803-812

Forman BM, Umesono K, Chen J, Evans RM (1995c) Unique response pathways are established by allosteric interactions among nuclear hormone receptors. Cell 81:541-550

Fujishima H, Sanchez Mejia RO, Bingham CO, 3rd, Lam BK, Sapirstein A, Bonventre JV, Austen KF, Arm JP (1999) Cytosolic phospholipase A2 is essential for

both the immediate and the delayed phases of eicosanoid generation in mouse bone marrow-derived mast cells. Proc Natl Acad Sci U S A 96:4803-4807

Fukami K, Takenawa T (1992) Phosphatidic acid that accumulates in platelet-derived growth factor-stimulated Balb/c 3T3 cells is a potential mitogenic signal. J Biol Chem 267:10988-10993

Funk CD (2001) Prostaglandins and leukotrienes: advances in eicosanoid biology. Science 294:1871-1875

Fyrst H, Pham DV, Lubin BH, Kuypers FA (1996) Formation of vesicles by the action of acyl-CoA:1-acyllsophosphatidylcholine acyltransferase from rat liver microsomes: optimal solubilization conditions and analysis of lipid composition and enzyme activity. Biochemistry 35:2644-2650

Ganesh Bhat B, Wang P, Kim JH, Black TM, Lewin TM, Fiedorek FT, Jr., Coleman RA (1999) Rat sn-glycerol-3-phosphate acyltransferase: molecular cloning and characterization of the cDNA and expressed protein. Biochim Biophys Acta 1439:415-423

Garrington TP, Johnson GL (1999) Organization and regulation of mitogen-activated protein kinase signaling pathways. Curr Opin Cell Biol 11:211-218

Giguere V, Tremblay A, Tremblay GB (1998) Estrogen receptor beta: re-evaluation of estrogen and antiestrogen signaling. Steroids 63:335-339

Gijon MA, Spencer DM, Kaiser AL, Leslie CC (1999) Role of phosphorylation sites and the C2 domain in regulation of cytosolic phospholipase A2. J Cell Biol 145:1219-1232

Gish W, States DJ (1993) Identification of protein coding regions by database similarity search. Nat Genet 3:266-272

Glaser KB, Lock YW (1995) Regulation of prostaglandin H synthase 2 expression in human monocytes by the marine natural products manoalide and scalaradial. Novel effects independent of inhibition of lipid mediator production. Biochem Pharmacol 50:913-922

Gonchar MV, Sergeeva MG, Namgaladze DA, Mevkh AT (1998) Lack of direct connection between arachidonic acid release and prostanoid synthesis upon differentiation of U937 cell. Biochem Biophys Res Commun 249:829-832

Gonzalez-Baro MR, Granger DA, Coleman RA (2001) Mitochondrial glycerol phosphate acyltransferase contains two transmembrane domains with the active site in the N-terminal domain facing the cytosol. J Biol Chem 276:43182-43188

Green S, Walter P, Kumar V, Krust A, Bornert JM, Argos P, Chambon P (1986) Human oestrogen receptor cDNA: sequence, expression and homology to v-erb-A. Nature 320:134-139

Guo Z, Krucken J, Benten WP, Wunderlich F (2002) Estradiol-induced nongenomic calcium signaling regulates genotropic signaling in macrophages. J Biol Chem 277:7044-7050

Gupta D, Jin YP, Dziarski R (1995) Peptidoglycan induces transcription and secretion of TNF-alpha and activation of lyn, extracellular signal-regulated kinase, and rsk signal transduction proteins in mouse macrophages. J Immunol 155:2620-2630

Habib A, Creminon C, Frobert Y, Grassi J, Pradelles P, Maclouf J (1993) Demonstration of an inducible cyclooxygenase in human endothelial cells using

antibodies raised against the carboxyl-terminal region of the cyclooxygenase-2. J Biol Chem 268:23448-23454

Haldar D, Vancura A (1992) Glycerophosphate acyltransferase from liver. Methods Enzymol 209:64-72

Hammond LE, Gallagher PA, Wang S, Hiller S, Kluckman KD, Posey-Marcos EL, Maeda N, Coleman RA (2002) Mitochondrial glycerol-3-phosphate acyltransferase-deficient mice have reduced weight and liver triacylglycerol content and altered glycerolipid fatty acid composition. Mol Cell Biol 22:8204-8214

Hass R, Bartels H, Topley N, Hadam M, Kohler L, Goppelt-Strube M, Resch K (1989) TPA-induced differentiation and adhesion of U937 cells: changes in ultrastructure, cytoskeletal organization and expression of cell surface antigens. Eur J Cell Biol 48:282-293

Hatch GM (1994) Cardiolipin biosynthesis in the isolated heart. Biochem J 297 (Pt 1):201-208

Hatch GM (1998) Cardiolipin: biosynthesis, remodeling and trafficking in the heart and mammalian cells (Review). Int J Mol Med 1:33-41

Heacock AM, Uhler MD, Agranoff BW (1996) Cloning of CDP-diacylglycerol synthase from a human neuronal cell line. J Neurochem 67:2200-2203

Hernandez M, Bayon Y, Sanchez Crespo M, Nieto ML (1999) Signaling mechanisms involved in the activation of arachidonic acid metabolism in human astrocytoma cells by tumor necrosis factor-alpha: phosphorylation of cytosolic phospholipase A2 and transactivation of cyclooxygenase-2. J Neurochem 73:1641-1649

Herschman HR (1996) Prostaglandin synthase 2. Biochim Biophys Acta 1299:125-140

Hill EM, Bader T, Nettesheim P, Eling TE (1996) Retinoid-induced differentiation regulates prostaglandin H synthase and cPLA2 expression in tracheal epithelium. Am J Physiol 270:L854-862

Hinds TS, West WL, Knight EM (1997) Carotenoids and retinoids: a review of research, clinical, and public health applications. J Clin Pharmacol 37:551-558

Hirai H, Tanaka K, Yoshie O, Ogawa K, Kenmotsu K, Takamori Y, Ichimasa M, Sugamura K, Nakamura M, Takano S, Nagata K (2001) Prostaglandin D2 selectively induces chemotaxis in T helper type 2 cells, eosinophils, and basophils via seven-transmembrane receptor CRTH2. J Exp Med 193:255-261

Hla T, Lee MJ, Ancellin N, Paik JH, Kluk MJ (2001) Lysophospholipids--receptor revelations. Science 294:1875-1878

Hla T, Neilson K (1992) Human cyclooxygenase-2 cDNA. Proc Natl Acad Sci U S A 89:7384-7388

Hodis HN, Mack WJ, LaBree L, Mahrer PR, Sevanian A, Liu CR, Liu CH, Hwang J, Selzer RH, Azen SP (2002a) Alpha-tocopherol supplementation in healthy individuals reduces low-density lipoprotein oxidation but not atherosclerosis: the Vitamin E Atherosclerosis Prevention Study (VEAPS). Circulation 106:1453-1459

Hodis HN, Mack WJ, Lobo R (2002b) Antiatherosclerosis interventions in women. Am J Cardiol 90:17F-21F

Hoff T, DeWitt D, Kaever V, Resch K, Goppelt-Struebe M (1993) Differentiation-associated expression of prostaglandin G/H synthase in monocytic cells. FEBS Lett 320:38-42

Hooks SB, Ragan SP, Lynch KR (1998) Identification of a novel human phosphatidic acid phosphatase type 2 isoform. FEBS Lett 427:188-192

Hostetler KY (1982) Polyglycerophospholipids: phosphatidylglycerol, diphosphatidylglycerol, and bis (monoacylglycerol) phosphate. In: Hawthorne JN, Ansell GB (eds) Phospholipids. Elsevier, Amsterdam, pp 215-261

Hovius R, Lambrechts H, Nicolay K, de Kruijff B (1990) Improved methods to isolate and subfractionate rat liver mitochondria. Lipid composition of the inner and outer membrane. Biochim Biophys Acta 1021:217-226

Hovius R, Thijssen J, van der Linden P, Nicolay K, de Kruijff B (1993) Phospholipid asymmetry of the outer membrane of rat liver mitochondria. Evidence for the presence of cardiolipin on the outside of the outer membrane. FEBS Lett 330:71-76

Hwang ST, Urizar NL, Moore DD, Henning SJ (2002) Bile acids regulate the ontogenic expression of ileal bile acid binding protein in the rat via the farnesoid X receptor. Gastroenterology 122:1483-1492

Ingham PW (2001) Hedgehog signaling: a tale of two lipids. Science 294:1879-1881

Jamal Z, Martin A, Gomez-Munoz A, Brindley DN (1991) Plasma membrane fractions from rat liver contain a phosphatidate phosphohydrolase distinct from that in the endoplasmic reticulum and cytosol. J Biol Chem 266:2988-2996

James SY, Williams MA, Kelsey SM, Newland AC, Colston KW (1997) The role of vitamin D derivatives and retinoids in the differentiation of human leukaemia cells. Biochem Pharmacol 54:625-634

Jiang F, Gu Z, Granger JM, Greenberg ML (1999) Cardiolipin synthase expression is essential for growth at elevated temperature and is regulated by factors affecting mitochondrial development. Mol Microbiol 31:373-379

Jiang YJ, Hatch GM, Mymin D, Dembinski T, Kroeger EA, Choy PC (2001) Modulation of cytosolic phospholipase A(2) by PPAR activators in human preadipocytes. J Lipid Res 42:716-724

Jiang YJ, Lu B, Choy PC, Hatch GM (2003) Regulation of cytosolic phospholipase A2, cyclooxygenase-1 and -2 expression by PMA, TNFalpha, LPS and M-CSF in human monocytes and macrophages. Mol Cell Biochem 246:31-38

Johnston SR, Lu B, Scott GK, Kushner PJ, Smith IE, Dowsett M, Benz CC (1999) Increased activator protein-1 DNA binding and c-Jun NH2-terminal kinase activity in human breast tumors with acquired tamoxifen resistance. Clin Cancer Res 5:251-256

Kai M, Wada I, Imai S, Sakane F, Kanoh H (1996) Identification and cDNA cloning of 35-kDa phosphatidic acid phosphatase (type 2) bound to plasma membranes. Polymerase chain reaction amplification of mouse H2O2-inducible hic53 clone yielded the cDNA encoding phosphatidic acid phosphatase. J Biol Chem 271:18931-18938

Karas RH (2002) Animal models of the cardiovascular effects of exogenous hormones. Am J Cardiol 90:22F-25F

Katzenellenbogen BS, Korach KS (1997) A new actor in the estrogen receptor drama--enter ER-beta. Endocrinology 138:861-862

Kelley RI, Cheatham JP, Clark BJ, Nigro MA, Powell BR, Sherwood GW, Sladky JT, Swisher WP (1991) X-linked dilated cardiomyopathy with neutropenia, growth retardation, and 3-methylglutaconic aciduria. J Pediatr 119:738-747

Kennedy EP (1961) Biosynthesis of complex lipids. Fed Proc Fed Am Soc Exp Biol 20:934-940

Kennedy EP (1989) Discovery of the pathways for the biosynthesis of phosphatidylcholine. In: Vance DE (ed) Phosphatidylcholine Metabolism. CRC Press, Boca Raton, pp 1-9

Kennedy EP (1992) Sailing to Byzantium. Annu Rev Biochem 61:1-28

Kent C (1995) Eukaryotic phospholipid biosynthesis. Annu Rev Biochem 64:315-343

Kozak M (2002a) Emerging links between initiation of translation and human diseases. Mamm Genome 13:401-410

Kozak M (2002b) Pushing the limits of the scanning mechanism for initiation of translation. Gene 299:1-34

Kramer RM, Sharp JD (1997) Structure, function and regulation of Ca2+-sensitive cytosolic phospholipase A2 (cPLA2). FEBS Lett 410:49-53

Kuroda A, Sugiyama E, Taki H, Mino T, Kobayashi M (1997) Interleukin-4 inhibits the gene expression and biosyntheis of cytosolic phospholipase A2 in lipopolysaccharide stimulated U937 macrophage cell line and freshly prepared adherent rheumatoid synovial cells. Biochem Biophys Res Commun 230:40-43

Kurokawa R, DiRenzo J, Boehm M, Sugarman J, Gloss B, Rosenfeld MG, Heyman RA, Glass CK (1994) Regulation of retinoid signalling by receptor polarity and allosteric control of ligand binding. Nature 371:528-531

Lambeth JD, Ryu SH (1996) Glycerolipids in signal transduction. In: Vance DE, Vance J (eds) Biochemistry of Lipids, Lipoproteins and Membranes. Vol 31. Elsevier Science V.B., Amsterdam, pp 37-254

Lands WE, Hart P (1965) Metabolism of plasmalogen. 3. Relative reactivities of acyl and alkenyl derivatives of glycerol-3-phosphorylcholine. Biochim Biophys Acta 98:532-538

Langenbach R, Loftin CD, Lee C, Tiano H (1999) Cyclooxygenase-deficient mice. A summary of their characteristics and susceptibilities to inflammation and carcinogenesis. Ann N Y Acad Sci 889:52-61

Lanz RB, McKenna NJ, Onate SA, Albrecht U, Wong J, Tsai SY, Tsai MJ, O'Malley BW (1999) A steroid receptor coactivator, SRA, functions as an RNA and is present in an SRC-1 complex. Cell 97:17-27

Lashkari DA, DeRisi JL, McCusker JH, Namath AF, Gentile C, Hwang SY, Brown PO, Davis RW (1997) Yeast microarrays for genome wide parallel genetic and gene expression analysis. Proc Natl Acad Sci U S A 94:13057-13062

Lehner R, Kuksis A (1995) Triacylglycerol synthesis by purified triacylglycerol synthetase of rat intestinal mucosa. Role of acyl-CoA acyltransferase. J Biol Chem 270:13630-13636

Leslie CC (1997) Properties and regulation of cytosolic phospholipase A2. J Biol Chem 272:16709-16712

Letunic I, Goodstadt L, Dickens NJ, Doerks T, Schultz J, Mott R, Ciccarelli F, Copley RR, Ponting CP, Bork P (2002) Recent improvements to the SMART domain-based sequence annotation resource. Nucleic Acids Res 30:242-244

Lewin TM, Granger DA, Kim JH, Coleman RA (2001) Regulation of mitochondrial sn-glycerol-3-phosphate acyltransferase activity: response to feeding status is unique in various rat tissues and is discordant with protein expression. Arch Biochem Biophys 396:119-127

Lewis TS, Shapiro PS, Ahn NG (1998) Signal transduction through MAP kinase cascades. Adv Cancer Res 74:49-139

Leygue E, Dotzlaw H, Lu B, Glor C, Watson PH, Murphy LC (1998) Estrogen receptor beta: mine is longer than yours? J Clin Endocrinol Metab 83:3754-3755

Li F, Ambrosini G, Chu EY, Plescia J, Tognin S, Marchisio PC, Altieri DC (1998) Control of apoptosis and mitotic spindle checkpoint by survivin. Nature 396:580-584

Lien E, Sellati TJ, Yoshimura A, Flo TH, Rawadi G, Finberg RW, Carroll JD, Espevik T, Ingalls RR, Radolf JD, Golenbock DT (1999) Toll-like receptor 2 functions as a pattern recognition receptor for diverse bacterial products. J Biol Chem 274:33419-33425

Lin LL, Wartmann M, Lin AY, Knopf JL, Seth A, Davis RJ (1993) cPLA2 is phosphorylated and activated by MAP kinase. Cell 72:269-278

Lockwood JF, Cao J, Burn P, Shi Y (2003) A Human Intestinal Monoacylglycerol Acyltransferase: Differential Features in Tissue Expression and Activity. Am J Physiol Endocrinol Metab

Lodish A, Berk A, Zipursky L, Matsudaira P, Baltimore D, Darnell J (2000) Molecular Cell Biology. W.H.Freeman & Co., New York

Lu B, Dotzlaw H, Leygue E, Murphy LJ, Watson PH, Murphy LC (1999) Estrogen receptor-alpha mRNA variants in murine and human tissues. Mol Cell Endocrinol 158:153-161

Lu B, Leygue E, Dotzlaw H, Murphy LJ, Murphy LC (2000) Functional characteristics of a novel murine estrogen receptor-beta isoform, estrogen receptor-beta 2. J Mol Endocrinol 25:229-242

Lu B, Leygue E, Dotzlaw H, Murphy LJ, Murphy LC, Watson PH (1998) Estrogen receptor-beta mRNA variants in human and murine tissues. Mol Cell Endocrinol 138:199-203

Mangelsdorf DJ, Evans RM (1995) The RXR heterodimers and orphan receptors. Cell 83:841-850

Mangelsdorf DJ, Thummel C, Beato M, Herrlich P, Schutz G, Umesono K, Blumberg B, Kastner P, Mark M, Chambon P, et al. (1995) The nuclear receptor superfamily: the second decade. Cell 83:835-839

Marill J, Idres N, Capron CC, Nguyen E, Chabot GG (2003) Retinoic acid metabolism and mechanism of action: a review. Curr Drug Metab 4:1-10

Marks F, Gschwendt M (1996) Protein kinase C. In: Marks F (ed) Protein Phosphorylation. VCH Publishers, Inc., Weinheim, pp 81-116

Martin A, Gomez-Munoz A, Jamal Z, Brindley DN (1991) Characterization and assay of phosphatidate phosphatase. Methods Enzymol 197:553-563

Mcewen BS, Alves SE (1999) Estrogen actions in the central nervous system. Encocr Rev 20:279-307

McKenna NJ, Lanz RB, O'Malley BW (1999a) Nuclear receptor coregulators: cellular and molecular biology. Endocr Rev 20:321-344

McKenna NJ, Xu J, Nawaz Z, Tsai SY, Tsai MJ, O'Malley BW (1999b) Nuclear receptor coactivators: multiple enzymes, multiple complexes, multiple functions. J Steroid Biochem Mol Biol 69:3-12

McPhail LC (2002) Glycerolipids in signal transduction. In: Vance DE, Vance J (eds) Biochemistry of Lipids, Lipoproteins and Membranes. Vol 36. Elsevier Science B.V., Amsterdam, pp 315-339

Mehta K (2003) Retinoids as regulators of gene transcription. J Biol Regul Homeost Agents 17:1-12

Menard S, Pupa SM, Campiglio M, Tagliabue E (2003) Biologic and therapeutic role of HER2 in cancer. Oncogene 22:6570-6578

Mendelsohn ME (2002) Genomic and nongenomic effects of estrogen in the vasculature. Am J Cardiol 90:3F-6F

Merrill AH, Sandhoff K (2002) Sphingolipids: metabolism and cell signalling. In: Vance DE, Vance J (eds) Biochemistry of lipids, lipoproteins and membranes. Vol 36. Elsevier Science B.V., Amsterdam, pp 373-406

Mestre JR, Subbaramaiah K, Sacks PG, Schantz SP, Tanabe T, Inoue H, Dannenberg AJ (1997) Retinoids suppress epidermal growth factor-induced transcription of cyclooxygenase-2 in human oral squamous carcinoma cells. Cancer Res 57:2890-2895

Miano JM, Berk BC (2001) Retinoids: new insight into smooth muscle cell growth inhibition. Arterioscler Thromb Vasc Biol 21:724-726

Moncada S, Vane JR (1979) Arachidonic acid metabolites and the interactions between platelets and blood-vessel walls. N Engl J Med 300:1142-1147

Monneret G, Gravel S, Diamond M, Rokach J, Powell WS (2001) Prostaglandin D2 is a potent chemoattractant for human eosinophils that acts via a novel DP receptor. Blood 98:1942-1948

Morii H, Ozaki M, Watanabe Y (1994) 5'-flanking region surrounding a human cytosolic phospholipase A2 gene. Biochem Biophys Res Commun 205:6-11

Morteau O, Morham SG, Sellon R, Dieleman LA, Langenbach R, Smithies O, Sartor RB (2000) Impaired mucosal defense to acute colonic injury in mice lacking cyclooxygenase-1 or cyclooxygenase-2. J Clin Invest 105:469-478

Murakami S, Iwaki D, Mitsuzawa H, Sano H, Takahashi H, Voelker DR, Akino T, Kuroki Y (2002) Surfactant protein A inhibits peptidoglycan-induced tumor necrosis factor-alpha secretion in U937 cells and alveolar macrophages by direct interaction with toll-like receptor 2. J Biol Chem 277:6830-6837

Nagy L, Thomazy VA, Shipley GL, Fesus L, Lamph W, Heyman RA, Chandraratna RA, Davies PJ (1995) Activation of retinoid X receptors induces apoptosis in HL-60 cell lines. Mol Cell Biol 15:3540-3551

Nakajima H, Kizaki M, Ueno H, Muto A, Takayama N, Matsushita H, Sonoda A, Ikeda Y (1996) All-trans and 9-cis retinoic acid enhance 1,25-dihydroxyvitamin D3-induced monocytic differentiation of U937 cells. Leuk Res 20:665-676

Nakamura T, Lin LL, Kharbanda S, Knopf J, Kufe D (1992) Macrophage colony stimulating factor activates phosphatidylcholine hydrolysis by cytoplasmic phospholipase A2. Embo J 11:4917-4922

Nalefski EA, Sultzman LA, Martin DM, Kriz RW, Towler PS, Knopf JL, Clark JD (1994) Delineation of two functionally distinct domains of cytosolic phospholipase A2, a regulatory Ca(2+)-dependent lipid-binding domain and a Ca(2+)-independent catalytic domain. J Biol Chem 269:18239-18249

Narumiya S, FitzGerald GA (2001) Genetic and pharmacological analysis of prostanoid receptor function. J Clin Invest 108:25-30

Nathan C, Sporn M (1991) Cytokines in context. J Cell Biol 113:981-986

Needleman P, Turk J, Jakschik BA, Morrison AR, Lefkowith JB (1986) Arachidonic acid metabolism. Annu Rev Biochem 55:69-102

Neuville P, Bochaton-Piallat ML, Gabbiani G (2000) Retinoids and arterial smooth muscle cells. Arterioscler Thromb Vasc Biol 20:1882-1888

Newmeyer DD, Ferguson-Miller S (2003) Mitochondria: releasing power for life and unleashing the machineries of death. Cell 112:481-490

Niles RM (2003) Vitamin A (retinoids) regulation of mouse melanoma growth and differentiation. J Nutr 133:282S-286S

Nusing RM, Mohr S, Ullrich V (1995) Activin A and retinoic acid synergize in cyclooxygenase-1 and thromboxane synthase induction during differentiation of J774.1 macrophages. Eur J Biochem 227:130-136

Olsson IL, Breitman TR (1982) Induction of differentiation of the human histiocytic lymphoma cell line U-937 by retinoic acid and cyclic adenosine 3':5'-monophosphate-inducing agents. Cancer Res 42:3924-3927

Ospina JA, Krause DN, Duckles SP (2002) 17beta-estradiol increases rat cerebrovascular prostacyclin synthesis by elevating cyclooxygenase-1 and prostacyclin synthase. Stroke 33:600-605

Ozaki M, Morii H, Qvist R, Watanabe Y (1994) Interleukin-1 beta induces cytosolic phospholipase A2 gene in rats C6 glioma cell line. Biochem Biophys Res Commun 205:12-17

Paik J, Blaner WS, Sommer KM, Moe R, Swisshlem K (2003) Retinoids, retinoic acid receptors, and breast cancer. Cancer Invest 21:304-312

Paulauskis JD, Sul HS (1988) Cloning and expression of mouse fatty acid synthase and other specific mRNAs. Developmental and hormonal regulation in 3T3-L1 cells. J Biol Chem 263:7049-7054

Paulson JC (1989) Glycoproteins: what are the sugar chains for? Trends Biochem Sci 14:272-276

Paulson JC, Colley KJ (1989) Glycosyltransferases. Structure, localization, and control of cell type-specific glycosylation. J Biol Chem 264:17615-17618

Paydas S, Yavuz S, Disel U, Sahin B, Canbolat T, Tuncer I (2003) Vasculitis associated with all trans retinoic acid (ATRA) in a case with acute promyelocytic leukemia. Leuk Lymphoma 44:547-548

Peng B, Lu B, Leygue E, Murphy LC (2003) Putative functional characteristics of human estrogen receptor-beta isoforms. J Mol Endocrinol 30:13-29

Pettus BJ, Bielawska A, Spiegel S, Roddy P, Hannun YA, Chalfant CE (2003) Ceramide kinase mediates cytokine and calcium ionophore-induced arachidonic acid release. J Biol Chem

Phizicky E, Bastiaens PI, Zhu H, Snyder M, Fields S (2003) Protein analysis on a proteomic scale. Nature 422:208-215

Pluschke G, Hirota Y, Overath P (1978) Function of phospholipids in Escherichia coli. Characterization of a mutant deficient in cardiolipin synthesis. J Biol Chem 253:5048-5055

Raetz CR (1990) Biochemistry of endotoxins. Annu Rev Biochem 59:129-170

Ria R, Roccaro AM, Merchionne F, Vacca A, Dammacco F, Ribatti D (2003) Vascular endothelial growth factor and its receptors in multiple myeloma. Leukemia 17:1961-1966

Ridgway ND, Vance DE (1992) Phosphatidylethanolamine N-methyltransferase from rat liver. Methods Enzymol 209:366-374

Ross-Macdonald P, Coelho PS, Roemer T, Agarwal S, Kumar A, Jansen R, Cheung KH, Sheehan A, Symoniatis D, Umansky L, Heidtman M, Nelson FK, Iwasaki H, Hager K, Gerstein M, Miller P, Roeder GS, Snyder M (1999) Large-scale analysis of the yeast genome by transposon tagging and gene disruption. Nature 402:413-418

Rossouw JE (2002a) Hormones for coronary disease-full circle. Lancet 360:1996-1997

Rossouw JE (2002b) Hormones, genetic factors, and gender differences in cardiovascular disease. Cardiovasc Res 53:550-557

Rubanyi GM, Kauser K, Johns A (2002) Role of estrogen receptors in the vascular system. Vascul Pharmacol 38:81-88

Rudd PM, Elliott T, Cresswell P, Wilson IA, Dwek RA (2001) Glycosylation and the immune system. 291:2370-2376

Sampey AV, Hall PH, Mitchell RA, Metz CN, Morand EF (2001) Regulation of synoviocyte phospholipase A2 and cyclooxygenase 2 by macrophage migration inhibitory factor. Arthritis Rheum 44:1273-1280

Sanjanwala M, Sun GY, Cutrera MA, MacQuarrie RA (1988) Acylation of lysophosphatidylcholine in bovine heart muscle microsomes: purification and kinetic properties of acyl-CoA:1-acyl-sn-glycero-3-phosphocholine O-acyltransferase. Arch Biochem Biophys 265:476-483

Sato T, Michizu H, Hashizume K, Ito A (2001a) Hormonal regulation of PGE2 and COX-2 production in rabbit uterine cervical fibroblasts. J Appl Physiol 90:1227-1231

Sato TK, Overduin M, Emr SD (2001b) Location, location, location: membrane targeting directed by PX domains. Science 294:1881-1885

Schaeffer HJ, Weber MJ (1999) Mitogen-activated protein kinases: specific messages from ubiquitous messengers. Mol Cell Biol 19:2435-2444

Schlame M, Brody S, Hostetler KY (1993) Mitochondrial cardiolipin in diverse eukaryotes. Comparison of biosynthetic reactions and molecular acyl species. Eur J Biochem 212:727-735

Schlame M, Rustow B (1990) Lysocardiolipin formation and reacylation in isolated rat liver mitochondria. Biochem J 272:589-595

Schneider N, Lanz S, Ramer R, Schaefer D, Goppelt-Struebe M (2001) Up-regulation of cyclooxygenase-1 in neuroblastoma cell lines by retinoic acid and corticosteroids. J Neurochem 77:416-424

Seger R, Krebs EG (1995) The MAPK signaling cascade. Faseb J 9:726-735

Sellmayer A, Obermeier H, Weber C (1997) Intrinsic cyclooxygenase activity is not required for monocytic differentiation of U937 cells. Cell Signal 9:91-96

Shibata H, Spencer TE, Onate SA, Jenster G, Tsai SY, Tsai MJ, O'Malley BW (1997) Role of co-activators and co-repressors in the mechanism of steroid/thyroid receptor action. Recent Prog Horm Res 52:141-164; discussion 164-145

Shibata Y, Bjorkman DR, Schmidt M, Oghiso Y, Volkman A (1994) Macrophage colony-stimulating factor-induced bone marrow macrophages do not synthesize or release prostaglandin E2. Blood 83:3316-3323

Singer SJ, Nicolson GL (1972) The fluid mosaic model of the structure of cell membranes. Science 175:720-731

Singh H, Beckman K, Poulos A (1993) Exclusive localization in peroxisomes of dihydroxyacetone phosphate acyltransferase and alkyl-dihydroxyacetone phosphate synthase in rat liver. J Lipid Res 34:467-477

Smith CJ, Morrow JD, Roberts LJ, 2nd, Marnett LJ (1993) Differentiation of monocytoid THP-1 cells with phorbol ester induces expression of prostaglandin endoperoxide synthase-1 (COX-1). Biochem Biophys Res Commun 192:787-793

Smith WL (1989) The eicosanoids and their biochemical mechanisms of action. Biochem J 259:315-324

Smith WL, DeWitt DL, Garavito RM (2000) Cyclooxygenases: structural, cellular, and molecular biology. Annu Rev Biochem 69:145-182

Smith WL, Murphy RC (2002) The eicosanoids: cyclooxygenase, Lipoxygenase, and epoxygenase pathways. In: Vance DE, Vance J (eds) Biochemistry of Lipids, Lipoproteins and Membranes. Vol 36. Elsevier Science B.V., Amsterdam, pp 341-369

Spittler A, Willheim M, Leutmezer F, Ohler R, Krugluger W, Reissner C, Lucas T, Brodowicz T, Roth E, Boltz-Nitulescu G (1997) Effects of 1 alpha,25-dihydroxyvitamin D3 and cytokines on the expression of MHC antigens, complement receptors and other antigens on human blood monocytes and U937 cells: role in cell differentiation, activation and phagocytosis. Immunology 90:286-293

Stamps AC, Elmore MA, Hill ME, Kelly K, Makda AA, Finnen MJ (1997) A human cDNA sequence with homology to non-mammalian lysophosphatidic acid acyltransferases. Biochem J 326 (Pt 2):455-461

Tatusov RL, Koonin EV, Lipman DJ (1997) A genomic perspective on protein families. Science 278:631-637

Tilley SL, Coffman TM, Koller BH (2001) Mixed messages: modulation of inflammation and immune responses by prostaglandins and thromboxanes. J Clin Invest 108:15-23

Tran K, Wong JT, Lee E, Chan AC, Choy PC (1996) Vitamin E potentiates arachidonate release and phospholipase A2 activity in rat heart myoblastic cells. Biochem J 319 (Pt 2):385-391

Uetz P, Giot L, Cagney G, Mansfield TA, Judson RS, Knight JR, Lockshon D, Narayan V, Srinivasan M, Pochart P, Qureshi-Emili A, Li Y, Godwin B, Conover D, Kalbfleisch T, Vijayadamodar G, Yang M, Johnston M, Fields S, Rothberg JM (2000) A comprehensive analysis of protein-protein interactions in Saccharomyces cerevisiae. Nature 403:623-627

Uetz P, Hughes RE (2000) Systematic and large-scale two-hybrid screens. Curr Opin Microbiol 3:303-308

Urizar NL, Liverman AB, Dodds DT, Silva FV, Ordentlich P, Yan Y, Gonzalez FJ, Heyman RA, Mangelsdorf DJ, Moore DD (2002) A natural product that lowers cholesterol as an antagonist ligand for FXR. Science 296:1703-1706

van den Bosch H (1974) Phosphoglyceride metabolism. Annu Rev Biochem 43:243-277

Vance DE (1996) Glycerolipid biosynthesis in eukaryotes. In: Vance DE, Vance J (eds) Biochemistry of Lipids, Lipoproteins and Membranes. Vol 31. Elsevier Science B.V., Amsterdam, pp 153-178

Vance DE (2002) Glycerolipid biosynthesis in eukaryotes. In: Vance DE, Vance J (eds) Biochemistry of Lipids, Lipoproteins and Membranes. Vol 36. Elsevier Science B.V., Amsterdam, pp 205-231

Vaz FM, Houtkooper RH, Valianpour F, Barth PG, Wanders RJ (2003) Only one splice variant of the human TAZ gene encodes a functional protein with a role in cardiolipin metabolism. J Biol Chem

Vegeto E, Bonincontro C, Pollio G, Sala A, Viappiani S, Nardi F, Brusadelli A, Viviani B, Ciana P, Maggi A (2001) Estrogen prevents the lipopolysaccharide-induced inflammatory response in microglia. J Neurosci 21:1809-1818

Voelker DR (1984) Phosphatidylserine functions as the major precursor of phosphatidylethanolamine in cultured BHK-21 cells. Proc Natl Acad Sci U S A 81:2669-2673

Voelker DR (1997) Phosphatidylserine decarboxylase. Biochim Biophys Acta 1348:236-244

Voelker DR (2002) Lipid assembly into cell membranes. In: Vance DE, Vance J (eds) Biochemistry of Lipids, Lipoproteins and Membranes. Vol 36. Elsevier Science B.V., Amsterdam, pp 205-231

Vreken P, Valianpour F, Nijtmans LG, Grivell LA, Plecko B, Wanders RJ, Barth PG (2000) Defective remodeling of cardiolipin and phosphatidylglycerol in Barth syndrome. Biochem Biophys Res Commun 279:378-382

Waggoner DW, Martin A, Dewald J, Gomez-Munoz A, Brindley DN (1995) Purification and characterization of novel plasma membrane phosphatidate phosphohydrolase from rat liver. J Biol Chem 270:19422-19429

Walter P, Green S, Greene G, Krust A, Bornert JM, Jeltsch JM, Staub A, Jensen E, Scrace G, Waterfield M, et al. (1985) Cloning of the human estrogen receptor cDNA. Proc Natl Acad Sci U S A 82:7889-7893

Welch HC, Coadwell WJ, Stephens LR, Hawkins PT (2003) Phosphoinositide 3-kinase-dependent activation of Rac. FEBS Lett 546:93-97

West J, Tompkins CK, Balantac N, Nudelman E, Meengs B, White T, Bursten S, Coleman J, Kumar A, Singer JW, Leung DW (1997) Cloning and expression of two human lysophosphatidic acid acyltransferase cDNAs that enhance cytokine-induced signaling responses in cells. DNA Cell Biol 16:691-701

Weston CR, Davis RJ (2002) The JNK signal transduction pathway. Curr Opin Genet Dev 12:14-21

Weston CR, Lambright DG, Davis RJ (2002) Signal transduction. MAP kinase signaling specificity. Science 296:2345-2347

White DA (1973) The phospholipid composition of mammalian tissues. In: Ansell GG, Hawthorne JN, Dawson RMC (eds) From and Function of Phospholipids. Elsevier Scientific Publishing Co., Amsterdam, pp 441-482

Willson TM, Brown PJ, Sternbach DD, Henke BR (2000) The PPARs: from orphan receptors to drug discovery. J Med Chem 43:527-550

Willy PJ, Umesono K, Ong ES, Evans RM, Heyman RA, Mangelsdorf DJ (1995) LXR, a nuclear receptor that defines a distinct retinoid response pathway. Genes Dev 9:1033-1045

Wilton DC, Waite M (2002) Phospholipases. In: Vance DE, Vance J (eds) Biochemistry of Lipids, Lipoproteins and Membranes. Vol 36. Elsevier Science B.V., Amsterdam, pp 291-311

Wong JT, Tran K, Pierce GN, Chan AC, O K, Choy PC (1998) Lysophosphatidylcholine stimulates the release of arachidonic acid in human endothelial cells. J Biol Chem 273:6830-6836

Wright SD, Ramos RA, Tobias PS, Ulevitch RJ, Mathison JC (1990) CD14, a receptor for complexes of lipopolysaccharide (LPS) and LPS binding protein. Science 249:1431-1433

Wu T, Ikezono T, Angus CW, Shelhamer JH (1994) Characterization of the promoter for the human 85 kDa cytosolic phospholipase A2 gene. Nucleic Acids Res 22:5093-5098

Xie W, Herschman HR (1996) Transcriptional regulation of prostaglandin synthase 2 gene expression by platelet-derived growth factor and serum. J Biol Chem 271:31742-31748

Xu J, Weng YI, Simonyi A, Krugh BW, Liao Z, Weisman GA, Sun GY, Simoni A (2002) Role of PKC and MAPK in cytosolic PLA2 phosphorylation and arachadonic acid release in primary murine astrocytes. J Neurochem 83:259-270

Xu XM, Tang JL, Chen X, Wang LH, Wu KK (1997) Involvement of two Sp1 elements in basal endothelial prostaglandin H synthase-1 promoter activity. J Biol Chem 272:6943-6950

Yang Q, Sakurai T, Kakudo K (2002) Retinoid, retinoic acid receptor beta and breast cancer. Breast Cancer Res Treat 76:167-173

Yao XL, Cowan MJ, Gladwin MT, Lawrence MM, Angus CW, Shelhamer JH (1999) Dexamethasone alters arachidonate release from human epithelial cells by induction of p11 protein synthesis and inhibition of phospholipase A2 activity. J Biol Chem 274:17202-17208

Yeagle P (1989) Lipid regulation of cell membrane structure and function. FASEB J 3:1833-1842

Yen CL, Farese RV, Jr. (2003) MGAT2, a monoacylglycerol acyltransferase expressed in the small intestine. J Biol Chem 278:18532-18537

Yen CL, Stone SJ, Cases S, Zhou P, Farese RV, Jr. (2002) Identification of a gene encoding MGAT1, a monoacylglycerol acyltransferase. Proc Natl Acad Sci U S A 99:8512-8517

Yet SF, Lee S, Hahm YT, Sul HS (1993) Expression and identification of p90 as the murine mitochondrial glycerol-3-phosphate acyltransferase. Biochemistry 32:9486-9491

Yet SF, Moon YK, Sul HS (1995) Purification and reconstitution of murine mitochondrial glycerol-3-phosphate acyltransferase. Functional expression in baculovirus-infected insect cells. Biochemistry 34:7303-7310

Yeung YG, Richard Stanley E (2003) Proteomic approaches to the analysis of early events in CSF-1 signal transduction. Mol Cell Proteomics

Yokoyama C, Tanabe T (1989) Cloning of human gene encoding prostaglandin endoperoxide synthase and primary structure of the enzyme. Biochem Biophys Res Commun 165:888-894

Zhang FX, Kirschning CJ, Mancinelli R, Xu XP, Jin Y, Faure E, Mantovani A, Rothe M, Muzio M, Arditi M (1999) Bacterial lipopolysaccharide activates nuclear factor-kappaB through interleukin-1 signaling mediators in cultured human dermal endothelial cells and mononuclear phagocytes. J Biol Chem 274:7611-7614

Zhang M, Mileykovskaya E, Dowhan W (2002) Gluing the respiratory chain together. Cardiolipin is required for supercomplex formation in the inner mitochondrial membrane. J Biol Chem 277:43553-43556

Zhu H, Bilgin M, Bangham R, Hall D, Casamayor A, Bertone P, Lan N, Jansen R, Bidlingmaier S, Houfek T, Mitchell T, Miller P, Dean RA, Gerstein M, Snyder M (2001) Global analysis of protein activities using proteome chips. Science 293:2101-2105

Zhu H, Klemic JF, Chang S, Bertone P, Casamayor A, Klemic KG, Smith D, Gerstein M, Reed MA, Snyder M (2000) Analysis of yeast protein kinases using protein chips. Nat Genet 26:283-289

Zhu H, Snyder M (2001) Protein arrays and microarrays. Curr Opin Chem Biol 5:40-45

Zhu H, Snyder M (2003) Protein chip technology. Curr Opin Chem Biol 7:55-63

Zhuang YH, Sainio EL, Sainio P, Vedeckis WV, Ylikomi T, Tuohimaa P (1995) Distribution of all-trans-retinoic acid in normal and vitamin A deficient mice: correlation to retinoic acid receptors in different tissues of normal mice. Gen Comp Endocrinol 100:170-178